TECHNISCHE UNIVERSITÄT MÜNCHEN

Lehrstuhl für Biotechnologie der Nutztiere

New methods for transgenesis in rabbits: Cell-mediated transgenesis and transposons

Tobias Roland Richter

Vollständiger Abdruck der von der Fakultät Wissenschaftszentrum Weihenstephan für Ernährung, Landnutzung und Umwelt der Technischen Universität München zur Erlangung des akademischen Grades eines

Doktors der Naturwissenschaften

genehmigten Dissertation.

Vorsitzender: Univ.-Prof. Dr. D. Haller

Prüfer der Dissertation:

1. Univ.-Prof. A. Schnieke, Ph.D.
2. Priv.-Doz. Dr. S. E. Ulbrich

Die Dissertation wurde am 24.10.2012 bei der Technischen Universität München eingereicht und durch die Fakultät Wissenschaftszentrum Weihenstephan für Ernährung, Landnutzung und Umwelt am 06.05.2013 angenommen.

Für meine Eltern

Die höchste Form des Glücks ist ein Leben mit einem gewissen Grad an Verrücktheit.

Erasmus von Rotterdam

Men love to wonder, and that is the seed of science.

Ralph Waldo Emerson

ABSTRACT

The ability to generate transgenic rabbits (*Oryctolagus cuniculus*) in a fast and efficient way would benefit biomedical research. So far, transgenic rabbits were produced by pro-nuclear micro-injection of DNA molecules into fertilized oocytes or intra-cytoplasmic sperm injection. These methods are characterized by a very low efficiency and formation of concatemeres, which can result in gene silencing. Low transgenic expression may also be due to position effects. Here, two different methods are used, cell-mediated transgenesis by nuclear transfer (NT) and improved micro-injection by the use of transposons. Each method is suitable for a particular purpose and proofs of principle applications are shown.

In order to have appropriate cells for the cell-mediated transgenesis, two different cell types (pluripotent rabbit embryonic stem cells (rbESCs) and multipotent rabbit mesenchymal stem cells (rbMSCs)) were characterized and assessed. For this, efficient techniques for their isolation and culture were developed as well as efficient methods to transfect them. RbESCs showed by RT-PCR expression of essential stem cell markers: *Oct4*, *Nanog*, *Sox2*, *FoxD3*, *Rex1*, *Nodal*, *DPPA5*, *BMP4* and *TERC*. Additionally, Oct4 was detected as protein by immunostaining. When exposed to differentiating conditions (via embryoid bodies), cells showed distinct phenotypes and expressed markers for the three germ layers *Nestin* (exoderm), *Desmin* (mesoderm) and *Hnf4a* (endoderm) that were detected by RT-PCR. Further, rbESCs stably transfected with *eGFP* and transferred into wild type 8-cell-stage embryos contributed to the inner cell mass as revealed by the expression of *eGFP* in rbESCs derived from those embryos. The 2nd cell type, rbMSC, was derived from bone-marrow and adipose tissue. Their successful differentiation (adipogenic, osteogenic and chondrogenic) was verified by specific staining. Both rbESCs and rbBM-MSCs were compared for their ability to support foetal development after nuclear transfer where rbMSCs were found to be more suitable for cell-mediated transgenesis. To assess if rbMSCs were also suitable for the production of gene targeted rabbits, cells were transfected with a targeting vector to replace exon 3 of the rabbit *hprt* gene with a PGK-Neo-pA cassette by homologous recombination. Resulting rabbits with a dysfunctional HPRT could provide an animal model for the human Lesch-Nyhan syndrome.

In order to improve the efficiency of micro-injection of naked DNA into fertilised oocytes, a transposon-based system (Sleeping Beauty - SB) was developed to integrate genes of interest (GOI) into the rabbit genome as stable single-copies. To assess this vector system for production of transgenic rabbits the red fluorescent marker *mCherry* under control of a chimeric cytomegalovirus immediate-early enhancer/modified chicken β-actin

promoter/chicken β-globin intron sequence (CAGGs) was used. To determine the optimal ratio of transposase to vector *in vitro* both constructs were transfected into rbMSCs. Information from these experiments were then used to produce transgenic rabbits, 3 out of 18 foetuses (17%, d 21 *p.c.*) showed a uniform expression of *mCherry*. PCR analysis revealed that none of the negative foetuses carried *mCherry*. Furthermore, PCR results showed that the transposase-bearing vector was not integrated.

To obtain an animal model for Diabetes mellitus, a SB vector carrying the Akita-mutated *insulin* was designed and proved functional in cell-culture assays. This was then followed by preliminary *in vivo* experiments.

ZUSAMMENFASSUNG

Die Möglichkeit, transgene Kaninchen (*Oryctolagus cuniculus*) schnell und effizient zu generieren, würde die biomedizinische Forschung fördern. Transgene Kaninchen wurden bisher durch pronukleare Mikroinjektion von DNA in befruchtete Eizellen oder intrazytoplasmatische Injektion von Spermien erzeugt. Allerdings sind diese Methoden durch sehr geringe Effizienz und die Bildung von Konkatemeren, was zur Stilllegung von Genen in Folge von Positionseffekten führen kann, gekennzeichnet. In dieser Arbeit werden zwei Methoden, die zellvermittelte Transgenese durch Kerntransfer und eine verbesserte Mikroinjektion durch das Nutzen von Transposonen, angewandt. Jede Methode ist für bestimmte Zwecke geeignet und Anwendungen zum Nachweis des Wirkprinzips werden gezeigt.

Um geeignete Zellen für die zellvermittelte Transgenese zu erhalten, wurden zwei verschiedene Zelltypen charakterisiert und bewertet. Die gewählten Zelltypen sind pluripotente embryonale Kaninchenstammzellen (rbESCs) und multipotente mesenchymale Kaninchenstammzellen (rbMSCs). Es wurden sowohl effiziente Methoden für ihre Isolierung und Kultivierung als auch Methoden zu ihrer Transfektion entwickelt. RbESCs zeigten die Expression von essentiellen Stammzellmarkern (*Oct4*, *Nanog*, *Sox2*, *FoxD3*, *Rex1*, *Nodal*, *DPPA5*, *BMP4* und *TERC*) in der RT-PCR. Zusätzlich konnte Oct4 als Protein durch Immunfärbung nachgewiesen werden. Wenn rbESCs Differenzierungsbedingungen mittels embryonalen Körperchen ausgesetzt wurden, zeigten sich verschiedene Phänotypen und die Expression von Markern in der RT-PCR, die charakteristisch für jede der drei Keimlinien sind: *Nestin* (Exoderm), *Desmin* (Mesoderm) und *Hnf4a* (Endoderm). Anschließend wurden mit *eGFP* stabil transfizierte rbESCs in 8-Zell-Stadium-Embryonen eingeführt, woraufhin die *eGPF*-rbESCs zur Entstehung der inneren Zellmasse beitrugen, was durch die Expression von *eGFP* in den wiederum daraus erhaltenen rbESCs nachgewiesen wurde. Der zweite verwendete Zelltyp, rbMSCs, wurde sowohl aus Knochenmark als auch aus Fettgewebe gewonnen. Deren erfolgreiche Differenzierung in Adipozyten, Chondrozyten und Osteoblasten wurde durch spezifische Färbungen nachgewiesen. Beide Zelltypen, rbMSCs und rbBM-MSCs, wurden auf ihre Verwendbarkeit für Kerntransferexperimente verglichen. Es zeigte sich, dass rbMSCs besser für die zellvermittelte Transgenese geeignet sind. Um zu ermitteln ob rbMSCs auch für die Produktion von Kaninchen mit gezielten Genmodifikation geeignet sind, wurden männliche rbMSCs mit einem Targetingvektor transfiziert, welcher das Exon 3 des Kaninchengens *hprt* mit einer PGK-Neo-pA Kassette durch homologe Rekombination ersetzt. Daraus entstehende Kaninchen mit einem nicht funktionellen HPRT sind als Modelltiere für das menschliche Lesch-Nyhan-Syndrom geeignet.

Um die Mikroinjektion von nackter DNA in befruchtete Eizellen zu verbessern, wurde ein auf Transposonen basiertes System (Sleeping Beauty, SB) entwickelt, um gewünschte Gene in das Kaninchengenom als stabile Einzelintegration und ohne die Bildung von Konkatemeren einzufügen. Das Transposonsystem besteht aus zwei Vektoren, um die Integration des Transposasegens zu verhindern. Einer trägt das gewünschte Gen und der andere das Enzym. Um dieses Vektorsystem für die Gewinnung transgener Kaninchen zu bewerten, wurde das rot fluoreszierende Markergen *mCherry* unter Kontrolle des CAGGs Promoters in rbMSCs transfiziert und *in vitro* das optimale Verhältnis Transposase zu Vektor bestimmt. Dieses wurde dann genutzt um transgene Kaninchen durch Mikroinjektion in befruchtete Eizellen zu gewinnen. In diesem Experiment wurden die Föten am Tag 21 der Trächtigkeit analysiert, wobei sich zeigte, dass 3 von 18 Föten (17%) eine gleichmäßige Expression von *mCherry* aufwiesen. Die anschließende PCR zeigte außerdem, dass keiner der nicht *mCherry* exprimierenden Föten eine Kopie dieses Genes aufwies. Weiterhin wurde durch PCR gezeigt, dass der Transposase tragende Vektor nicht integriert wurde. Um ein Tiermodel für Diabetes mellitus zu generieren, wurde ein SB-System mit mutiertem Insulingen entworfen. Hierbei wurde die Akitamutation in das Kaninchengen *insulin* eingefügt, was in Zellkulturversuchen seine Funktionalität zeigte. Anschließend wurden vorbereitende Experiment *in vivo* durchgeführt.

Table of contents

INTRODUCTION - 1 -

1.1 TRANSGENIC ANIMALS - 1 -

1.1.0.1 Rabbits as animal model for biomedicine - 2 -

1.1.1 TRANSPOSON-BASED TRANSGENESIS - 3 -

1.1.1.1 Microinjection - 3 -

1.1.1.2 Transposons - 4 -

1.1.1.2.1 Sleeping Beauty - 5 -

1.1.2 CELL-MEDIATED TRANSGENESIS - 6 -

1.1.2.1 Pluripotent cells - 7 -

1.1.2.1.1. Molecular basis of pluripotency - 9 -

1.1.2.2 Multipotent cells - 11 -

1.2 DISEASES TO MODEL - 13 -

1.2.1 DIABETES MELLITUS - 13 -

1.2.1.1. Molecular basis of diabetes mellitus - 14 -

1.2.1.2. Diabetic model organisms - 17 -

1.2.1.2.1. Mechanism of the destruction of β-cells - 18 -

1.2.2 LESCH-NYHAN SYNDROME - 19 -

1.2.2.1 Molecular basis of Lesch-Nyhan syndrome - 19 -

1.2.2.2 Model organisms for Lesch-Nyhan syndrome - 21 -

1.2.2.3 Rabbit hprt gene - 21 -

1.3 AIMS OF THE THESIS - 23 -

2 MATERIAL AND METHODS - 24 -

2.1 MATERIAL - 24 -

2.1.1 EQUIPMENT - 24 -

2.1.2 CONSUMABLES - 25 -

2.1.3 CHEMICALS - 26 -

2.1.4 KITS - 27 -

2.1.5 ENZYMES FOR MOLECULAR BIOLOGY - 27 -

2.1.6 CLONING VECTORS - 27 -

2.1.7 CHEMICALS FOR SOUTHERN BLOT ANALYSIS - 28 -

2.1.8 MISCELLANEOUS - 28 -
2.1.9 STRAINS OF *ESCHERICHIA COLI* - 29 -
2.1.10 MEDIA AND ANTIBIOTICS FOR BACTERIAL CULTURE - 29 -
2.1.11 MAMMALIAN CELLS - 29 -
2.1.12 MEDIA AND ADDITIVES FOR MAMMALIAN CELL CULTURE - 29 -
2.1.13 ANIMALS - 31 -
2.1.14 OLIGONUCLEOTIDES - 31 -
2.1.14.1 Oligonucleotides for vector construction - 31 -
2.1.14.2 Oligonucleotides for PCR amplifications - 31 -
2.1.14.3 Oligonucleotides for sequencing - 33 -
2.1.15 COMPUTER SOFTWARE - 34 -
2.2 METHODS - 35 -
2.2.1 MICROBIOLOGICAL WORK - 35 -
2.2.1.1 Growing *E. coli* - 35 -
2.2.1.2 Storage of *E. coli* - 35 -
2.2.1.3 Transformation of electro-competent *E. coli* - 35 -
2.2.1.4 Making recombineering-competent *E. coli* - 36 -
2.2.2 MOLECULAR BIOLOGICAL WORK - 36 -
2.2.2.1 Isolation of DNA - 36 -
2.2.2.1.1 Isolation of plasmid and BAC from E. coli - 36 -
2.2.2.1.2 Isolation of mammalian genomic DNA - 37 -
2.2.2.2 Manipulation of DNA - 37 -
2.2.2.2.1 Restriction endonuclease digestion - 37 -
2.2.2.2.2 Treatment of DNA with Klenow fragment - 38 -
2.2.2.2.3 Dephosphorylation of DNA - 38 -
2.2.2.2.4 Agarose gel-electrophoresis - 38 -
2.2.2.2.5 Extraction of DNA from agarose gels - 39 -
2.2.2.2.6 Ligation of DNA fragments - 39 -
2.2.2.2.7 Purification of DNA by Phenol-Chloroform-Isoamylalcohol - 39 -
2.2.2.2.8 DNA precipitation - 39 -
2.2.2.2.9 Introduction of single base mutations - 40 -
2.2.2.3 DNA concentration determination - 40 -
2.2.2.4 Polymerase Chain Reaction (PCR) - 40 -
2.2.2.5 Sequencing of DNA - 42 -
2.2.2.6 Southern Blot analysis of DNA - 42 -

2.2.2.6.1 Preparation of the probe - 42 -
2.2.2.6.2 Southern Blot - 43 -
2.2.2.7 Isolation of RNA - 44 -
2.2.2.8 Reverse Transcriptase Polymerase Chain Reaction (RT-PCR) - 45 -
2.2.3 MAMMALIAN CELL CULTURE WORK - 45 -
2.2.3.1 Media for mammalian cell culture - 46 -
2.2.3.2 Isolation and culture of primary cells - 47 -
2.2.3.2.1 Isolation of mouse embryonic feeder cells - 47 -
2.2.3.2.2 Preparation of feeder plates - 47 -
2.2.3.2.3 Isolation and culture of putative rabbit embryonic stem cells - 47 -
2.2.3.2.4 Isolation and culture of rabbit mesenchymal stem cells - 48 -
2.2.3.2.5 Isolation and culture of rabbit fibroblast-like cells - 49 -
2.2.3.2.6 Isolation of rabbit foetal cells - 49 -
2.2.3.2.7 Culture of rat insulinoma cells - 49 -
2.2.3.3 Cryopreservation and thawing of mammalian cells - 50 -
2.2.3.4 Differentiation of stem cells - 50 -
2.2.3.4.1 Differentiation of rabbit putative embryonic stem cells - 50 -
2.2.3.4.2 Differentiation of rabbit mesenchymal stem cells - 51 -
2.2.3.5 Karyotyping by Fluorescence in-situ hybridisation - 52 -
2.2.3.6 Crystal violet staining - 52 -
2.2.3.7 Transfection of mammalian cells - 53 -
2.2.3.7.1 Chemical transfection - 53 -
2.2.3.7.2 Electroporation - 53 -
2.2.3.7.3 Nucleofection - 53 -
2.2.3.8 Generation of stable genetically modified cells - 53 -

3 RESULTS - 54 -

3.1 TRANSPOSON-MEDIATED TRANSGENESIS - 54 -
3.1.1 CONSTRUCTION OF RABBIT *INSULIN* EXPRESSION VECTORS - 54 -
3.1.2 VERIFICATION OF THE FUNCTIONALITY OF INSULIN EXPRESSION VECTORS - 55 -
3.1.3 VERIFICATION OF THE FUNCTIONALITY OF SLEEPING BEAUTY TRANSPOSON SYSTEM - 57 -
3.1.4 GENERATION OF TRANSGENIC RABBITS BY TRANSPOSON-MEDIATED TRANSGENESIS - 58 -
3.1.4.1 Generation of transgenic rabbits carrying mCherry red fluorescent protein - 59 -
3.1.4.2 Generation of transgenic rabbits carrying mutated rabbit *insulin* - 61 -
3.1.5 SUMMARY - 62 -

3.2 CELL-MEDIATED TRANSGENESIS - 63 -

3.2.1 PLURIPOTENT STEM CELLS - 63 -

3.2.1.1 Derivation of rabbit pluripotent stem cells - 63 -

3.2.1.2 Optimisation of the *in vitro* culture of rabbit putative embryonic stem cells - 64 -

3.2.1.3 Assessment of optimal transfection methods for rabbit embryonic stem cells - 68 -

3.2.1.4 Differentiation of rabbit embryonic stem cells *in vitro* - 70 -

3.2.1.4.1 Spontaneous differentiation of rbESCs - 70 -

3.2.1.4.2 Directed differentiation of rbESCs - 72 -

3.2.1.5 Contribution of rabbit embryonic stem cells to the inner cell mass - 73 -

3.2.2 MULTIPOTENT STEM CELLS - 74 -

3.2.2.1. Characterisation of rabbit MSCs - 74 -

3.2.2.2. Differentiation of rabbit MSCs - 77 -

3.2.2.3. Assessment of optimal transfection methods for rabbit MSCs - 79 -

3.2.2.3.1. Transfection with plasmids - 79 -

3.2.2.3.2. Transfection with bacterial artificial chromosomes - 81 -

3.2.3 ASSESSMENT OF NUCLEAR TRANSFER COMPETENCE - 82 -

3.2.4 TARGETING OF RABBIT *HPRT* - 83 -

3.2.4.1 Construction of bacterial artificial chromosome targeting vector - 83 -

3.2.4.2 Construction of a conventional rabbit *hprt* targeting plasmid - 84 -

3.2.4.3 Gene targeting of rabbit $hprt^{Neo}$ in mesenchymal stem cells - 85 -

3.2.4.3.1 BAC targeting of hprt - 85 -

3.2.4.3.2 Conventional targeting of hprt - 85 -

3.2.5 SUMMARY - 87 -

4 DISCUSSION - 89 -

4.1 TRANSPOSON-MEDIATED TRANSGENESIS - 89 -

4.1.1 FUNCTIONALITY OF CONSTRUCTED SLEEPING BEAUTY VECTOR SYSTEM - 90 -

4.1.2 GENERATION OF TRANSGENIC RABBITS BY TRANSPOSON-MEDIATED TRANSGENESIS - 90 -

4.1.2.1 Influence of Sleeping Beauty on the integration and expression of the transgene - 92 -

4.1.2.2 Improvements for transposon-mediated transgenesis - 94 -

4.1.3 FUNCTIONALITY OF RABBIT *INSULIN* EXPRESSION VECTORS - 96 -

4.1.3.1 Implications of Ins^{Akita} rabbits - 98 -

4.2 CELL-MEDIATED TRANSGENESIS - 101 -

4.2.1 PLURIPOTENT CELLS - 101 -

4.2.1.1 Pluripotency is influenced by extrinsic factors - 101 -

4.2.1.2 Plasticity of pluripotent cells - 106 -
4.2.1.3 Pluripotent signalling network - 107 -
4.2.1.4 Pluripotency of rabbit cells - 108 -
4.2.1.5 Differentiation of pluripotent cells - 111 -
4.2.1.6 Generation of rabbit chimeras - 112 -
4.2.1.7 Improvements for the derivation of rabbit pluripotent cells - 112 -
4.2.2 MULTIPOTENT CELLS - 113 -
4.2.2.1 Differentiation of multipotent cells - 114 -
4.2.2.2 Heterogeneity of mesenchymal stem cells - 115 -
4.2.2.3 Ageing of mesenchymal stem cells - 115 -
4.2.3 COMPETENCE OF PLURIPOTENT AND MULTIPOTENT RABBIT STEM CELLS FOR NT - 116 -
4.2.3.1 Influencing factors for nuclear transfer - 118 -
4.2.4 RB*HPRT* KNOCKOUT - 119 -
4.2.4.1 Generation of targeting constructs - 119 -
4.2.4.2 Selection of *hprt*^{Neo} cells - 119 -
4.2.4.3 Improvements for the generation of *hprt* knockout cells - 122 -

5 ABBREVIATIONS - 125 -

6 LIST OF TABLES - 127 -

7 LIST OF FIGURES - 128 -

8 APPENDIX - 131 -

8.1 CONSTRUCTION OF RABBIT *INSULIN* EXPRESSION VECTORS - 131 -
8.2 CONSTRUCTION OF SLEEPING BEAUTY TRANSPOSON SYSTEM - 132 -
8.3 GENERATION OF TRANSGENIC RABBITS CARRYING MCHERRY - 133 -
8.4 MUTAGENESIS OF A BACTERIAL ARTIFICIAL CHROMOSOME - 133 -
8.5 CONSTRUCTION OF A RABBIT *HPRT* TARGETING CONSTRUCT - 134 -

9 LITERATURE - 136 -

10 ACKNOWLEDGMENT - 183 -

11 CURRICULUM VITAE - 185 -

INTRODUCTION

1.1 Transgenic animals

Transgenesis refers to the introduction of an exogenous gene, transgene, into an organism which then is transmitted to the offspring. This involves random integrations as well as targeted integrations. However, other definitions include also the experimental modification of the genomic sequence without introduction of exogenous genes.

Transgenic animals are powerful tools in biomedical research. In 1980 the first transgenic animal was produced by pronuclear DNA microinjection into the fertilised mouse oocyte [1,2]. Five years later the first transgenic rabbits, pigs and sheep were generated in the same way [3,4]. Generally, transgenesis is achieved by inserting exogenous DNA by different methods, e.g. chemical-based and non-chemical transfection of plasmid vectors, transduction of viral vectors and microinjections. Nowadays, the toolbox to obtain transgenic animals includes cell-mediated transgenesis, sperm-mediated DNA transfer, intracytoplasmic injection of sperm heads containing transgenic DNA (ICSI), retro-, lenti- and adenoviral vectors, small interfering ribonucleic acids, meganucleases, zinc finger nucleases (ZFNs), transcription activator-like effector hybrid nucleases (TALENs) and transposons. An overview to achieve transgenic animals is given in Fig. 1.

The first famous transgenic livestock was Herman the bull [5] producing lactoferrin. For the expression of human proteins also transgenic sheep, pigs, rabbits, mice and rats were generated [6–8]. Here, the most prominent example is the expression of human α-1-antitrypsin in sheep [9,10]. Most important for livestock biotechnology, Schnieke *et al.* (1997) [11] cloned for the first time a live sheep from previously genetically manipulated cells. Today, a lot of medicines and immunisations are produced in transgenic animals [12–14].

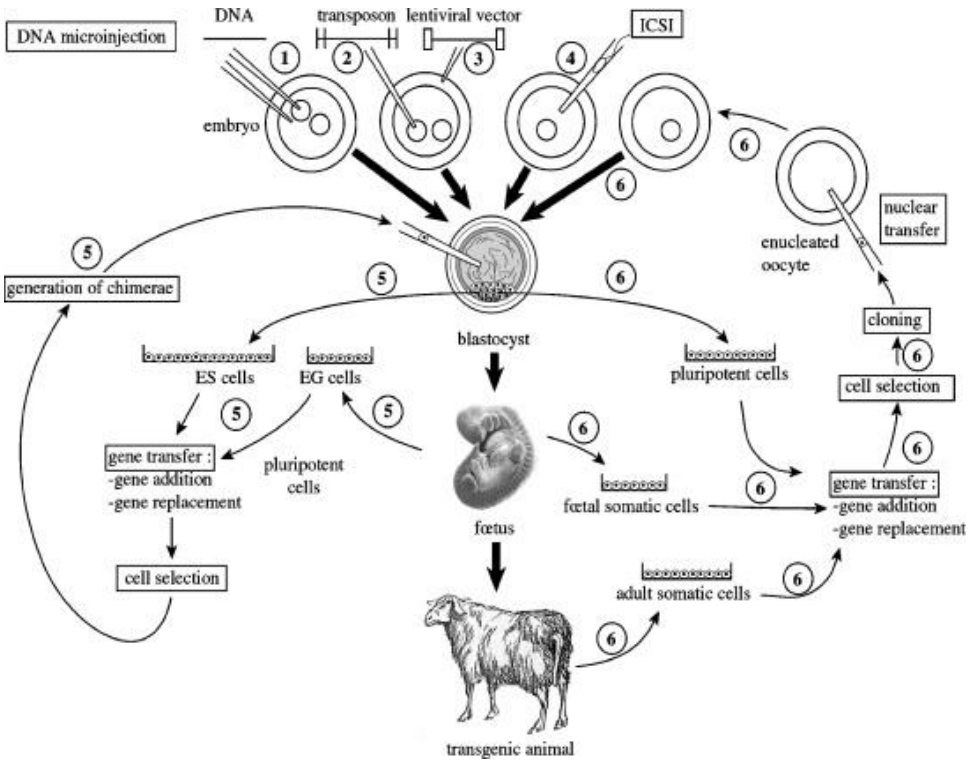

Figure 1: Overview of different methods to achieve transgenic animals.
The simplest way is the micromanipulation of the zygote by injecting exogenous DNA 1-3. Injection of 1: naked DNA and 2: transposons into the cytoplasm or into pronuclei. 3: Lentiviral vectors are infectious and therefore injected into the perivitelline space. 4: Sperms carrying the transgene are microinjected into the oocyte (ICSI). 5/6: Cells can be obtained from different stages of a developing animal and also from an adult. Those cells were made transgenic *in vitro* and selected for the transgene. When these cells were given into blastocysts (5), a chimeric animal will be achieved. On the other hand, the nucleus of these cells can be injected into an enucleated oocyte (6) resulting in a transgenic animal. Adapted from Houdebine (2009) [15]

1.1.0.1 Rabbits as animal model for biomedicine

The rabbit (*Oryctolagus cuniculus*) is an omnivore that originates from the southwest of Europe. It was tamed and kept as a meat supplier. This domestication began in about the 3rd century BC by the Romans after the conquest of Spain. Based on coat colour and other visible traits, different breeds were developed during the 19th century.

In addition to their high fertility (65% conception rate), rabbits have a high number of offspring (5 – 12). The gestation time is 30 – 33 days and rabbits become sexual mature with 4 – 5 months of age. After approx. 44 days *postpartum*, rabbits can be fertilised again, having 4 – 7 litters per year. In addition, rabbits have a much longer life span (5 – 8 years) compared to rodents.

Rabbits used as experimental animals are most commonly the Dutch breed (agouti) with a weight of less than 3 kg and the white New Zealand breed (albino) with a weight of 3 – 6 kg. There are only a small number of inbred strains, e.g. ZIKA. Compared to mouse and rat, the number of rabbits in biomedical research is relatively low and is approx. 1% of all reported experimental animals. The research areas for which they are used include toxicity,

teratogenicity and pyrogenic tests, the production of antisera, the setting of biologically active substances, studies on atherosclerosis and surgical models [16].

The first transgenic rabbits were established by microinjection in 1985 [3,4] and later by improved microinjection [17]. Nevertheless, the broad use of rabbits in biomedical research is hampered by the lack of methods for precise genetic engineering. Albeit rabbit models are used in research, their phenotype results from spontaneous mutations [18,19] or imprecise microinjections [20, review].

Rabbits are in use as animal model already more than 100 years [21,1097]. As experimental model organism, rabbits are anatomically, physiologically and genetically more similar to humans, than to mice and rats [22,23]. Also, rabbit strains exhibit a more diverse genetic background than mouse strains. This could mimic the diverse human genetic situation more accurately. Thus, rabbits are more appropriate to study complex diseases such as atherosclerosis, diabetes mellitus (DM) and lipid metabolism. In particular, the disease phenotypes of distinct transgenic rabbit models are closer to humans then to rodents [24, review]. In the research of acromegaly, only the rabbit perfectly showed the same phenotype as humans, but not the pig model [25–27]. Furthermore, a rabbit model of hypertrophic cardiomyopathy showed all characteristic symptoms observed in humans [28–32]. In the research of infectious diseases, like tuberculosis, rabbits are superior to mice and guinea pigs [33–35]. Beside human, chimpanzee and gibbon, only rabbits are susceptible to infections with human immunodeficiency virus (HIV), albeit the progression of the disease acquired immunodeficiency syndrome (AIDS) is very slow [36–40]. For cancer science (e.g. leukaemia), different rabbit models are available [41–44].

Rabbits not only serve as biomedical models but are also used for the production of therapeutic proteins [45,46]. Already in 1990 human interleukin-2 was produced in the milk of transgenic rabbits [47]. Today, rabbits are well established in the production of human polyclonal antibodies and other pharmaceutical proteins [48–52, reviews: 46,53–56]. Importantly, there is no known transmission of severe diseases and pathogens to humans.

1.1.1 Transposon-based transgenesis

To simply insert a foreign DNA sequence into a genome the method of pronuclear DNA microinjection has been most commonly used. But at least in mice other methods, such as viral vectors or transposons can be more efficient in the production of transgenic animals.

1.1.1.1 Microinjection

During microinjection foreign DNA is injected into the pronuclei of fertilised oocytes. As mentioned, the first transgenic animal as well as first transgenic livestock were achieved with

this method. Although microinjection has been used for more than 20 years this method is fraught with many disadvantages since microinjection is very inefficient and expensive. Typically, depending on the species, less than 1 – 4% of treated embryos are transgenic [4, reviews: 57–60]. Generally, injected DNA integrates as concatemeres (multiple copies of the exogenous fragment with a total size of 70 – 100 kb) that are prone to silencing [62, review: 61]. It is difficult to predict the site of integration of transgenic DNA and the resulting expression pattern and level. Due to the relatively late integration during development, founder animals are predominantly mosaic for the transgene [63, review].

1.1.1.2 Transposons

Since microinjection alone is a very inefficient method, attempts to improve this method have been made. One option is the use of viral vectors but due to the high infectious potential of viruses and therefore difficult work flow it is desirable to reduce their usage for genetic applications. In addition, viruses do not integrate at random but have strong preferences for actively transcribed genes [64, review: 65]. An alternative enhancement is the microinjection of transposons [66].

Transposons are ordinary repetitive and mobile genetic components of genomes amounting for about 45% of its size [67]. However, most of them are not intact and therefore not mobile. Based on their transposition mechanisms they are grouped into two classes. Class I elements, retrotransposons, use an RNA intermediate for their transposition by a copy-and-paste mechanism. Class II elements, DNA transposons, transpose by a cut-and-paste mechanism. Only 3% of the genome consists of these class II elements [67,68]. The different members of DNA transposons are grouped into super families that are Tc1/mariner, piggyBac, Merlin, Ginger, Mutator, Transib, Sola, Zator, Pogo, TP36, IS630, hAT, P and others [69, review].

DNA transposons activate themselves as the transposase enzyme is encoded by the transposon itself. It excises and re-integrates by a very precise cut-and-paste mechanism. The transposase gene is flanked by inverted terminal repeats (ITR) which are binding sites for the transposase. After transposase-mediated excision of the element, it becomes subsequently integrated into a new genomic site. All DNA-transposons identified in mammalian genomes so far are not functional due to non-functional transposase genes. The mechanisms involved during transposition are reviewed by Claeys Bouuaert and Chalmers (2010) [70].

Genetically reconstructed and/or modified transposons have been shown to enable transgenesis in different species such as worms [71–73], sea squirt [74], flies [75,76], fish [77], frogs [78,79], mice [80–83], rats [84,85] and human cells [86–88].

1.1.1.2.1 Sleeping Beauty

The name Sleeping Beauty (SB) refers to the awakening of a Tc1/mariner superfamily-based transposon after more than 10 million years of evolutionary sleep [89–91]. DNA transposons of this superfamily (e.g. SB, Minos, Passport) are found in all vertebrates but are inactive due to the accumulation of mutations [92]. Since SB was constructed for the purpose to deliver defined DNA sequences into vertebrate genomes it is a synthetic DNA transposon. For this, fossil transposase sequences found in salmonid fishs (*Salmo salar* and *Oncorhynchus mykiss*) were reconstructed. Today, SB is the most widely used transposon system in vertebrates [reviews: 93,94]. The SB transposase protein (SBase) consists of 360 amino acids (aa) and recognizes the flanking ITRs (Fig. 2). It binds to ITRs, catalyses first the excision and then the integration into random sites within the genome [95]. However, there is a requirement for a TA dinucleotide at the target site, typical for transposons of this superfamily [96]. In addition, surrounding the TA dinucleotide are palindromic consensus sequences [97–99]. There are approx. 200 million TA sites in the mammalian genome. This target site selection is primarily determined by the DNA structure [98]. In principle, the integration pattern of SB is random, apart from the TA dinucleotide dependence. Nevertheless, some hotspots and cold regions are widespread within the genome. This regional preference differs among distinct transposon systems. In the chromatin context, SB does not show preference for transcription units [100]. If SB integrates into transcription sites this occurs mostly into introns. Upon integration of SB the TA site becomes duplicated. When excised, this duplication results in a typical footprint consisting of characteristic nucleotides (TAG(T/A)CTA) [101–103].

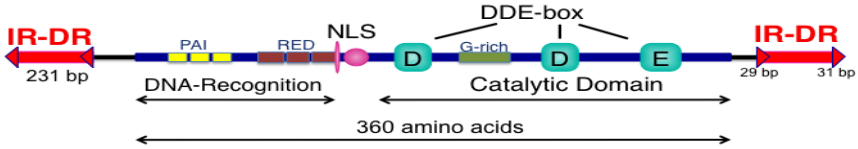

Figure 2: Principle structure of the Sleeping Beauty transposon.
The transposase, flanked by ITRs (red), consists of 360 aa and has two functionally domains: The catalytic domain is responsible for the excision and, upon DNA recognition by the DNA recognition domain, for the integration into a new locus. PAI and REC are two paired box sequences. The DDE box refers to positions of conserved aspartic acid (D) and glutamic acid (E) and is a functional characteristic in biochemistry. G-rich is a sequence rich in glycine (G). NLS is the nuclear localisation signal. The ITR consist of inverted repeats which contain short direct repeats (29/31 bp). Adapted from Hackett (2011) [104]

For its use in research, SB is designed as a two vector system to have a non-autonomous transposon (Fig. 3). Hence, SB is not able to excise and re-insert itself. The necessary transposase is supplied in *trans* by a 2nd vector directed by a promoter of choice. On the other vector, the transposon (consisting only of ITRs) including the gene of interest (GOI) is encoded. To enable the SBase to perform the transposition, the GOI is flanked by ITRs (231 bp) which contain two short direct repeats (29 bp and 31 bp) (Fig. 2). For maximal

transposition rate, this difference in length is essential [105]. Those repeat motifs were isolated from another salmon, *Tanichthys albonubes* [105,106].

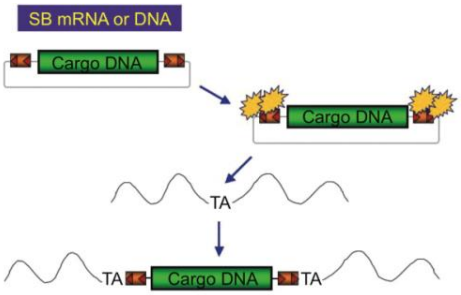

Figure 3: Transposition of the Sleeping Beauty system.
The GOI (cargo DNA) is flanked by the recognition sequences (ITRs). The transposase (SBase) is delivered as DNA or mRNA in *trans*. Upon expression of SBase it binds to ITRs (two molecules per ITR) and randomly to a TA dinucleotide in the genome. Then, SBase catalyses the excision of the cargo and its integration into the new locus. During the integration process, the TA dinucleotide becomes duplicated. Adapted from Geurts (2003) [107]

The first derived SBase containing all motifs required for its function, SB10, was improved over the last decade by various modifications of its DNA sequence which resulted in a more stable molecule, SB100 [66,108–112]. SB100 has about 100 times higher activity than SB10. An even more important fact for the aims of this thesis, SB100 allows the titration of its concentration to obtain single copy integrations. This was not possible with previous versions that failed in transposition below a certain threshold [66]. In 2009, SB100 became molecule of the year by the International Society for Molecular and Cell Biology and Biotechnology Protocols and Research (ISMCBBPR).

In research, SB is widely used for insertional mutagenesis [113–119] or gene transfer [106,120–124]. A possible limitation for the use of transposons is their dependency on cargo size [106]. In general, efficiency decreases with an increase in cargo size. Thus, the optimal cargo size is below 6 kb [108].

Contrary to SB is piggyBac (PB) which is also a DNA transposon. PB belongs to another superfamily and is also widely used in research. PB prefers transcription units and especially inserts into transcription start sites [125]. However, the Tc1/mariner family (except Passport, which has preference for transcription units [126]) possess the most random integration preference of all known transposon families [83,125,127].

1.1.2 Cell-mediated transgenesis

To have the opportunity to obtain genetically modified organisms with precise genetic modifications it is important to have a cell type allowing both transfection and selection processes as well as successful nuclear transfer (NT) or chimera formation. To obtain transgenic animals by cell-mediated transgenesis, the transgenic cells can be used in two different ways.

One possibility is the NT in which the nucleus of the transgenic cell is transferred into an enucleated oocyte that then becomes activated followed by the transfer of the developing embryo into a foster mother [128–130, reviews]. The other possibility can be performed only with pluripotent cells and is called chimera formation. Hereby, transgenic pluripotent cells were injected into the early embryo, mostly at blastocyst stage [131,132, reviews]. Again, the developing embryo is transferred into the foster mother. The advantage of NT is that offspring are 100% transgenic, if the donor cell was transgenic. On the other hand, chimera formation is easier to perform but offspring need to be outbred to obtain 100% transgenic animals. The first chimeric animals were reported by Brinster (1974) [133], Papaioannou *et al.* (1975) [134] and Mintz and Illmensee (1975) [135].

The targeted specific modification of the genome cannot be achieved with transposons. The precise modification is mainly achieved by homologous recombination (HR) [136, review]. Here, the homologous sequence of the exogenous DNA activates the natural DNA repair mechanism of the cell. The process of site directed mutagenesis of a desired genetic locus by HR is called gene targeting. The targeting by HR was successfully established by Mario R. Capecchi, Oliver Smithies and Martin J. Evans in mice applying embryonic stem cells (ESCs) [137–144]. However, the first targeting of a gene was reported in 1985 in two different cell types by targeting the *β-globin* gene with *neomycin resistance* (*neo*) [145]. The targeted cells can be selected *in vitro* and then used for NT or chimera formation to achieve transgenic animals. When the cells used for NT are not embryonic but somatic, the process is called somatic cell nuclear transfer (SCNT). The breakthrough in livestock using SCNT was reported in 1997 with Dolly the sheep [146–148]. Shortly after, the first transgenic livestock was produced by SCNT [11] followed by the production of a gene targeted sheep [149]. In total, successful SCNT was reported in 16 mammalian species including rabbits. However, the success rate measured on live births is very low (1 – 3%) [150–156]. Even when animals are born they often suffer and die due to various different abnormalities [147,149,157–159; reviews: 160,161]. Further, no gene targeting was shown in rabbits due to a lack of ESCs and difficulties in SCNT. Nevertheless, the success rate can be increased by applying pluripotent cells. Those cells require less reprogramming of early developmental genes [162].

1.1.2.1 Pluripotent cells

The term pluripotency refers to the cell's ability to grow indefinitely and to differentiate into any cell type of an adult organism. Always, pluripotent cells have the ability to self-renew, they divide continuously in the undifferentiated state. The definition of pluripotency was first formulated in 1954 by Stevens and Little [163].

There are different types of cells referred to as pluripotent. First of all there are embryonic stem cells (ESC) that were first established from mouse blastocysts in 1981 [164–166]. To proof the contribution of ESCs to the germ line, ESCs are injected into blastocyst staged embryos. Following, these cells will contribute to the development of the whole embryo. Since that organism originated from two genetically different cell populations it is called a chimera. The first chimera obtained from ESCs was reported 1984 [167] and the contribution to germ line was shown. Later, 1998, human ESCs could be derived [168]. Naturally, cells with an activated pluripotency network can be found *in vivo* in the morula, inner cell mass (ICM), epiblast (epiblast stem cells (EpiSCs)) and the germ lineage (primordial germ cells (embryonic germ cells) and male adult germline stem cells) [169–173]. From rabbits, putative embryonic germ cells were reported [174].

Also in an *in vivo*, but pathological condition, pluripotent cells are found in teratocarcinomas [163,175–178]. For several years, these embryonic carcinoma cells were the only pluripotent cells kept *in vitro*. Their differentiation capabilities were first described by Kleinsmith and Pierce (1964) [179].

ESCs are the most widely used pluripotent cells and seen as a prototype for pluripotency. ESCs are *in vitro* cultured cells isolated from the ICM of the blastocyst stage (Fig. 4).

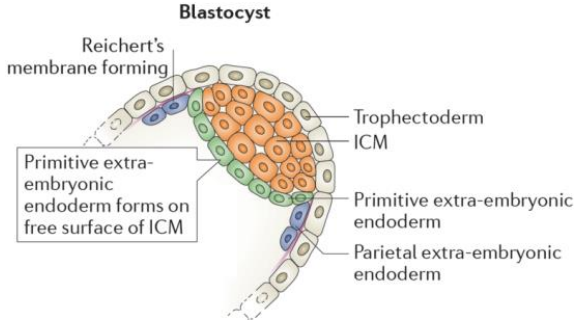

Figure 4: Early specification of cells in the blastocysts.
Embryonic cells possess positional information already in the morula stage that result in first differentiation events. Adapted from Evans (2011) [180]

As a possible alternative to ESCs, induced pluripotent stem cells (iPSC) were established in 2006 from the mouse in the laboratory of Shinya Yamanaka and Kazutoshi Takahashi using four transcription factors (TFs; Oct4, Sox2, c-Myc and Klf4) [181]. During following years, a lot of effort was spent in this new field. It was shown that iPSCs can be generated from different cell types and also from human cells beside other species [182,183]. Further, various factors were used and distinct experimental setups proofed to be successful for the induction pluripotency [184,185, review: 186]. Finally, it was possible to reprogram somatic cells only by the transduction of recombinant proteins, albeit with lower efficiency [187].

1.1.2.1.1. Molecular basis of pluripotency

Pluripotency is controlled by a number of cell signalling pathways. In humans, the predominant pathways are transforming growth factor β (TGFβ) and basic fibroblast growth factor (bFGF) that cooperate to maintain pluripotency [188,189]. TGF-β belongs to a superfamily with more than 40 members, including activin, Nodal and bone morphogenic proteins (BMPs) [190, review]. TGFβ signals via activin/Nodal through Smad2/3/4 whereas bFGF signals via the FGF receptor (FGFR) through mitogen-activated protein kinase (MAPK) and Akt pathways (Fig. 6) [192, review: 191]. The phosphoinositide 3-kinase (PI3K)/Akt pathway is also activated by the insulin-like growth factor 1 (IGF1) [193,194]. Further, pluripotency is promoted by the Wnt pathway through the activation of β-catenin (Fig. 6) [195–198, reviews: 199–201] and this effect is mainly due to the enhancement of proliferation [202]. All the signalling results in the expression of the three key TFs *Oct4*, *Sox2* and *Nanog* [203–205]. These factors regulate their own expression in an auto regulatory network and in feed-forward loops thereby activating the expression of ESC-specific genes (Fig. 5) [206–209, review: 210]. Other scientists count Tcf3 to the core circuit, because it is co-localised with Oct4 and Nanog to more than 1000 promoters, including *Oct4*, *Sox2* and *Nanog* [198]. All those factors are markers for pluripotency. Of those, prominent TFs in ESCs are Oct4, Sox2, Nanog, Stat3, Sall4, Smad1, Dax1, Esrrb, Hesx1, Klf4/5, Tcfcp211, Zfp143 and Zic3 whereas factors important for ESC signalling are Tcf3, Cdx2, Fgf2, Lefty2, Zic3 and Skil [211–214, review: 215]. If the balance in the core factors gets disturbed, pluripotency is lost and cells differentiate into cell types of the three germ layers: endoderm, mesoderm and ectoderm. In humans, the primary pathway for differentiation is BMP, which uses Smad1/5/8 that inhibits the expression of *Nanog* but activates the expression of differentiation-specific genes. Notch is also involved in differentiation, which signals through the notch intracellular domains.

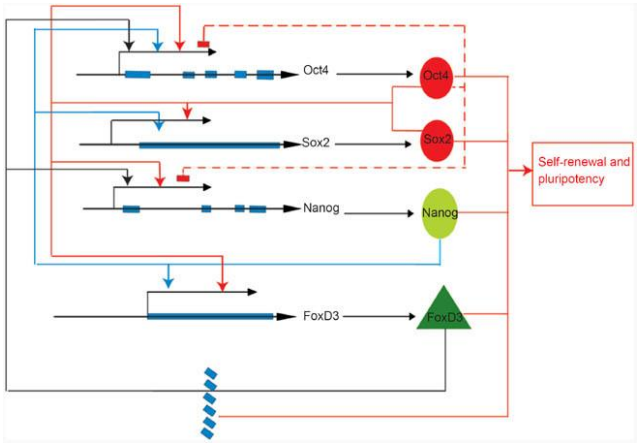

Figure 5: Regulatory network of key transcription factors.
Oct4 and Sox2 are acting together to activate the expression of themselves, *Nanog* and *FoxD3* acting in an auto regulatory network and feed forward loops. The balance of those factors needs to be tightly regulated to maintain a stable pluripotent state. Adapted from Pan and Thomson (2007) [216]

Markers for pluripotency can be also found on the cell surface. In hESCs cell surface markers of pluripotency are the glycolipid stage specific embryonic antigens 3/4 (SSEA3/4) and the glycoproteins TRA-1-60/81 [217,218; reviews: 219–223].

In mESCs, the solely surface marker for pluripotency is SSEA1. The most prominent extrinsic factor to maintain murine pluripotency is the leukaemia inhibitory factor (LIF) [224–231]. LIF belongs to the IL-6 cytokine family. LIF maintains pluripotency by activating three major pathways: Janus kinase/signal transducer and activator of transcription 3 (Jak/STAT3), PI3K/Akt and Src homology 2 domain-containing tyrosine phosphatase 2 (SHP2)/MAPK while the most important is the activation of STAT3 (Fig. 6) [232–235, reviews: 236–239]. Hence, activation of the Akt pathway is important in both mESCs and hESCs [240]. In mESCs more than 2500 binding sites for STAT3 were found. Of those, one third are co-occupied by Oct4, Nanog and Sox2 [241,242]. Further, STAT3 prevents the differentiation into endoderm and mesoderm in collaboration with BMP4 [243,244]. Hereby, BMP4 activates inhibitors of differentiation genes (Id) (Fig. 6) [245,246]. In hESCs, BMP4 leads to mesodermal differentiation in absence of STAT3 activation [247,248].

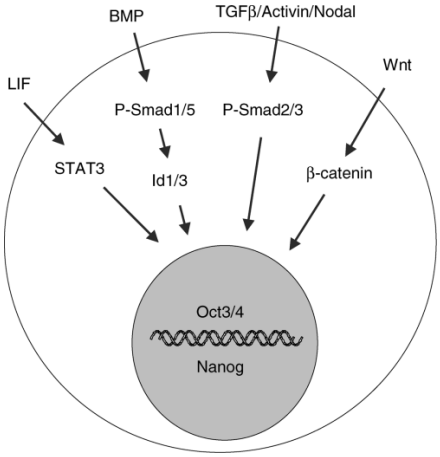

Figure 6: Extrinsic factors maintaining pluripotency in ESCs.
This overview summarises pathways including their most prominent signalling molecules that result in the expression of both pluripotency core factors *Oct4* and *Nanog*. LIF and BMP4 are responsible for pluripotency of mESCs (left side) but TGFβ/activin/Nodal and Wnt for pluripotency of hESCs (right side). Adapted from Valdimarsdottir and Mummery (2005) [191]

Crucial functional criteria to prove pluripotency are: a) differentiation of pluripotent cells into cells representing all three germ layers, b) active pluripotency TFs c) teratoma formation and d) formation of chimera with contribution of the pluripotent cells to the germline. The most stringent assay is tetraploid complementation. Upon injection into a 4n blastocyst, pluripotent cells are able to give rise to an entire embryo [249, review: 250].

Pluripotent stem cells were successfully verified only for mouse, rat and human [251,252]. For several livestock species ES-like cells and primordial germ cell cultures were reported but without any definite proof [253]. Nevertheless some pluripotent cell isolates were capable to

produce chimeric animals but without contribution to the germ line as reported for pig (EG-like cells) [254] and cattle (ES-like cells) [255]. The isolation, culture and characterisation of rabbit ESCs (rbESCs) were reported by six different groups albeit with contradicting findings regarding the expression of pluripotency markers and its molecular signalling (4.2.1.4).
To date, nothing is known about naturally occurring pluripotent cells in the mammalian soma. However, somatic cells can be induced to become pluripotent by experimentally techniques: NT, direct reprogramming and cell fusion. The induction process needs to reactivate the transcriptional regulatory network characteristic for pluripotency (Fig. 5).

1.1.2.2 Multipotent cells

To have an alternative for pluripotent cells to obtain transgenic rabbits, multipotent cells were used in this work. The existence of stem cells in mammals was proposed already in 1906 by Maximow [256]. Indeed, Maximow (1910) [257] proved later the originating of blood cells from a common precursor. These precursor cells are located in the bone marrow and the clonal nature of bone marrow cells was proven by Becker *et al.* (1963) [258] and Siminovitch *et al.* (1963) [259].
Multipotent mesenchymal stem cells (MSC) are a diverse subset of precursors present in the stromal fraction in many tissues of the adult (Fig. 7) [260,261,263; review: 262]. Originally, MSCs were found in the stromal adherent fraction of the bone-marrow [264–266]. MSCs in adipose tissue (A-MSC) were found much later [267,268] but are easier to isolate [269, review].
MSCs show a fibroblast-like phenotype [270], arise from the lateral mesoderm and are self-renewing. Due to a lack of unique markers, human MSCs are characterized by the expression of specific surface markers (e.g. *CD44, CD90, CD166, CD271, SSEA4* and *D7-FIB*) but are negative for others (e.g. *CD11b, CD19, CD45* and *HLADR*) [271–278]. However, this expression profile varies with isolation procedure and passage.
Multipotency of MSCs refers to the ability to differentiate functionally into cells forming the cartilage (chondrocytes) [279–281], fibroblasts (building tendons and ligaments, skin) [282,283], stromal cells [284], osteocytes [281,285,286], astrocytes [287], adipocytes [281] and myocytes [288,289], which form cardiac muscle, smooth muscles and skeletal muscles [290, review]. Further studies revealed also the differentiation into endothelial cells [291], hepatocytes [292–294] and endocrine cells [295,296]. Also, MSCs possess immunoregulatory properties [297 and 298, reviews]. The general functions of MSCs are organ homeostasis and wound healing [299].

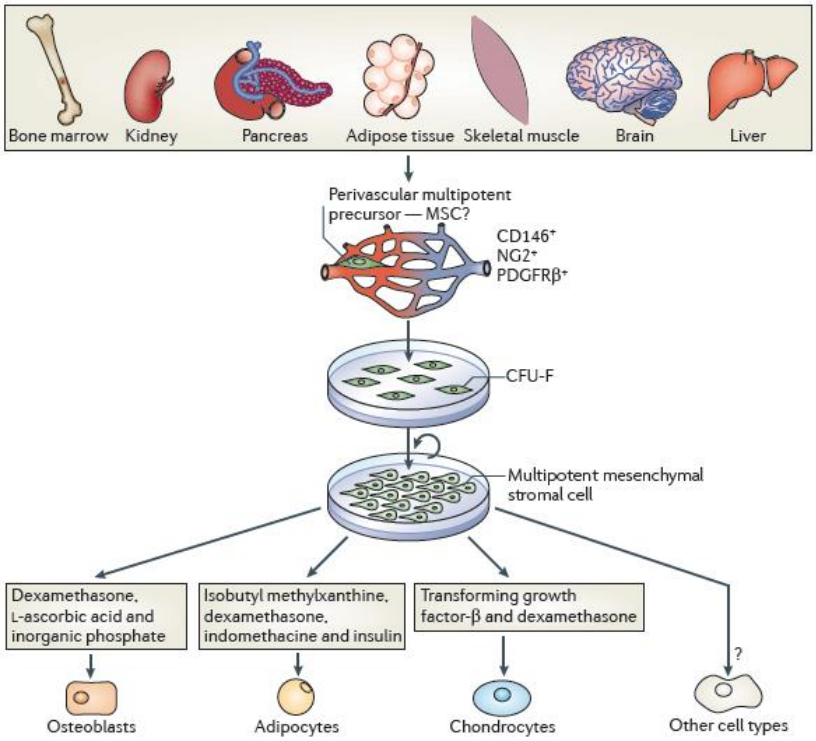

Figure 7: Occurrence of mesenchymal stem cells.
MSCs can be derived from various tissues in an adult body. When taken in culture they are able to self-renew but also to differentiate. Upon administration of specific factors, differentiation can be guided into osteoblasts, adipocytes and chondrocytes. These three differentiations are a hallmark of MSCs. Adapted from Nombela-Arrieta *et al*. (2011) [262]

Bone marrow MSCs (BM-MSC) are located in perivascular niches in the bone-marrow parenchyma and are associated with hematopoietic stem cells (HSCs) and regulate the homeostatic turnover of non-haematopoietic stromal cells and the maintenance of (HSC) [302–304, reviews: 300,301]. BM-MSCs differentiate to replace mature osteoblasts and adipocytes [264,285; review: 305]. Some studies showed that BM-MSCs can differentiate into cells usually arising from a different germ layer like neurons (ectoderm) [306–308] and cardiomyocytes (mesoderm) [289,309,310; reviews: 311,312].

A-MSCs are located perivascular together with pericytes and endothelial cells [313–316]. Like BM-MSCs, A-MSC can differentiate into cells other than the mesodermal lineage: endothelial- and epithelial cells, neural cells, hepatocytes and pancreatic islet cells [317, review].

MSCs are present at an extremely low frequency in tissues, e.g. 0.001% in the bone marrow [318,319]. Other cells resident in bone marrow are red blood cells, white blood cells, platelets, adipocytes, hematopoietic precursors and endothelial progenitors. A-MSCs are more frequent in their niche (up to 3%) [320–322].

1.2 Diseases to model

Via genetic engineering the molecular basis of a disease can be recapitulated in an animal model. However, due to the lack of functional ES cells few genetically defined rabbit disease models have so far been reported. To develop the necessary technology for rabbits two types of models were chosen: expression of a dominant negative mutation to produce a rabbit model for diabetes mellitus (DM) and gene inactivation of the *hprt* gene to develop a Lesch-Nyhan syndrome model.

This chapter describes both diseases including their causes, molecular characteristics, available models and their limitations.

1.2.1 Diabetes mellitus

Worldwide, there are already 1.46 billion overweighed and 495 million obese adults [323]. It is predicted that the number of diabetics is increasing by the year 2050 by more than 50% to 552 million people. In the United States, one in four adults has DM (announcement at the 71st American Diabetes Association (ADA) meeting in San Diego, CA, USA (June 24 - 28, 2011)). Further, the number of adults with DM has doubled within the past three decades [324]. Also, childhood obesity is increasing. In the USA, 10% of infants are overweight and more than 20% in the age group of 2 – 5 [325]. According to the newest figures, 16.9% of the age group 2 – 19 years are obese [326]. In adults, 68.8% are overweighed and 35.7% are obese [327]. From this development, this disease and its complications cause enormous economic costs.

General symptoms of DM are hyperglycaemia, polyuria and polydipsia. Accompanying symptoms are an impairment of growth and higher susceptibility to infections. Later consequences of DM are coronary artery disease, stroke, sexual dysfunction, kidney failures, loss of vision and amputations amongst others [328 and 329, reviews]. Indeed, 80% of all deaths in diabetic patients are due to atherosclerosis [330, review]. In general, DM compromises the life quality and shortens the life span.

DM refers to a heterogeneous group of distinct metabolic diseases. The hallmark of these diseases is the common hyperglycaemia caused by defects in the secretion and/or action of insulin [331 and 332, reviews]. The dysfunction of insulin producing β-cells in the pancreas leading to an inadequate supply belongs to the secretory defects. Based on the cause, DM is divided in type I and II. A reduced action of insulin is a result of a decreased response of liver, muscle and adipose tissue to insulin which is called peripheral insulin resistance and leads to overt hyperglycaemia and ultimately to DM II [329,336–338; reviews: 333–335]. Therefore, type II is also

called non-insulin dependent DM, since administration of insulin (e.g. injections) has with time decreasing effects.

A cause for DM, or at least predisposition, are mutations and polymorphisms in genes coding for TFs and enzymes involved in *insulin* action pathways [339–341]. Additional, the life style, especially the diet, has an important impact in the development of this disease. Thus, a prominent risk factor for DM II is obesity.

1.2.1.1. Molecular basis of diabetes mellitus

The islets are the endocrine part of the pancreas and account for 1 – 2% of its mass. Islet cells are responsible for secreting the key hormones for the regulation of carbohydrate metabolism. According to their function, islet cells can be divided into distinct cell types: α- (glucagon), β- (insulin), γ- (pancreatic polypeptide), δ- (somatostatin) and ε-cells (ghrelin) [342, review]. It is worth to note that very small proportions of insulin are secreted by the thymus [343,344], brain [345], lachrymal glands [346] and salivary glands [347,348]. The main function of β-cells is the sensing of elevations of blood glucose levels through expressed glucose transporters across the cell membrane which then triggers the calcium dependent insulin secretion. After expression of *insulin*, the signalling sequence becomes cleaved from the primary amino acid (aa) sequence (preproinsulin) and proinsulin is packed into vesicles that migrate to the Golgi apparatus. Here, the C-peptide becomes cleaved and insulin gets its biological active form. Insulin is transported in granules to the cell membrane [349,350; reviews: 351–355]. The secretion of insulin is influenced mainly by the glucose concentration but also by other metabolites and hormones.

The cause of type I DM are malfunctions of the immune system [356]. This results in a cell-mediated auto-immune attack of the pancreas and final in its destruction [357, review]. This chronic inflammatory process is called insulitis. Reasons for the emergence of type I are interactions between genetic susceptibility and environment, but also mutations of *insulin* [358].

Type II as a polygenic syndrome having various aetiologies and is characterized by a combination of an insensitivity of various tissues to insulin as well as β-cell dysfunction resulting in a lack in the secretion of insulin pathways [334,359–361]. This type of DM is a result of long-term high blood glucose levels, which leads to oxidative stress and glucose toxicity in β-cells. In addition, chronic hyperglycaemia leads ultimately to malfunction of β-cells and their apoptosis [362–364, reviews]. Due to the high blood glucose level, either from diet, insensitivity of glucose metabolising organs to insulin (insulin resistance) or both, the β-cells receive insulin releasing signals. Since the action of insulin cannot circumvent the high blood glucose, β-cells produces more and more insulin which leads to a mismatch in the folding capacity of the ER and demand. Thus, the permanent overload of β-cell ER results in chronic ER stress and its

consequences (Fig. 8). Several pathways (activation of protein kinase C, autooxidation of glucose, formation of methylglyoxal, formation of sorbitol, metabolism of hexosamine and oxidative phosphorylation) lead to the formation of reactive oxygen species (ROS) (Fig. 8).

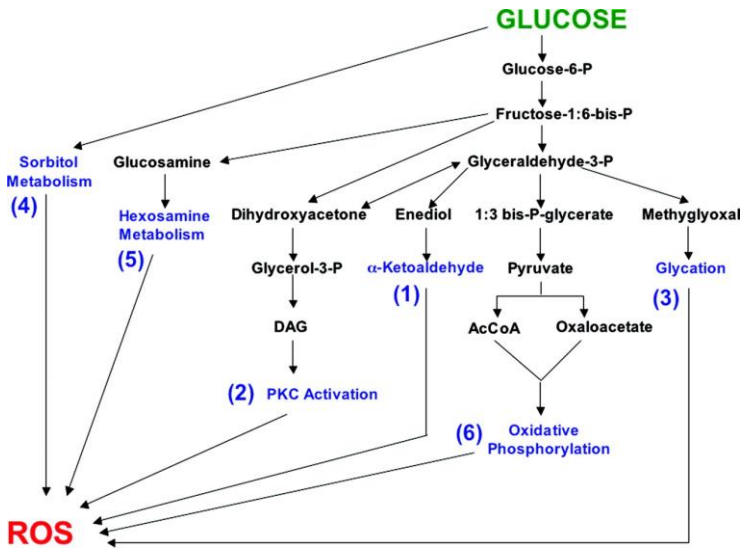

Figure 8: Metabolites of glucose pathways that result in an increase in reactive oxygen species.
If the glucose concentration cannot be regulated at physiologic level inflammatory processes are activated. Adapted from Robertson (2004) [365]

When ROS occur in excess and over long time this causes chronic oxidative stress that finally leads to increased apoptosis of β-cells [365–367, reviews]. The islets belong to those tissues that possess the lowest levels of intrinsic defences against oxidative stress [368]. Also, glucotoxicity impairs insulin expression due to missing expression of important TFs (e.g. PDX1, MafA) that normally bind to the *insulin* promoter. In addition, a high-fat diet, typically for western countries, leads to obesity and is a predisposing factor [369]. An excess of fat can have lipotoxic effects on β-cells and induce their apoptosis because too high fat leads to elevated levels of cholesterol, free fatty acids (FFA) and triglycerides in the blood (Figs. 9 and 10) [370, reviews: 361,371–373]. Also, a low degree of a chronic pro-inflammatory state is present in obesity which higher the level of ROS and lipoperoxides (Fig. 10) [374–376]. Direct induction of β-cell apoptosis was reported for permanent elevated levels of glucose [377,378] and FFAs [371, review].

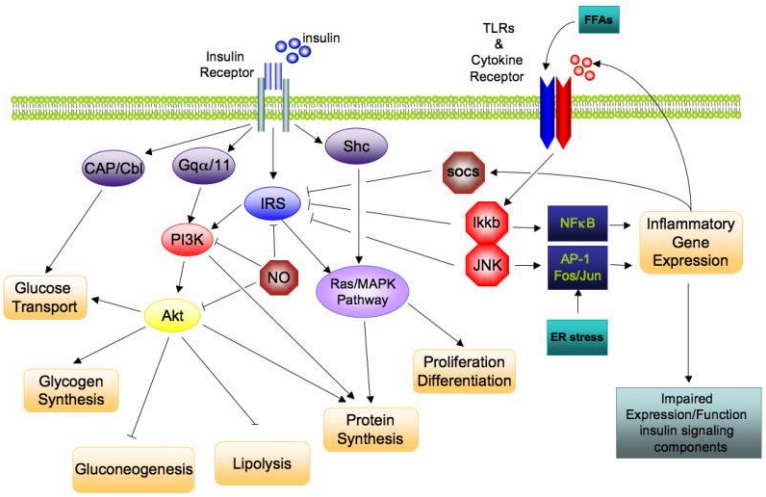

Figure 9: Insulin action and its inhibition.
On the left side the molecular regulation of insulin action upon its binding on its receptor leading to a decrease in glucose level is shown. On the right side the negative effects of free fatty acids (FFA) are indicated which circumvent the positive actions of insulin by inhibition of a central signalling molecule. These actions are amplified by ER stress and inflammation. Adapted from de Luca and Olefsky (2008) [367]

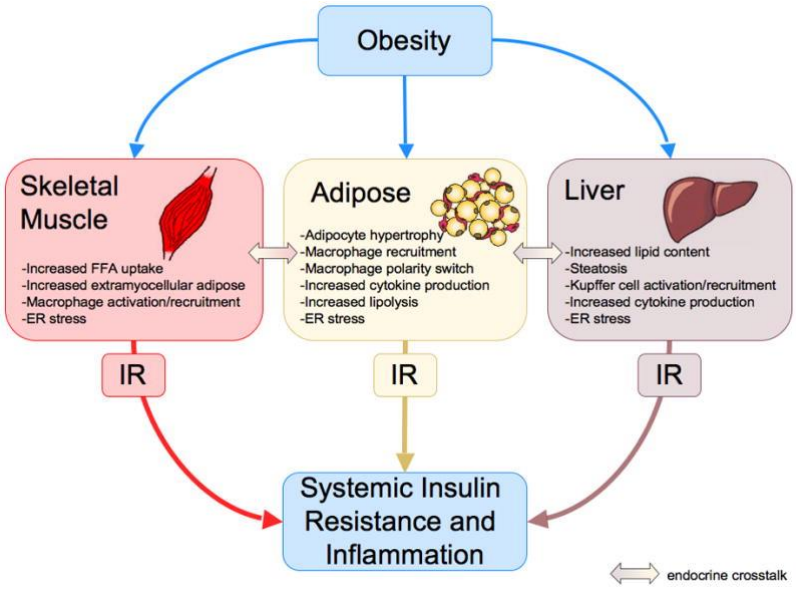

Figure 10: Summary of the negative consequences of obesity.
Obesity has negative influences on various organs, which finally results in resistance to insulin (IR). Later, IR becomes a systemic state. Adapted from de Luca and Olefsky (2008) [367]

Despite improved treatments, exogenous supply with insulin does not prevent long term complications. In general, diabetic patients possess a shorter life span [379,380]. The optimal treatment would be the transplantation of islets to restore its complex functions. The breakthrough in this field was achieved with the Edmonton Protocol [381]. Nevertheless, allogeneic transplantation is still a big risk. One major hurdle is graft rejection reactions [382–384] and on the other side functional considerations. So, the insulin secretion of transplanted islets is only 20 – 40% of that of healthy subjects. Even worse, the secretion capacity declines over time to a level of only ~10% 5 years after transplantation [385]. One explanation is the

recurrence of autoimmunity [386,387]. In addition, there is a need of 2 – 3 donors to obtain the minimal cell mass necessary for a single transplantation [388].

1.2.1.2. Diabetic model organisms

Since DM is a very complex disease and the *insulin* gene is conserved in various species, different species have been used as model organisms, e.g. mouse, rat, pig and minipig. The most common method is the destruction of β-cells by toxic chemicals like streptozotocin and alloxan. But also genetic mouse and rat models exist. Most of these models develop DM as a consequence of obesity. But also mice and rats that develop DM as consequence of mutations in the major histocompatibility complex exist. However, none of these models exactly recapitulates the human phenotype and all have some limitations [389, review].

An elegant method to model the phenotype of DM is the destruction of β-cells by a biological mechanism. For this, the Akita mutation of the mouse is ideal [390]. The autosomal dominant Akita mutation is a single base pair exchange from guanine to adenine which results in a change in the coding triplet (TGC → TAC) and finally in the aa from cysteine to tyrosine in the α-chain of insulin. Due to the missing cysteine the important bisulfide bond between the α- and β-chain cannot form (Fig. 11). In this mouse model the phenotype results from the destruction of β-cells due to the accumulation of misfolded insulin [391]. Also, these mice do not suffer from obesity or inflammatory reactions. They are born normal with normal islet size but are characterized by hypoinsulinemia and hyperglycemia. The onset of DM is at an age of 3 – 4 weeks. The general phenotype is similar to the human maturity onset diabetes in youth (MODY).

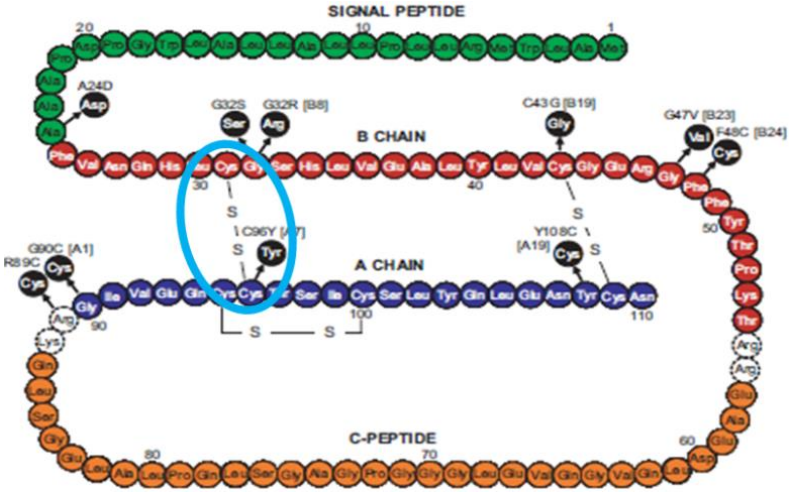

Figure 11: Amino acid sequence of preproinulin.
A chain is shown in blue, B chain in red, C peptide in orange and the signal peptide in green. The dashed positions indicate the cleavage sites for the conversion of proinsulin into insulin. Different mutations resulting in DM are shown. The disulphide bond affected by the Akita mutation is highlighted in blue. Adapted and modified from Støy *et al*. (2007) [392]

1.2.1.2.1. Mechanism of the destruction of β-cells

The misfolded insulin negatively affects the trafficking of non-mutated proinsulin (from the 2nd allele) [393]. Subsequently, these proteins are accumulated as complexes with binding immunoglobulin protein (BiP), a chaperone, in the endoplasmatic reticulum (ER) and finally results in apoptosis of these cells [390,391,394–397]. The ER is the side in the cell where disulphide formation and folding of secreted proteins takes place. As consequences to misfoldings, proteins involved in proper protein folding are overexpressed, particularly ER stress markers BiP and protein disulphide isomerase (PDI) (Fig. 12). PDI corrects errors in the disulphide bonding. These actions are a part of a cellular mechanism called quality control and in particular involve the unfolded protein response (UPR). It ensures that only correctly folded proteins are transported to the Golgi apparatus [398–401, reviews]. The UPR involves several steps. First, the cell increases the expression of ER process client proteins like chaperons and oxidases to increase the folding activities. In the case of this specific mutation of *insulin*, these processes fail. Hence, the cell tries to attenuate the protein biosynthesis to relieve the overload as a second mechanism (Fig. 12). Due to extrinsic stimuli, the β-cell receives *insulin* expression promoting signals. Thus, ER stress increases. A third step is the clearance by ER-associated degradation (ERAD) (Fig. 12). If the ER stress cannot be reduced, finally apoptosis becomes induced (Fig. 12) [402–410, reviews]. Commonly mentioned is that β-cells are one of the most vulnerable cells to ER stress. There are various diseases that result from protein misfolding, for instance α1-antitrypsin deficiency, cystic fibrosis, Alzheimer´s disease and haemophilia A and B.

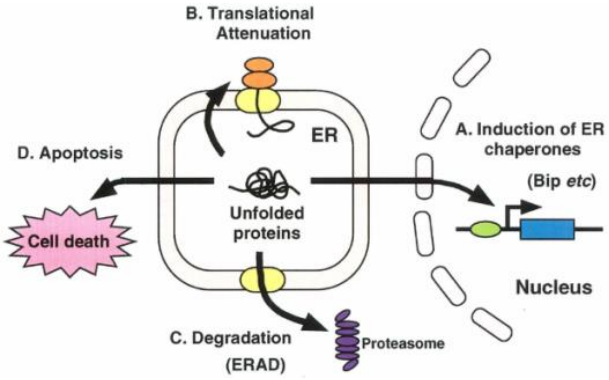

Figure 12: Cellular responses (UPR) to misfolded proteins.
In the first steps, the cell tries to resolve ER stress due to misfolded protein by increasing the folding capacity, attenuation of translation and degradation of unfolded proteins (ERAD). If those steps are not successful, the cell undergoes apoptosis. Adapted from Araki *et al*. (2003) [404]

Beside rodents and rabbits other animals were used as diabetic models such as cats, dogs, non-human primates and pigs [411, review]. In studies with rabbit models islet cells loss was induced by chemicals like alloxan (islet cell toxin). Mostly, the diabetic phenotype is stable only for several weeks. Recently, an alloxan model was developed suitable for experiments

lasting more than 1 year [412]. However, many complications of DM develop after a couple of years and can therefore not yet be modelled and examined in those rabbits. No transgenic rabbit model is yet available.

1.2.2 Lesch-Nyhan syndrome

The Lesch-Nyhan syndrome (LNS, prevalence between 1/235000 and 1/380000 live births) shows a clear familial distribution and almost limitation to males [413]. This disease was first described 1959 by Catel and Schmidt [414] and shortly after by Riley (1960) [415]. The disease was later elucidated by Lesch and Nyhan (1964) [416]. Three years later, Seegmiller identified the metabolic cause of LNS and the relationship between phenotype and mutations in the gene *hypoxanthine-guanine phosphoribosyl-transferase* (*hprt*) [417].

1.2.2.1 Molecular basis of Lesch-Nyhan syndrome

LNS is a metabolic disorder resulting from more than 300 distinct recessive mutations, including single base substitutions, deletions, insertions and duplications of the ubiquitously expressed X-chromosomal gene *hprt* [418–426]. This leads to a missing activity of the encoded enzyme (HPRT, EC 2.4.2.8) involved in the purine salvage pathway [427]. This enzyme catalyses the regeneration of both inosine mono phosphate (IMP) and guanosin mono phosphate (GMP) from hypoxanthine and guanine, respectively [428,429]. Hence, this enzyme is involved in the production of purines. The involvement of HPRT in purine metabolism was known from leukaemia studies [430,431]. The mild form of this disease with HPRT activities from 1 – 50% [432–434] is known as Kelley-Seegmiller syndrome or juvenile gout [435] with no or partly neurological abnormalities. The first functional analysis of *hprt* was performed by Melton *et al*. [436,437].

Any dysfunction of HPRT leads to an enormous overproduction of purine nucleotides by *de novo* synthesis [438,439]. Since purines become not reutilized, they are degraded which leads to an accumulation of uric acid in all body fluids and is present already at birth [440–444]. This causes hyperuricemia and hyperuricosuria which is associated with severe gout and kidney problems due to deposition of crystals of uric acids in the joints and in the kidney. In addition, the disease leads to neurological signs like poor muscle control, retardation of motor development, involuntary movements and mental retardation (spasticity) that appear in the first year of life. Developmental delay and hypotonia are evident by three to six months. In the 2nd life year, LNS is characterised by self-mutilating behaviour especially by biting of lips, tongue and fingers and head banging although the patients feel pain [445–456]. In addition, compulsive behaviour is seen including aggressiveness, vomiting and spitting albeit patients

often do not intend harm. Difficulty to understand the speech or lack of speech is very common. Mental retardation is reported with IQ scores varying from 25 – 101, with a mean score of approx. 60 [449,451,457–459].

Hprt is ubiquitously expressed, its highest activity was found in the basal ganglia in which also the highest dopamine concentration was found. The impairments of the nervous system are due to an imbalance of neurotransmitters [460–465] particularly from dysfunction of the striatum [466 and 467, reviews]. However, the structure of the brain appears normal [468]. Neurological deficits of LNS are due to lesions in striatal dopaminergic pathways [469–471]. Recently, the involvement of HPRT in the early development of dopamine neurons was found [472]. The lack of neurotransmitters in LNS results from the shortages of IMP and GTP and its di- and trinucleotides since signal transduction trough dopamine receptor requires GTP [473–475, reviews]. In addition, due to a higher rate of *de novo* purine synthesis to achieve required ATP levels, more oxidant stress is caused which leads to damages of dopaminergic systems [466,471,477; review: 476]. Due to low xanthine oxidase levels in the brain, the end product of purine metabolism is not uric acid but xanthine and hypoxanthine [478,479]. Indeed, these metabolites bind to benzodiazepine receptors and contribute to the pathogenesis [480–482]. In addition, hypoxanthine has direct cellular effects [483]. A lack of HPRT leads also to a poor utilization of vitamin B_{12}. Later, it comes to delayed growth and puberty. Often, testicular atrophy is a cause of LNS.

A very rare case is LNS in females which could occur by passing a mutated *hprt* gene from the mother and a new mutation of the father's *hprt* gene [470,484,486; review: 485]. Female carriers are usually unaffected but have an increase in uric acid excretion and an increased risk for gouty arthritis in later years.

The only available treatment for LNS is the application of allopurinol that allows survival until the 2nd or 3rd decade. Allopurinol preserves the renal function but nothing else.

Purines have an essential role in the cellular metabolism and are necessary components of nucleic acids precisely of the purine bases adenine and guanine. Due to the tremendous energy necessary in their *de novo* synthesis from aa and other precursors, 90% of purines are recycled in a salvage pathway. HPRT is a central enzyme in this process since it repatriates guanine and hypoxanthine (from adenine) into the DNA synthesis (Fig. 13). Dysfunction of HPRT leads to an increase in uric acid because purines cannot be reused and becomes degraded. On the other hand, the *de novo* synthesis becomes stimulated due to an excess of 5-phospho-D-ribosyl-1-pyrophosphate (PRPP). In turn, this activates amidophosphoryl-transferase (AMPRT) and causes hyperuricaemia and its consequences.

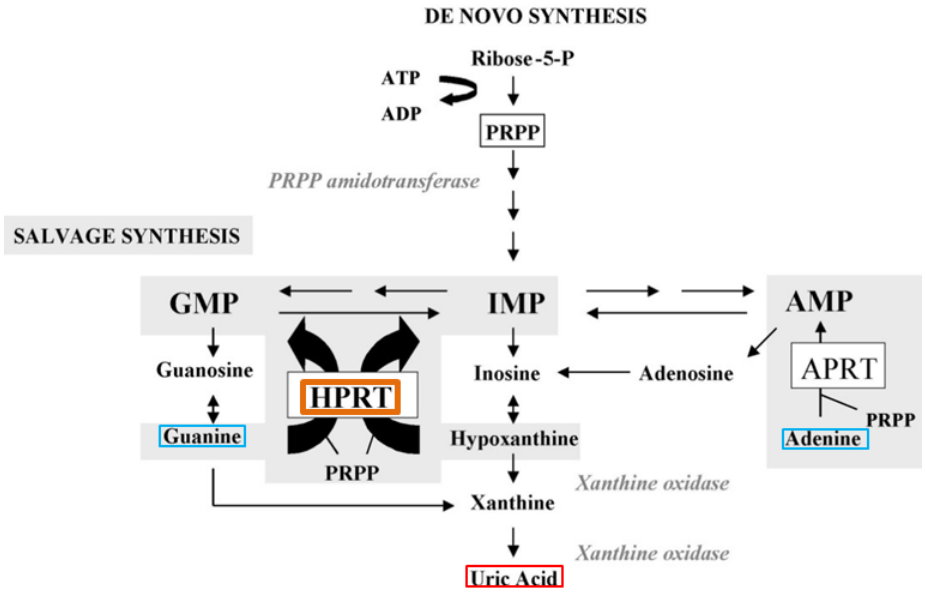

Figure 13: The central role of HPRT (orange box) in the recycling of adenine and guanine (blue boxes). When HPRT is not functional the salvage pathway will succumb. Hence, adenine and guanine will be completely degraded leading to an excess of uric acid (red box) and increased *de novo* synthesis. Adapted and modified from Torres and Puig (2007) [487]

1.2.2.2 Model organisms for Lesch-Nyhan syndrome

Already in 1972, a rat model for brain research was established: The neonate-lesioned rat [488]. Later it was found that this rat model resembles some of the characteristics of LNS including destruction of dopaminergic neurons and it's relation to self-injury [489–493, reviews: 494–496]. In 1983 the human *Hprt* gene was cloned and characterised [497]. Essential elements of the gene, as coding sequence, terminal untranslated regions and splicing sites, are highly conserved. The first animal model of LNS was derived of mESCs mutagenized by retroviral insertions which were then selected for loss of HPRT activity [498,499]. Due to the hemizygosity in males and the selectivity, *hprt* was one of the first genes chosen for gene targeting models [500]. Here, the correction of a mutated *hprt* gene was shown by HR [142]. Those mouse models provided only little information about the pathogenesis [501,502]. Furthermore, none of these mice showed the characteristic behavioural abnormalities [471,503–505]. Also, double knockout mice (*hprt* and *aprt*) are not suitable as model [506]. So far, all attempts to develop an appropriate animal model for LNS failed. However, important findings regarding neuropathogenesis and molecular relationships were achieved in these models [466, review].

1.2.2.3 Rabbit hprt gene

The structure of rb*hprt* is highly conserved and is similar to human *Hprt*. The human *Hprt* gene consists of 44 kb and 9 exons whereas the rb*hprt* consists of 47907 bp, of which only 802 bp are distributed within the 9 exons [507] (Fig. 14). Consequently, the rabbit HPRT protein consists of 218 aa. Shi *et al.* [507] also verified the ubiquitous expression of *hprt* in rabbits.

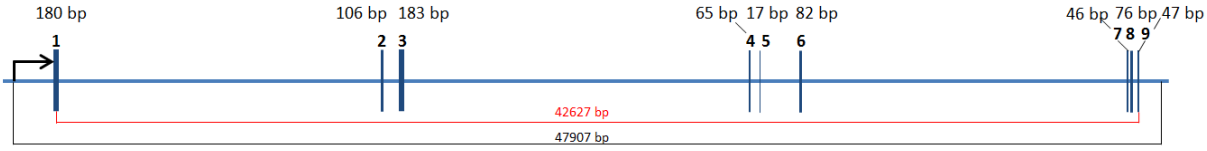

Figure 14: Structure of the rb*hprt* gene.
The size (47907 bp) and structure of rb*hprt* is visualised and exons (1 – 9, blue) are indicated to scale. The exact size of each exon is given above. The arrow visualises the promoter.

1.3 Aims of the thesis

The main aim of this thesis was to establish techniques to generate transgenic rabbits for biomedical research. For this, two different strategies, a direct method based on transposon vectors and different cell-mediated methods for transgenesis were to be evaluated. None of these techniques had so far been successfully established for the rabbit.

To assess if transposon vectors are suitable for efficient production of transgenic rabbits the sleeping beauty transposon systems was to be assessed using a reporter gene. If results looked promising then the newly developed method should be employed to produce a rabbit model for diabetes mellitus by introducing a transgene with a dominant negative mutation in the rabbit insulin gene. The mutation should be based on findings from the previously published Akita mouse model.

For the cell-mediated transgenesis the derivation, characterisation and genetic manipulation of rbESCs followed by production of chimeric rabbits was envisaged. Should this prove not successful a second strategy was to be employed, testing if the isolated ESCs or alternatively multipotent somatic stem cells such as mesenchymal cells were suitable for the derivation of nuclear transfer animals. Finally, cell-mediated transgenesis could be used to carry out the first gene targeting in rabbits. To show precise genetic engineering, the *hprt* gene was chosen for gene targeting. HPRT plays a crucial role in the purine salvage pathway. Its disruption leads to LNS.

2 MATERIAL AND METHODS

2.1 Material

2.1.1 Equipment

+4°C fridge	Beko Technologies GmbH, Dresden, Germany
-20°C freezer	Liebherr-International Deutschland GmbH, Biberach an der Riss, Germany
-80°C ultra-low temperature freezer	Thermo Electron GmbH, Karlsruhe, Germany
AxioCAM MRC camera	Zeiss AG, Oberkochen, Germany
Axiovert 25 microscope	Zeiss AG, Oberkochen, Germany
Bio Imaging System Gene Genius	Synoptics Ltd, Cambridge, United Kingdom
BioPhotometer	Eppendorf AG, Hamburg, Germany
Centrifuge 1-15	Sigma-Aldrich Chemie GmbH, Steinheim, Germany
Centrifuge 3-16	Sigma-Aldrich Chemie GmbH, Steinheim, Germany
Centrifuge 4K15C	Sigma-Aldrich Chemie GmbH, Steinheim, Germany
Centrifuge 5810	Eppendorf AG, Hamburg, Germany
Centrifuge Minispin	Eppendorf AG, Hamburg, Germany
Digital graphic printer UP-D895MD	Synoptics Ltd, Cambridge, United Kingdom
Electrophoresis chamber PerfectBlue mini	Peqlab Biotechnologie GmbH, Erlangen, Germany
Electrophoresis chamber HE 33 Mini	GE Medical Systems Deutschland GmbH & Co. KG, München, Germany
Electrophoresis chamber CSSU1214	Thermo Electron GmbH, Karlsruhe, Germany
Electrophoresis chamber CSSU78	Thermo Electron GmbH, Karlsruhe, Germany
Electrophoresis power supply EPS 301	GE Medical Systems Deutschland GmbH & Co. KG, München, Germany
Electroporator Multiporator	Eppendorf AG, Hamburg, Germany
Electroporator Nucleofector Device	Lonza Cologne GmbH, Köln, Germany
Handy Step Multipipette	Brand GmbH & Co. KG, Wertheim, Germany
Heating block VLM2Q	VLM GmbH, Bielefeld, Germany
Ice maker	Brice Italia S.r.l., Villa Cortese (MI), Italy
Ika MS2 Minishaker RCO	IKA-Werke GmbH & Co. KG, Staufen, Germany
Ika-Combimag RCO	IKA-Werke GmbH & Co. KG, Staufen, Germany
Improved Neubauer chamber	Brand GmbH & Co. KG, Wertheim, Germany
Incubator	Binder GmbH, Tuttlingen, Germany
Laminar Flow Hood HERAsafe Type HSP	Heraeus Instruments GmbH, Osterode, Germany
Liquid nitrogen storage system	Messer Group GmbH, Griesheim, Germany
Microwave NN-E202W	Panasonic K.K., Kadoma, Japan
Mr. Frosty freezing device	Nalgene Nunc International Corporation, Rochester, USA
Orbital shaker	Thermo Electron GmbH, Karlsruhe, Germany
PCR cycler DNA Engine DYAD	MJ Research Inc., Waltham, USA
pH meter Cyberscan 510	Eutech Instruments Europe B.V., Nijkerk, The Netherlands
Pipette BioHit m10, m100, m1000	Biohit Group, Helsinki, Finland
Pipette Pipetman P20, P200, P1000	Gilson Inc., Middleton, USA
Pipette Pipetman Ultra U2	Gilson Inc., Middleton, USA
Pipetus reddot	Belden Electronics GmbH, Schalksmühle, Germany

Power supply EC 105	Thermo Electron GmbH, Karlsruhe, Germany
Power supply EPS 301	GE Medical Systems Deutschland GmbH & Co. KG, München, Germany
Pulsed field gel electrophoresis device	Bio-Rad Laboratories Inc., Hercules, USA
Pure water system Astacus	membraPure GmbH, Bodenheim, Germany
Rainin Pipet-Lite (2, 20, 200 and 1000 µl)	Mettler-Toledo GmbH, Giessen, Germany
Scale 440-33N	Kern & Sohn GmbH, Balingen-Frommen, Germany
Scale APX-1502	Denver Instrument GmbH, Göttingen, Germany
Steri-Cycle CO2 incubator	Thermo Electron GmbH, Karlsruhe, Germany
Vacuum centrifuge DNA110 Speed Vac	GMI Inc., Ramsey, USA
Vortex Genie 2	Scientific Industries Inc., New York, USA
Vortex Mixer	VELP Scientifica srl, Usmate, Italy
Waterbath	Thermo Electron GmbH, Karlsruhe, Germany

2.1.2 Consumables

0.5 ml, 1.5 ml and 2.0 ml reaction tubes	Brand GmbH & Co. KG, Wertheim, Germany
14 ml Round bottom tube with ventilation lid	BD, Franklin Lakes, USA
15 and 50 ml centrifugation tubes	Corning Inc., New York, USA
50 ml high speed centrifugation tubes	SPL Life Sciences, Eumhyeon-ri, Korea
Cell culture dish (6, 10 and 15 cm)	Corning Inc., New York, USA
Cell culture flasks (25, 75, 150 cm²)	Corning Inc., New York, USA
Cell culture plates (4-, 6-, 12-, 24-, 48- and 96-well)	Corning Inc., New York, USA
Cell scratcher	Corning Inc., New York, USA
Cryopreservation tube	Corning Inc., New York, USA
Cuvettes	Brand GmbH & Co. KG, Wertheim, Germany
Disposable inoculating loop (10 µl)	Cole-Parmer Instrument Corporation, Vernon Hils, USA
Electroporation cuvettes (2 and 4 mm)	Peqlab Biotechnologie GmbH, Erlangen, Germany
Filter Stericup and Steritop (0.22 µm)	Merck KGaA, Darmstadt, Germany
Glass capillaries	Brand GmbH & Co. KG, Wertheim, Germany
Glass pasteur pipettes	Brand GmbH & Co. KG, Wertheim, Germany
Glassware (bottles, flasks)	Paul Marienfeld GmbH & Co. KG, Lauda Königshofen, Germany
Hybond-N^+ nylon transfer membrane	GE Healthcare Ltd., Little Chalfont, United Kingdom
Injection needles (0.3 x 13 mm)	BD, Franklin Lakes, USA
Microscope slides	Gerhard Menzel, Glasbearbeitungswerk GmbH & Co. KG, Braunschweig, Germany
Petri dish (10 cm)	Brand GmbH & Co. KG, Wertheim, Germany
Photometer cuvettes UVette	Eppendorf AG, Hamburg, Germany
Pipette tips (2, 20, 200, 1000 µl)	Brand GmbH & Co. KG, Wertheim, Germany
Pipette tips with filter (2, 20, 200, 1000 µl)	Mettler-Toledo GmbH, Giessen, Germany
Rotilabo blotting paper (1 mm)	Carl Roth GmbH & Co. KG, Karlsruhe, Germany
Scalpels	Megro GmbH & Co. KG, Wesel, Germany
Sterile filter 0.22 µm	Sartorius AG, Göttingen, Germany
Sterile plastic pipettes (1, 2, 5, 10, 25 ml)	Corning Inc., New York, USA
Syringes	Henke, Sass, Wolf GmbH, Tuttlingen, Germany

2.1.3 Chemicals

1,4-Dithiothreitol (DTT)	Sigma-Aldrich Chemie GmbH, Steinheim, Germany
2-Mercaptoethanol	Sigma-Aldrich Chemie GmbH, Steinheim, Germany
2-Propanol	Carl Roth GmbH & Co. KG, Karlsruhe, Germany
4´,6-Diamidino-2-phenylindol (DAPI)	Sigma-Aldrich Chemie GmbH, Steinheim, Germany
Acetic acid	Sigma-Aldrich Chemie GmbH, Steinheim, Germany
Alcian blue	Sigma-Aldrich Chemie GmbH, Steinheim, Germany
Biozym LE Agarose	Biozym Scientific GmbH, Hessisch Oldendorf, Germany
Bovine Serum Albumin (BSA), pH 7.0	PAA Laboratories GmbH, Pasching, Austria
Bromophenol blue	Sigma-Aldrich Chemie GmbH, Steinheim, Germany
Chloroform	Sigma-Aldrich Chemie GmbH, Steinheim, Germany
D-Glucose	Sigma-Aldrich Chemie GmbH, Steinheim, Germany
Dimethylsulfoxid (DMSO)	Sigma-Aldrich Chemie GmbH, Steinheim, Germany
Ethanol	Honeywell Specialty Chemicals Seelze GmbH, Seelze, Germany
Ethidium bromide solution	Sigma-Aldrich Chemie GmbH, Steinheim, Germany
Ethylenediaminetetraacetic acid (EDTA)	Sigma-Aldrich Chemie GmbH, Steinheim, Germany
Formaldehyde	Sigma-Aldrich Chemie GmbH, Steinheim, Germany
Formaldehyde, para-	Sigma-Aldrich Chemie GmbH, Steinheim, Germany
Formalin (37% (v/v))	Sigma-Aldrich Chemie GmbH, Steinheim, Germany
Formamide (deionized)	Sigma-Aldrich Chemie GmbH, Steinheim, Germany
GenAgarose L.E.	Genaxxon BioScience GmbH, Ulm, Germany
Glycerol	Sigma-Aldrich Chemie GmbH, Steinheim, Germany
Glycine	Carl Roth GmbH & Co. KG, Karlsruhe, Germany
HEPES	Invitrogen GmbH, Darmstadt, Germany
Ficoll 400	GE Healthcare Ltd., Little Chalfont, United Kingdom
Hydrochloric acid	Sigma-Aldrich Chemie GmbH, Steinheim, Germany
Maleic acid	Sigma-Aldrich Chemie GmbH, Steinheim, Germany
Methanol	Carl Roth GmbH & Co. KG, Karlsruhe, Germany
Oil Red O	Sigma-Aldrich Chemie GmbH, Steinheim, Germany
Orange G dye	Sigma-Aldrich Chemie GmbH, Steinheim, Germany
Phenol : Chloroform : Isoamylalcohol (25 : 24 : 1)	Sigma-Aldrich Chemie GmbH, Steinheim, Germany
Silver nitrate	Sigma-Aldrich Chemie GmbH, Steinheim, Germany
Sodium acetate	Carl Roth GmbH & Co. KG, Karlsruhe, Germany
Sodium chloride	Sigma-Aldrich Chemie GmbH, Steinheim, Germany
Sodium citrate tribasic dihydrate	Sigma-Aldrich Chemie GmbH, Steinheim, Germany
Sodium hydroxide	Sigma-Aldrich Chemie GmbH, Steinheim, Germany
Sodium thiosulfate	Sigma-Aldrich Chemie GmbH, Steinheim, Germany
Sodium pyruvate	Invitrogen GmbH, Darmstadt, Germany
Sodiumdodecylsulfate (SDS)	Sigma-Aldrich Chemie GmbH, Steinheim, Germany
Sucrose	Sigma-Aldrich Chemie GmbH, Steinheim, Germany
Trizma base	Sigma-Aldrich Chemie GmbH, Steinheim, Germany
Tris hydrochloride	Sigma-Aldrich Chemie GmbH, Steinheim, Germany
Trizol	Invitrogen GmbH, Darmstadt, Germany
Tween 20	Sigma-Aldrich Chemie GmbH, Steinheim, Germany

2.1.4 Kits

GenElute Mammalian Genomic DNA Miniprep Kit	Sigma-Aldrich Chemie GmbH, Steinheim, Germany
Human MSC Nucleofector kit	Lonza Cologne GmbH, Köln, Germany
MACSelect K^k Tranfected Cell Selection kit	Miltenyi Biotec GmbH, Bergisch Gladbach, Germany
NucleoBond Xtra Maxi	Macherey-Nagel GmbH & Co. KG, Düren, Germany
NucleoBond Xtra Midi	Macherey-Nagel GmbH & Co. KG, Düren, Germany
NucleoSpin Plasmid Quick Pure	Macherey-Nagel GmbH & Co. KG, Düren, Germany
Qiagen Large-Construct Kit	Qiagen N.V., Venlo, The Netherlands
Quick Change II-E Site-Directed Mutagenesis Kit	Agilent Technologies Inc., Santa Clara, USA
Total RNA Isolation System SV	Promega Corporation, Fitchburg, USA
Transcriptor Universal cDNA Master	Roche Deutschland Holding GmbH, Grenzach-Wyhlen, Germany
Turbo DNA free	Applied Biosystems, Foster City, USA
Wizard SV Gel and PCR Clean-Up System	Promega Corporation, Fitchburg, USA

2.1.5 Enzymes for molecular biology

Antarctic Phosphatase	New England Biolabs Inc., Ipswich, USA
Calf Intestine Phosphatase (CIP)	New England Biolabs Inc., Ipswich, USA
DNA Polymerase I Large (Klenow) Fragment	New England Biolabs Inc., Ipswich, USA
GoTaq DNA Polymerase	Promega Corporation, Fitchburg, USA
M-MuLV Reverse Transcriptase	New England Biolabs Inc., Ipswich, USA
OmniTaq DNA Polymerase	OLS Omni Life Science GmbH & Co. KG, Bremen, Germany
Phusion High-Fidelity DNA Polymerase	New England Biolabs Inc., Ipswich, USA
Platinum Taq DNA Polymerase	Invitrogen GmbH, Darmstadt, Germany
Proteinase K	Sigma-Aldrich Chemie GmbH, Steinheim, Germany
Restriction endonucleases	New England Biolabs Inc., Ipswich, USA
Restriction endonucleases BplI, PscI	Fermentas GmbH, St. Leon-Rot, Germany
RNAse A solution	Sigma-Aldrich Chemie GmbH, Steinheim, Germany
SuperScript III Reverse Transcriptase	Invitrogen GmbH, Darmstadt, Germany
SuperScript One-Step RT-PCR System with Platinum *Taq* High Fidelity	Invitrogen GmbH, Darmstadt, Germany
T4 DNA Ligase	New England Biolabs Inc., Ipswich, USA
TURBO DNA-free	Applied Biosystems, Foster City, USA

2.1.6 Cloning vectors

BAC containing rabbit *hprt*	BACPAC Resources, Children´s Hospital, Oakland, USA
BAC-mCherry-Neo	laboratory stock
pBluescript-3xpA	created by Dr. Nousin Rezaei
pcDNA-3-PGK-Neo	created by Dr. Hagen Wieland
pCAGGs-eGFP	kind gift of Prof. Elly Tanaka
pCAGGs-mCherry	kind gift of Prof. Elly Tanaka

pCAGGs-SB100	kind gift of Dr. Thomas Floss
pGEM-T Easy Vector System I	Promega Corporation, Fitchburg, USA
pBluescript SK+	Agilent Technologies Inc., Santa Clara, USA
pjet1.2/blunt	Fermentas GmbH, St. Leon-Rot, Germany
pl452	kind gift of Prof. Eckhard Wolf
pMACS-K^k II	Miltenyi Biotec GmbH, Bergisch Gladbach, Germany
pPGK-eGFP1-Neo	created by Dr. Hagen Wieland
pPGK-Neo	created by Dr. Hagen Wieland
pREPROII	kind gift of Dr. Ralf Kühn
pSL1180 Amersham	GE Healthcare Ltd., Little Chalfont, United Kingdom
pT2BDS3	kind gift of Dr. Thomas Floss
pT2-SB-βgeo	kind gift of Dr. Thomas Floss
pUC-19	Invitrogen GmbH, Darmstadt, Germany

2.1.7 Chemicals for Southern Blot analysis

AGFA Cronex 5 X-Ray film	Röntgen Bender GmbH & Co. KG, Baden-Baden, Germany
AGFA Developer G 150 for X-Ray film	Röntgen Bender GmbH & Co. KG, Baden-Baden, Germany
AGFA Fixer G 354 for X-Ray film	Röntgen Bender GmbH & Co. KG, Baden-Baden, Germany
Anti-Digoxigenin-AP, Fab fragments	Roche Deutschland Holding GmbH, Grenzach-Wyhlen, Germany
Blocking Reagent	Roche Deutschland Holding GmbH, Grenzach-Wyhlen, Germany
CDP-Star	Roche Deutschland Holding GmbH, Grenzach-Wyhlen, Germany
DIG Easy Hyb Granules	Roche Deutschland Holding GmbH, Grenzach-Wyhlen, Germany
Digoxigenin-11-2'-deoxy-uridine-5'-triphosphate, alkaline-labile (DIG-labelled dUTP)	Roche Deutschland Holding GmbH, Grenzach-Wyhlen, Germany
DNA molecular weight marker VII, Digoxigenin-labelled	Roche Deutschland Holding GmbH, Grenzach Wyhlen, Germany

2.1.8 Miscellaneous

100 bp ladder	New England Biolabs Inc., Ipswich, USA
1 kb ladder	New England Biolabs Inc., Ipswich, USA
dNTPs	Biomers.net GmbH, Ulm, Germany
RNase Away	Carl Roth GmbH & Co. KG, Karlsruhe, Germany
Mid Range II PFG Marker	New England Biolabs Inc., Ipswich, USA

2.1.9 Strains of *Escherichia coli*

DH10b (Genotype: F^- endA1 recA1 galE15 galK16 nupG rpsL ΔlacX74 Φ80lacZΔM15 araD139 Δ(ara,leu)7697 mcrA Δ(mrrhsdRMS-mcrBC) λ^-; Invitrogen GmbH, Darmstadt, Germany

K12 ER2925 dam^-/dcm^- (Genotype: ara-14 leuB6 fhuA31 lacY1 tsx78 glnV44 galK2 galT22 mcrA dcm-6 hisG4 rfbD1 R(zgb210::Tn10)TetS endA1 rpsL136 dam13::Tn9 xylA-5 mtl-1 thi-1 mcrB1 hsdR2); New England Biolabs Inc., Ipswich, USA

SW106 derived from EL350, contains an *ara*-inducible *Cre* gene (Genotype: DH10B [l*cl*857 (*cro–bio*A) <> araC-PBADcre]); kind gift of Prof. Eckhard Wolf

2.1.10 Media and antibiotics for bacterial culture

Difco lysogeny broth base — BD, Franklin Lakes, USA
S.O.C. medium — Invitrogen GmbH, Darmstadt, Germany

Antibiotic	Supplier	Stock solution	Working concentration
Ampicillin	Sigma-Aldrich Chemie GmbH, Steinheim, Germany	100 mg/ml	100 µg/ml
Chloramphenicol	Sigma-Aldrich Chemie GmbH, Steinheim, Germany	20 mg/ml	20 µg/ml
Kanamycin	Sigma-Aldrich Chemie GmbH, Steinheim, Germany	30 mg/ml	30 µg/ml

2.1.11 Mammalian Cells

Cell line	Organism	Description	Source
INS1-E	Rat	Insulinoma cells	Kind gift of Eckhard Lammert, with permission of Claes B. Wollheim
MEF	Mouse	Mouse embryonic fibroblasts	This work
MEF-MITO	Mouse	Mitomycin-treated MEFs	homemade
MEF-Neo-MITO	Mouse	MEF-MITO from a *neo*-transgenic mice strain	homemade
rbESC	Rabbit	Embryonic stem cells	This work
rbFB-1	Rabbit	Muscle derived fibroblasts	This work
rbMSC-A	Rabbit	Adipose tissue derived mesenchymal stem cells	This work
rbMSC-BM	Rabbit	Bone-marrow derived mesenchymal stem cells	This work

2.1.12 Media and additives for mammalian cell culture

3-Isobutyl-1-methylxanthin (IBMX) — Sigma-Aldrich Chemie GmbH, Steinheim, Germany
6-Bromoindirubin-3´-oxime — Merck KGaA, Darmstadt, Germany
6-Thioguanine — Sigma-Aldrich Chemie GmbH, Steinheim, Germany
Accutase — PAA Laboratories GmbH, Pasching, Austria

Activin A	Sigma-Aldrich Chemie GmbH, Steinheim, Germany
Advanced Dulbecco's Modified Eagle's Medium (Advanced DMEM)	Invitrogen GmbH, Darmstadt, Germany
Amphotericin B	PAA Laboratories GmbH, Pasching, Austria
Ascorbic acid	Sigma-Aldrich Chemie GmbH, Steinheim, Germany
Basic fibroblast growth factor, human (bFGF, FGF-2)	Genaxxon BioScience GmbH, Ulm, Germany
β-Glycerophosphate	Sigma-Aldrich Chemie GmbH, Steinheim, Germany
Cell Culture Water, EP-grade	PAA Laboratories GmbH, Pasching, Austria
Chicken serum	PAA Laboratories GmbH, Pasching, Austria
Demecolcine	PAA Laboratories GmbH, Pasching, Austria
Dexamethasone (water-soluble)	Sigma-Aldrich Chemie GmbH, Steinheim, Germany
Dulbecco's Modified Eagle's Medium (DMEM), high glucose (4.5 g/l)	PAA Laboratories GmbH, Pasching, Austria
Dulbecco's PBS, without Ca^{+} & Mg^{2+}	PAA Laboratories GmbH, Pasching, Austria
Fetal calf serum, ES qualified (FCS)	PAA Laboratories GmbH, Pasching, Austria
G418	PAA Laboratories GmbH, Pasching, Austria
Gelatine type B (bovine skin)	Sigma-Aldrich Chemie GmbH, Steinheim, Germany
Gentamycin	PAA Laboratories GmbH, Pasching, Austria
Glasgow Modified Eagle's Medium BHK-21 + Glutamine, - Tryptose Phosphate Broth	Invitrogen GmbH, Darmstadt, Germany
GlutaMAX	Invitrogen GmbH, Darmstadt, Germany
Hanks Balanced Salt Solution	Biochrom AG, Berlin, Germany
Heparin	Sigma-Aldrich Chemie GmbH, Steinheim, Germany
Hypoosmolar Buffer	Eppendorf AG, Hamburg, Germany
Indomethacin	Sigma-Aldrich Chemie GmbH, Steinheim, Germany
Insulin-like growth factor 2 (IGF2)	Sigma-Aldrich Chemie GmbH, Steinheim, Germany
Isobutylmethylxanthine (IBMX)	Sigma-Aldrich Chemie GmbH, Steinheim, Germany
ITS+1	Sigma-Aldrich Chemie GmbH, Steinheim, Germany
jetPei	Polyplus-transfection SA, Illkirch, France
Leukaemia inhibitory factor (LIF)	homebrew
LIF (ESGRO)	Merck KGaA, Darmstadt, Germany
Lipofectamine 2000	Invitrogen GmbH, Darmstadt, Germany
Lymphocyte separation medium	PAA Laboratories GmbH, Pasching, Austria
MACSelect K^{k} MicroBeads	Miltenyi Biotec GmbH, Bergisch Gladbach, Germany
Metafectene	Biontex Laboratories GmbH, Planegg, Germany
Nanofectin	PAA Laboratories GmbH, Pasching, Austria
Non-essential aa (NEAA)	PAA Laboratories GmbH, Pasching, Austria
Penicillin/Streptomycin solution	PAA Laboratories GmbH, Pasching, Austria
Promofectine	PromoCell GmbH, Heidelberg, Germany
Retinoic acid	Sigma-Aldrich Chemie GmbH, Steinheim, Germany
ROCK-Inhibitor (Y-27632 dihydrocholride monohydrate)	Sigma-Aldrich Chemie GmbH, Steinheim, Germany
RPMI 1640 with L-Glutamine	PAA Laboratories GmbH, Pasching, Austria
SatisFection	Agilent Technologies Inc., Santa Clara, USA
Sodium pyruvate solution	PAA Laboratories GmbH, Pasching, Austria
TCM	Minitüb GmbH, Tiefenbach, Germany
Transforming growth factor beta (TGF-β1)	MorphoSys AG, Martinsried/Planegg, Germany
Trypsin EDTA	PAA Laboratories GmbH, Pasching, Austria

Turbofect	Fermentas GmbH, St. Leon-Rot, Germany

2.1.13 Animals

Rabbits: albino Zimmermannkanichen (ZIKA) hybrid strain

Mice: C57BL6 strain, C57BL6-neo strain

All animals were housed in own facilities. Animal experiments were approved by the animal experimentation ethical committee of TU Munich and performed in accordance with the European Union Normative for Care and Use of Experimental Animals.

2.1.14 Oligonucleotides

Oligonucleotides were synthesized by biomers.net GmbH, Ulm, Germany, Sigma-Aldrich Chemie GmbH, Steinheim, Germany and Eurofins MWG GmbH, Ebersberg, Germany.

The recognition sequence of restriction endonucleases is underlined.

The number of bases refers to each respective primer pair.

2.1.14.1 Oligonucleotides for vector construction

Oligonucleotide name	Sequence 5´- 3´	Product size
rbIns 5´region-fwd	GGTGGTGCAGGGACTACAGA	
rbIns 5´region-rev	AGCCTCTGTGCGTATGTGTG	1187 bp
rbIns ex1-fwd	GGCGGGGGGCGTGGGGGGCGCGGGCA	
rbIns ex3-rev	GAGGTGACCAGCAGACAGGTCTGT	824 bp
rbIns g303a-fwd	CGGCATCGTGGAGCAGTGTTACACCAGCATCT	
rbIns g303a-rev	AGATGCTGGTGTAACACTGCTCCACGATGCCG	-
rbHPRT-exon2-EcoRI-fwd	ATGAATTCAATTTCCAGACATACTCAGCAGTG	
rbHPRT-exon2-NheI-rev	ATCGATCGTGTCCATAATGAGTCCATGAGG	478 bp
rbHPRT-exon4-BamHI-rev	ATGGATCCGACCAGTCAACAGGGGACAT	
rbHPRT-exon4-NotI-rev	ATCGCCGGCGCTGCAACTGTCACCCACACT	476 bp

2.1.14.2 Oligonucleotides for PCR amplifications

Oligonucleotide name	Sequence 5´- 3´		Product size
Oct4-fwd	TGGTGCCGTGAAGCTGGA		
Oct4-rev	GCCCTTCTGGCGCCGGTT	two isoforms	380, 488 bp
Nanog-fwd	AGCTCCAGCAGAATTGTC		
Nanog-rev	TACTCATCCACGCAGAGA		386 bp
Rex1-fwd	AGTCAACGCCAGGTATTC		
Rex1-rev	TATGAGCCAGCAACTGAG		469 bp
FoxD3-fwd	GCCCAAGAACAGCCTAGTGA		

FoxD3-rev	GGGTCCAGGGTCCAGTAGTT	255 bp
Nodal-fwd	GTGCTCCACTCCAACCTCTC	
Nodal-rev	GCTTGGGGTAGATGATCCAA	226 bp
TERC-fwd	CTAACTGAGCAGGGCGTAGG	
TERC-rev	GTGCAAGTCCCACAGCTCAG	379 bp
DPPA5-fwd	GAAGACCTGAAAGATCCAGA	
DPPA5-rev	AGGACTGGAAACTGGCTTCA	320 bp
BMP4-fwd	AAAGTCGCCGAGATTCAGG	
BMP4-rev	GAGTCTGATGGAGGTGAGT	635 bp
Nestin-fwd	TTTGCAGATGAGGAAGAGAG	
Nestin-rev	ATGCTCTGACTCCTCCAAG	444 bp
Desmin-fwd	AGCAGGAGATGATGGAATAC	
Desmin-rev	TCCAGCAGCTTCCGGTAGG	277 bp
Hnf4a-fwd	CCTCAAAGCCATCATCTTC	
Hnf4a-rev	GAAGAGCTTGATGAACTGGA	220 bp
Nudel-fwd	TCTGTTACCGCCATTAGAGG	
Nudel-rev	ATGACTCAGAGCTGCACTTG	380 bp
Gapdh-fwd	GGAGCCAAACGGGTCATCATCTC	
Gapdh-rev	GAGGGGCCATCCACAGTCTTCT	233 bp
PGK-Neo-genomic-fwd	TTGACAATTAATCATCGGCATAGT	
PGK-Neo-genomic-rev	TTATTAGGAAAGGACAGTGGGAGT	1001 bp
Intron1-PGK-fwd	GCAAGGTCTATCTTTTCCCAAA	
Intron1-PGK-rev	TAAAGCGCATGCTCCAGACT	2002 bp
pA-intron4-fwd	CCTTCTAGTTGCCAGCCATC	
pA-intron4-rev	GGCACAGTGGCTTTAGCTGT	2000 bp
rbHPRT-ctrl-ex2-fwd	TCTCATACCTTAATTTCCTTTGGTAGA	
rbHPRT-ctrl-ex2-rev	GTCGGTCTTGACAAAAAGAACC	998 bp
rbHPRT-ctrl-ex4-fwd	AGGATCTCCTGTCATCTCACCTT	
rbHPRT-ctrl-ex4-rev	TCTTAATGATTGATTGAAAGCAGTG	974 bp
rbHPRT-ctrl-ex7-fwd	AATTAACAGCCTGCTGGTGAAAAG	
rbHPRT-ctrl-ex7-rev	TTGTATTTTGCTTTTCCAGTTTCA	1070 bp
rbHPRT-ex3-c-fwd	GACTTTGATTTCTTGGTCCTAAACA	
rbHPRT-ex3-e-rev	CATAAGGAGAGATCATGAGGAAAAA	1003 bp
SB100-fwd	AGACCTCAGAAAAAGAATTGTAGACCT	
SB100-rev	TAGCATTGCCTTTAAATTGTTTAACTT	986 bp
SB100b-fwd	AAGACCTCAGAAAAAGAATTGTAGACC	
SB100b-rev	GTAGCATTGCCTTTAAATTGTTTAACT	988 bp

SB-Ins-rev-5-a-fwd	CTCGTTTTTCAACTACTCCACAAAT		
SB-Ins-rev-5-a-rev	TTCCTCAGCATTCTTAACAAAAGAC		505 bp
SB-Cherry-fwd	CAGCCATTGCCTTTTATGGT		
SB-Cherry-rev	TTCAGCTTCAGCCTCTGCTT		1004 bp
SO-Cherry-2-fwd	AAGGGCGAGGAGGATAACAT		
SO-Cherry-2-rev	ACATGAACTGAGGGGACAGG		205 bp
Cherry-BbsI-3`-fwd	AAGGGCGAGGAGGATAACAT		
Cherry-BbsI-3`-rev	CTTCAGCTTCAGCCTCTGCT		510 bp
Cherry-BbsI-5`-fwd	TGGACGAGCTGTACAAGTAAGAAT		
Cherry-BbsI-5`-rev	ACAAACAATAGTTTTGGCAAGTCA		1002 bp
RT-INS-fwd	TGGTCCTCTGCAGACTGGAT		
RT-INS-rev	GGCACCCCTAGTTGCAGTAGT	mRNA	330 bp
		DNA	666 bp

2.1.14.3 Oligonucleotides for sequencing

Oligonucleotide name	Sequence 5´- 3´
rbHPRT-exon2-fwd	TTACGCCAAGCTCGAAATTA
rbHPRT-exon2-rev	CCGGTAGAATTTCGACGAC
rbHPRT-exon4-fwd	TCACTATAGGGCGAATTGGA
rbHPRT-exon4-rev	AGCTTGCGGAACCCTTAATA
rbHPRT-3´-site-a-rev	GCATGGAAAGGATGAGACAGA
rbHPRT-3´-site-b-rev	TGCCTCCATGATAAACTGCTT
rbHPRT-5´-site-a-fwd	GGTCTATCTTTTCCCAAAACTTGA
rbHPRT-51 fwd and 73 rev	CACAGGGGCAGACATCAGTA
rbHPRT-51 fwd and 73 rev-b	CCATACCCACCTACCTATCCTTC
rbHPRT-51 fwd and 73 rev-c	CATTACGTCGAGGACTTGGAA
rbHPRT-51-fwd	GAACCCACTCAAATGCATATTTC
rbHPRT-51-b-fwd	CATCCCCCTCACAGCTTATG
rbHPRT-51-rev	TGCTCCTGCCGAGAAAGTAT
rbHPRT-51-b-rev	GGGCATGGAGTACATGTGG
rbHPRT-51-c-rev	TGTGGAATTGTGAGCGGATA
rbHPRT-73-fwd	GGAAAGGGACTGGCTGCTAT
rbHPRT-73-b-fwd	CCACTCAAATGCATATTTCTTGA
rbHPRT-73-rev	GATTGACTCAAAATCTGGCATAA
Ins complete	CAGGGACTACAGAACGCTTTGG
rbIns ex3_2-rev	GTCCTCTGCAGACCAGATCC
rbIns-Mut-seq	GAGCGCCATCTTGTTCTCTC
rbIns-pA-fwd	GCCCGCTACAGATCAGGGAGGAC

pjet1.2 Sequencing Primer-fwd	CGACTCACTATAGGGAGAGCGGC
pjet1.2 Sequencing Primer-rev	AAGAACATCGATTTTCCATGGCAG

2.1.15 Computer Software

Axiovision 3.1	Zeiss AG, Oberkochen, Germany
Basic local alignment search tool (BLAST)	http://www.ncbi.nlm.nih.gov/blast/Blast.cgi
GeneSnap 6.01	Synoptics Ltd, Cambridge, United Kingdom
Microsoft Office:Mac 2003/2007	Microsoft Deutschland GmbH, Unterschleißheim, Germany
Primer 3	Whitehead Institute, http://frodo.wi.mit.edu
VectorNTI 10	Invitrogen GmbH, Darmstadt, Germany
ClustalW2 alignments	http://www.ebi.ac.uk/Tools/clustalw2

2.2 Methods

All work was carried out at room temperature (RT), if not stated otherwise.

2.2.1 Microbiological work

All work was carried out under sterile conditions in class II laminar air flow cabinets. Before usage, media and consumables were sterilized by autoclaving for 20 min at 121°C. Non-autoclaveable additives were filter-sterilised (0.22 µm pore size).

2.2.1.1 Growing *E. coli*

To obtain single colonies after transformation, from liquid cultures or from cryopreserved stocks, *E. coli* were plated on LB (lysogeny broth) agar plates containing the proper antibiotics (final concentration of 100 µg/ml ampicillin, 30 µg/ml kanamycin and 20 µg/ml chloramphenicol) and incubation overnight (o/n) at 37°C and 32°C in case of *E. coli* containing a bacterial artificial chromosome (BAC), respectively.

For small scale preparations of plasmid and BAC, 5 ml of LB were inoculated with a single colony of *E. coli*, proper antibiotics were added and incubated o/n at 37°C and 32°C, respectively, while shaking at an agitation of 230 rpm.

For larger amounts of plasmid- and BAC-DNA, a 5 ml culture, but incubated for 8 h, was transferred into 300 ml LB (Maxiprep) or 500 ml LB (BAC-prep).

2.2.1.2 Storage of *E. coli*

Plates and liquid cultures were kept at 4°C for up to two weeks. For long term storage, 500 µl of a fresh grown overnight liquid culture, arose from a single colony, were mixed with 99% (v/v) glycerol and frozen at -80°C.

2.2.1.3 Transformation of electro-competent *E. coli*

Electro-competent *E. coli* (50 µl) were thawed on ice, 2 µl and 5 µl of a ligation reaction or 1 ng of plasmid DNA was added and mixed by pipetting. The mixture was transferred into precooled electroporation cuvettes (2 mm), bacterial cells were pulsed at 2500 V for 5 ms in a multiporator and 500 µl of prewarmed LB were added. This mixture was transferred to a 1.5 ml reaction tube and incubated at 37°C while shaking at an agitation of 230 rpm for 45 min. Afterwards, 20 to 200 µl of the suspension were plated onto LB agar plates as described.

2.2.1.4 Making recombineering-competent *E. coli*

Freshly streaked *E. coli*, previously transformed with BAC-rb*hprt*, were grown until OD_{600} 0.3 – 0.4. Then, this culture was incubated at 42°C for 15 min while shaking and put immediately into ice-water while shaking and incubated on ice for 20 min. All following steps were carried out at 4°C. The bacteria culture was centrifuged at 3500 x g for 10 min and the supernatant (s/n) was removed. The pellet was resuspended in 1 ml ice-cold 10% (v/v) glycerol/H_2O. The centrifugation and resuspension was repeated two more times. Then, aliquots of 50 µl were frozen at -80°C.

2.2.2 Molecular biological work

All reactions and solutions were prepared with sterile double distilled H_2O (ddH_2O). All sensitive reactions (e.g. polymerase chain reaction (PCR), work with RNA) were assembled applying pipette tips with filter.

2.2.2.1 Isolation of DNA

2.2.2.1.1 Isolation of plasmid and BAC from E. coli

a) Small scale isolation of plasmid and BAC (Miniprep)

Depending on the aim of this isolation step, Miniprep was performed by alkaline lysis method (for more DNA, time consuming) or non-alkaline lysis method (fast procedure, cheaper, less DNA).

For alkaline lysis method, 2 ml of a 5 ml o/n culture were pelleted by centrifugation at 16000 x g for 1 min. S/n was discarded, pellet was first resuspended in 100 µl resuspension solution (2 mM sucrose, 10 mM EDTA, 25 mM Trizma-HCl, pH 8.0) then in 200 µl lysis solution (0.2 M NaOH, 1% (w/v) SDS) and lysed for 3 min. Lysis was stopped by adding 150 µl neutralisation solution (3 M sodium acetate, pH 4.8) and the sample was incubated on ice for 30 min. After centrifugation for 10 min at 16000 x g, s/n was transferred to a new reaction tube and DNA was precipitated by adding 1 ml 95% EtOH. The sample was centrifuged for 15 min at 16000 x g and s/n discarded. The DNA pellet was washed twice first with 80% then with 95% EtOH. Each washing step was followed by centrifugation for 10 min at 16000 x g. After removal of s/n, pellet was air-dried and DNA dissolved in 50 µl ddH_2O containing 20 µg/ml RNAse A to remove bacterial RNA contamination.

For non-alkaline lysis method [508], 2 ml of a 5 ml o/n culture were pelleted by centrifugation at 16000 x g for 1 min and 1.5 ml of s/n were discarded; pellet was resuspended in remaining liquid (500 µl) and mixed with 500 µl non-alkaline lysis solution

(6 M lithium-acetate, 2 mM EDTA, 0.5% (w/v) SDS, pH 4.8), incubated for 5 min and centrifuged at 10000 x g for 10 min. The s/n was transferred to a new reaction tube and DNA was precipitated by adding 800 µl isopropanol and centrifugation at 10000 x g for 10 min. The s/n was removed, pellet washed in 1 ml 70% EtOH, centrifuged at 16000 x g for 1 min and the s/n was discarded and the pellet air-dried. Finally, the DNA was dissolved in 20 µl ddH_2O containing 20 µg/ml RNAse A to remove bacterial RNA contamination.

For sensitive subsequent reactions, miniprep was performed applying the NucleoSpin Plasmid QuickPure kit according to manufacturer's instructions.

b) Large scale isolation of plasmid

Midi- and Maxipreps of plasmid DNA were performed applying the NucleoBond Xtra Midi- or Maxi kit according to manufacturer's instructions from 50 or 300 ml o/n cultures.

c) Large scale isolation of BAC

Maxipreps of BAC DNA were performed applying the Qiagen Large-Construct kit according to manufacturer's instructions from 500 ml o/n cultures.

2.2.2.1.2 Isolation of mammalian genomic DNA

Depending on the sensitiveness of subsequent reactions, mammalian genomic DNA was isolated by a quick and dirty method or highly pure with a kit.

a) Igepal solution isolation

To obtain genomic DNA from cell samples, the cell-Trypsin-EDTA mixture was centrifuged at 16000 x g for 10 min after detaching from the culture plate. The s/n was removed, the cell pellet was resuspended in 50 µl Igepal buffer (50 mM Tris-HCl, 50 mM KCl, 3.15 mM $MgCl_2$, 0.25% (v/v) Igepal, 0.5% (v/v) Tween 20, pH 8.0) containing Proteinase K (1 mg/ml) and incubated at 60°C for 90 min followed by an incubation at 95°C for 15 min. Then, the mixture was centrifuged at 16000 x g for 15 min and 5 µl of the s/n was used for screening PCR.

b) Kit-based isolation

To obtain high pure mammalian genomic DNA, the GenElute Mammalian Genomic DNA Miniprep Kit was used according to manufacturer's instructions.

2.2.2.2 Manipulation of DNA

2.2.2.2.1 Restriction endonuclease digestion

For the restriction digestion of DNA 2 to 3 U of restriction endonuclease per µg were used according to manufacturer's instructions. To verify putative restriction patterns, around 1 µg

of DNA was digested. For quantitate preparations of plasmid DNA, fragments up to 20 µg were used. Depending on the following work flow the restriction endonuclease was heat inactivated according to manufacturer's instructions.

2.2.2.2.2 Treatment of DNA with Klenow fragment

To converse disturbing overhangs on DNA fragments to blunt ends, the DNA Polymerase I Large (Klenow) fragment was used according to manufacturer's instructions. This enzyme forms blunt ends by removing 3´ overhangs and filling in 5´ overhangs. To terminate the reaction, 0.5 M EDTA solution was added to a final concentration of 25 mM EDTA and the mixture was incubated at 75°C for 15 min.

2.2.2.2.3 Dephosphorylation of DNA

To prevent self-ligation of plasmid DNA 5´ and 3´ phosphate groups were removed by applying Calf Intestine Phosphatase (CIP) or Antarctic Phosphatase according to manufacturer's instructions.

2.2.2.2.4 Agarose gel-electrophoresis

To separate DNA fragments according to their size, to isolate DNA fragments after restriction digest and to estimate the concentration of the DNA agarose gel-electrophoresis was used. Depending on the (expected) size of DNA fragments, DNA was separated on 0.8 to 1.5% (w/v) agarose gels in an electric field ranging from 80 to 120 V in TAE (40 mM Trizma base, 20 mM acetic acid, 1 mM EDTA, pH 8.0) or TBE buffer (90 mM Trizma base, 90 mM boric acid, 2 mM EDTA, pH 8.0). All gels contained 0.1 µg/ml ethidium bromide to visualize the DNA by UV light at 254 nm excitation wavelength in the Gene Genius Bioimaging System. Before loading onto the gel, samples were mixed with 5 x gel loading buffer (50% (v/v) glycerol, 10 mM EDTA, 0.1% (w/v) SDS, traces of bromophenol blue). 100 bp and/or 1 kb DNA ladder was used to determine the size and estimate the concentration of DNA fragments.

To separate DNA fragments larger than 10 kb (up to 200 kb), pulsed field gel electrophoresis was used. For this, the DNA was separated on a 1% (w/v) agarose gel in 0.5 x TAE in a pulsed electric field at 60 V and 15 s pulse in 0.5 x TAE at 12°C for 16 h. Before loading onto the gel, 3 µg of each sample was mixed with 1/3 volume gel loading buffer (15% Ficoll 400 (w/v), traces of Orange G dye). 1 kb DNA ladder and Mid Range PFG marker II were used to determine the size and estimate the concentration of DNA fragments. To visualize the DNA bands, the gel was stained in EtBr-containing 0.5 x TAE buffer after the separation.

2.2.2.2.5 Extraction of DNA from agarose gels

To obtain desired DNA fragments from agarose gels, the gels were put on a UV table, fragments were cut out with a clean scalpel and the DNA was purified applying the Wizard SV gel and PCR Clean-Up System kit according to manufacturer's instructions.

2.2.2.2.6 Ligation of DNA fragments

To ligate DNA fragments in a molar ratio (vector : insert) of 1 : 3 (sticky ends) or 1 : 5 (blunt ends), T4 DNA ligase was used according to manufacturer's instructions and usually incubated at RT for 2 h (sticky ends), followed by an incubation at 4°C o/n (only for blunt ends). For difficult to ligate fragments, the reaction was incubated at 16°C o/n, 1 µl of T4 DNA ligase was added and again incubated at 16°C o/n.

2.2.2.2.7 Purification of DNA by Phenol-Chloroform-Isoamylalcohol

To concentrate and purify DNA obtained from preceding procedures, such as restriction digests, the Phenol-Chloroform-Isoamylalcohol method was used. The DNA to purify was filled up with TE buffer (10 mM Tris, 1 mM EDTA) to a sufficient amount (usually 500 µl) and mixed with the same volume Phenol-Chloroform-Isoamylalcohol solution. This mixture was centrifuged at 16000 x g for 2 min and the upper, aqueous phase was transferred into a new reaction tube. Then, 1/10 volume NaAcetate (pH adjusted to 5.2 with glacial acetic acid) as well as 2.5 fold volume EtOH (100%) was added and mixed. To precipitate the DNA, the mixture was incubated at -20°C for 25 min and centrifuged at 16000 x g for 15 min (4°C). The s/n was discarded; the pellet was washed with 200 µl EtOH (80%) and centrifuged at 16000 x g for 2 min (4°C). The s/n was discarded and the pellet air dried under a laminar flow hood. Finally, the pellet was dissolved in 40 µl Tris-low EDTA (10 mM Tris, 0.1 mM EDTA).

2.2.2.2.8 DNA precipitation

To obtain sterile DNA for transfections into mammalian cells, the DNA was precipitated by adding 0.1 volumes of 3 M NaCl and 2 volumes of 100% EtOH (-20°C). The mixture was incubated at -80°C for 2 h or at -20°C o/n. Then, the solution was centrifuged at 16000 x g for 10 min. The following steps were done under sterile conditions. The s/n was discarded, pellet was washed in 1 ml 70% EtOH, followed by centrifugation at 16000 x g for 5 min. The s/n was discarded, pellet air dried under a laminar flow hood and dissolved in 50 to 200 µl Tris-low EDTA (10 mM Tris, 0.1 mM EDTA).

2.2.2.2.9 Introduction of single base mutations

In order to introduce the single base pair mutation (G to A, Akita mutation) into the rabbit *insulin* gene (rb*Ins*), it was previously subcloned into a cloning vector and the mutation was inserted according to manufacturer's instructions of the PCR-based Quick Change II-E Site-Directed Mutagenesis Kit. The necessary oligonucleotides (rbIns g303a, 2.1.14.1) were designed using the Quick Change Primer Design program (genomics.agilent.com). The kit includes the removing of the initial vector, clean-up and electroporation into kit´s own *E. coli* and medium.

The PCR program applied to introduce the mutation was as follows:

Initial denaturation	95°C	30 s	
Denaturation	95°C	30 s	x 16
Annealing	55°C	1 min	
Extension	68°C	3 min 50 s	
Cooling	8°C	∞	

2.2.2.3 DNA concentration determination

Routinely, DNA concentrations were measured applying the BioPhotometer according to manufacturer's instructions. Alternatively, DNA concentration was estimated by comparing the sample with the NEB ladder DNA on TBE agarose gels.

2.2.2.4 Polymerase Chain Reaction (PCR)

PCR was used to amplify fragments from plasmid, BAC and genomic DNA for cloning purposes or the verification of the presence of a given DNA fragment. PCR was performed according to manufacturer's instructions. In the following, purposes of each PCR reaction are described and the capital letter indicates the concerning cycling conditions in Table 1.

A) The PGK-Neo-polyA (mouse phosphoglycerate kinase promoter (PGK) directing *neo*) was amplified from the vector pcDNA3 using Omni-Taq-DNA-Polymerase.

B) Two fragments of BAC-rbHPRT were amplified using Phusion-DNA-Polymerase under the same cycling conditions. These both fragments (Fig. 15) were needed for cloning of the recombineering vector.

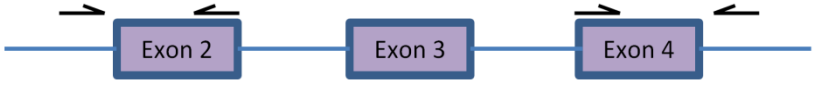

Figure 15: Two PCR amplicons of rb*hprt* for subsequent cloning purposes.

C) Two fragments (Fig. 16) of the final recombineered BAC-rbHPRT^{Neo} were amplified using Go-Taq-DNA-Polymerase for analysis under the same cycling conditions.

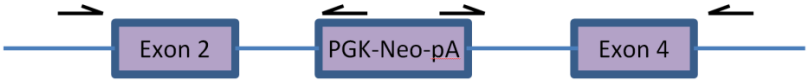

Figure 16: Two PCR amplicons of BAC-rbHPRT^{Neo} for analysing purposes.

D) Amplification of the promoter of rb*Ins* using Phusion polymerase for cloning purposes. Amplicon overlaps with fragment E) and shares a unique restriction site (Fig. 17).

E) Amplification of the transcription unit of rb*Ins* using Phusion polymerase for cloning purposes. Amplicon overlaps with fragment D) and shares a unique restriction site (Fig. 17). The Akita mutation will be introduced into this amplicon (2.2.2.2.9).

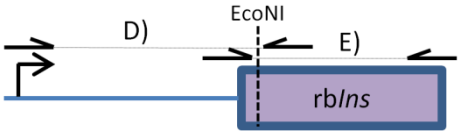

Figure 17: PCR amplicons of rb*Ins* for cloning purposes.
Both amplicons D) and E) overlapping the unique restriction site EcoNI which is used to ligate both amplicons after introduction of the Akita mutation.

Table 1: PCR cycling parameters concerning to the amplifications described above.

	A)		B)		C)		D)		E)	
Initial denaturation	94°C	2 min	94°C	2 min	95°C	2 min	98°C	2 min	98°C	2 min
Denaturation	94°C	30 s	94°C	30 s	95°C	45 s	98°C	10 s	98°C	10 s
Annealing	57°C	45 s	57°C	45 s	66°C	45 s	67°C	30 s	65°C	30 s
Extension	72°C	2 min	72°C	1.5 min	72°C	2.16 min	72°C	20 s	72°C	20 s
Cycles	25		25		35		30		30	
Final extension	-		-		72°C	5 min	72°C	7 min	72°C	7 min
Cooling	8°C	∞	8°C	∞	8°C	∞	8°C	∞	8°C	∞

F) Amplification of a small part of the rb*Ins*^{Akita} expression vector pINS^{Akita} using Go-Taq-DNA-Polymerase for analysing purposes.

G) Amplification of a part of the expression vector pT2-SB-CAGGs-mCherry (cytomegalovirus early enhancer/chicken b-actin promoter (CAGGs) directing expression of red fluorescent protein *mCherry* flanked by IRs of SB transposon) using oligonucleotides Cherry-BbsI-3`-fwd and Cherry-BbsI-3`-rev with Go-Taq-DNA-Polymerase for analysing purposes.

H) Amplification of a part of the SB100 expression vector pCAGGsSB100 using oligonucleotides SB100-fwd and SB100-rev with Go-Taq-DNA-Polymerase for analysing purposes.

Table 1 (continued): PCR cycling parameters concerning to the amplifications described above.

	F)		G)		H)	
Initial denaturation	95°C	2 min	95°C	2 min	95°C	2 min
Denaturation	95°C	45 s	95°C	45 s	95°C	45 s
Annealing	61°C	45 s	63°C	45 s	61°C	45 s
Extension	72°C	30 s	72°C	1 min	72°C	1 min
Cycles	35		35		35	
Final extension	72°C	5 min	72°C	5 min	72°C	5 min
Cooling	8°C	∞	8°C	∞	8°C	∞

2.2.2.5 Sequencing of DNA

DNA sequencing was performed by Eurofins MWG GmbH (Ebersberg, Germany) or according to manufacturer's instructions of the BigDye Terminator v1.1 cycle Sequencing Kit. If PCR products are supposed for sequencing with the usage of BigDye Terminator, the DNA was cleaned up SAP buffer and ExoI. For this, 100 ng of DNA were mixed with 2 µl BigDye Reaction mix, 2 µl BigDye Sequencing Buffer, 2.5 pmol of sequencing primer filled up to a final volume of 10 µl with H_2O and run in a thermocycler with following program:

Initial denaturation	96°C	15 s	
Denaturation	96°C	10 s	x 35
Annealing	60°C	4 s	
Extension	60°C	4 min	
Cooling	8°C	∞	

Further processing was performed by Dr. K. Flisikowski (Chair of Animal Breeding, TUM).

2.2.2.6 Southern Blot analysis of DNA

Southern Blot hybridisation was used to analyse the copy number of *mCherry* integrated into the rabbit genomic DNA.

2.2.2.6.1 Preparation of the probe

For the detection of DNA fragments on the membrane probes labelled with Digoxigenin-11-2'-deoxy-uridine-5'-triphosphate (DIG) were used. Here, a DIG-dUTP : dTTP ratio of 1 : 3 was used. For this, a PCR was set up to amplify a 205 bp fragment of the *mCherry* cassette with the oligonucleotide pair SO-Cherry-2-fwd and SO-Cherry-2-rev using 10 pg of the vector pT2BDS3-SB-polylinker-rev-mCherry. A second PCR using the same oligonucleotides was set up without (w/o) DIG to compare labelled and unlabelled probes by gel electrophoresis. The PCRs were set up according to manufacturer's instructions of the Go-Taq

Polymerase with using only 0.6 µl of dNTPs (40 mM) and run in a thermocycler with following program:

Initial denaturation	95°C	2 min	
Denaturation	95°C	45 s	x 35
Annealing	60°C	45 s	
Extension	72°C	12 s	
Final extension	72°C	5 min	
Cooling	8°C	∞	

To analyse the labelling of the probe, the DIG-labelled and the non-labelled samples were loaded onto a 1.5% (w/v) TAE agarose gel. Due to the incorporation of DIG, the labelled probe was expected to be slightly larger than the non-labelled one.

2.2.2.6.2 Southern Blot

For the Southern Blot, 10 µg of genomic DNA per lane was digested with 30 U BlpI for 4 h according to manufacturer's instructions and loaded onto a 1% (w/v) 1x TBE gel w/o EtBr. Next, 2 µl DIG-labelled molecular weight marker VII and 6 µl 1 kb ladder was loaded onto the gel. The gel was run at 40 V for 18 h. To determine the separation of DNA, the lane with the 1 kb ladder was cut off, stained in 1 x TAE containing EtBr for 15 min and visualized with UV light. All following steps were carried out with gentle shaking, if not stated otherwise. The DNA was depurinated by incubate the gel in 250 mM HCl for 10 min. Then, the gel was rinsed with dH_2O and incubated twice in denaturation solution (0.5 M NaOH, 1.5 M NaCl) for 15 min and again rinsed with dH_2O. The gel was incubated twice in neutralization solution (0.5 M Tris-HCl pH7.5, 1.5 M NaCl) for 15 min and rinsed with dH_2O. Afterwards, the gel was equilibrated in 20 x SSC (3 M NaCl, 0.3 M NaCitrate, adjusted to pH 7 with 1 M HCl) for 10 min. The gel was assembled in a capillary blot according to the manual and the DNA was blotted onto the Hybond-N^+ membrane o/n. After blotting, the membrane was washed twice in 2 x SSC and the DNA was linked to it by an incubation at 120°C for 30 min. The membrane was covered with DIG Easy Hyb and incubated for 1 h in a rotating 50 ml centrifugation tube. 2.5 µl of the probe were diluted in 50 ml ddH_2O, incubated at 95°C for 5 min and mixed with 2.5 ml of pre-warmed (37°C) DIG Easy Hyb (hybridisation solution). The DIG Easy Hyb was discarded from the membrane; the hybridisation solution was added and incubated in the rotating tube at 47.7°C o/n. The next day, the hybridisation solution was discarded, the membrane was incubated twice in low stringency buffer (2 x SSC, 0.1% (v/v) SDS) for 15 min and then the membrane was incubated twice in pre-warmed

(54°C) high stringency buffer (0.5 x SSC, 0.1% (v/v) SDS) at 54°C for 15 min. The membrane was incubated in washing buffer (0.1 M maleic acid, 0.15 M NaCl, 0.3% (v/v) Tween 20, adjusted to pH 7.5 with NaOH) for 2 min, blocking solution (1 x blocking solution in washing buffer) was added and incubated for 1 h. Then, antibody solution (blocking solution, anti-Digoxygenin-AP Fab fragments 1:10000) was added and the membrane was incubated for 30 min. The membrane was incubated twice in washing buffer for 15 min and then incubated in detection buffer (0.1 M Tris-HCl, 0.1 M NaCl, pH 9.5) for 3 min. The membrane was taken out of the tray and was sealed into a plastic wrap. Before closing the wrap, the chemiluminescent substrate (1:100 in detection buffer) was added drop wise to the membrane. The sealed membrane was exposed to X-ray films for 5 min to 1 h.

2.2.2.7 Isolation of RNA

For RNA isolation from mammalian cells, the cells were detached with accutase, centrifuged at 340 x g for 5 min and resuspended in Trizol or in lysis buffer from the Total RNA Isolation System SV kit.

In case of the Total RNA Isolation System SV kit, RNA was isolated according to manufacturer's instructions.

In case of using Trizol reagent, cells were resuspended in 4 ml Trizol, incubated for 5 min and this suspension was transferred into 2 ml reaction tubes. Then, 200 µl of chloroform were added, the tubes were briefly inverted for 15 s and the mixture was incubated for 3 min. Subsequently, the tubes were centrifuged at 12000 x g for 15 min at 4°C and the upper, aqueous phase was transferred carefully into fresh tubes and after addition of 500 µl isopropanol (-20°C) incubated for 10 min. After centrifugation at 12000 x g for 10 min at 4°C s/n was discarded and the pellet was washed in 1000 µl 70% (v/v) EtOH (-20°C). The tubes were centrifuged at 7500 x g for 5 min at 4°C, the s/n was discarded, and the pellet was air-dried and dissolved in 50 µl of H_2O by incubation at 60°C for 10 min.

To remove contaminating DNA, Turbo DNA free kit was used according to manufacturer's instructions.

Finally, the RNA concentration was measured with a photo-spectrophotometer and, if not used immediately, stored at -80°C.

The quality of the RNA was checked by loading 5 µl RNA (100 ng/µl) (mixed with 15 µl formamide (100%) and 5µl 5 x loading buffer, incubated at 65°C for 5 min) on 1.5% 1 x TBE agarose gels as described (2.2.2.2.4).

2.2.2.8 Reverse Transcriptase Polymerase Chain Reaction (RT-PCR)

RT-PCR was performed by a one-step or two-step protocol. For the one-step protocol RT-PCRs were carried out using SuperScript III One-step RT-PCR system according to manufacturer's instructions and run in a thermo cycler with programs listed in Table 2.

A) For *Oct4*, *Nanog*, *Rex1* and *TERC*

B) For *Nestin*, *Desmin*, *Hnf4α* and *Gapdh*

C) For *Nodal*, *FoxD3*, *DPPA5* and *BMP4*

For the two-step protocol, RNA was transcribed into cDNA in a separate reaction using M-MuLV Reverse Transcriptase or Transcriptor Universal cDNA Master kit according to manufacturer's instructions. Then, 1 µl of the cDNA-sysnthesis reaction was used to set up the PCR according to manufacturer's instructions of the Go-Taq Polymerase with program listed in Table 2.

D) rb*Ins*

Table 2: PCR cycling parameters concerning to the amplifications described above.

	A)		B)		C)		D)	
Reverse transcription of RNA into cDNA	50°C	45 min	50°C	45 min	55°C	45 min	-	
Initial denaturation	94°C	2 min	94°C	2 min	94°C	2 min	95°C	2 min
Denaturation	94°C	30 s	94°C	20 s	94°C	15 s	95°C	45 s
Annealing	54°C	30 s	56°C	20 s	62°C	30 s -1°C^{-cycle}	60°C	45 s
Extension	68°C	1 min	72°C	20 s	72°C	1 min	72°C	18 s
Cycles	10		35		10		35	
Denaturation	95°C	30 s	-		94°C	15 s	-	
Annealing	56°C	30 s	-		59°C	30 s	-	
Extension	68°C	1 min +1 s^{-cycle}	-		72°C	1 min	-	
Cycles	30		-		30		-	
Final extension	-		72°C	5 min	-		72°C	5 min
Cooling	8°C	∞	8°C	∞	8°C	∞	8°C	∞

2.2.3 Mammalian cell culture work

All work in tissue culture was performed in safety level S1 laboratories in a class II airflow cabinet under sterile conditions. All consumables were autoclaved before use or sterile single packed disposables were used. All solutions prepared outside of the airflow cabinet or were not sterile were autoclaved, or if not possible, filter sterilized (0.22 µm) before use.

Generally, all media, accutase / trypsin were pre-warmed to 37°C before use. The handling of cells occurred always under sterile conditions. Periodically, the medium was tested for the presence of mycoplasma contamination by the use of PCR method. The PCR was performed by Magret Bahnweg.

In principle, all cells were cultured w/o antibiotics and antimycotics, if not stated otherwise, in a cell culture incubator at 37°C in a 5% CO_2 humidified atmosphere in cell culture well plates, cell culture dishes or cell culture flasks with ventilation lids. The cells were inspected regularly under an inverted microscope for the state of confluence, signs of stress, media etc. The medium was replaced every 2 to 3 days and cells were subcultured (passaged) before they reached a confluent monolayer. For this, the medium was removed, the cells were washed with D-PBS and the cells were detached by incubation with accutase or trypsin at 37°C, 5% CO_2. When cells were detaching, the reaction was stopped by adding the appropriate medium and the cell suspension was centrifuged at 340 x g for 5 min, resuspended in growth medium and transferred to into new culture vessel.

For the used cells, the medium, passaging ratios and selection antibiotic concentrations are shown in Table 3. Selection antibiotic concentrations were determined in dose response curves.

Table 3: Summary of all mammalian cell lines used in this thesis.
For each cell line, the corresponding medium, splitting ratio and, if applied, antibiotic concentration is given.

Cell line	Growth medium	Subculture ratio	Selection antibiotics concentration
INS1-E	INS1-E	1 : 2 to 1 : 4	G418: 25 µg/ml
MEF	DMEM+	-	-
MEF-MITO	DMEM+	-	-
MEF-Neo-MITO	DMEM+	-	-
rbESC	CM++	1 : 1 to 1 : 6	G418: 150 µg/ml
rbFB-1	DMEM+	1 : 2 to 1 : 4	G418: 200 µg/ml
rbA-MSC	MSC	1 : 4	G418: 500 µg/ml
rbBM-MSC	MSC	1 : 4	G418: 500 µg/ml 6-TG: 6 µg/ml

2.2.3.1 Media for mammalian cell culture

DMEM+
DMEM (4.5 g/l glucose)
2 mM GlutaMAX
0.1 mM Non-essential amino acids
10% (v/v) FCS

INS1E medium
RPMI 1640
1 mM Na-Pyruvate
1 mM GlutaMAX
11.2 mM HEPES
0.175 mM 2-Mercaptoethanol
10% (v/v) FCS

MSC medium
advanced DMEM
2 mM GlutaMAX
0.1 mM Non-essential amino acids
10% (v/v) FCS
5 ng/ml bFGF

Cryopreservation medium
70% (v/v) growth medium
20% (v/v) FCS
10% (v/v) DMSO

Embryo medium
80% (v/v) TCM
20% (v/v) FCS
0.5 mg/ml gentamycin

CM++
conditioned medium
(DMEM+ cultured on MEFs)
300 U/ml LIF
10 ng/ml bFGF

CM+++
CM++
0.1 µM ROCK-inhibitor

Differentiation medium	Embryoid body differentiation medium 1	Embryoid body differentiation medium 2
Glasgow-MEM BHK-21	DMEM/F12	DMEM/F12
1 mM Na-Pyruvate	0.1 mM Non-essential amino acids	0.1 mM Non-essential amino acids
0.1 mM Non-essential amino acids	1 mM GlutaMAX	1 mM GlutaMAX
2 mM GlutaMAX	100 µM 2-Mercaptoethanol	100 µM 2-Mercaptoethanol
35 nM 2-Mercaptoethanol	20% (v/v) FCS	2% (v/v) FCS
10% (v/v) FCS		

2.2.3.2 Isolation and culture of primary cells

2.2.3.2.1 Isolation of mouse embryonic feeder cells

Pregnant mice were sacrificed at day 13.5 *post coitum* (*p.c.*) and washed with 80% EtOH. After uteri dissection, the foetuses were separated and washed 3 x in D-PBS. To remove neural cells and as much blood as possible the heads, livers, and hearts were cut out and discarded. The remaining bodies of the foetuses were washed 3 x in D-PBS and minced with a razor blade. The minced foetuses were rinsed with 15 ml of trypsin/EDTA/chicken serum and incubated at 37°C and 5% CO_2 for 15 min. The solution containing minced tissues was transferred into a 50 ml conical tube and incubated for 2 min at room temperature (RT) to settle down bigger clumps. Afterwards, s/n was transferred into a 50 ml conical tube, filled up to 50 ml with DMEM+ (containing 100 µg/ml Penicillin/Streptomycin solution (Pen/Strep)) and centrifuged at 340 x g for 5 min. After centrifugation the pellet was resuspended in 50 ml DMEM+ (containing 100 µg/ml Pen/Strep) and plated onto 75 cm^2 flasks. Further cultivation, expansion and mitomycin C treatment procedures were carried out by Angela Zaruba and Peggy Müller.

Before using, the MEF-MITO cells were tested by cultivating them in a 6-well plate (covered with 0.1% (v/v) gelatine in D-PBS) in DMEM+. The quality and colony formation of MEF-MITOs were tested.

2.2.3.2.2 Preparation of feeder plates

Depending on the purpose, 6- or 12 well plates or rather 25- or 75 cm^2 flasks were coated by adding 0.1% gelatine solution for at least 20 min. Gelatine was removed and thawed MEF-MITOs (1 vial per plate, 1 vial per 25 cm^2 flask and 2 vials for 75 cm^2 flask) were plated with DMEM+. The plates with feeder cells were prepared at least 2 h before using them for the cultivation of rbESCs.

2.2.3.2.3 Isolation and culture of putative rabbit embryonic stem cells

Rabbit embryos were obtained by flushing explanted oviducts of superovulated rabbits 19 h *p.c.* and cultured in embryo medium until hatching blastocyst stage. ICM cells were isolated mechanically with sterile needles and plated immediately onto one well of a 12 well plate with feeder cells in CM++. Seven to ten days after initial plating, the ICM outgrowths

(explants) were mechanically dissected and individually re-seeded onto new feeder layers in 12 well plates and continued in culture always on feeder layers. Putative rbESCs spontaneously differentiate when passaged as big clusters (>50 cells). For this, they were routinely passaged as small clumps of cells (10 - 20 cells) using accutase. Mostly, CM++ was supplemented with ROCK-i (10 µM/ml). A sample of the medium was taken on a regular basis to check for the absence of mycoplasmas.

2.2.3.2.4 Isolation and culture of rabbit mesenchymal stem cells

MSCs can be derived both from bone-marrow and adipose tissue. Accordingly, two different methods to obtain these cells were applied.

For the isolation of MSCs from bone-marrow, stromal cells were isolated from the femurs and tibia of 5 week old rabbits. All equipment was cleaned with 80% EtOH and washed in sterile D-PBS. The remaining tissues around the bones were removed, bones were cleaned with 80% EtOH and epiphyses were opened with a saw. The bone-marrow was flushed thoroughly into petri dishes with advanced DMEM and transferred into 50 ml centrifugation tubes while eliminating bigger clumps. The petri dishes were rinsed twice with advanced DMEM and also transferred into the tubes. Then, the solution was filtered through a steel mesh, transferred into 50 ml centrifugation tubes and centrifuged at 600 x g for 10 min. Before removing the whole s/n, the fatty layer on top was removed; the pellet was resuspended in 20 ml MSC-medium (supplemented with 100 µg/ml Pen/Strep and 100 µg/ml Amphotericin B, also in following steps) and centrifuged at 600 x g for 5 min. The s/n was removed and pellet was resuspended in 20 ml MSC-medium. If there was more than one 50 ml tube at the beginning, the cells were pooled after each centrifugation step. At the end, cells were seeded onto 75 cm^2 flasks in MSC-medium. The medium was changed every day after rinsing twice with D-PBS to remove non adherent and hematopoietic cells. Three days after isolation, medium was changed to MSC-medium w/o antibiotics. When cells reached a confluence of 80% they were frozen and stored in liquid N_2. For each flask, a medium sample was taken to verify the absence of mycoplasmas.

For the isolation of MSCs from adipose tissue, fat tissue was isolated with a scalpel of 5 week old rabbits. All equipment was cleaned with 80% EtOH and washed in sterile D-PBS. Tissue was minced with scalpel and scissors and digested in 10 ml sterile filtered collagenase type I/D-PBS (1 mg/ml) at 37°C with shaking every 5 min. Next, the suspension was filtered through a 100 µm cell strainer to remove connective tissue and clumps. This filtrate was resuspended in an equal volume of MSC-medium (supplemented with 100 µg/ml Pen/Strep and 100 µg/ml Amphotericin B, also in following steps), centrifuged at 1000 x g for 10 min,

s/n was removed, pellet was resuspended in 20 ml MSC-medium and seeded onto one 150 cm^2 flask. Following proceedings were the same as described for BM-MSCs.
Both, A-MSCs and BM-MSCs were routinely grown in MSC-medium and passaged using accutase before they reached 80% confluence.

2.2.3.2.5 Isolation and culture of rabbit fibroblast-like cells

For the isolation of fibroblast-like cells, a piece of around 3 cm was cut off of the hind leg muscle of a just now sacrificed male 13 week old rabbit, washed with D-PBS and minced with a scalpel. The minced tissue was rinsed with 15 ml of trypsin/EDTA/chicken serum and incubated at 37°C and 5% CO_2 for 15 min. Then, the tissue was vortexed and minced further while pipetting up and down. The incubation and mincing process was repeated 2 x with incubation times of 10 and 5 min. After the last incubation, in order to settle down bigger clumps, the s/n was transferred into 50 ml conical tubes and filled up to 50 ml with DMEM+ (containing 100 µg/ml Pen/Strep and 100 µg/ml Amphotericin B) and centrifuged at 340 x g for 5 min. After centrifugation the pellet was resuspended in 50 ml DMEM+ (containing 100 µg/ml Pen/Strep and 100 µg/ml Amphotericin B) and plated onto two 75 cm^2 flasks. After 8 days, the cells were passaged, pooled and plated onto four 75 cm^2 flasks with DMEM+. Four days later, three flasks were frozen, while RNA was isolated from the cells of the fourth flask.

2.2.3.2.6 Isolation of rabbit foetal cells

For the isolation of foetal cells, rabbit foetuses 21 day *p.c.* were washed in D-PBS, a piece of around 1 cm was cut off, again washed with D-PBS and minced with a scalpel. Remaining carcasses were frozen at -80°C. The minced tissue was rinsed with 15 ml of trypsin/EDTA/chicken serum and incubated at 37°C and 5% CO_2 for 15 min. Then, the tissue was vortexed and minced further while pipetting up and down. The incubation and mincing process was repeated 2 x with incubation times of 10 and 5 min. After the last incubation to settle down bigger clumps, the s/n was transferred into 50 ml conical tubes and filled up to 50 ml with DMEM+ (containing 100 µg/ml Pen/Strep and 100 µg/ml Amphotericin B) and centrifuged at 340 x g for 5 min. After centrifugation the pellet was resuspended in 25 ml DMEM+ (containing 100 µg/ml Pen/Strep and 100 µg/ml Amphotericin B) and plated onto one 150 cm^2 flasks and cultured.

2.2.3.2.7 Culture of rat insulinoma cells

Rat insulinoma cell line INS1E was cultured in 75 cm^2 flasks in INS1E medium.

2.2.3.3 Cryopreservation and thawing of mammalian cells

For cryopreservation, cells were washed with D-PBS, detached with accutase, pelleted by centrifugation at 340 x g for 5 min and resuspended in culture medium (depends on cell type) and cryopreservation medium in a 1:1 ratio. The cryotubes were placed in a freezing container and frozen down at -80°C**.** For long-term storage, cryotubes were stored in a liquid nitrogen system.

Cryotubes containing frozen cells (either from liquid nitrogen or -80°C) were thawed in a 37°C water bath, washed with 1 ml of appropriate medium in a conical tube and were centrifuged at 340 x g for 5 min. The s/n was discarded, the pellet was resuspended in culture medium and plated onto flask or plate and incubated.

2.2.3.4 Differentiation of stem cells

2.2.3.4.1 Differentiation of rabbit putative embryonic stem cells

Rabbit putative ESCs were differentiated by creating embryoid bodies (EBs) using suspension culture and hanging drops.

Suspension culture

In a procedure similar to passaging, after centrifugation cell clumps were resuspended in 5 ml differentiation medium and plated onto a 10 cm bacterial dish (Petri dish) and incubated for 5 days. The plate was observed daily for the formation of cystic structures. After 5 days, the medium containing floating EBs was transferred into a 15 ml conical tube and incubated for 30 min, to settle down EBs. The s/n was removed, fresh differentiation medium was added carefully and EBs were resuspended by gentle pipetting. EBs were transferred to a gelatine coated 6 well plate, where they were allowed to attach and observed every other day.

Hanging drops

The first steps are similar to the derivation of EBs in suspension culture. RbESCs cultured one passage w/o feeder cells were resuspended in embryoid body differentiation medium 1 (2.2.3.1) and the cells were counted. The cell number was adjusted at 500, 1000, 3000, 5000, 6000 and 7000 cells per 40 µl, whereby 40 µl is the volume of the drop. Drops were given to the inner side of the lid of a bacterial dish; the lid was turned what allowed the drops to hang along the gravitation force gradient. The plate was filled with D-PBS, to avoid drying of the drops. Hanging drops were incubated for 10 days. Afterwards, EBs were transferred to a gelatine-coated 12 well plates with embryoid body differentiation medium 1, where they were allowed to attach. After three days, the medium was changed to embryoid body differentiation medium 2 and changed 3 x per week.

2.2.3.4.2 Differentiation of rabbit mesenchymal stem cells

Adipogenic differentiation

For the adipogenic differentiation 2 x 10^5 cells were plated per well of a 6 well plate using MSC medium. After 48 h, the medium of 3 wells was replaced by adipogenesis medium (Advanced DMEM, 0.1 mM NEAA, 2 mM GlutaMAX, 10% FCS (v/v), 5 ng/ml bFGF, 50 µM 3-isobutyl-1-methylxanthine, 1 µM dexamethasone, 1 x ITS+1, 100 µM indomethacin) whereas MSC medium was used for the other three wells (control) and incubated for 21 days. The medium was changed 2 to 3 x per week. Then, the cells were washed twice with D-PBS, fixed for 5 min. with fixation solution (10% (v/v) formaldehyde/methanol) and the cells were washed 3 x with dH_2O. The cells were covered with Oil Red O solution (1.5 parts Oil Red O (0.3% (v/v)) in isopropanol and 1 part ddH_2O) and incubated for 30 min at RT. Oil Red O solution was rinsed off with ddH_2O. The lipid droplets in the cells stained red and were documented.

Osteogenic differentiation

For the osteogenic differentiation, 3 x 10^4 cells were plated per well of two 6 well plates using MSC medium. After 48 h, the medium of 6 wells was replaced by osteogenesis medium (Advanced DMEM, 0.1 mM NEAA, 2 mM GlutaMAX, 10% FCS (v/v), 5 ng/ml bFGF, 10 µM β-glycerol phosphate, 100 nM dexamethasone, 50 µg/ml ascorbic acid) whereas MSC medium was used for the other six wells (control) and cells were incubated for 21 days. The medium was changed 2 to 3 x per week for 21 days. Then, 3 wells of both the differentiated cells and of the control were used for staining of calcium deposits.

To stain the calcium deposits, the cells were washed twice with D-PBS, fixed for 5 min with fixation solution (10% (v/v) formaldehyde/methanol) as described above. Then, 1 ml of the staining solution (5% (w/v) silver nitrate/ddH_2O) was added per well, incubated for 30 min in the dark and the cells were washed 3 x with dH_2O. One ml dH_2O was added per well and the cells were exposed to UV light (254 nm) for 30 min. After, the H_2O was removed, 1 ml per well of sodium thiosulfate (5% (w/v)/H_2O) was added and incubated for 5 min. The cells were washed 3 x with dH_2O. The calcium deposits stained brownish/black and were documented.

Chondrogenic differentiation

For the chondrogenic differentiation, 5 x 10^5 cells per 15 ml centrifugation tube were centrifuged for 5 min at 340 x g, s/n was discarded, pellet was washed with D-PBS and centrifuged again for 3 min at 3400 x g. The s/n was removed, chondrogenesis medium (Advanced DMEM, 0.1 mM NEAA, 2 mM GlutaMAX, 10% FCS (v/v), 10 ng/ml TGF-β) was added very carefully to not destroy the pellet and cells were incubated in 2 x 15 ml

centrifugation tubes whereas in other 2 x 15 ml centrifugation tubes MSC medium (2.2.3.1) was used (controls). The medium was changed 2 x per week for 21 days. Then, the medium was discarded; the pellet was washed twice with D-PBS and dried by air.
The deposition of proteoglycan was made visible by staining with alcian blue. For this, pellets were covered with alcian blue solution (1% (w/v) alcian blue, 3% (v/v) acetic acid, H_2O (pH 2.5)), incubated for 30 min and washed 3 x with dH_2O.

2.2.3.5 Karyotyping by Fluorescence in-situ hybridisation

To assess the normal rabbit karyotype of established rbESC lines, the number and morphology of chromosomes was assessed with the use of fluorescence *in situ* hybridisation (FISH).
To achieve a sufficient number of dividing cells, rbESCs were grown in a 75 cm^2 flask. Once the cells reached 80 – 90% confluence, the cell cycle was blocked in the methaphase stage by adding demecolcin and incubation for 4 h at 37°C. Cells were detached with accutase, pelleted by centrifugation at 340 x g for 5 min, and resuspended in 500 µl of DMEM+. Subsequently, the cell suspension was slightly vortexed. During vortexing, 10 ml of 0.8% (v/v) NaCitrate was added drop-wise. After incubation at 37°C for 25 min, the cell suspension was centrifuged at 300 x g for 5 min and resuspended in 2 ml fixative (MeOH/glacial acetic acid (3:1)). The centrifugation and fixing steps were repeated 2 x. After the last centrifugation step, cell pellet was resuspended in 1 ml fixative and incubated at -20°C for 10 min. Afterwards, cell suspension was dropped onto pre-chilled glass slides and immediately transferred onto a warm table (40°C) to dry. Dry chromosome spreads were stained with DAPI solution (2 mg/ml in TBST (20 mM Tris-Cl pH 7.4, 0.15 M NaCl, 0.05% Tween-20)) for 3 min, washed 3 x with ddH_2O and air-dried at RT in the dark. Before covering with coverslips, slides were mounted with 35 µl of anti-fade and stored in the dark at RT. The metaphase spreads were observed and counted under fluorescence microscope.

2.2.3.6 Crystal violet staining

Cells in culture were stained by this method, to make easily visible especially colonies but also the confluence. For this, the medium was removed, cells were washed with D-PBS and fixative was added for 5 min at RT. The fixative was removed, cells were washed 3 x with D-PBS and crystal violet staining solution was added and incubated 5 min at RT. Finally, staining solution was removed and cells were washed with ddH_2O. Stained cells were subjected to air drying.

2.2.3.7 Transfection of mammalian cells

2.2.3.7.1 Chemical transfection

The day before the transfection, the cells were split onto a 6 well plate in order to reach a confluence of 80 – 90%. The transfection was carried out according to the manufacturer's instructions of jetPei, Lipofectamine 2000, Metafectene, Nanofectin, Promofectin, SatisFection and Turbofect.

2.2.3.7.2 Electroporation

To prepare the cells for electroporation they were detached with accutase in a process similar to passaging. After the centrifugation step, the s/n was discarded and the pellet was resuspended in hypoosmolar buffer (37°C) to obtain a cell concentration of 5 x 10^5 to 1.5 x 10^7 cells/ml. For each electroporation, 750 µl of the cell suspension were then mixed with 50 µl isoosmolar buffer containing DNA (variable amounts) and incubated 5 to 10 min at RT. This suspension was given in a 4 mm cuvette, electroporated with a single pulse at 300 V for 500 µs and incubated for 5 to 10 min at RT. Then, 1 ml culture medium was added and the cell suspension was plated onto tissue culture vessels and incubated.

2.2.3.7.3 Nucleofection

Since it is not possible to adjust relevant parameters, the method was performed strictly to the manufacturer's instructions. To perform the reaction, the human MSC Nucleofector kit was used where for a single reaction, 5 x 10^5 cells and 2 - 15 µg of DNA were used. The particular nucleofection programs were chosen according to suggestions of technical support.

2.2.3.8 Generation of stable genetically modified cells

For cell selection purposes, the optimal antibiotic concentration was determined by dose response curves. For this, the cells were seeded with the corresponding required minimum confluence on 12 well plates. Into each well, the antibiotic was added in ascending concentration or already in a certain range. A control well with medium w/o antibiotic was included. The medium containing antibiotic was changed 2 – 3 x per week. After 10 days, the lowest concentration at which no living cells can be seen was selected.

To select for stably transfected cells, the medium was replaced with fresh medium and the appropriate antibiotic (Table 3) was added two days after the transfection. The medium containing antibiotic was changed 2 – 3 x per week until single colonies were visible

3 RESULTS

3.1 Transposon-mediated transgenesis

In this section, the method of genetic manipulation using the sleeping beauty transposon system was established. Therefore, transposon vectors for the proof of its functionality were produced and tested both *in vitro* and *in vivo*. Further, the rabbit *insulin* was cloned, Akita mutation introduced and finally proofed to be functional. The detailed information concerning vector construction is given in appendix.

3.1.1 Construction of rabbit *insulin* expression vectors

To show the functionality of the Akita mutation in rabbit insulin, the mutated *insulin* needs to be expressed in an *in vitro* system.

At the outset of this project no sequence data regarding rabbit *insulin* were available, thus it was identified based on homology to human, mouse and rat insulin genes. During the time period of this project the sequence of rabbit *insulin* become available in the GenBank (access number: DP001064.1).

Both the promoter region and transcription unit were amplified using primer pair rbIns-5'region (promoter) and oligonucleotides rbIns-ex1-fwd and rbIns-ex3-rev (transcription unit) (see 2.1.14.1). The resulting fragments, whose correctness was verified by restriction digests, were each ligated into the cloning vector pjet1.2 and again verified by restriction digests and sequencing.

In order to insert the desired Akita mutation (transition of guanine to adenine at position 303) into the rabbit *insulin* gene the Quick Change II-E Site-Directed Mutagenesis kit was used. After transformation, positive colonies were identified by colony PCR, restriction digests and sequencing. It was found that all sequences were correct and the desired mutation was inserted.

In the next step, the two parts of *insulin*, promoter and either the mutated or non-mutated transcription unit were combined.

In a final cloning step, a poly adenylation signal (polyA) was added to both *insulin* and Ins^{Akita} expression vectors. For this, the vectors from the previous step were linearized and the 3 x polyA cassette (5´- 3´: SV40, bovine growth hormone and CMV) was inserted. The final vectors (Fig. 18) were verified by restriction digests and sequencing with oligonucleotides rbIns-pA-fwd, pjet1.2 Sequencing Primer-fwd and –rev. It was found that all sequences were

correct. Thus, both *insulin* and *Ins*^{Akita} expression vectors, pINS^{WT} and pINS^{Akita}, were successfully constructed and were used in further experiments.

Figure 18: Schematic draw of rabbit *insulin* and 3 x poly adenylation signal placed behind.
The sizes of promoter, coding sequence and pA are indicated. The red asterisk marks the transition of guanine to adenine at position 303. In the control vector, this mutation is missing.

3.1.2 Verification of the functionality of insulin expression vectors

To verify the functionality of the mutated and non-mutated *insulin* expression vectors, the *insulin* expressing insulinoma cell line INS1E was transfected with either pINS^{WT} or pINS^{Akita}. Upon transfection with pINS^{Akita}, it is expected that INS1E cells will die due to the mutation which causes a misfolding of INS (discussion 4.1.1). Both vectors were co-transfected with pPGK-Neo using a 10 : 1 molar ratio for selection reasons. For both vectors, 3 µg, 4 µg, 5 µg, 6 µg and 7 µg of DNA per well of a 6-well plate were transfected applying nanofection. After two days, INS1E cells were subjected to G418 selection. After 12 days, colony formation was observed. No cells survived after transfection with pINS^{Akita} whereas cells transfected with the non-mutated version (pINS^{WT}) were growing normal (Fig. 19).

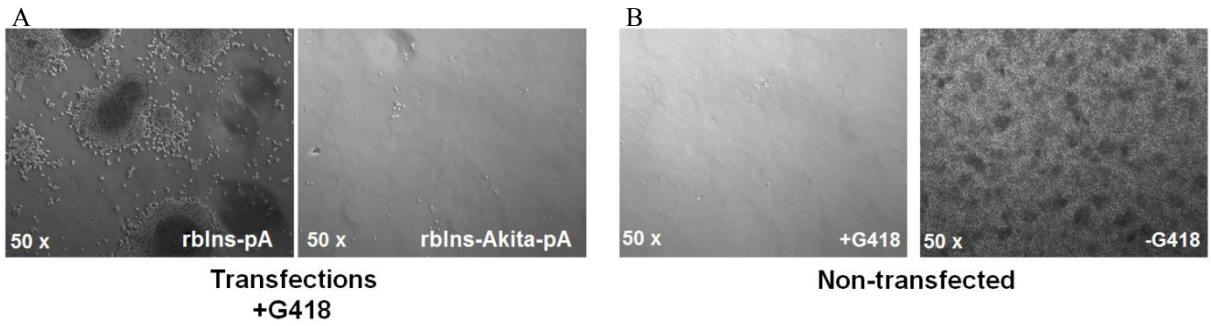

Figure 19: Co-transfection of either pINS^{Akita}: pPGK-Neo (10 : 1) or pINS^{WT} : pPGK-Neo (10 : 1) into INS1E cells.
A) Cells transfected with pINS^{WT} grew under G418 selection, whereas cells transfected with pINS^{Akita} died. **B)** Non-transfected cells died under G418 selection (negative control) but grew w/o selection pressure (positive control).

To show that the promoter is active in insulin-producing cells only, both vectors were co-transfected into rabbit fibroblasts (rbFB-1) as described for INS1E cells. As fibroblasts do not express *insulin*, transfection with any *insulin* expression vectors was expected to not affect fibroblast growing properties. Indeed, it was shown that neither of the two vectors (pINS^{WT} and pINS^{Akita}) had any influence on the growth of rbFB-1 (Fig. 20).

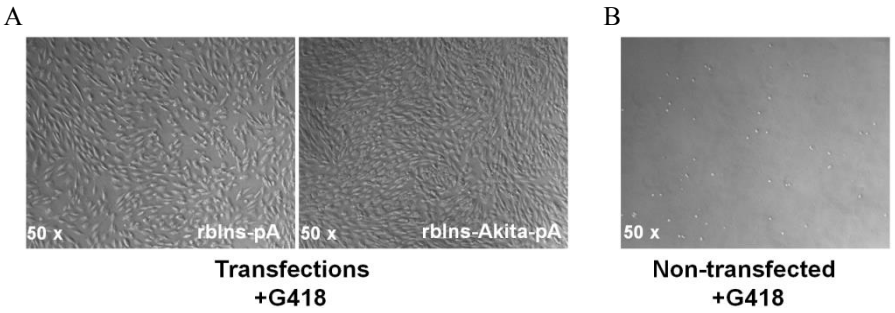

Figure 20: Co-transfection of either pINS^{Akita} : pPGK-Neo (10 : 1) or pINS^{WT} : pPGK-Neo (10 : 1) into rbFB-1.
A) Cells transfected with pINS^{WT} grew under G418 selection as well as cells transfected with pINS^{Akita}. **B)** Non-transfected cells died under G418 selection (negative control).

It was shown in the above experiments, that both *insulin* expression vectors are functional. Importantly, it was shown that insulin is expressed in insulin expressing cells only and not in others thereby verifying the specificity of the promoter. However, these results are only based on phenotypic observations. To verify the expression of *Ins^{Akita}* on molecular level (by RT-PCR), a different experimental setup needs to be performed. As shown, *Ins^{Akita}*-expressing cells are dying, minimizing the isolation efficiency of intact total RNA. Therefore, to verify the expression of *Ins^{Akita}*, total RNA needs to be isolated soon after transfection and after onset of transgene expression but prior to induced cell death. To enrich for transfected cells the selection procedure of the MACS-system was used 24 h after transfection.

The selection vector pMACSK^{k} II expresses a specific cell surface marker allowing selection for successfully transfected cells. pINS^{WT} or pINS^{Akita} was co-transfected with pMACSK^{k} II in a mass ratio of 5 : 1 (*Insulin* expression vector : pMACSK^{k} II) using 7 µg total DNA per well of a 6 well plate. Each of the two combinations was done in quadruple.

For RT-PCR, total RNA was isolated at two time points (24 h and 48 h post transfection). After verification of the intactness of RNA, RT-PCR with oligonucleotides RT-INS-fwd and RT-INS-rev was performed. The primer pair used for this reaction was designed to amplify both RNA (303 bp) and DNA (666 bp) of rabbit *insulin*.

Specific band (303 bp) for mRNAs for both *Ins^{WT}* and *Ins^{Akita}* were present on the agarose gel, whereas non-transfected cells did not show any band as well as water control (Fig. 21). The absence of insulin DNA contamination in the RNA samples was verified by the lack of the 666 bp band. Only DNA control (pINS^{Akita}) showed a characteristic band at the expected size. Those results proofed the expression of both *pIns^{WT}* and *Ins^{Akita}*.

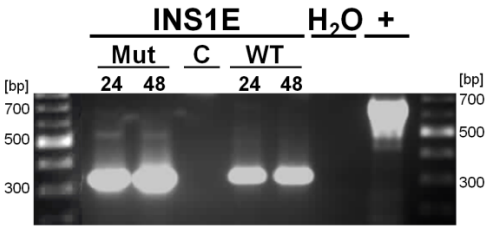

Figure 21: RT-PCR for rabbit *insulin* of co-transfected INS1E cells using either pINS^{Akita} : pMACSK^{k} II (5 : 1) or pINS^{WT} : pMACSK^{k} II (5 : 1).
Total RNA was isolated 24 h and 48 h post transfection. Mut: Co-transfection of pINS^{Akita} : pMACSK^{k} II, C: non-transfected INS1E cells (negative control), WT: Co-transfection of pINS^{WT} and pMACSK^{k}, +: pINS^{Akita} DNA. Primer pair detects both DNA (666 bp) and mRNA (330 bp).

3.1.3 Verification of the functionality of Sleeping Beauty transposon system

In the previous experiments (3.1.2), the two vectors carrying rabbit *insulin* and the Akita mutation proofed to be functional. In the next step, the Sleeping Beauty (SB) transposon system was verified for functionality in the rabbit. For this, a visible marker (red fluorescence protein mCherry) was used. To verify the functionality of the constructed SB system in rabbits, an *in vitro* assay was performed. In addition, it was proofed that the known phenomenon of transposase overproduction inhibition occurs also in rabbits. Hence, the optimal ratio of *SB100* to gene of interest (GOI) was determined.

For subcloning, *SB100 transposase* was cloned into pCAGGseGFP of which the *enhanced green fluorescent protein* (*eGFP*) cassette was removed by restriction digest. The correctness of the resulting transposase expression vector pCAGGsSB100 (Fig. 22 A) was verified by restriction digests.

The vector bearing the transposase recognition sequences (SB-IRs) was prepared to be ready for simple insertion of any GOI. For this, the vector pT2BDS3 was digested to remove unnecessary sequences between IRs. Then, the superlinker of pSL1180 Amersham, was subcloned between both SB-IRs into pT2BDS3. The resulting pT2-SB-polylinker was verified by restriction digest.

Afterwards, the first GOI, *CAGGs-mCherry*, was subcloned from pCAGGs-mCherry into the superpolylinker resulting in the vector pT2-SB-CAGGs-mCherry (Fig. 22 B), which was verified by restriction digests and sequencing.

Figure 22: Two vector SB-system.
The transposase, necessary for transposition of target gene, is delivered as a separate vector. **A)** Schematic draw of pCAGGsSB100. The SB100 transposase is directed by a CAGGs promoter and stopped by rabbit β-globin polyA. **B)** Schematic draw of the transposable *mCherry* red fluorescence transgene vector pT2-SB-CAGGs-mCherry. *mCherry* is directed by CAGGs promoter and stopped by rabbit β-globin polyA. The expression cassette is flanked by SB inverted repeats (IR) and has a total size of 3145 bp.

In a first experiment, the optimum molar ratio of pT2-SB-CAGGs-mCherry to pCAGGsSB100 was determined. The four molar ratios used were: 1 : 1, 1 : 0.5, 1 : 0.1 and 1 : 0.01. For this, 3 µg of total vector DNA per well of a 6 well plate was transfected into rbMSCs using nanofectin. As a control, rbMSCs were transfected with pT2-SB-CAGGs-mCherry and pCAGGsSB100 separately.

48 h after transfection it could be shown that transfection efficiency increased with decreasing amount of pCAGGsSB100 (transposase) (Fig. 23 A). Thus, the phenomenon of overproduction inhibition was shown to occur in rabbit MSCs and the functionality of SB system was verified. As expected, a control transfection of pT2-SB-CAGGs-mCherry alone resulted in moderate expression of *mCherry* (Fig. 23 B). However, the number of fluorescing cells was 2-fold higher when co-transfected with pCAGGsSB100 at a 1 : 0.01 ratio. The control transfection of pCAGGsSB100 alone resulted in no *mCherry* expression.

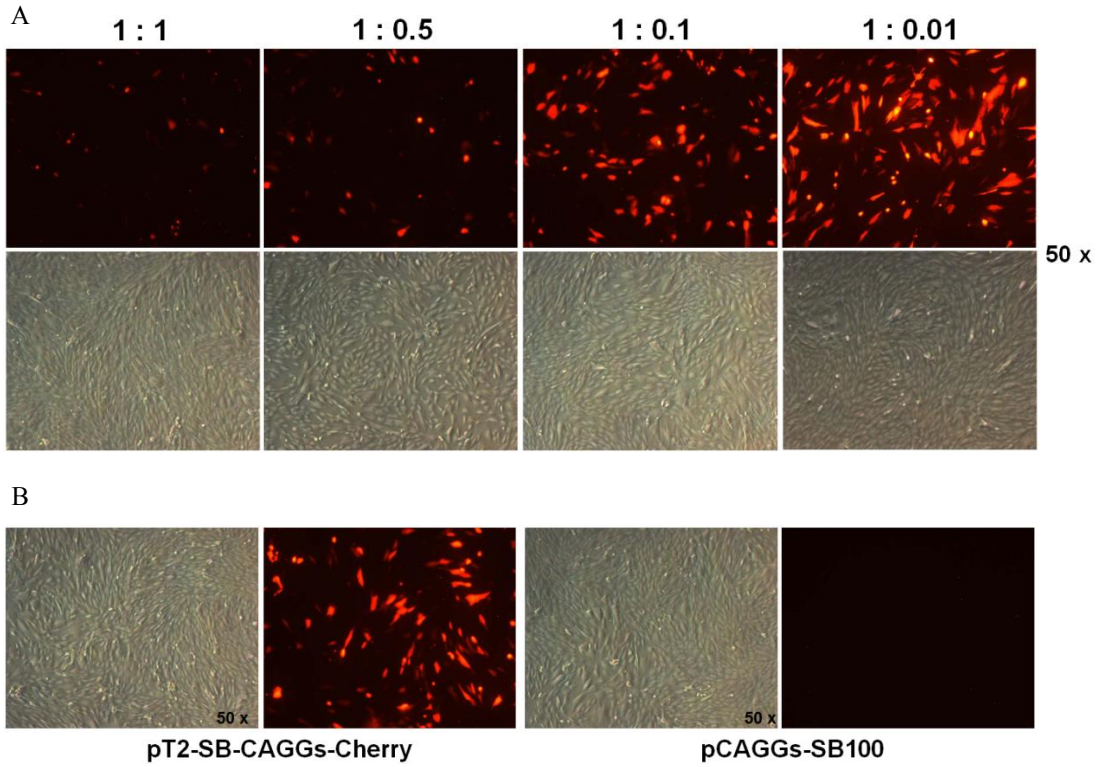

Figure 23: Verification of the functionality of SB vector system by the use of *mCherry* red fluorescent transgene in rbBM-MSC P1.
A) Co-transfection of transposable vector (pT2-SB-CAGGs-mCherry) and transposase expression vector (pCAGGsSB100) in distinct ratios (1 : 1, 1 : 0.5, 1 : 0.1 and 1 : 0.01). **B)** Controls: Transfection of each vector (pT2-SB-CAGGs-mCherry and pCAGGsSB100) alone.

3.1.4 Generation of transgenic rabbits by transposon-mediated transgenesis

To generate transgenic rabbits, vector DNA of GOI and transposase at a total concentration of 0.4 ng/µl was microinjected into rabbit fertilised oocytes. Afterwards, the developing embryos were transferred to surrogate mothers.

The vector carrying the GOI (*mCherry* or *Ins*^{Akita}) was used as circular as well as linear (linearized by XmnI) vector in these experiments.

3.1.4.1 Generation of transgenic rabbits carrying mCherry red fluorescent protein

Based on the results of the *in vitro* experiments (3.1.3), a ratio of 1 : 0.01 (pT2-SB-CAGGs-mCherry to pCAGGsSB100) was used for microinjection. Table 4 summarises these experiments. A total of 19 surrogate mothers were used of which 8 got pregnant and a total of 29 foetuses could be recovered at day 21 *p.c.* Of those, 14 were transgenic and the transgenesis frequencies of recovered embryo per surrogate mother were ranging from 25 to 90%.

Table 4: Summary of the microinjection experiments of SB-system with *mCherry* as transgene.
For each injection experiment the number of injected embryos, the number of embryos transferred to surrogate mother, the number of recovered foetuses (day 21 *p.c.*), the number of transgenic foetuses and the corresponding transgenic frequencies per recovered embryos are given.

No. of injected embryos	No. of surrogate mothers	No. of transferred embryos	No. of recovered foetuses	No. of transgenic foetuses	Transgenic frequency of recovered embryos [%]
60	1	24	10	9	90
74	2	36	3	2	66.7
		38	0	-	-
8	1	8	1	0	0
46	1	24	0	-	-
62	2	29	8	2	25
		25	0	-	-
31	1	17	2	0	0
41	2	23	0	-	-
		18	0	-	-
48	1	38	3	0	0
74	2	39	2	1	50
		38	0	-	-
97	2	45	0	-	-
		52	0	-	-
72	2	36	2	0	0
		36	0	-	-
75	2	30	0	-	-
		30	0	-	-

The transgenic status of all foetuses was analysed by PCR with primer pair SB-Cherry. The correct identity of the obtained PCR products was proven by restriction digests. Further, the sensitivity of targeting PCRs was determined. It was found that 5 copies of pT2-SB-CAGGs-mCherry were necessary to obtain a band on the agarose gel.

From 18 foetuses fibroblast-like cells were also isolated. Cells in culture were observed for mCherry expression visible by red fluorescence (Fig. 24 A). All those cells exhibiting red fluorescence also showed a positive band for *mCherry* in the PCR (Fig. 24 B). As expected, cells not exhibiting red fluorescence were negative for *mCherry* in the PCR. Further, *mCherry* positive cells were tested for integration of the co-transfected vector pCAGGsSB100. It was demonstrated that this vector was not integrated (Fig. 24 C).

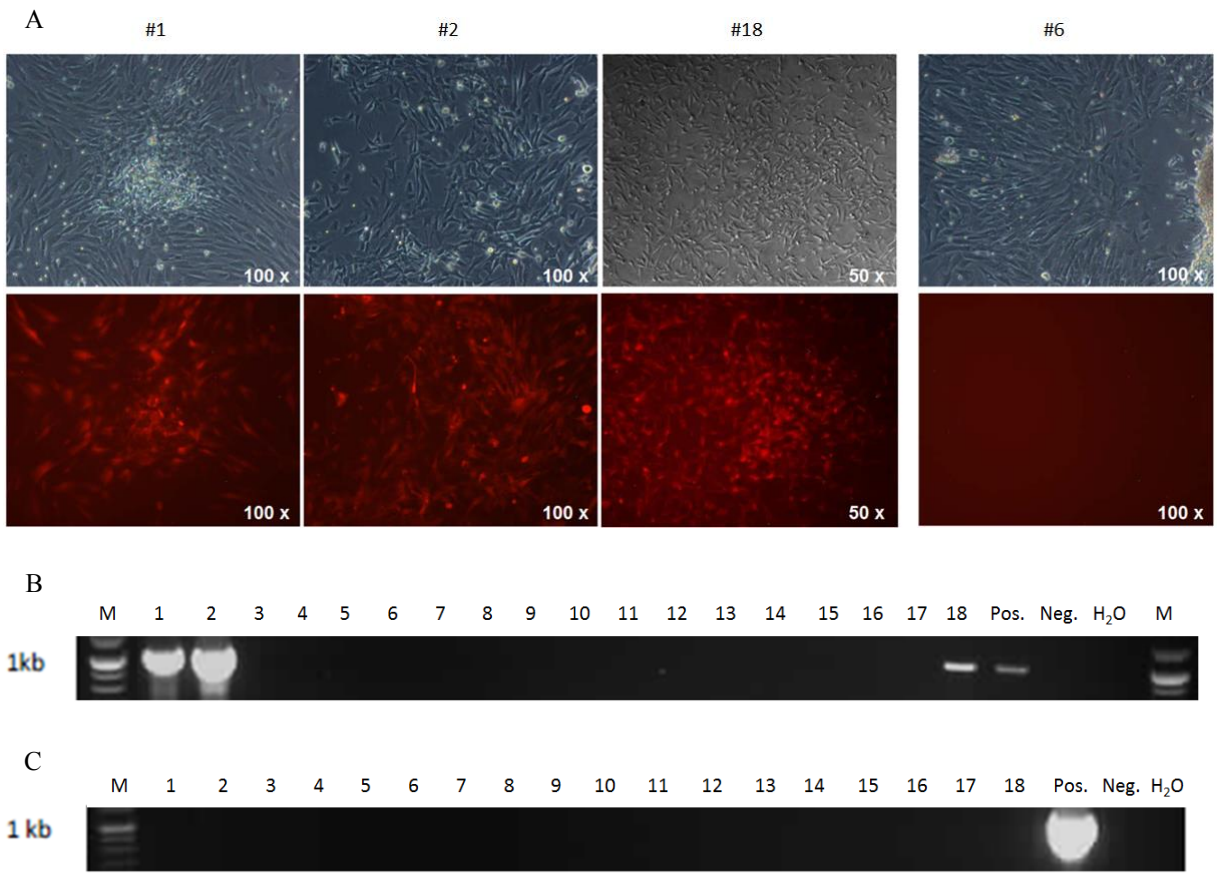

Figure 24: Transgenic rabbit foetuses obtained by applying mCherry SB-transposon system.
A) Isolated and cultured foetal fibroblasts expressing red fluorescent *mCherry* (# 1, 2 and 18) and exemplary foetal fibroblasts of a negative foetus (# 6). **B)** PCR for *mCherry* on genomic DNA isolated of cultured foetal fibroblasts. Pos.: pT2-SB-CAGGs-mCherry DNA, Neg.: wild type (wt) DNA **C)** PCR for SB100 on genomic DNA isolated of cultured foetal fibroblasts. Pos.: pCAGGsSB100 DNA, Neg.: wt DNA

To assess the copy number of integrated pT2-SB-CAGGs-mCherry, Southern Blot analysis was performed. For this, 11 µg of genomic DNA of *mCherry* positive foetuses and of wild type (wt) animals was restriction digested with BlpI (Fig. 25). Before using these digests for Southern Blot and to verify the DNA amount, a volume corresponding to 1 µg was taken out and run on an agarose gel. Due to the random integration of SB, it is not possible to predict a precise band size on the Southern Blot. Although a second restriction site could be chosen, but then it is not possible to assess the copy number.

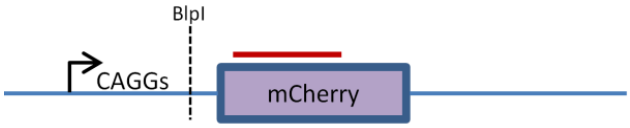

Figure 25: Location of the recognition site of the restriction enzyme BlpI on the vector pT2-SB-CAGGs-mCherry.
The bold red line indicates the annealing of the Southern Blot hybridisation probe. Positions are not to scale.

The Southern Blot verified the integration of pT2-SB-CAGGs-mCherry in all samples but not in WT. In each sample lane, two bands are visible which indicates a double integration of pT2-SB-CAGGs-mCherry into the rabbit genome (Fig. 26).

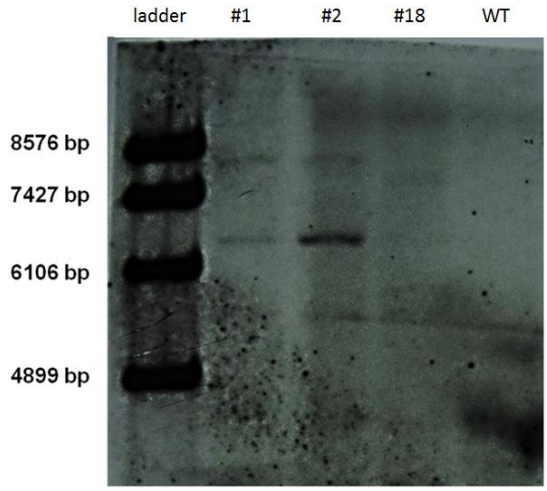

Figure 26: Southern Blot analysis of DNA of the three positive foetuses and of WT as negative control.
In each lane of samples #1, #2 and #18 two bands are visible, but no band in WT genomic DNA control.

3.1.4.2 Generation of transgenic rabbits carrying mutated rabbit *insulin*

Since the SB system with *mCherry* resulted in promising outcomes both in tissue culture and animal experiments and the *insulin* vector proved its functionality in tissue culture experiments as well, the *Ins*^{Akita} cassette including 3x polyA was cloned into pT2-SB-polyinker. The resulting vector pT2-SB-INS^{Akita} (Fig. 27) was successfully verified by restriction digests and sequencing.

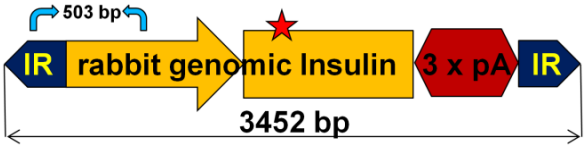

Figure 27: Schematic draw of pT2-SB-INS^{Akita} bearing the transposable rabbit *Ins*^{Akita} transgene and artificial 3x polyA.
The expression cassette is flanked by SB inverted repeats (IR) and has a total size of 3452 bp. Blue arrows indicate the annealing sites of primer pair SB-Ins-rev-5-a used for subsequent analysis.

Again, the vector was linearized and a ratio of 1 : 0.01 (pT2-SB-INS^{Akita} to pCAGGsSB100) was used. The injection procedure and conditions were the same as for *mCherry* (3.1.4.1). In these experiments, embryos were not transferred to surrogate mothers but kept *in vitro* until blastocyst stage. Due to legal restrictions, no transfer into surrogate mothers could be carried out. Therefore, blastocysts were cultivated separately on 24 well plates until hatching. Prior to DNA analysis, cultivation of cells was carried out to minimize false positive results due to non-integrated vector DNA that may still present after microinjection. Thus, cells obtained from hatched embryos were grown until 95% confluence. In two rounds of microinjections genomic DNA was isolated of 57 embryos that grew out and PCR analysis was performed to verify the presence of pT2-SB-INS^{Akita}. Here, it is important that at least one primer does not anneal in the rabbit *insulin* sequence. Hence, primer pair SB-Ins-rev-5-a was used. The PCR analysis confirmed the presence of pT2-SB-INS^{Akita} in the outgrowths of 54 embryos

(Table 5, Fig. 28). For each microinjection round, these results correspond to transgenic frequencies of 31.6% and 72% per initially cultivated embryo, respectively. In a further PCR reaction, the absence of pCAGGsSB100 was verified in all 57 embryos (data not shown). The third round of injections with 34 cultivated embryos resulted in no hatching embryos.

Table 5: Summary of the microinjection experiments of SB-system with rabbit *Ins*^{Akita} as transgene.
Here, embryos were cultivated *in vitro* until 95% confluence of the outgrowth, genomic DNA was isolated and analysed by PCR for the presence of pT2-SB-INS^{Akita}.

No. of injected embryos	No. of cultivated embryos	No. of hatched embryos	No. of transgenic embryos	Transgenic frequency of hatched embryos [%]
58	57	20	18	90
52	50	37	36	97.3
34	34	0	-	-

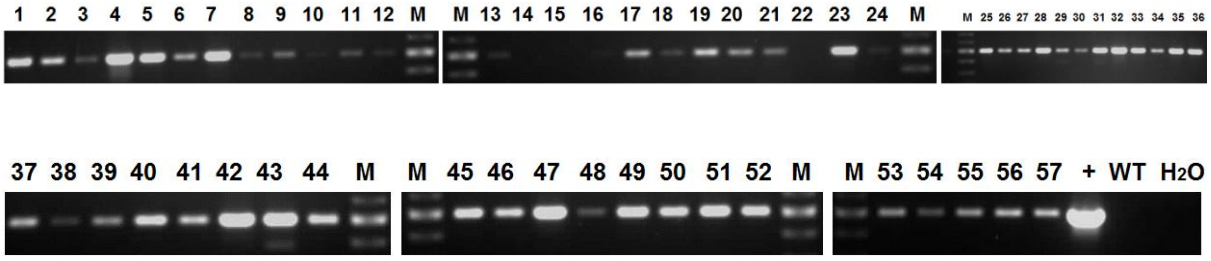

Figure 28: PCR analysis of putative transgenic rabbit embryos obtained applying SB-transposon system.
PCR for SB-IR/rabbit *insulin* on genomic DNA isolated of cultured embryonic cells. +: positive control pT2-SB-INS^{Akita} DNA, WT: negative control WT DNA, M: 100 bp ladder.

3.1.5 Summary

To obtain transgenic rabbits by the method of transposon-mediated transgenesis, important technical prerequisites were established and valuated. Thus, the Sleeping Beauty transposon system was successfully established and applied in the rabbit. Using a *mCherry* reporter construct, a high percentage of transgenic red fluorescent rabbit foetuses was obtained. Furthermore, to obtain a transgenic rabbit for biomedical research, a high percentage of transgenic blastocysts using a rabbit *Ins*^{Akita} construct was shown. Further experiments with this construct could not be performed due to missing legal permissions.

3.2 Cell-mediated transgenesis

In this chapter results of the isolation, characterisation and manipulation of both pluripotent and multipotent stem cells are described, which may support cell-mediated transgenesis.

3.2.1 Pluripotent stem cells

During my Master thesis [509] I attempted to isolate rbESCs. However, it was not possible to maintain a pure ESC-like phenotype. The routinely used medium was conditioned medium supplemented with LIF, bFGF and ROCK-i (CM+++). All rbESCs in culture underwent to some extend differentiation resulting in a mixed population of rbESCs and differentiated cells. Morphological, rbESCs were defined by the formation of round colonies with clear margins. The rounded and tightly packed cells exhibited a high nucleus/cytoplasm ratio with prominent nucleoli. To obtain pure rbESC colonies, the method of isolation of inner cell mass (ICM) cells and their further cultivation was modified.

The preliminary results of the Master thesis include the verification of expression of *Oct4*, *Nanog*, *FoxD3*, *Nodal*, *Rex1*, *DPPA5*, *TERC* and *BMP4* by RT-PCR and the verification of alkaline phosphatase (AP) activity by chemical staining method and OCT4 by immunostaining. In addition, one chimeric rabbit was born. Further, the karyotype of distinct lines appeared to be stable in low and high passages.

3.2.1.1 Derivation of rabbit pluripotent stem cells

In this section, several experiments are described to optimise the derivation of rbESCs.

It has been shown in the Master thesis that the insulin-like growth factor 2 (IGF2) has a positive effect on the culture of rbESCs. Therefore, in a first experiment the ICM of 48 blastocysts was isolated and cultivated in two distinct media: a) in conditioned medium supplemented with 3 factors LIF, bFGF and ROCK-i (CM+++ (2.2.3)) and additionally supplemented with IGF2 (20 ng/ml) (24 isolations) and b) the other 24 ICM cells were cultured in CM++ (w/o bFGF) but supplemented with IGF2 (20 ng/ml). After 8 days, 15 ES-like colonies in medium (a) containing IGF2 and 14 colonies in same medium but w/o bFGF (b) became visible. There were no morphologic differences in those colonies. Also, their growth and morphologic characteristics during further growth did not change visibly.

In a further experiment, similar conditions were applied. Here, the ICM of 18 blastocysts was cultured in CM+++ supplemented with IGF2 (20 ng/ml), whereas the ICM of 18 other blastocysts was cultured in CM+++. Of the first group, 12 explants could be achieved and of the 2nd group 11 explants. Different from the previous experiment, some lines cultured in

CM+++ and additional IGF2 supplementation grew as perfect monolayers without morphological signs of other cell types and exhibited typical ES-like morphology present in all cells of the concerning line. Those lines were also alkaline phosphatase (AP) positive as verified by chemical AP staining. One line was subjected to differentiation assays and induced to differentiate into cells of the three germ layers by addition of bFGF, activin A and retinoic acid. However, only differentiation into a fibroblast like phenotype could be observed.

Another attempt was to isolate cells of the developing rabbit embryo at different stages, ranging from morula to early blastocyst. Usually, ICM was isolated exclusively from early to late blastocyst stage. In comparison, 32 explants out of 35 embryos from early to late blastocyst stages could be obtained (91.4%), whereas only 5 explants out of 36 embryos from morula to early blastocyst stage could be achieved (13.9%).

During all experiments, 48 lines of putative rbESCs could be established in this thesis.

3.2.1.2 Optimisation of the *in vitro* culture of rabbit putative embryonic stem cells

The line rbESC-5 (established in the master thesis) was used for most experiments and characterised intensively. To reveal the optimal culture conditions of rbESCs, rbESC-5 at passage 13 was tested in a combination of both absence and presence of LIF, ROCK-i and bFGF in both basic media CM and mES (standard mESC medium) (Table 6). In addition, IGF2 was added w/o any other supplementation into both CM and mES.

Table 6: Overview of the supplements and their combinations used to reveal the optimal conditions.
Each combination was used in both CM and mES. Note that the combination of CM 6 is identical to CM++ and CM 8 is identical to CM+++ of previous experiments.

	Combinations								
Supplement	1	2	3	4	5	6	7	8	9
LIF	-	-	-	+	-	+	+	+	-
ROCK-Inhibitor	-	-	+	-	+	-	+	+	-
bFGF	-	+	-	-	+	+	-	+	-
IGF2	-	-	-	-	-	-	-	-	+

This medium experiment was conducted over a period of 33 days and 5 passages. The cells were assessed 3 x per week on the basis of what showed before to be typical rbES-like morphology (3.2.1). The first assessment was three days after initial seeding of the cells (Tables 7 and 8). Usually, this is the time the first colonies become visible after thawing. The results as means of morphologic description are given in (Tables 7 and 8).

Table 7: Summary of the morphologic results of the medium condition experiment using CM as basic medium.
The combination # refers to the combination of supplements outlined in Table 6.

Combination #	3 days post seeding	33 days post seeding
1	Some ES-like cells, lot of differentiation	Mainly ES-like colonies, but also differentiated cells
2	More ES-like cells compared to #1, but also lot of differentiation	Mainly ES-like colonies, but also differentiated cells
3	Mainly ES-like cells, few differentiation	Almost exclusively differentiated cells, nearly no ES-like cells
4	No ES-like cells, only differentiated cells	Some nearly perfect and big ES-like colonies, lot of differentiation
5	Mainly ES-like colonies, few differentiation	Some ES-like colonies, lot of differentiation
6 (= CM++)	Mainly ES-like cells, lot of differentiation	Some big ES-like colonies, also differentiation
7	Mainly ES-like cells, very few differentiated cells	Almost exclusively differentiated cells, very few ES-like cells
8 (= CM+++)	Lot of ES-like cells, more differentiation compared to #5	Mainly ES-like colonies, but also differentiation
9	Almost no ES-like cells, lot of differentiation	Some nearly perfect and big ES-like colonies, bit of differentiation

Table 8: Summary of the morphologic results of the medium condition experiment using mES medium as basic medium.
The combination # refers to the combination of supplements outlined in Table 6.

Combination #	3 days post seeding	33 days post seeding
1	Lot of differentiation	Mainly ES-like colonies, but also differentiated cells
2	Lot of differentiation	Mainly almost perfect ES-like colonies, but also differentiated cells
3	Some ES-like cells, differentiation	Some few ES-like colonies, lot of differentiated cells
4	No ES-like cells, lot of differentiation	Some nearly perfect and big ES-like colonies, lot of differentiation
5	Mainly ES-like cells, almost no differentiation	Some ES-like colonies, lot of differentiation
6	Lot of differentiation	Lot of small ES-like colonies, also differentiated cells
7	Mainly ES-like cells, but no colonies, few of differentiation	Some few ES-like colonies, differentiation
8	Only few ES-like cells, lot of differentiation	No ES-like colonies, nearly no ESCs
9	Only few ES-like cells, lot of differentiation	Some nearly perfect and big ES-like colonies, bit of differentiation

These experiments revealed positive and negative effects of the used supplements. Surprisingly, if ROCK-i was used exclusively in both standard media (CM++ and CM+++), nearly all cells differentiated (Table 9, Fig. 29). This condition was even worse than without any supplementation. However, when ROCK-i was used in combination with LIF, the morphologies improved and were good when bFGF was supplemented as third compound. Surprisingly, this was only so for CM as basic medium but not when mES was used. As shown already for the derivation of rbESCs, the supplementation of IGF2 enhanced *in vitro*

cultivation in both mES and CM. This experiment showed that most suitable media might be CM supplemented with LIF + bFGF + IGF2 and LIF + bFGF + ROCK-i. The latter one was used routinely (CM+++). During the course of experiments, typical ES-like cells with nearly perfect morphology were observed over 3 passages in CM w/o any supplements but disappeared later. This indicated the easy to influence putative pluripotent state.

Table 9: Complete overview of the results of the medium condition experiment.
Good looking morphological results are highlighted in green whereas negative ones are highlighted in red. Morphologic observations are ranked by numbers from 1 (best) to 6 (worst).

rbESC-5 P13	CM	mES
+LIF	3	3
+bFGF	3	2-
+ROCK-i	5	4-
+IGF2	2	2
+LIF, +ROCK-i	4	4
+LIF, +bFGF	2	3
+bFGF, +ROCK-i	4	4
+LIF, +bFGF, +ROCK-i	2	5
-	3	3

1: perfect rbESCs
2
3
4
5
6: complete differentiation

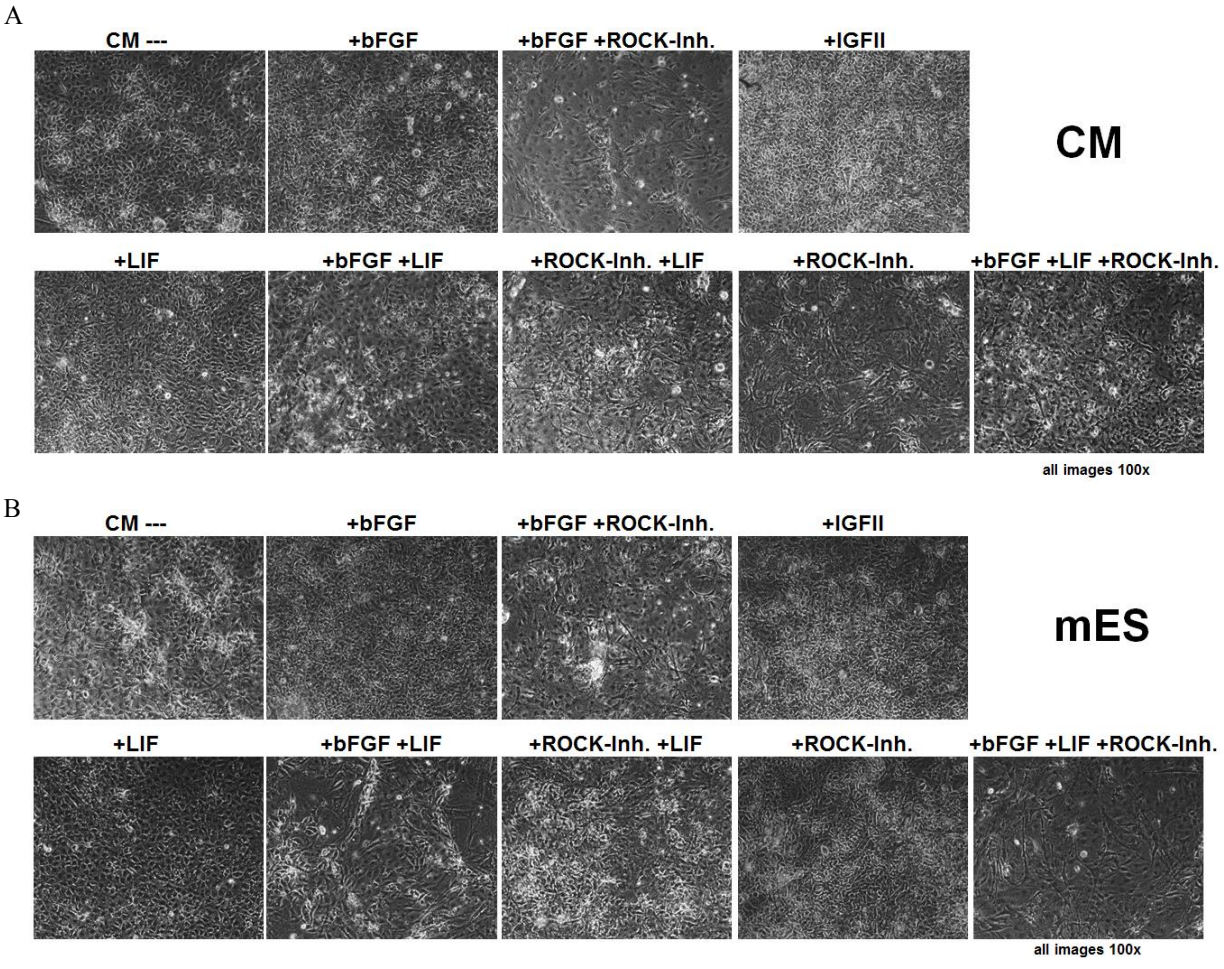

Figure 29: Typical morphology of putative rbESCs under specific conditions of the medium composition experiment.
The both basic media (CM (A) and mES (B)) were supplemented with the indicated combinations of molecules and morphological assessed.

In an additional experiment that was conducted at the same time, rbESC line 5 P14 was cultured under three different conditions: CM+++ but w/o feeder cells, CM and mES. This experiment was conducted over 78 days. The cells grew for 14 passages (CM: 11 passages) under those conditions. The cells in CM exhibited a slower proliferation rate and reached three passages fewer compared to cells in the two other media. Remarkably, rbES-like cells under all three conditions grew as perfect monolayers (Fig. 30). As a rapid morphological test, the cells cultured w/o feeders were changed from CM+++ to DMEM+, in which they changed their morphology within 3 passages dramatically to typical fibroblast-like phenotype indicative for differentiation. A karyotyping of the three sublines derived from CM, mES and CM+++ but w/o feeder cells was performed to assess the integrity of the chromosomes (Table 10) which was shown to be normal. Since the diploid rabbit karyotype consists of 44 chromsomes (Fig. 31) it is expected that the majority of chromosome counts reveals this number. Indeed, the mode of each subline was 44. However, the percentage of cells exhibiting exactly 44 chromosomes differs between the sublines. Nevertheless, cells exhibiting more than 44 chromomes were around 7 – 8%, except cells that were cultured without feeders. These cells exhibited more then 44 chromosomes at a higher frequency (16.4%).

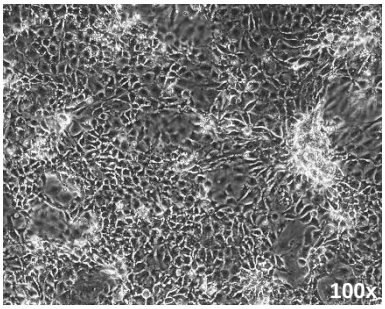

CM---

Figure 30: Typical morphology of the long term medium experiment of rbESC in CM.

Table 10: Summary of counted chromosomes obtained from karyotyping of cells cultivated under stated conditions.

No. of Chr.	-MEF-MITO CM+++	CM	mES
< 44	31 (46.3%)	33 (58,9%)	49 (48,5%)
44	25 (37.3%)	19 (33,9%)	49 (48,5%)
> 44	11 (16.4%)	4 (7,1%)	8 (7,9%)
total	67	56	101
mode	44	44	44

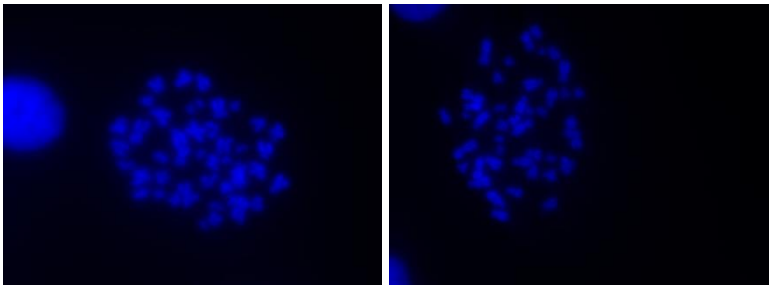

Figure 31: Typical karyotype of rabbit normal diploid chromosome set after DAPI staining.

To estimate the ability of rbESCs for NT, experiments were performed with non-transfected as well with stably transfected rbESCs (3.2.1.3). Since these experiments were done also with MSCs, the results are summarized in chapter 3.2.3.

3.2.1.3 Assessment of optimal transfection methods for rabbit embryonic stem cells

To reveal the optimal method for transfection of rbESCs, different methods were assessed.

In a first experiment, the method of electroporation was applied on rbESC-5 P12 using distinct cell concentrations ($1x10^6$ and $1x10^7$ cells/ml) and different amounts (1, 5 and 10 µg) of *eGFP* expressing plasmid (pEGFP-C1). As negative control, electroporation w/o DNA was performed. After 48 h, cells were observed for green fluorescence. In general, there were nearly no colonies with ESC-like phenotype visible and expression of *eGFP* was only detected when 10 µg DNA in combination with 10^6 cells/ml were used. Five and nine days after electroporation, there was no fluorescence visible at all due to a massive loss of cells except two *eGFP*-expressing ESC-like colonies (1 µg DNA, 10^6 cells/ml and 10 µg DNA, 10^6 cells/ml).

Since electroporation did not provide in satisfying results, three distinct particle-based transfection reagents (Lipofectamine 2000, Nanofectin and TurboFect) were used to transfect the line rbESC-5 at passage 11 with the plasmid pPGK-eGFP1-Neo. For each transfection reagent varying amounts were used in combination with 1 and 2 µg of plasmid DNA (Table 11). Each combination was done twice in 24 well plates. For this, the suppliers' recommendations were scaled down.

Table 11: Combinations of transfection reagents.
Overview of the used reagents, their concentration and their combination with distinct amounts of vector DNA (pPGK-eGFP1-Neo).

Reagent	Lipofectamine 2000	Nanofectin	TurboFect
A [µl]	0.5	1.2	1
B [µl]	1	3.2	1.5
C [µl]	2	6.4	2
D [µl]	3	8	2.8

After 24 h, the transient expression of *eGFP* was assessed. The results showed a clear tendency that the higher the amount of each reagent the higher the number of eGFP positive cells (Table 12, Fig. 32). Contrary, no clear tendency can be seen when different amounts of pPGK-eGFP1-Neo were used. When Lipofectamine 2000 was used, the higher amount of pDNA resulted in higher number of green cells. But when using Nanofectin and TurboFect, the lower amount (1 µg) of pDNA most often resulted in higher numbers of green cells as 2 µg. Overall, the application of TurboFect resulted in the least eGFP positive cells compared

to Lipofectamine 2000 and Nanofectin. Nanofectin resulted in the highest transfection efficiencies (Fig. 32). Hence, these parameters (8 µl Nanofectin and 1 µg pDNA) were chosen for further transfections.

Table 12: Overview of the results obtained applying different reagents in different concentrations and in different combinations with distinct amounts of pPGK-eGFP1-Neo.
Amount of cells exhibiting eGFP fluorescence is indicated by a scale ranging from no fluorescence (-) up to very high expression (+++).

DNA [µg] / Reagent	Lipofectamine 2000		Nanofectin		TurboFect	
	1	2	1	2	1	2
A	(+)	+(+)	-	-	-	(+)
B	+	+(+)	++	+	+	+
C	++	++	++(+)	++(-)	++	+
D	++(+)	+++	+++	++	(+)	++

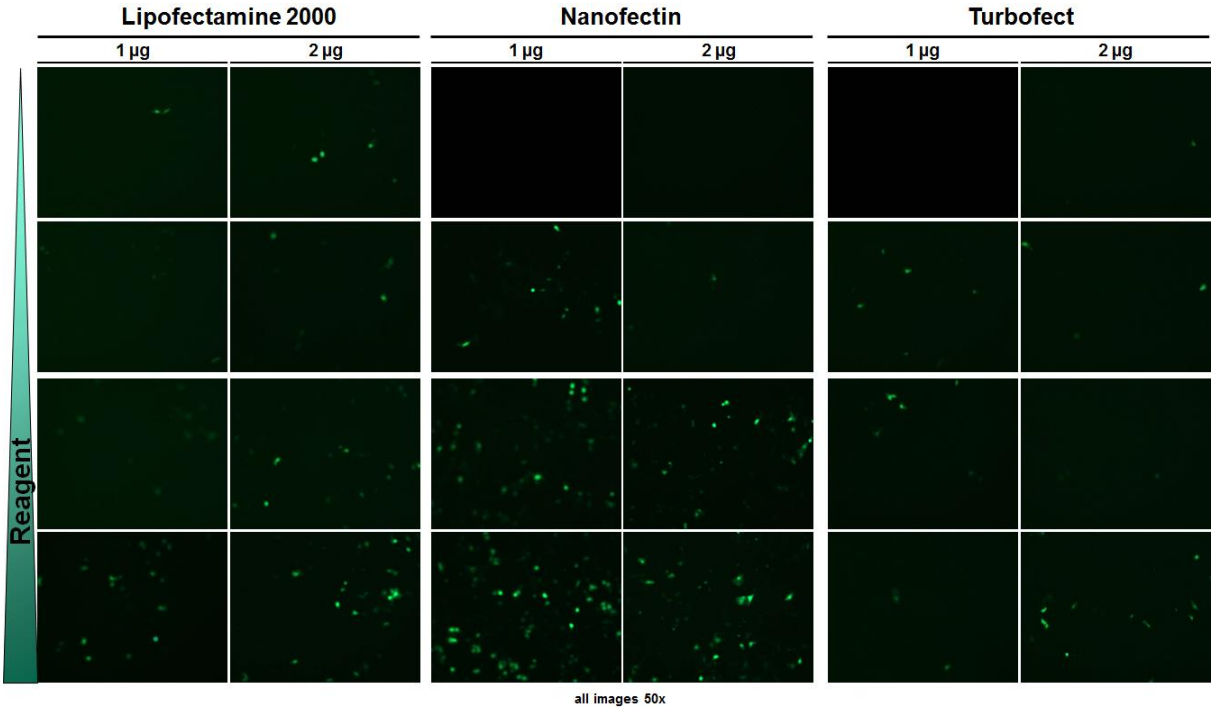

Figure 32: Transfection of rbESC-5 P11 with the plasmid pPGK-eGFP1-Neo applying different transfection reagents, 4 distinct concentrations and each in combination with 1 and 2 µg plasmid DNA.
Images showing typical eGFP fluorescence of each combination 24 h post transfection.

Since feeder cells (MEF-MITOs) were present during the above transfections, it was tested if rbESCs could be transfected in the absence of feeders. Hence, pPGK-eGFP1-Neo was transfected using Nanofectin into the line rbESC-5 at passage 12 in the presence or absence of feeder cells, which resulted in positive outcomes for both experiments.

3.2.1.4 Differentiation of rabbit embryonic stem cells *in vitro*

A hallmark of ESCs is their pluripotent differentiation potential. This potential needs to be verified by differentiation of pluripotent cells into cells of each of the three germ lines: mesoderm, endoderm and ectoderm.

To assess the differentiation potential of the obtained rbESC lines, different methods were used for their differentiation into distinct cell types. Differentiation assays were adapted to available protocols developed for human and mouse ESCs.

3.2.1.4.1 Spontaneous differentiation of rbESCs

For differentiation, the method of EB formation was performed using 500, 1000, 3000, 5000, 6000 and 7000 cells per 40 µl droplets. All droplets were cultured under distinct conditions that are outlined in Fig. 33. Variations were done in the time scale: culture of hanging drops (2, 4 or 6 d) and afterwards in suspension culture (3 or 6 d). Further, the influence of various differentiation media (2.2.3) was assessed. For comparison, the formation of EBs was induced solely in suspension culture.

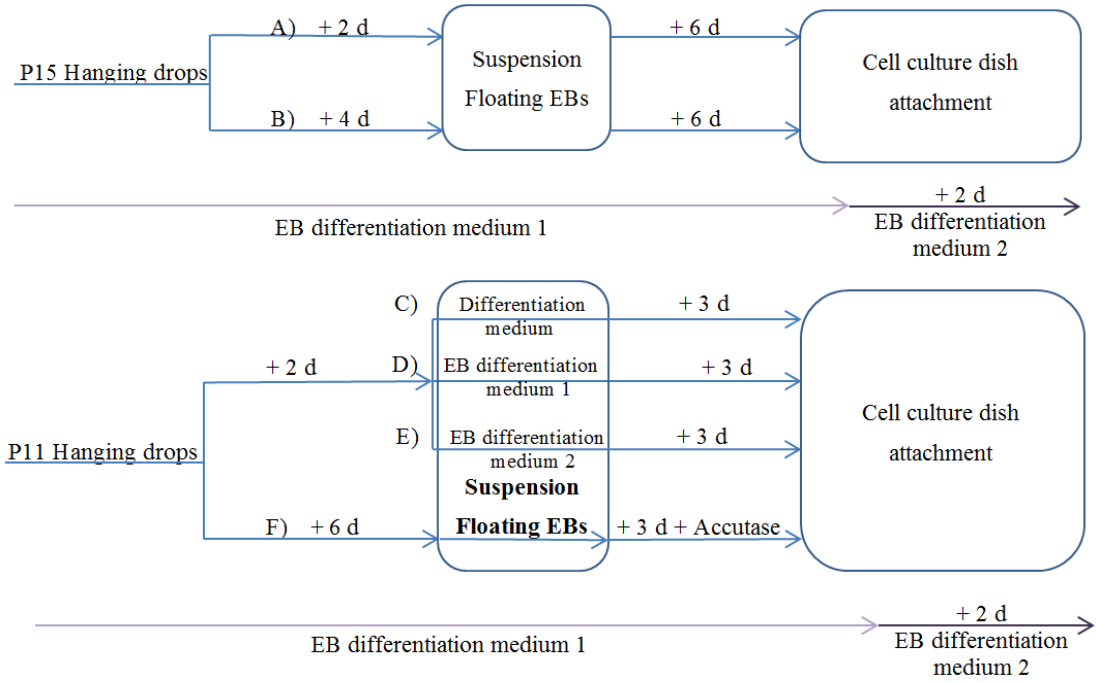

Figure 33: Overview of applied conditions to differentiate rbESCs.
After cultivation as hanging drops, formed aggregates were cultured in suspension and then transferred to gelatine covered cell culture plates. **A)** Hanging drops for 2 d, suspension culture for 6 d, both in EB differentiation medium 1, 2 d on cell culture plate in EB differentiation medium 2. **B)** Hanging drops for 4 d, suspension culture for 6 d, both in EB differentiation medium 1, 2 d on cell culture plate in EB differentiation medium 2. **C)** Hanging drops for 2 d in EB differentiation medium 1, suspension culture for 3 d in differentiation medium, 2 d on cell culture plate in EB differentiation medium 2. **D)** Hanging drops for 2 d in EB differentiation medium 1, suspension culture for 3 d in EB differentiation medium 1, 2 d on cell culture plate in EB differentiation medium 2. **E)** Hanging drops for 2 d in EB differentiation medium 1, suspension culture for 3 d in EB differentiation medium 2, 2 d on cell culture plate in EB differentiation medium 2. **F)** Hanging drops for 6 d, suspension culture for 3 d, both in EB differentiation medium 1, before transfer to attachment plates aggregates were dissociated with accutase, 2 d on cell culture plate in EB differentiation medium 2.

Morphologically, aggregates most similar to mouse EBs were achieved with 3000, 4000 and 5000 cells per droplet (Fig. 34). Lower cell numbers did not form EB-like structures or did not give rise to outgrown colonies on attachment plates. Albeit forming dense structures, also high cell numbers did not result in round EB like structures. The most typical EB like structures were obtained with 3000 cells per droplet. Further, it was shown that distinct differentiation medium compositions (2.2.3) used had only a minor effect on the formation of EBs and their resulting outgrowths. Also, the different cultivation periods did not have a significant impact. The most obvious observation was that outgrowths of hanging drop EBs were remarkably different in their morphology and its diversity to those formed only in suspension culture.

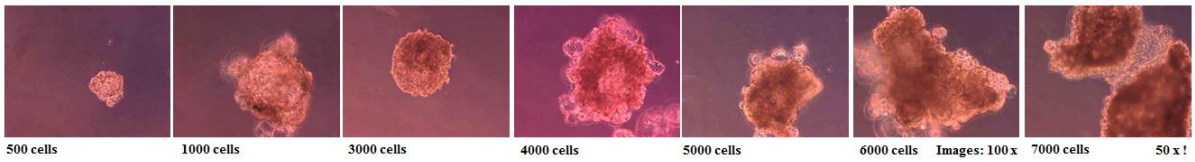

Figure 34: Typical aggregates formed during EB differentiation experiments.
Number of cells per droplet is given. The size of aggregates correlates with number of cells used per droplet. However, only aggregates formed with 3000 cells per droplet formed typical EB-like structures. Note that magnification of the image of 7000 cells/droplet is only 50 x, all other images are 100 x.

During microscopic observations lipid-like droplets (*Gutta adipis*) were seen in outgrown aggregates from hanging drop cultures and were positively stained with Oil-Red-O (Fig. 35). This strongly indicates an adipogenic differentiation of rbESCs and verifies a differentiation into mesoderm. Contrary, outgrowths of EBs obtained only in suspension culture did not show lipid-like droplets and did not stain. Since the differentiation media did not contain a compound forcing adipogenesis, the observed mesodermal differentiation might be spontaneous. Further, these findings show again that the differentiation by suspension culture alone is less successful as hanging drop method.

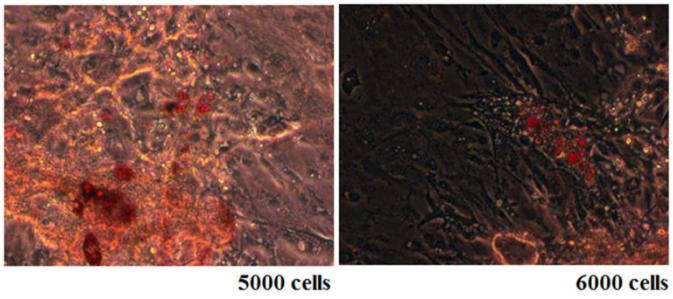

Figure 35: Lipid droplets stained by Oil-Red-O in outgrown cells of attached EB-like structures.
The outgrowths of hanging drop EB-like structures formed lipid-like droplets that stained positive with Oil-Red-O. Number of cells indicates the number used per droplet for EB formation.

One differentiation gave also rise to spontaneous active beating cardiomyocytes (video available).

3.2.1.4.2 Directed differentiation of rbESCs

In a further experiment the directed differentiation of rbESCs into distinct cells of the three germ layers, namely endoderm, mesoderm and ectoderm, was performed by the addition of defined chemicals (bFGF, activin A and retinoic acid), which were proven to direct differentiation of both mouse [247,510,511; review: 512] and human [513] ESCs. The EB formation was again performed in all three differentiation media, each for two different time frames (2 and 5 d in hanging drop culture) and 4000, 5000, 6000 and 7000 cells per droplet. After subsequent suspension culture, all floating aggregates were split 1 : 4 onto 12 well plates covered with 0.1% gelatine, cultured in differentiation medium supplemented with 10 ng/ml bFGF (for mesodermal differentiation), 20 ng/ml activin A (for endodermal differentiation) and 1 µM retinoic acid (for ectodermal differentiation) (Fig. 36).

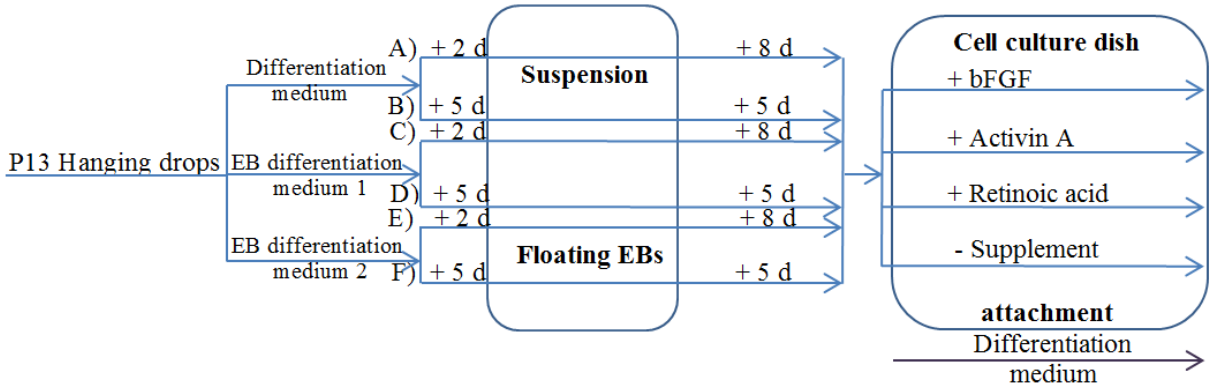

Figure 36: Outline of the differentiation strategy to direct differentiation into cells belonging to the three germ layers.
After suspension culture, all aggregates were pooled and split in 4 parts to attachment plates covered with 0.1% gelatine. Then, specific chemicals were added to differentiation medium. One group was left w/o supplementation as control. **A)** Hanging drops for 2 d, suspension culture for 8 d, both in differentiation medium. **B)** Hanging drops for 5 d, suspension culture for 5 d, both in differentiation medium. **C)** Hanging drops for 2 d, suspension culture for 8 d, both in EB differentiation medium 1. **D)** Hanging drops for 5 d, suspension culture for 5 d, both in EB differentiation medium 1. **E)** Hanging drops for 2 d, suspension culture for 8 d, both in EB differentiation medium 2. **F)** Hanging drops for 5 d, suspension culture for 5 d, both in EB differentiation medium 2.

Five days after supplementation with differentiation inducing chemicals, each group showed same cell types, most of them having fibroblast-like phenotype (data not shown).

To elucidate possible active differentiation processes based on the expression of marker genes, RT-PCR analysis was performed. For comparison, RNA was isolated from undifferentiated cell lines. The quality of all RNAs was checked on agarose gels and found to be intact. Then, RT-PCR was performed according to the one-step protocol. As controls, RNA of MEF-MITO and of rbFB-1 (fibroblasts) was used. RT-PCR was carried out for *Oct4*, *Sox2*, *Nestin*, *Desmin*, *Hnf4α*, *Bmp4* and as control for *Gapdh*. For human *Oct4*, two different isoforms were reported due to alternative splicing [514]. Since the existence of an atypical splice donor site was found in rabbit *Oct4* [515], RT-PCT was performed for both possible isoforms. In

a first experiment, those primer pairs were tested on the lines rbESC-5 and rbFB-1 (Fig. 37 A). Bands for the differentiation markers (*Desmin* (mesoderm), *Nestin* (ectoderm) and *Hnf4α* (endoderm)) were found in the cell line rbESC-5 that should be undifferentiated. Similar results were obtained in a second experiment in which RNA of different sources (undifferentiated cells (rbESC-45 and -46), differentiated rbESCs (EB, diff. P5 and P7) and controls (rbFB-1, MEF). For each total RNA RT-PCR for *Bmp4*, *Desmin*, *Nestin* and *Hnf4α* was performed (Fig. 37 B – D). Again, markers indicative for differentiation are present in undifferentiated rbESC-45 and -47 but also in differentiated rbESCs. However, RNA isolated directly from EBs did not give a band for *Bmp4* and *Desmin*. Further, the markers *Desmin* and *Nestin* seem to be expressed in the controls (rbFB-1, MEF).

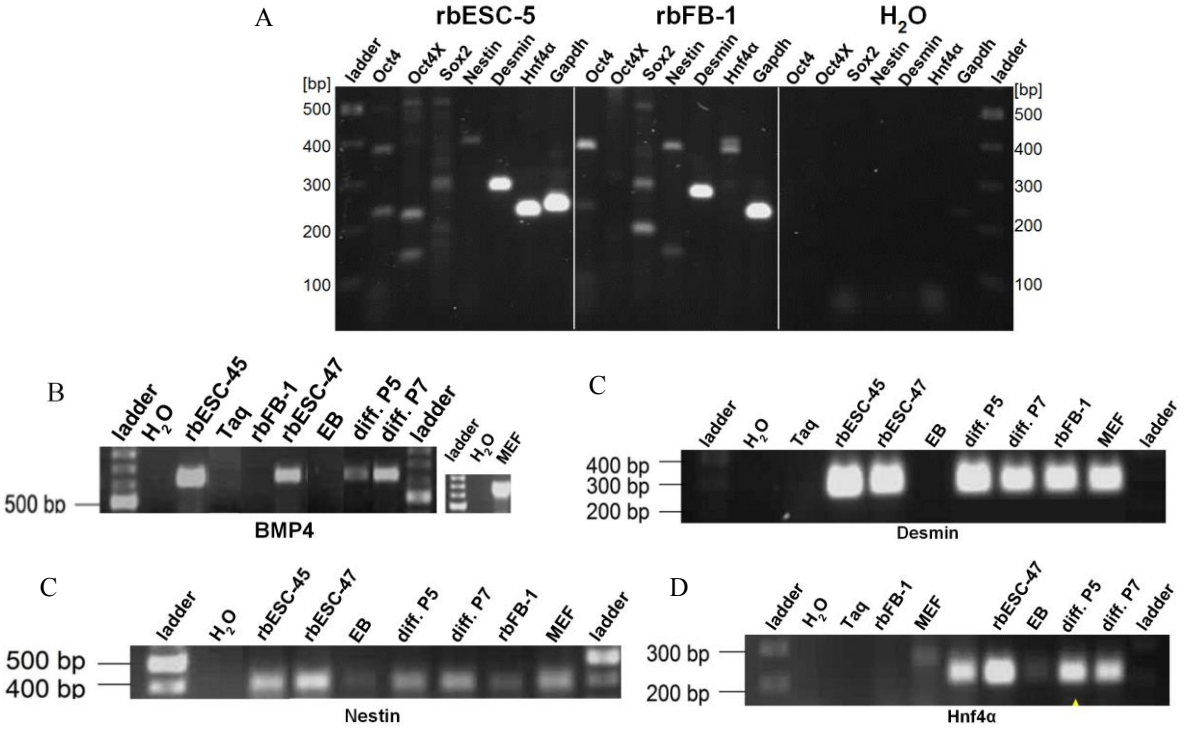

Figure 37: RT-PCR analysis of differentiation markers.
A) Total RNA was isolated from rbESC-5 and rbFB-1 to perform RT-PCR. **B) – D)** Total RNA was isolated from undifferentiated rbESC lines, from EB-like aggregates and from outgrown and induced EB-like aggregates. For control, total RNA was isolated from rbFB-1 and MEF-MITO. Differentiation markers used for RT-PCR are **B)** BMP4, **C)** Desmin, **D)** Nestin and **E)** Hnf4α.

Additionally, PCR products were sequenced to reveal the identity using either the PCR products directly or after subcloning into pjet1.2/blunt vector. The identity of following sequences to the corresponding gene could be verified: *Sox2*, *Nanog*, *FoxD3*, *Rex1*, *Nodal*, *Terc*, *Hnf4α*.

3.2.1.5 Contribution of rabbit embryonic stem cells to the inner cell mass

A proof of pluripotency is the contribution of ESCs to the ICM of the developing embryo. To assess the contribution of rbESCs, eight stably transfected rbESC-5 P25 (with pPGK-eGFP1-

Neo) were transferred into 8-cell-stage embryos by microinjection. A total of 36 embryos were injected and cultured *in vitro* to hatching blastocyst stage. The ICM was isolated and cells were cultured. Out of the 36 embryos, 17 explants (47%) were obtained and 12 (33%) went to passage 2. These 12 lines were then subjected to G418 selection at passage 3. Nine lines (75%) survived selection indicating the presence of pPGK-eGFP1-Neo. In addition, a PCR analysis of genomic DNA isolated from all 12 lines revealed that all those lines surviving G418 selection were positive for the pPGK-eGFP1-Neo transgene construct (Fig. 38). However, expression of *eGFP* analysed by fluorescence microscopy could only be detected in 5 lines but corresponded to the G418 selection and PCR results. These results show that the injected rbESCs may have contributed to the developing embryo. That finding is an indicator for pluripotency.

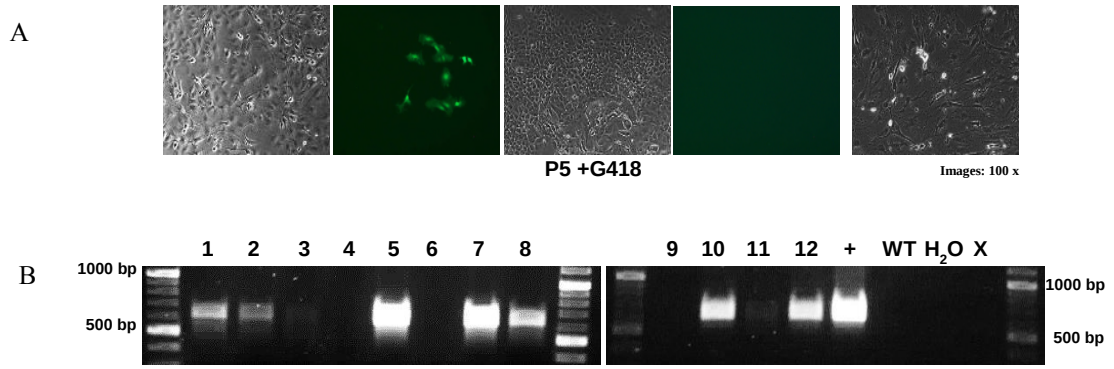

Figure 38: Assessment of the contribution of rbESCs to the developing rabbit embryo.
Eight stably transfected (pPGK-eGFP1-Neo) rbESCs were injected per 8-cell-stage embryo. In late blastocyst stage, ICM was isolated and cultured. Cells in P3 were subjected to G418 selection over 3 passages. **A)** Cells bearing pPGK-eGFP1-Neo were resistant to G418 and were growing (Images on the left); some expressed *eGFP* (left) whereas others did not (middle). Right image shows cells not resistant to G418. **B)** PCR for *eGFP* on genomic DNA of all obtained explants. +: positive control (pPGK-eGFP1-Neo), WT: negative control (WT DNA), X: empty lane.

3.2.2 Multipotent stem cells

Multipotent stem cells could serve as a possible alternative to ESCs for cell-mediated transgenesis including gene targeting. The generation of transgenic animals with multipotent cells would require NT.

3.2.2.1. Characterisation of rabbit MSCs

Mesenchymal stem cells (MSCs) were isolated from bone marrow (BM-MSCs) and fat tissue (A-MSCs) and assessed for growth rate, colony formation and differentiation capability.

To reveal the growth rate of both MSC lines, a growth curve assay was performed. For this, 1.5 x 10^5 cells were seeded in each 25 cm^2 flask and cultivated under standard conditions or under reduced O_2 conditions in a triple gas incubator (37°C, 5% CO_2, 5% O_2, 90% N_2). BM-

MSCs and A-MSCs were cultured in triplicates starting at P1 and finishing the experiment after P9. Over the course of the experiment, the cells did not change their morphology neither under standard nor under reduced O_2 conditions (Fig. 39). They maintained the typical spindle-shaped cell body.

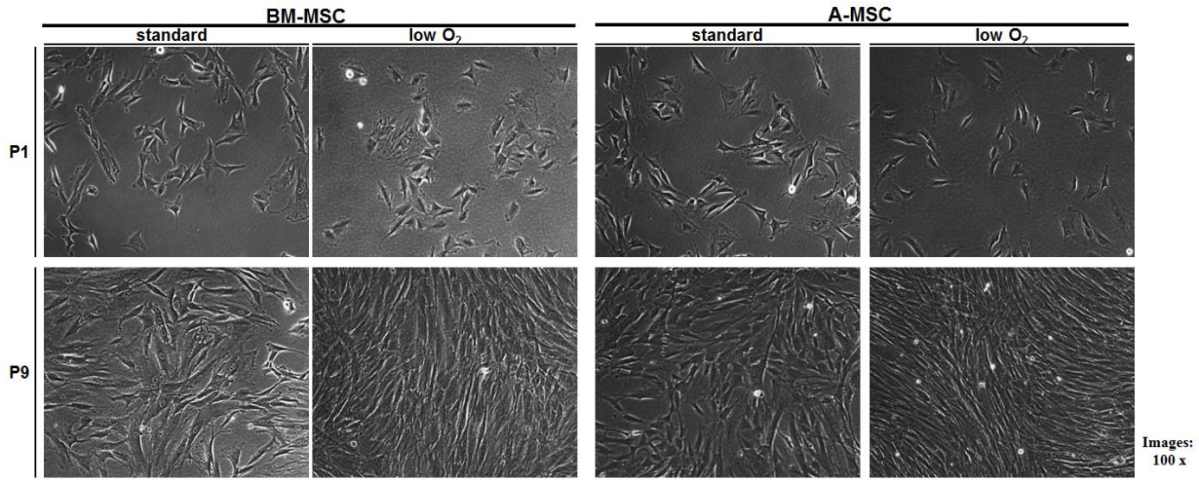

Figure 39: Typical morphology of rabbit BM-MSC and A-MSC under standard cell culture conditions and under reduced O_2 conditions each at P1 and P9.

When the cells reached a confluence of 80%, they were passaged and re-seeded at 1.5 x 10^5. After each passaging, cells were counted and a growth curve of each line was created (Fig. 40). It showed that the condition with reduced O_2 resulted in higher cell numbers for both BM- and A-MSCs. However, A-MSCs resulted in higher cell numbers for both conditions compared to BM-MSCs. Further, a slight decrease of growth rate can be seen for both A- and BM-MSCs under standard condition at higher passages (P8 – P9) but not in the condition with reduced O_2.

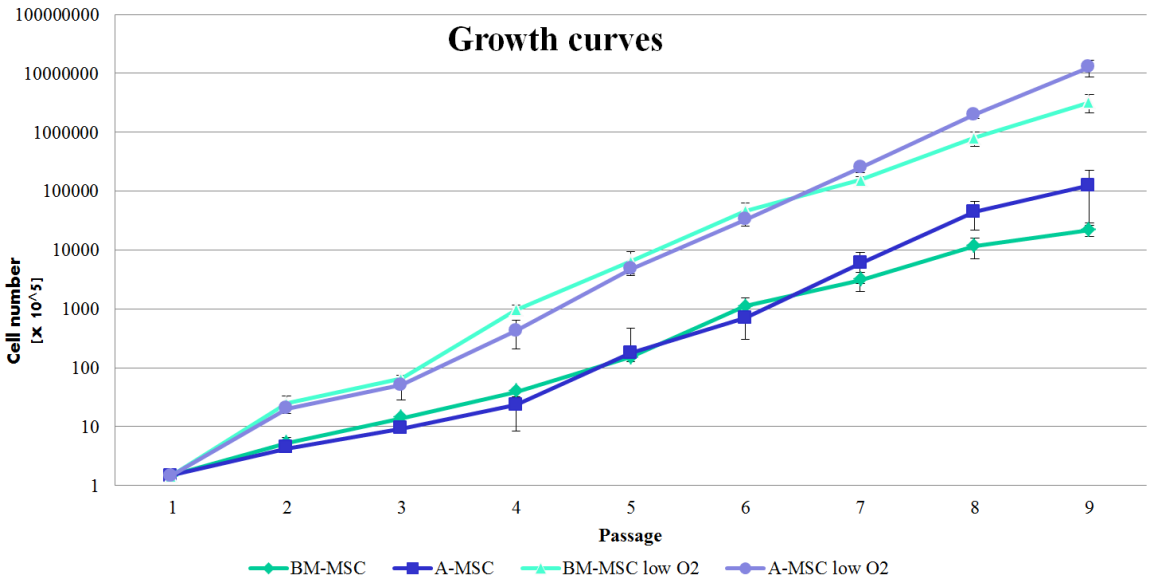

Figure 40: Growth curves obtained from data collected during the culture of rabbit BM-MSC and A-MSC under standard cell culture conditions and under reduced O_2 conditions over 9 passages.
Starting cell number was 1.5 x 10^5 cells.

Population doubling times were calculated in accordance with the growth curves. A-MSCs possess the shorter doubling time (26 and 29 h). The population doubling times for both A- and BM-MSCs are shorter under reduced O_2 then under standard conditions (Table 13). Thus, the optimal condition to culture rbMSCs is under reduced O_2 concentration.

Table 13: Population doubling times of rabbit BM-MSC and A-MSC cultivated under standard cell culture conditions and under reduced O_2 conditions over 9 passages.

Population doubling times [h]			
standard		reduced O_2	
BM-MSC	A-MSC	BM-MSC	A-MSC
34.73	29.33	28.51	26.09

The growth characteristics of rbMSCs were further assessed by colony forming assays. For this, 5 x 10^3 cells of A- or BM-MSCs were plated onto 15 cm dishes in triplicates. After 14 days in culture, established colonies were stained with crystal violet dye (Fig. 41). Here, it showed that A-MSCs have the potential to establish colonies at much higher frequency compared to BM-MSCs when seeded at very low cell densities. In general, A-MSCs showed to have a higher growth potential then BM-MSCs.

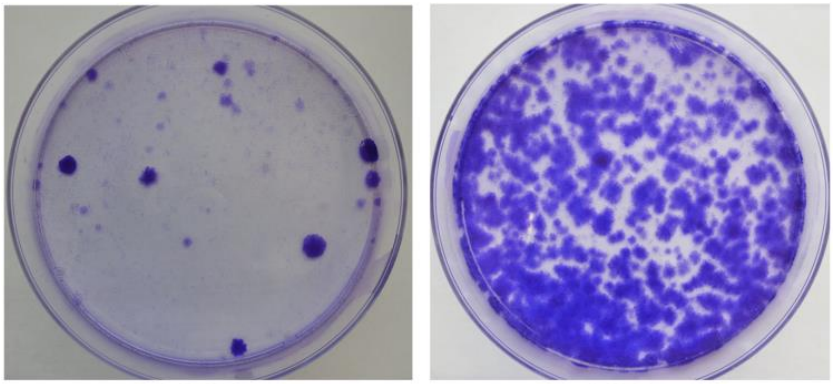

Figure 41: Colony forming assay of rbBM-MSC and rbA-MSC.
5000 cells per 15 cm were seeded and stained after 14 d in culture.

To verify the positive effect of bFGF on the culture of rbMSCs, both BM- and A-MSCs (P4) were cultured in the presence (standard medium) or absence of bFGF. Both lines cultured w/o bFGF stopped growing and underwent senescence (Fig. 42). Thus, the supplementation of bFGF is essential for the culture of rbMSCs.

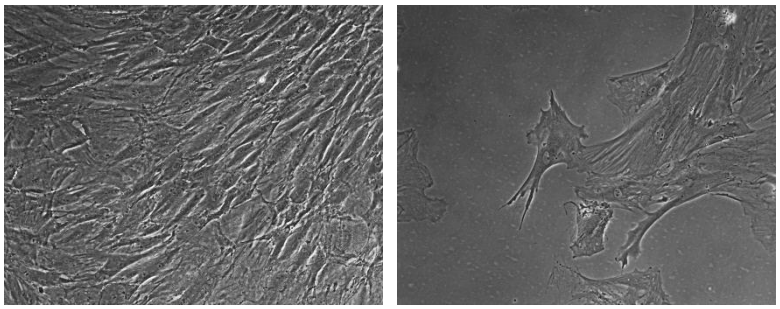

Figure 42: Dependency of rbMSCs on the supplementation of bFGF as verified on BM-MSC.
W/o supplementation with bFGF cells stop growth and go into senescence.

3.2.2.2. Differentiation of rabbit MSCs

The multipotential character of MSCs was tested by standard differentiation assays: adipogenesis, osteogenesis and chondrogenesis as described in material and methods. Experiments were done in triplicates.

The potential for adipogenesis of both A- and BM-MSCs was verified by the staining with Oil-Red-O indicating the presence of lipid droplets (Fig. 43). However, the cells showed morphologic differences after adipogenesis. A-MSCs grew as three dimensional loose cell layers but did not detach whereas BM-MSC still grew as tight monolayer.

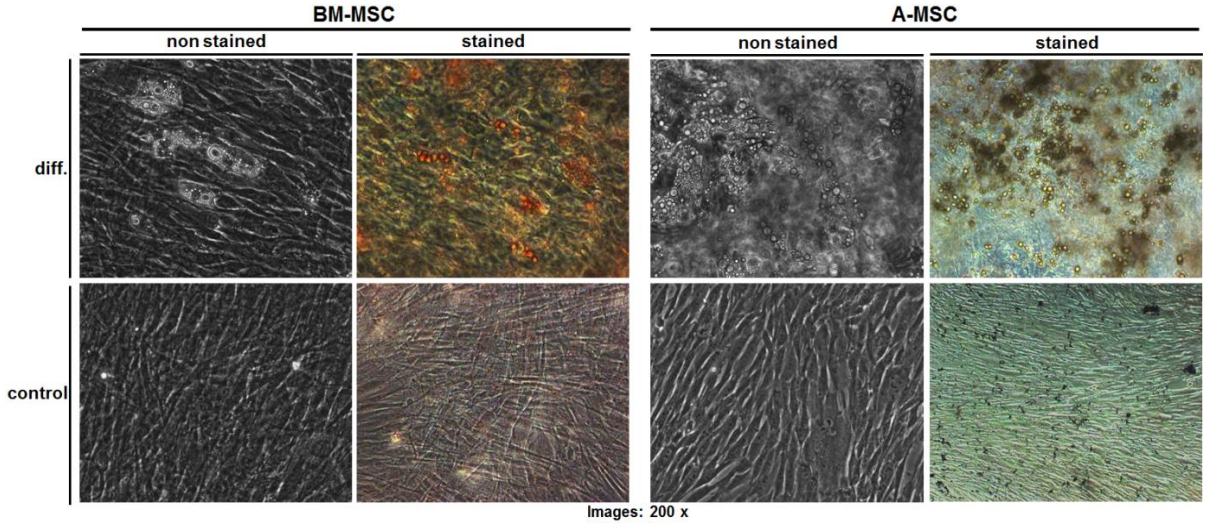

Figure 43: Multipotency of rbMSCs. BM-MSCs and A-MSCs cultured under conditions inducing adipogenic differentiation.
Differentiation was verified by Oil-Red-O staining.

The potential for osteogenesis could be verified for BM-MSCs by silver nitrate staining but not for A-MSCs (Fig. 44). Again, morphologic differences after osteogenesis could be observed. BM-MSCs changed their morphology to an endothelial like form consisting of round and small cells whereas A-MSC did not change their morphology.

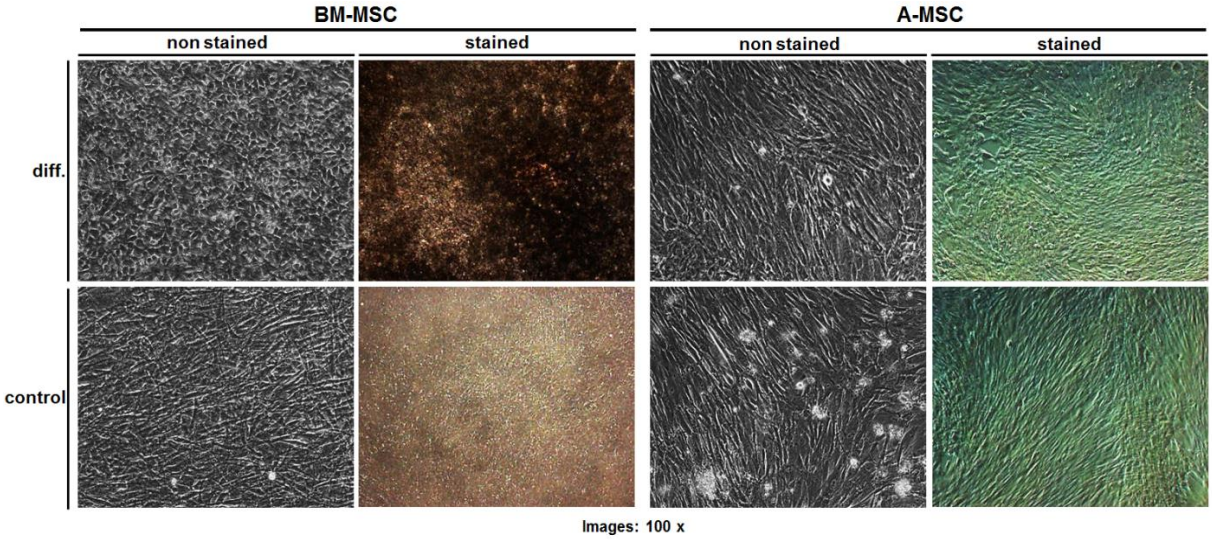

Figure 44: Multipotency of rbMSCs. BM-MSCs and A-MSCs cultured under conditions inducing osteogenic differentiation.
Differentiation was verified by silver nitrate staining.

The potential for chondrogenesis of both A- and BM-MSCs was verified by pellet formation (Fig. 45) and subsequent staining. Again, morphologic differences could be observed. BM-MSCs formed a small compact and dense pellet after chondrogenesis, whereas the pellet formed by A-MSCs was not dense but loose and fluffy.

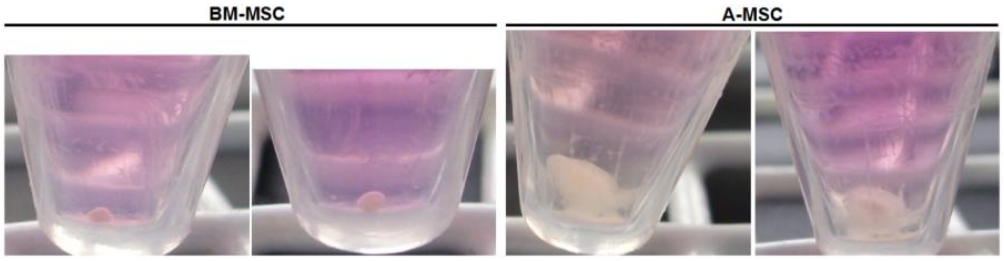

Figure 45: Multipotency of rbMSCs.
BM-MSCs and A-MSCs cultured under conditions inducing chondrogenic differentiation thereby dense pellets became formed.

Nevertheless, the homogenous deposition of proteoglycan in the pellets was successfully stained by alcian blue. Mucopolysaccharides appeared blue in pellets formed by both A- and BM-MSCs (Fig. 46).

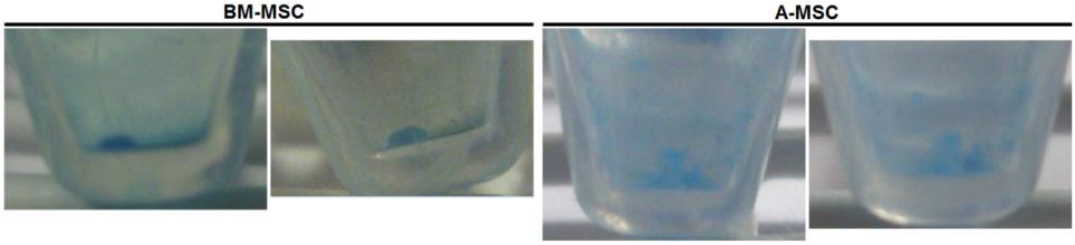

Figure 46: Multipotency of rbMSCs.
Pellets of BM-MSCs and A-MSCs stained positive with alcian blue verifying differentiation.

In summary, both A- and BM-MSCs could be differentiated into distinct cells. However, A-MSCs failed to differentiate into osteocytes.

3.2.2.3. Assessment of optimal transfection methods for rabbit MSCs

In further experiments, different methods were tested for their ability to transfect rbMSCs. As it is known that transfection efficiency depends also on the vector size, different constructs varying in their size such as plasmids (standard constructs up to 20 kb) and BACs (large constructs up to 250 kb) were used.

3.2.2.3.1. Transfection with plasmids

To allow drug selection of transfected cells the SV40-Neo-pA cassette of pcDNA-3 was subcloned into pCAGGs-mCherry vector. The functionality of the resulting vector pCAGGs-mCherry-Neo was successfully verified in cell culture experiments (data not shown).

Both BM- and A-MSCs were examined for their transfection efficiency. For this, pCAGGs-mCherry-Neo and two transfection methods (nanofection and nucleofection) were applied.

For nanofection, 3 µg pDNA were used per well of a 6-well-plate with 9.6 µl Nanofectin per well. Experiments were done in triplicates. For negative control, three wells of each line were left non-transfected.

For nucleofection, 2 µg pDNA were used per reaction with 5×10^5 cells. Cells were nucleofected with by the supplier recommended programs C-17 and U-23. For negative control, 5×10^5 cells were left non-transfected.

After 24 h post-transfection, the transient expression was determined by fluorescence microscopy (Fig. 47). All transfected cells showed red fluorescence albeit at different frequencies. For nanofection, no clear difference between A- and BM-MSCs was visible. Contrary, differences were observable for nucleofection experiments. Here, for BM-MSCs the program U-23 resulted in higher fluorescence frequencies then C-17 whereas the result for A-MSCs was vice versa. For each experiment the triplicate wells were pooled, cells were counted and 5×10^5 cells of each experiment were seeded per 10 cm dish (resulting in three dishes per experiment) and cultivated with the addition of G418 (500 µg/ml) to select for stable integration. After selection process, clonal cell colonies were counted and examined for *mCherry* expression (Table 14). For BM-MSCs transfected with nanofectin 21 colonies appeared of which 19 (90%) showed red fluorescence whereas for A-MSCs only 6 colonies appeared of which 5 (83%) showed red fluorescence. For nucleofection, the results were different. Here, for BM-MSCs 4 (C-17) and 5 (U-23) colonies appeared, but none showed red fluorescence. On the other hand, for A-MSCs many more colonies appeared: 30 for C-17 and 28 for U-23 of which 18 (60%) and 22 (79%) showed red fluorescence, respectively.

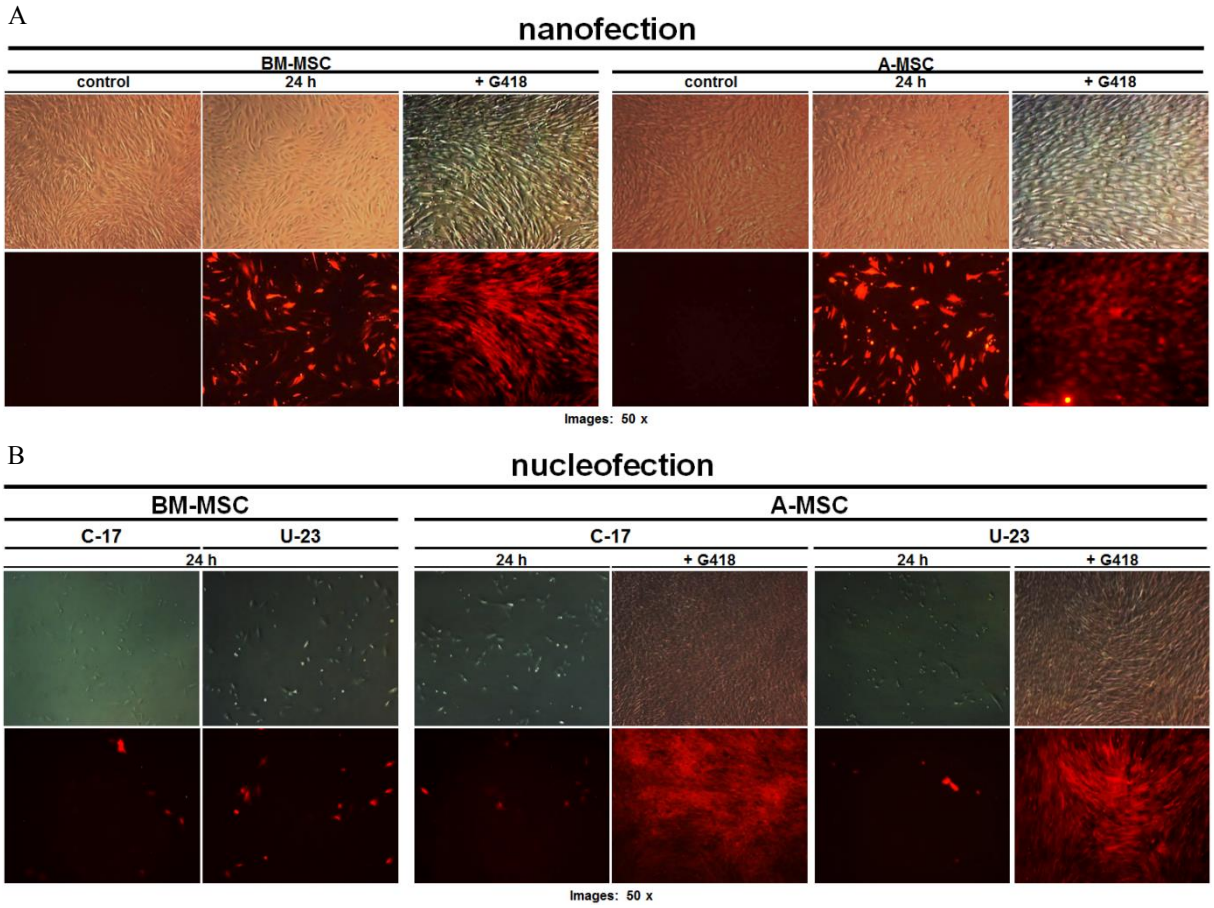

Figure 47: Transfection of rbBM-MSCs and A-MSCs using pCAGGs-mCherry-Neo.
A) Transfection by nanofection. Both BM-MSCs and A-MSCs were stably transfected. **B)** Transfection by nucleofection. BM-MSC could not stably transfected with both applied programs whereas A-MSCs were stably transfected with programs C-17 and U-23.

Table 14: Assessment of transfection efficiencies of rbBM-MSCs and A-MSCs applying different methods
Successful transfections are highlighted in red.

transfection method		fluorescence	BM-MSC	A-MSC
nucleofection	C-17	Yes	0 (0%)	18 (60%)
		No	4	12
	U-23	Yes	0 (0%)	22 (79%)
		No	5	6
nanofectin		Yes	19 (90%)	5 (83%)
		No	2	1

The results show that A- and BM-MSCs could be successfully transfected and stable colonies could be established. The results (Table 14) revealed that the most efficient method to transfect BM-MSCs is nanofection. Also, nanofection of BM-MSCs resulted in the highest transfection efficiency (90%). However, nucleofection of A-MSCs with the program U-23 resulted in a higher number of red fluorescent colonies but with a minor efficiency (79%). Based on these results and the differentiation assays, BM-MSCs were chosen for further experiments. Thus, to determine the most efficient DNA-nanofectin-ratio BM-MSCs were transfected with 2, 3 and 4 µg of pCAGGs-mCherry-Neo each with 9.6 µl and 16 µlnanofectin. Transient expression of *mCherry* was determined by fluorescence microscopy

48 h post-transfection. No differences were found in the transfection efficiency when different amounts of nanofectin were used. A DNA amount of 4 µg showed the lowest percentage of red fluorescent cells, but there was no significant difference between 2 µg and 3 µg (data not shown). Thus, for further experiments 9.6 µl of nanofectin and 2 µg of DNA were used.

3.2.2.3.2. Transfection with bacterial artificial chromosomes

To optimize the transfection of MSCs with large constructs, the vector BAC-mCherry-Neo (120 kb) was used in a nucleofection experiment with program C-17 using vector amounts of 5, 7.5, 10 and 12.5 µg. The vector BAC-mCherry-Neo has a similar size as the targeting vector BAC-rbHPRT^{Neo}. After 48 h, it was found that the amount of fluorescent cells increased with an increasing amount of vector DNA (data not shown). Best results were obtained with 12.5 µg.

As transfection efficiency with large BAC constructs was low, four additional transfection reagents were tested in their ability to transfect MSCs using BAC-mCherry-Neo. Promofectin was used with 2 and 4 µg BAC-DNA each with 4 and 8 µl of the reagent. SatisFection was used with 2 µg BAC-DNA and 3 µl reagent. jetPei was used with 3 µg BAC-DNA and 6 µl reagent. An exception is Metafectene, which is used on detached cells. Here, 20 µg BAC-DNA and 20 µl reagent was used with 1.3 x 10^6 cells and plated afterwards onto 1 well of a 6-well plate.

After 24 h, transfection efficiencies were determined by microscopy as means of mCherry fluorescence. Transfection efficiencies were very low for Metafectene and jetPei (Fig. 48). The combination of 2 µg BAC-DNA and 4 µl promofectin gave the best result, but overall efficiency remained low.

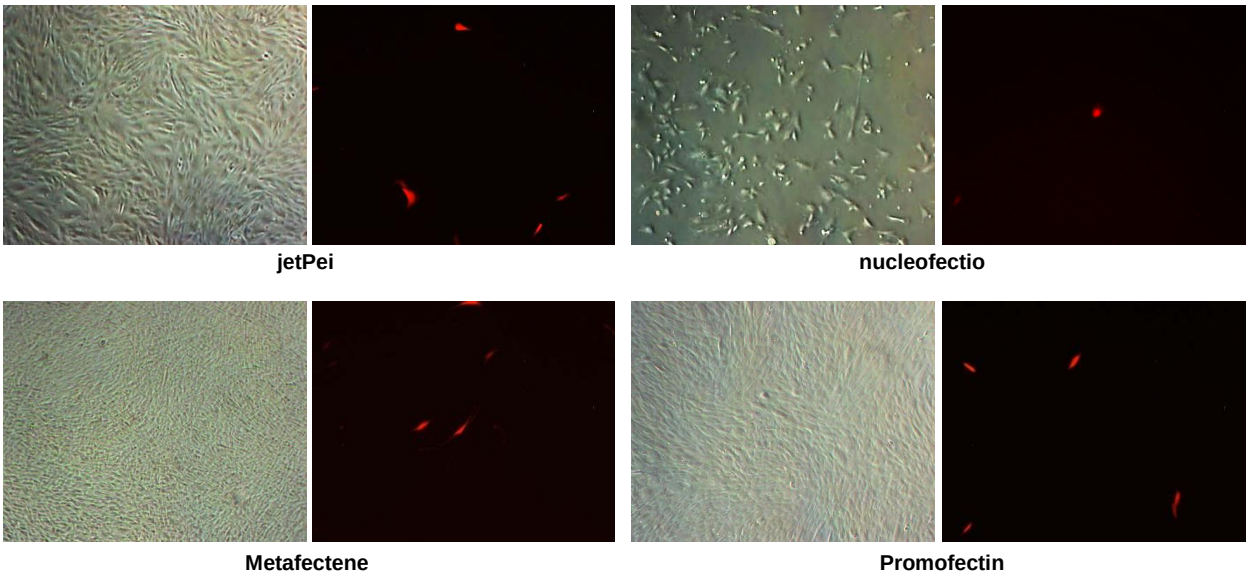

Figure 48: Transfection of rbBM-MSCs with vector BAC-mCherry-Neo applying different methods. Cells were transfected with distinct methods but none outperformed regarding transfection efficiencies as determined by mCherry fluorescence 24 h post-transfection. The picture of nucleofection is from an experiment using 12.5 µg BAC-DNA; the picture of Promofectin is from the combination of 2 µg BAC-DNA and 4 µl reagent. Images: 100x.

3.2.3 Assessment of nuclear transfer competence

Since the main goal was to define a cell type with the highest competence for NT and the production of transgenic rabbits, BM-MSCs were compared with rbESCs. Both cell lines showed to be efficiently and stably transfectable. Hence, both non-transfected and stably transfected rbESCs and BM-MSCs were used for NT. All NT experiments were performed by the groupf of Prof. Eckhard Wolf and have been published [516].

For NT, six independently derived rbESC lines were used and more than 2000 embryo reconstructions were performed. Of those, 85% fused and of these 86% underwent cleavage which finally resulted in a blastocyst rate of 23% (Table 15 A). Remarkably, rbESCs did not lead to a live born animal at all when embryos were transfferred into surrogate mothers (Table 15 B). However, it has been shown that both non-transfected as well as genetically manipulated BM-MSCs result in higher rates of fusion (94% and 93%), cleavage (89% and 92%), blastocysts (38% and 55%) and live borns (2% and 4%) compared to rbESCs (Table 15). During these experiments, the first live cloned rabbit could be achieved from genetically manipulated cells.

Table 15: Assessment of the potential of rbESCs, rbBM-MSCs and stably transfected rbBM-MSCs (*eGFP*) for NT
A) Development of reconstructed embryos *in vitro*. **B)** Development of reconstructed embryos *in vivo*. Adapted and modified from Zakhartchenko *et al*. (2011) [516]

A

Donor cells	Fused	Cleaved	Blastocysts[a]
rbESCs	1858/2181 (85%)	1239/1821 (86%)	243/1054 (23%)
rbBM-MSCs	793/844 (94%)	698/786 (89%)	48/128 (38%)
eGFP-rbMSCs	412/444 (93%)	377/409 (92%)	97/178 (55%)

[a] Percentages relate to the number of embryos fused and cultured further.

B

Donor cells	Transferred embryos/recipients	Pregnant recipients	Rabbits born[a]
rbESCs	607/23	12/2	0
rbBM-MSCs	483/13	9/13	10 (2%)
eGFP-rbMSCs	216/8	4/8	8 (4%)

[a] Percentages relate to the total number of embryos transferred.

In addition, rabbit fibroblasts (rbFB) were tested for NT [516]. These fibroblasts were isolated of animals obtained from NT experiments described above using stably transfected rbBM-MSCs (*eGFP*). This experiment was a test if cloned but non-viable rabbits could be rescued. Indeed, two live born rabbits could be obtained from fibroblasts from previously cloned transgenic rabbits (Table 16 B). Further, the obtained rates of fusion, cleavage and blastocysts (Table 16 A) were similar compared to MSCs as donor cells.

Table 16: Assessment of the potential of rabbit fibroblasts for NT obtained from cloned *eGFP*-transgenic animals.
A) Development of reconstructed embryos *in vitro*. **B)** Development of reconstructed embryos *in vivo*. Adapted and modified from Zakhartchenko *et al*. (2011) [516]

A

Donor cells	Fused	Cleaved	Blastocysts[a]
rbFB-eGFP-rbMSC-A	341/377 (90%)	274/341 (80%)	39/75 (52%)
rbFB-eGFP-rbMSC-B	566/607 (93%)	487/409 (86%)	27/76 (36%)

[a] Percentages relate to the number of embryos fused and cultured further.

B

Donor cells	Transferred embryos/recipients	Pregnant recipients	Rabbits born[a]
rbFB-eGFP-rbMSC-A	188/6	3/6	2 (1%)
rbFB-eGFP-rbMSC-B	365/8	7/8	0

[a] Percentages relate to the total number of embryos transferred.

3.2.4 Targeting of rabbit *hprt*

Classical, targeting vectors can be divided into four categories depending on the purpose: conditional~, insertional~, knock-in~ and replacement vector. To target *hprt*, a replacement vector design was constructed. During the time period of this project the sequence of rabbit *hprt* become available in the GenBank (access number: EF219063.1). In this thesis, two different strategies for gene targeting were assessed: The targeting of rabbit *hprt* by BAC vector and by traditional targeting vector.

3.2.4.1 Construction of bacterial artificial chromosome targeting vector

The sequence of rabbit *hprt* is 48.9 kb and was present on a ~120 kb BAC vector. To excise essential exons and to replace them with a selection cassette the technique of recombineering

was employed. This requires a targeting vector with short (~500 bp) homologous sequences (Fig. 49). The construction of this vector (pl452-rbHPRT, Fig. 50) was achieved by Ala El Din Samara in his Bachelor-thesis.

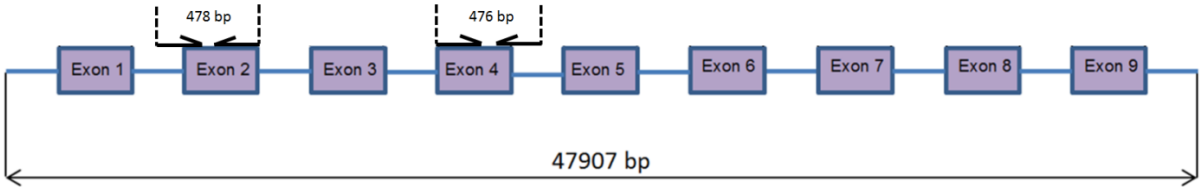

Figure 49: Amplification of two parts of rb*hprt* for subsequent cloning.
One fragment includes a part of intron 1 and exon 2 (478 bp) and the other fragment includes exon 4 and a part of intron 4 (476 bp).

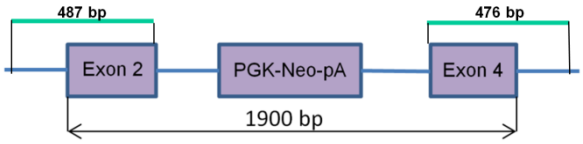

Figure 50: pl452-rbHPRT.
Exon 2 and 4 of rb*hprt* were subcloned into pl452 to obtain a vector for subsequent recombineering. Size of the both homology arms used for recombineering are highlighted in green.

In the next step BAC-rbHPRT was transferred into *E. coli* SW 106. Then, the backbone of the vector pl452-rbHPRT was removed and this cassette (Fig. 50) was transformed into the prepared *E. coli* SW 106 to replace exon 3 by recombineering. Successfully recombineered clones (Fig. 51) were selected by ampicillin and chloramphenicol and verified by PCR analysis (data not shown).

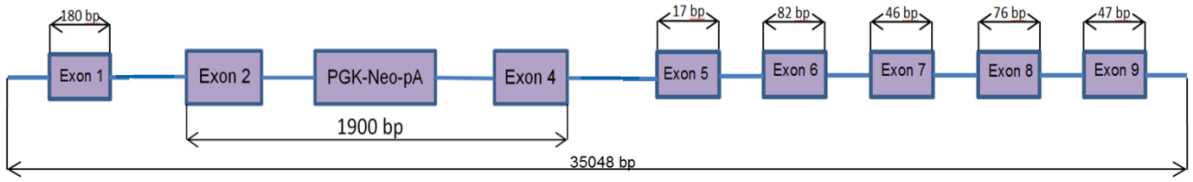

Figure 51: Structure of rb*hprt*^{Neo} located on a BAC after successful recombineering thereby decreasing the overall size of rb*hprt*.
This construct was used for transfections.

For the subsequent transfection, the BAC-rbHPRT^{Neo} (~120 kb) had to be linearized. Since the whole sequence of the complete BAC is not known, various restriction endonucleases were tested and it revealed that FseI is a single cutter and was used for linearization.

3.2.4.2 Construction of a conventional rabbit *hprt* targeting plasmid

As an alternative strategy, a classical targeting vector was constructed. For this, the exon 2-PGK-Neo-exon 4 fragment was digested from BAC-rbHPRT^{Neo}, ligated into the vector pBluescript SK+ resulting in prbHPRT^{Neo} and subjected to sequencing. It was found that all sequences were correct. This final vector provides 2797 bp homology on the left arm (5´) and 3896 bp homology on the right arm (3´) (Fig. 52).

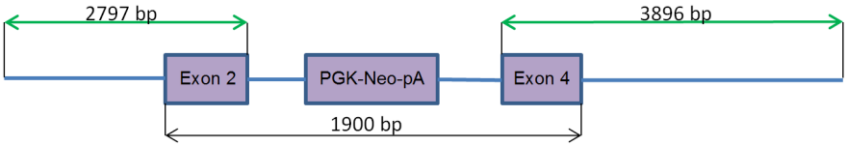

Figure 52: Structure of the targeting vector prbHPRT^{Neo}.
The size of the both homology arms for homologous recombination is highlighted in green.

3.2.4.3 Gene targeting of rabbit *hprt*^{Neo} in mesenchymal stem cells

Since *hprt* is an X-chromosomal gene, male cells comprise only one allele. For a functional knockout, only this allele needs to be targeted which allows the selection with 6-Thioguanine (6-TG).

BM-MSCs originating from a male rabbit were transfected by previously established methods (3.2.2.3.2). In all transfections, where BAC-rbHPRT^{Neo} was used, the DNA was purified with the Qiagen Large-Construct Kit.

3.2.4.3.1 BAC targeting of hprt

In preliminary experiments, rbBM-MSC P1 were transfected at 70% confluence using 1 and 1.5 µg of FseI linearized BAC-rbHPRT^{Neo}. After consecutive selection with G418 and 6-TG no colonies could be obtained.

In further experiments, FseI-linearized BAC-rbHPRT^{Neo} (precipitated by Phenol-Chlorofrom-Isoamylalcohol) was transfected by nucleofection (5 and 12.5 µg; program C-17) into rbBM-MSC P1. However, after consecutive selection with G418 and 6-TG no colonies could be obtained.

Since attempts to generate single clones of transfected rbBM-MSCs failed, transfected rbBM-MSCs were mixed with the triple amount of non-transfected cells 2 – 4 days after the transfection and seeded for G418 selection. It is expected that the non-transfected cells will support the transfected cells that are stressed and seeded at very low confluence. Upcoming cell colonies were passaged to 48-well plates and exposed to 6-TG selection. Cell colonies resistant to G418 and the following 6-TG selection were subjected to PCR analysis to detect targeting events. With this modified selection method, 162 resistant colonies could be obtained. However, PCR analysis (Fig. 54 A) revealed that those colonies were false positive (data not shown).

3.2.4.3.2 Conventional targeting of hprt

Despite spending lot of effort to generate targeted BM-MSCs using BAC vector, no targeting event could be verified. Consequently, the targeting construct was shortened as described (3.2.4.2). According to the results achieved for the transfection of BM-MSCs (3.2.2.3.1), rbBM-MSCs P1 were transfected using nanofectin with prbHPRT^{Neo} (Fig. 52) using 2 µg (2

wells) and 3 µg (3 wells) pDNA per well of a 6 well plate. Transfected rbMSCs were mixed with the triple amount of non-transfected cells 2 days after the transfection and seeded for G418 selection. Upcoming colonies were transferred each to 1 well of a 24 well plate in MSC medium w/o selection antibiotics (Fig. 53). Growing colonies were transferred to 1 well of a 6 well plate and subjected to 6-TG selection in MSC medium. Resistant colonies were split 1:4 whereas 2 parts were frozen, 1 part was sub cultured and 1 part was used for PCR analysis.

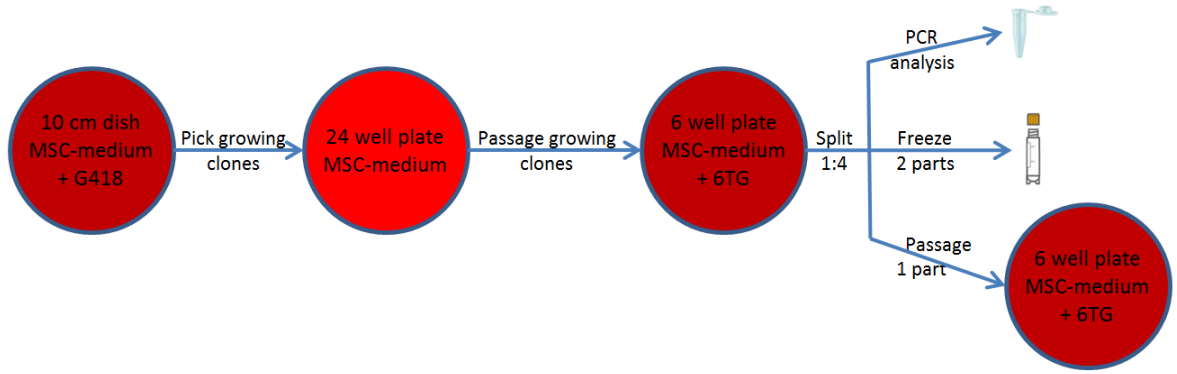

Figure 53: Overview of the applied selection strategy.
Transfected cells were seeded with the triple amount of non-transfected cells onto 10 cm dishes 48 h post transfection. G418 was added, growing colonies were passaged each to 1 well of a 24 well plate and cultured one passage w/o selection pressure. Growing colonies were passaged each into 1 well of 6 well plate with the 2nd selection antibiotic (6-TG). Colonies surviving this selection step were split 1:4, whereas 1 part was used for genomic DNA isolation and analysis, 2 parts were frozen and 1 part was subcultured under 6-TG selection.

The selection yielded in 142 G418 resistant colonies and 35 survived the subsequent 6-TG selection (Table 17). However, PCR analysis revealed that those colonies were false positive (data not shown). The sensitivity of the PCR assay was determined. It was found 10 copies of the rabbit genome are necessary to obtain a band on the agarose gel.

Table 17: Summary of *hprt* targeting experiments using a conventional targeting vector.
To obtain a targeted BM-MSC cell clone, different parameters (circular/linear vector, amount of DNA) were modified. After screening of all 6-TG resistant colonies only one was verified by PCR to be targeted.

Plasmid	DNA amount per well	Wells	# of G418 resistant colonies	# of 6-TG resistant colonies	PCR positive
circular	2 µg	2	49	7	0
	3 µg	3	93	28	0
linearized	1.7 µg	1	19	2	0
	3 µg	3	40	4	0
linearized	3 µg	4	246	55	1
circular	3 µg	8	202	14	0

Then, rbBM-MSCs P1 were transfected with linearized (XmnI – cuts in Amp^R) prbHPRT^{Neo} using 1.7 µg (1 well) and 3 µg (3 wells) per well. Selection strategy was the same as described above (Fig. 53). In total, 6 colonies were resistant to 6-TG (Table 17). Again, PCR analysis revealed that these colonies were false positive (data not shown).

In a last transfection experiment, rbBM-MSCs P1 were transfected with linearized (4 wells) and circular (8 wells) prbHPRT^{Neo} using 3 µg per well of a 6-well plate. Selection strategy was the same as described above. After G418 selection, 448 colonies were growing and 69 survived the subsequent 6-TG selection (Table 17). PCR analysis revealed that almost all

colonies, except one, were false positive. This colony no. 16 showed a band for *neo*^{R} in PCR analysis, but no band for exon 3 (Fig. 54). Most likely, this colony might be successfully targeted which would be the first targeting in rabbit cells. These cells can then be used for NT to produce gene targeted rabbits.

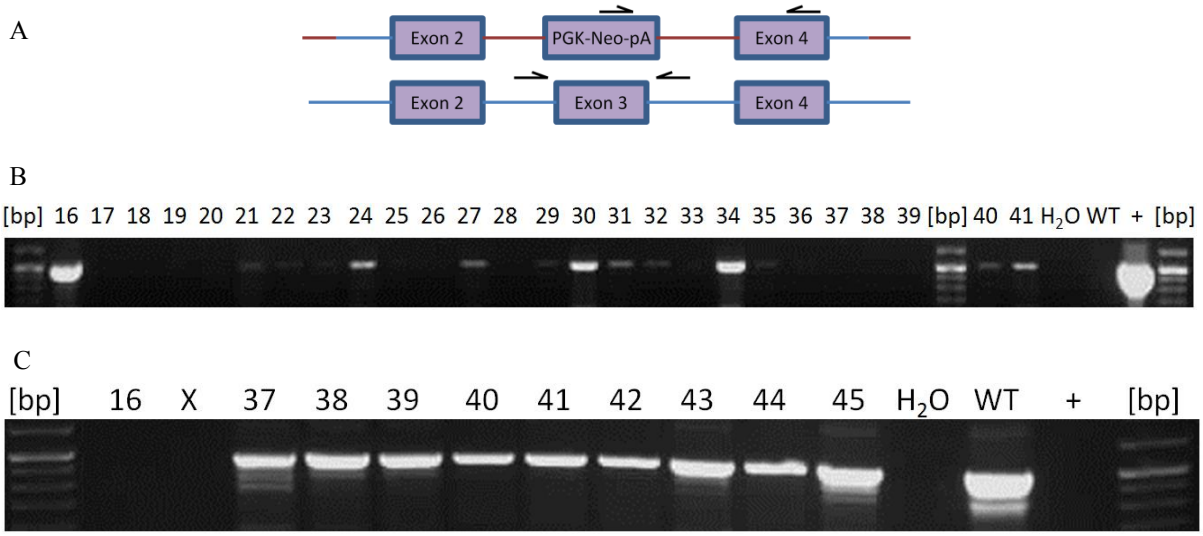

Figure 54: PCR analysis of rbBM-MSC colonies transfected with prbHPRT^{Neo} that were resistant against both G418 and 6-TG.
A) Binding sites of oligonucleotides used for PCR analysis. The primer pair indicating presence of targeting cassette anneals to the sequence of *Neo* and to exon 4 (upper panel). The primer pair indicating absence/presence of exon 3 anneals to intron 2 and intron 3 (lower panel). Genomic rb*hprt* sequences are indicated by blue lines, plasmid DNA are indicated by brown lines. **B)** PCR amplification of parts of PGK-*Neo* and exon 4. **C)** PCR amplification of exon 3 of rb*hprt*. Colony no. 16 shows a band for PGK-Neo-ex4 as well as a missing band for exon 3. +: control (prbHPRT^{Neo}), WT: control (WT DNA), X: empty lane. Note that both DNA controls (+/WT) serve as positive as well as negative controls in both different PCR amplifications due to the absence/presence of exon 3.

3.2.5 Summary

To obtain gene targeted rabbits by the method of cell-mediated transgenesis, important technical prerequisites were established and valuated. For this, different cell types were tested and characterised.

In the case of pluripotent rbESCs, no stable culture conditions could be established. However, the pluripotent potential was verified by the expression of crucial transcription factors, such as *Oct4* and *Nanog*. Pluripotency was further verified by the contribution of transgenic rbESCs to the ICM of developing embryos and by the achievement of one chimeric rabbit. Moreover, rbESCs were shown to differentiate into fibroblast-like cells, adipocytes and spontaneously active beating cardiomyocytes suggesting a mesodermal differentiation bias. However, the expression of markers for each germ layer could be revealed (*Desmin* (mesoderm), *Nestin* (ectoderm) and *Hnf4α* (endoderm)).

As an alternative cell type, rabbit A-MSC and BM-MSCs were established and characterised. The multipotency of BM-MSCs was verified by successful differentiations. Furthermore,

efficient transfection methods for rbMSCs as well as for rbESCs were established. The potential for cell-mediated transgenesis was successfully shown in nuclear transfer experiments. Totally, 18 live cloned rabbits from long-term cultured cells were achieved within this project. This is the highest number reported so far. Moreover, the first live cloned rabbit from genetically manipulated MSCs was achieved.

To obtain *hprt* knockout rabbits, rbBM-MSCs were transfected with targeting constructs whereby the *hprt* gene of one cell clone might be targeted by homologous recombination. This would be the first gene targeting in rabbits.

4 DISCUSSION

Today, the mouse is the most used animal in biomedical research due to well established genetic manipulative techniques. On the other hand, this animal model is very limited because of its small size and physiological investigations are not easily transferable to humans. There are some major metabolic and physiological differences and other animals resemble the human physiology more such as the pig, but it has limitations due to long generation times. The rabbit ideally fills the gap between small rodents and large livestock animals. Compared to livestock animals, the rabbit has shorter generation times and a large number of offspring. Due to its longer lifespan compared to mice and rats, the rabbit is very suitable for experimental human diseases that need longer observations. In addition, rabbits can be housed under specific conditions, for instance pathogen free. However, techniques to precisely genetically modify rabbits are not established and hamper the research. Therefore, the goal of this thesis is to extend the repertoire in the two areas of direct transgenesis and cell-mediated transgenesis.

The majority of genetically modified rabbits were established by using the breeds New Zealand white, Japanese white and Dutch belted. The Zimmermann Kaninchen (ZIKA, a hybrid strain of New Zealand White and Wiener Weißer) used in this thesis belongs to the minority in research [24, review].

In general, difficulties have arisen through a lack of genomic sequence data. At the beginning of the project, nearly no sequence data was available. Later, more and more rabbit sequences were stored in the GenBank with the adjunct “provisional”. At the end, a whole coverage of the rabbit genome was published, albeit some loci are still marked as a gap.

4.1 Transposon-mediated transgenesis

Due to high efficiency, integration as single copies, but being non-infectious, SB combines advantages of viruses and naked DNA. Since viruses and cellular organisms co-evolved, cells developed important defence mechanisms against viral infections. Non-viral vectors, such as SB, can avoid many but not all of these defences [517–519]. The most common non-viral gene delivery is simple plasmids. Plasmids have a very low integration rate and often turn off the expression of their transgene due to cellular responses. Additionally, the delivery of plasmids into cells is a difficult and inefficient process. SB can overcome at least the first obstacles due to a precise integration and stable transgene expression [520,521]. Importantly, the integration of transposons avoids multiple tandem integrations and also the formation of concatemeres.

Further, transposons facilitate single copy integration. Compared to retroviruses, DNA transposons have genome wide a more random distribution [522]. Since SB is a non-viral DNA molecule, therefore S1, production and delivery costs are much lower compared to viral vectors [523].

A prerequisite to apply DNA transposons to a selected organism some criteria need to be fulfilled. The certain type of transposon needs to have sufficient transpositional activity and already present endogenous copies in the target genome need to be absent to avoid their mobilization. Further, the cargo capacity and integration site preferences are important for the choice of transposon type.

4.1.1 Functionality of constructed Sleeping Beauty vector system

In this section, the functionality of the constructed SB system was tested by the expression of *mCherry* transgene both *in vitro* in cell culture experiments and *in vivo* by microinjection into fertilised rabbit oocytes. The constructed SB transposon system, consisting of the transposon vector containing SB ITRs flanking the expression cassette of CAGGs promoter directing *mCherry* and the transposase vector containing the CAGGs promoter directing *SB100*, was transfected into rbBM-MSCs that were found to be positive for expression of red fluorescence *mCherry*. As reported, SB shows the phenomenon of overproduction inhibition [108,109,524,525]. On the other hand, a more recent study shows no overproduction inhibition for SB100 [526], but is contrary to the results of this thesis and most publications. In this thesis, the phenomenon of overproduction inhibition was clearly seen since the number of cells expressing *mCherry* visualized by red fluorescence increased with a decreasing amount of pCAGGs-SB100. Hence, the functionality of the constructed SB system was proven. It is also known, that under same conditions the transposition efficiency can be different in distinct cell types of the same species, but of course also in different species [94, review]. Thus, the results obtained on rbBM-MSCs cannot be generalised to integration properties in other rabbit cells.

4.1.2 Generation of transgenic rabbits by transposon-mediated transgenesis

The aim of this part was to establish a transposon system for injection into fertilised rabbit oocytes and thereby generating transgenic rabbits. This was the method of choice for the generation of Ins^{Akita} rabbits. As proof of principle a transposon carrying the marker *mCherry* was constructed and transgenic rabbit foetuses were successfully achieved. In this work, the SB system was established by co-microinjection of pT2-SB-CAGGs-mCherry to pCAGGsSB100 in a molar ratio 1 : 0.01. In the first rounds of transfections, foetuses were

analysed by PCR for the presence of *mCherry*. Here, in independent rounds of microinjections transgenic frequencies per recovered embryo of 66.7% and 90% could be achieved. Cells of recovered foetuses were isolated, cultured *in vitro* and investigated for mCherry red fluorescence. Transgene expression could be detected and *mCherry* expression coincided with presence or absence of vector DNA in the genome as confirmed by PCR analysis. Thus, no silencing of the transgene could be detected. Also, foetuses obtained on d 21 *p.c.* showed no obvious failures in phenotype but appeared normally developed. The higher transgenesis rate relies on transposition-mediated gene delivery that increases the efficiency of chromosomal integration. Importantly, it facilitates single-copy (monomeric) insertions. Despite the overall integration of transposons is random there is a higher frequency of integration into accessible euchromatic regions as shown by Mátés *et al.* (2009) [66] and Izsvák *et al.* (2010) [527]. This behaviour prevents gene silencing that is seen by Grabundzija *et al.* (2010) [112] after integration into heterochromatin. Further, the typical integration of transposons as single copies prevents silencing of the transgene since single integrated expression units are less prone for silencing by cellular mechanisms. SB does not show any preference to integrate into genes. However, transgene silencing by DNA methylation and histone deacetylation was observed by Garrison *et al.* (2007) [528] after SB-mediated gene integration which was shown to be dependent on the promoter (RSV or EF1α) used. Further, they reported that transgenes rich in CpG dinucleotides are prone to silencing by methylation even when integrated into active chromatin regions. Thus, they reported integration efficiencies between 41 to 52%. When using SB100, Mátés *et al.* (2009) [66] reported the generation of transgenic mice by pronuclear injection with frequencies of 45% at embryonic day 7 and 37% at birth. Those results are similar to the findings in this thesis. However, their results cannot be reliable compared due to different stages of analysis (d 7 *p.c.* and at birth vs. d 21 *p.c.*). Further, they reported 1 – 2 integrations per genome, what matches the findings in this work. Here, as indicated by Southern Blot, two foetuses showed two integrations of *mCherry* per genome whereas another foetus showed a single integration. However, in a study by Wilber *et al.* (2007) [529] larger variations in copy numbers were observed in hESCs showing 1 to more than 10 stable SB integrations per cell.

The transgenic frequency using SB-*mCherry* (25% and 50%) exceeded those of conventional microinjections in rabbits (varying from 1.2 to 23.4%) that resulted in a low transgenic rate (Table 18). Note, that transgenic frequency is calculated based on live born. Hence, results are not exactly comparable, as the results of this thesis were obtained on recovered foetuses and

not live born. In conclusion, the use of SB system in combination with microinjection resulted in higher transgenesis rate as conventional microinjections.

Table 18: Summary of all published microinjection experiments performed in rabbits.

No. of injected embryos	No. of live born	No. of transgenics	Notes	Ref.
1907	218	28 (12.8%)	copy numbers vary from 3 – 88 integrations per genome	4
246	21	3 (14.3%)		41
248	39	3 (7.7%)		42
552	47	11 (23.4%)		530
274	40	7 (17.5%)		37
665	19	2 (10.5%)		531
7100	411	27 (6.6%)	237 live born were examined for transgenesis	532
500	41	6 (14.6%)		533
1005	50	11 (22%)		534
560	64	6 (9.4%)		17
1530	51	3 (5.8%)		29
N/A	18	2 (11.1%)		535
367	43	3 (7%)		536
627	51	3 (5.9%)		49
87	28	4 (14.3%)	Used a combined method of DNA microinjection into isolated blastomeres and the following injection of this blastomeres to a 16 cell stage recipient which was implanted into foster mothers until compaction stage.	537
292	72	8 (11.1%)	Injections into both pronuclei	538
331	85	1 (1.2%)	Injection into one pronuclei	
			In *in vitro* culture experiments only 66% of double injected embryos proceeded to blastocyst stage, but 90% of single injected ones	
456	80	12 (15%)		539

4.1.2.1 Influence of Sleeping Beauty on the integration and expression of the transgene

Due to the late integration of naked DNA into the host genome of fertilised oocytes by microinjection, the resulting transgenic animals can be mosaic for the transgene [63, review]. This integration process is facilitated by the use of transposons. Nonetheless, since the transposase gene needs to be transcribed and translated into functional protein, the integration events of the gene of interest (GOI) could occur in later developmental stages which could result in mosaicism. Thus, the double integration indicated by Southern Blot obtained in this work does not necessarily mean a double integration but could be a hint for single integrations per genome occurred in different blastomeres of the developing embryo. This could be elucidated in F1 offspring or in F0 by FISH. Usually, in microinjections pDNA is used to obtain transgenic animals but also mRNA could be delivered by microinjection to obtain a transient expression. As reported by different groups, the generation of mosaics could be overcome by the use of SBase mRNA or even protein [79,80,529,540–543]. In addition, this procedure prevents the integration of the transposase bearing vector.

Also, the presence of the two bands obtained in Southern Blot could be due to a double integration; whereas the second integration could result from a re-mobilisation due to still present transient *SB100* expression. On the other hand, the double integration could originate from two integration events. Then the amount of transposon vector could be titrated to have a lower concentration. Thus, the readjustment of SB100 concentration would be necessary.

When analysing SB integrations, the phenomenon of local hopping should be considered. Local hopping describes transpositions whereby transposons integrate into *cis*-linked sites in the vicinity of the original donor site. This phenomenon is observed in all DNA-transposons. Wang *et al.* (2008) [522] described a frequency of 50% for local hopping in SB that was within an interval of 5 MB. However, as found by Luo *et al.* (1998), Fischer *et al.* (2001) and Carlson *et al.* (2003) [544–546], the chromosomal window as well the extent of local hopping varies drastically between distinct transposons systems, in different species as well in distinct loci.

As reported by Henikoff (1998) [61], the random integration of transgenes may inactivate or disturb the functioning of other genes or even cause severe unwanted effects. Additionally, Kues *et al.* (2006) [547] reports that transgenes can become silenced by epigenetic mechanisms. The higher transgenesis rate obtained by applying SB could be partly explained by the integration into transcriptional active euchromatine. Yant *et al*. (2005) [100] showed in a study on human cells and Liang *et al.* (2009) [526] on mESCs that the integration of SB is very close to random. Contrary, both groups verified that piggyBac (PB) hits more often genes. Further, Ivics *et al.* (2009) [93], Yant *et al.* (2005) [100] and Hackett *et al*. (2007) [548] found that those integrated into genes, the majority of insertions was in introns. In principle, the integration of naked DNA introduced by microinjection relies on the occurrence of double strand breaks (DSB) and the subsequent repair mechanism through non-homologous end joining (NHEJ). As shown by Brinster *et al*. (1985), Towbin *et al*. (2009) and Wako *et al*. (2010) [549–551], since around 60% of the mammalian genome consists of repetitive elements like centromeres, telomeres and short~/long interspersed elements (SINE/LINE) and also other non-transcribed sequences, the stochastic occurrence of DSB leads to integration in such regions followed by epigenetic silencing of the transgene. Obviously, SB prevents the integration into those sequences. In addition, SB prevents the formation of concatemeres which is commonly seen by traditional microinjection [549]. Also, Kues *et al.* (2006) [547] and Mátés *et al*. (2007) [552] showed that monomeric integrations obtained with transposons are less prone to silencing mechanism compared to concatemeric integrations.

As discussed above, the integration locus is crucial for proper expression of the transgene. Moreover, according to very recent findings, the majority of DNA consists of biochemically functional regions that are important for the proper expression protein coding genes [553,554]. By applying FISH, the integration loci could be figured out on chromosome level. This method is especially helpful, if multiple integrations were detected by Southern Blot. To exactly elucidate the integration sites of SB various groups performed a splinkerette PCR that became

developed further in recent years [522,555–559]. A further group focused on thermal asymmetric interlaced (TAIL) PCR to elucidate integration sites in a similar manner [560,561]. Another approach is the method of advanced inverse PCR that also allows the identification of integration sites on sequence level [562]. Wilson *et al*. (2007) [125] and Yant *et al.* (2000) [563] using a more laborious way by subcloning the regarding fragments into plasmids followed by sequencing.

4.1.2.2 Improvements for transposon-mediated transgenesis

Often, nuclei are difficult to identify during injections. This was also observed in this study. Hence, injections were not reliable. This could be overcome by cytoplasmic injection which simplifies the delivery of the transposon system. As shown by Sumiyama *et al*. (2010) [564], cytoplasmic microinjection causes less damage to oocytes and leads to higher viability. This group reported a transgenesis rate of 30 - 66.7% using Tol2 in mice. With pronuclear injection they achieved a rate of 20%. As reported by Garrels *et al. (*2011) [565], microinjection into cytoplasm does not decrease the efficiency of SB100 in livestock. On the other hand, Brinster *et al*. (1985) [549] and Sumiyama *et al*. (2010) [564] reported that cytoplasmic injection of vector DNA alone is significantly less efficient as pronuclear injection. The findings in this thesis of low survival rate of injected embryos could be due to damage that unavoidably occurs during microinjections and due to toxic effects of foreign DNA. As reported by Sumiyama *et al*. (2010) [564], linear DNA could be more toxic than circular DNA during pronuclear injection. Since a linear pDNA (for transposon-transgene vector) was used in this thesis that might partly explain the low survival rate. Further, the amount of DNA and the volume of DNA solution that was injected are based on empirical experiences. Nevertheless, the size of the droplet to be injected varies from injection to injection and could of course have an influence on the embryos. Here, the microinjection into cytoplasm allows more tolerance as the cytoplasm is more voluminous as the nucleus.

An improvement of transgenesis rate could be the use of methylases. As shown by different groups methylation of SB transposon increases the transposition efficiency up to 9 fold [522,566–569]. As a result, the donor site becomes heterochromatinised and enhances SB transposition. Contrary, Wang *et al.* (2008) [522] showed that methylation of PB decreased transposition efficiency 12 fold. However, as reported by Carlson *et al.* (2011) [569], the transposon becomes reprogrammed during embryonic development and expressed in a manner characteristic for its specific locus.

When integrating transgenes into a host genome two processes need to be considered. One is the variability in the expression level and the other the decrease of expression over time [570, review: 571]. The expression of transgenes is controlled by its own promoter but also enhancers and insulators that both are provided either endo- or exogenously [572–575, reviews]. Additionally the integration loci itself is important for the expression of transgenes. As shown by Robertson *et al.* (1995) [576] the locus could become silenced by chromatin rearrangement which is known as position effect. Hence, integrations close to heterochromatin became silenced more often as in open euchromatin. Of course, the status of chromatin depends on the differentiation and function of the particular cell. As shown by Giraldo *et al*. (2003) [577] and van Keuren *et al*. (2009) [578], the use of insulators can prevent transgene silencing regardless of integration site and the use of enhancers leads to a reliable expression. Insulators need to be located on each side of the transgene [579, review]. However, insulators are neutral genetic elements; they do not act as activators or repressors. Nevertheless, insulators are not able to shield the transgene under each condition from silencing. Walisko *et al.* (2008) [580] and Dalsgaard *et al.* (2009) [581] successfully used insulators in combination with SB. In addition, insulators prevent the risk of *cis* activation of neighbouring genes on the integration side. However, Walisko *et al.* (2008) [580] found that SB has a very weak activity as enhancer or promoter for transcriptional activity of neighbouring genes.
Recently, Ammar *et al*. (2012) [582] showed site-specific integration of SB. Hereby, so called target fusion proteins were applied. This would allow targeted integrations with high efficiency. Previously, Wilson *et al*. (2005) [583] applied the fusion of transposons with zinc fingers to allow site directed transposition albeit with a very low efficiency.

Should problems arise following the analysis of transgenic rabbits, other DNA-transposon systems that were developed in the last years for transgenesis of higher eukaryotes could be used as they possess different characteristics, such as PB [82], Frog Prince [86,584], Minos [74,585], Tol1/2 [77,78,586] and Passport [587]. PB allows cargos up to 9.1 kb without a loss in efficiency whereas transposition is possible up to 14.3 kb albeit with decreasing efficiency. Distinct from SB and PB, Wu *et al.* (2006), Balciunas *et al.* (2006) and Koga *et al.* (2007) [588–590] reported that Tol1 and 2 does not show any preference for a specific sequence and no overproduction inhibition was observed. Further, Suster *et al*. (2009) [591] found that Tol2 transposes single copies of 66 – 120 kb. Hence, the Tol2 system could be an interesting alternative. Nevertheless, a very recent report shows the transposition of BACs (150 – 196 kb) on both SB- and PB constructs [1093]. However, the application of transposons has still limitations in the

generation of transgenic animals. Since the usual transposon system allows only gene addition, only dominant negative mutations can be introduced into the host genome. An interesting option could be inducible transposon systems, whose construction was shown [592,593].

4.1.3 Functionality of rabbit *insulin* expression vectors

The loss of β-cells is a hallmark of both Diabetes mellitus (DM) type I and II [594, review]. Hence, a model that shows progressive loss of these cells could serve as an optimal model. Interestingly, it was reported that the second *insulin* gene of rodents (mistakenly named *insulin I*) is a result of a transposition event 15 million years ago [595].

Contrary to mice and rats, the rabbit has only one *insulin* gene exactly like humans. This fact predisposes the rabbit as animal model for DM. In this work, functional units of rabbit *insulin* were estimated based on published sequence data from human and other species due to the high homology [596–598]. The sequence of human *Insulin* was elucidated 1980 [599].

The first report that the Akita mutation (1.2.1.2) leads to dysfunctionality of β-cells was from Wang *et al*. (1999) [391] in the maturity-onset diabetes of the young (Mody) mouse [390]. This Akita mouse model is widely used as a model for DM I. It is not accompanied with obesity and insulitis. Another report found this mouse suitable for modelling DM II due to the appearance of insulin resistance as a result of chronic hyperglycemia albeit without obesity [600]. Thus, this specific mutation and its effect could be an optimal model to study the common aetiology of both types DM I and II and associated complications. The Akita mutation leads to misfolding of INS because an essential disulphide bonds fails to form. That is due to the single base pair exchange from guanine to adenine which results in a change in the coding triplet (TGC → TAC) and finally in the aa from cysteine to tyrosine. Thus, the misfolded INS accumulates in the ER and induces a series of rescue mechanisms that finally result in apoptosis of β-cells [390,391,397].

A similar model is the Munich $Ins2^{C95S}$ mouse [601]. Here, the reason for development of DM is also a point mutation (T → A) on a prominent position resulting in malformation of insulin due to disruption of a disulphide bond. Summarised, the phenotype is very close to this of Akita mice because the cellular responses are the same following the misfolded protein that get stacked in the ER. However, both mutations, either in mice or humans, show sex specific variations. In males the phenotype is more severe than in females. It was speculated that it is due to an anti-diabetic effect of oestrogen [602, review].

Studies by Støy J *et al.* (2007) [392] and Edghill *et al.* (2008) [603] of different *insulin* mutations causing neonatal DM in humans revealed a mutation similar to that of the Akita mouse. Neonatal DM is very rare due to distinct monogenic mutations (like the Akita mutation). Most often DM is a result of multiple factors.

To introduce the Akita mutation into rabbits, rabbit genomic *Ins* was cloned, including promoter and transcription unit. Then, the Akita mutation was inserted. Finally, two expression vectors were obtained: pINS^{Akita} (mutated *Ins*) and pINS^{WT} (WT *Ins*). Both vectors contain an artificial triple polyA site. The functionality of constructed rabbit *insulin* expression vectors was verified in rat insulinoma cells (INS1E). These cells are very similar both in morphology and function to native β-cells [604–608]. Importantly, they are positive for *insulin* expression.

Upon transfection of pINS^{Akita} and pINS^{WT} into INS1E cells, the expression of both rabbit *Ins^{Akita}* and *Ins^{WT}* was successfully proven by RT-PCR. Further, the functionality of both *Ins^{Akita}* and *Ins^{WT}* was successfully verified in INS1E cells. Similar approaches like in this thesis to show the apoptotic action of *Ins^{Akita}* were performed by other groups. Araki *et al*. (2003) [609] transfected MIN6 cells (a mouse β-cell line) with mutated and non-mutated mouse *insulin*, respectively. The observations were the same as in this thesis: cells transfected with mutated *insulin* underwent apoptosis but not cells transfected with non-mutated *insulin*. Since INS1E cells transfected with *Ins^{Akita}* expression vector died but not control cells (*Ins^{WT}*), it is very likely that this effect is due to ER stress induced apoptosis. To proof the very likely action of ER stress induced apoptosis in INS1E cells, quantitative PCR for stress response molecules (e.g. *BiP*), factors involved in ERAD (e.g. *Hrd1*, *Sel1L*) or specific apoptosis inducing factors (e.g. *CHOP*, *caspase-12*) could be performed. That ER stress resulting from murine *Ins^{Akita}* causes apoptosis of INS1E cells was shown by Hartley *et al*. (2010) [610] who verified also the up regulation of stress markers, chaperons and ER-associated degradation genes. Directly, the bisulfide mispairing of *Ins^{Akita}* could be verified by non-reducing Tris-Tricine-urea-SDS-PAGE which was shown to have a very high sensitivity in this regard [611–613]. Importantly, this work demonstrates the action of *Ins^{Akita}* expression vector only in INS1E cells, but not in rabbit fibroblasts. This indicates that the promoter of the cloned *insulin* gene is functional and specific to insulin expressing cells. Further, the obtained results confirm the cell specific functionality of the constructed vectors.

Recently, the molecular linkage between diet, obesity, DM and finally the dysfunction of human and mouse β-cells was verified [614]. The trigger for the sequential molecular events leading to this dysfunction is elevated concentrations of free fatty acids (FFA) resulting from

a high fat diet. What follows is a series of typical metabolic disorders. In addition, a fatty liver develops and it comes to resistance to insulin [614]. This in turn leads to ER stress in β-cells and finally in their apoptosis. This ladder step could be modelled with the *Ins*^{Akita} rabbit. Interestingly and important, the lipid metabolism of rabbits closely resemble this of humans [615]. This indicates the usefulness of rabbits to study DM from the initial triggers until the overt disease.

4.1.3.1 Implications of *Ins*^{Akita} rabbits

Once the rabbit *Ins*^{Akita} model would be generated, it is necessary to detect its transcript and protein. According to publications, the presence of plasma insulin [616,617] and also pancreatic insulin [618,619] can be verified in foetal rabbits. In an analysis of Fletcher *et al*. (1982) [620], pancreatic insulin was found already at gestation day 22. Previously, Milner *et al*. (1969, 1975) [618,619] reported that insulin secretion precedes the glucoregulatory action.

Once the *Ins*^{Akita} rabbit is available, measurements of C-peptide, a marker for endogenous insulin production [621], would allow a rapid and validated quantification. Righettoni *et al*. (2010) [622] measured the blood glucose concentration indirectly through the exhaled air by determination of the acetone concentration with a tiny sensor chip.

Depending on the proceeding of DM upon *Ins*^{Akita} expression in rabbits or the research question, the expression of *Ins*^{Akita} could be controlled by applying the Tet-on system [623–626, review: 627]. Hereby the *insulin* promoter would direct the Tet-transactivator that, upon administration of doxycycline, would activate the Tet-promoter which directs *Ins*^{Akita}. Thus, *Ins*^{WT} would be secreted as naturally controlled but the expression of *Ins*^{Akita} could be controlled tissue specific and time dependent (spatiotemporal). Also, this system could be applied the other way around (Tet-off). Then, administration of doxycycline would switch off the expression of *Ins*^{Akita}. The Tet system could be cloned as one cassette and introduced by transposition into the rabbit genome.

In a healthy human, the β-cell mass is maintained by pancreatic stem cells also under difficult conditions like obesity and some states of insulin resistance [628, review]. Under pathologic conditions of DM, β-cells were destroyed and cannot become replaced by those stem cells. Notkins *et al*. (2001) [357] found that at the time of clinical diagnosis and overt DM (hyperglycaemia), already 70% of β-cell mass is destroyed. The introduction of the Akita mutation into rabbit *insulin* finally results in the destruction of β-cells and a lack of insulin. The underlying idea is to have an animal model for islet transplantation (Fig. 55). Successful and functional transplantation should supply the rabbit with insulin whose level is regulated according to blood glucose concentration. Later on, this could lead to new therapies for

human patients suffering on DM. The use of autologous stem cells for transplantation in autoimmune diseases has been reported [629, review]. Distinct efforts to cure DM I by cellular transplantation both in animals and humans were performed albeit with low success [630–634]. Also, a lot of research on islet transplantation in humans was already performed [381,635–637,642; reviews: 638–641]. Mattsson *et al*. (2002) [643] reported that often the transplantation fails due to disconnection from blood supply which results in too late revascularization leading to dysfunction. Hence, Zhang *et al.* (2004), Lai *et al*. (2005) and Su *et al*. (2007) [644–646] achieved improvements by overexpressing angiogenic growth factors. Miao *et al*. (2006) [647] expanded the findings by the administration of other growth factors and subsequent transplantation. A further attempt was the application of MSCs that enhance revascularisation, excrete immune-modulatory molecules and create a cytoprotective milieu [649, review: 648]. Olerud *et al*. (2009) [650] applied successfully the co-transplantation of neurospheres. Instead transplanting isolated islets the transplantation of whole pancreas was suggested for better prognosis and long term stabilisation of the glycaemic level [651, review]. On the other hand, Ricordi (2003) [652] and Froud *et al*. (2005) [653] reported that transplantation of islets is much simpler then pancreases. However, after interruption of immunosuppression, DM relapses [654, review]. All those facts highlight and underline the importance of a suitable animal model.

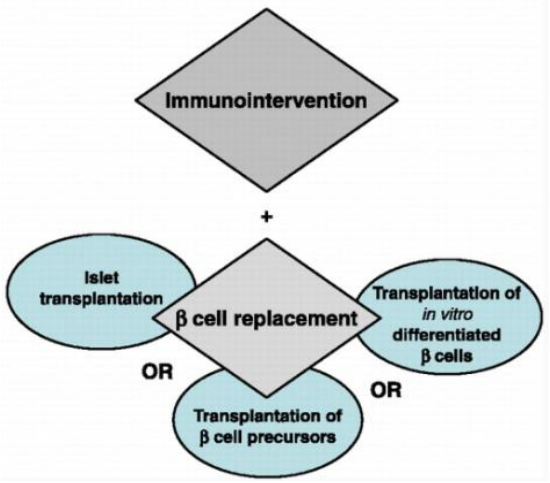

Figure 55: Overview of current strategies to restore the natural adaptive insulin providing function.
β-cells could be replaced by stem or precursor cells, by in vitro cultivated β-cells or transplantation of islets. However, intervention of immune reactions is necessary. Adapted from Couri and Voltarelli (2008) [655]

Due to the progress in stem cell biology and the opportunity to have patient specific, autologous stem cells either by isolation or full or partly reprogramming and their subsequent directed differentiation or transdifferentiation into islet cells, the need for immunosuppression decreases. Spontaneous *in vivo* differentiation of mESCs into INS producing cells was reported in the mouse [656] as well as a directed reprogramming approach of differentiated pancreatic exocrine cells into cells resembling β-cells [657]. Further, an approach that opens the

possibility for patient specific cells was developed by Kunisada *et al*. (2012) [1105] using reprogramming of human fibroblasts into iPSCs and their differentiation into insulin-producing cells. On the other hand, safety is still a matter. Today, there are no safely reproducible and convenient differentiation protocols available. Mostly, some cells present after differentiation possess still stem cell character. To prevent their possible carcinogenic action in the patient, those cells need to be efficiently eliminated before transplantation. Here, the *Ins*^{Akita} rabbit could serve as a valuable model.

Timper *et al*. (2006) [658] and Gao *et al*. (2008) [659] showed the transdifferentiation of hMSCs into INS producing β-cells. Since these protocols were also established using human A-MSCs [660–662], this could simplify the process as A-MSCs are obtainable in minimal surgical. Those differentiated islet cells could then serve as autologous transplants. First studies to use those cells were already performed in mice and rats [663,664]. Again, the rabbit could serve as optimal model. Due to carcinogenic risks when transplanting stem cells as observed in human patients [665,666] it must be shown that stem cells considered for transplantation meet the criteria by the International Society of Stem Cell Research [667].

Successfully established transgenic rabbits could then serve as models for human diseases of interest that have also huge impact, for instance Parkinson's disease. To model this disease a truncated parkin protein could be expressed. This causes cellular stress which results finally in apoptosis of specific neurons. It is known, that recessive mutations of *parkin* are the most common cause for this disease and that this gene is the most affected one albeit mutations in other genes lead to the same disease [668,669; reviews].

4.2 Cell-mediated transgenesis

Since numerous obstacles of SCNT are attributed to faulty epigenetic reprogramming of the cell nucleus, it is thought that cells with a higher potency prevent these circumstances. Hence, the aim of this work was to obtain pluripotent or at least multipotent rabbit cells. Typically, success rate (live births of transferred embryos) of mammalian SCNT is only 1 – 3% [670,671]. In general, a major influencing factor for efficient NT is the cell type. The cells should fulfil distinct criteria: high proliferation rate *in vitro*, amenable for genetic manipulations, stable chromosome number, support of HR and should undergo successful reprogramming after NT. Previously, the cloning of rabbits was reported only by two other groups [672,673] including one transgenic rabbit [674].

4.2.1 Pluripotent cells

Pluripotent cells are the cells with the highest potency cultivable in the laboratory. Totipotent cells are only available in the first cleavages of the developing embryo [675, reviews: 676–678]. Since verified rabbit pluripotent cells are not available today, attempts to cultivate those cells were carried out. As shown by our own work important markers could be verified indicating a pluripotent character of the isolated cells [509,516]. ES-like cells of rabbit have been reported albeit the formation of chimeras from cultured pluripotent cells was not shown [679–682]. Also, rabbit ES-like cells were not yet used for NT. Fang *et al.* (2006) [679] reported the ability of differentiated ES-like cells for successful NT. Surprisingly, the derivation of definitive pluripotent cells, regardless if ESCs or iPSCs, shows to be difficult in many species [683–688].

4.2.1.1 Pluripotency is influenced by extrinsic factors

According to the achieved results, optimal culture conditions for rbESCs could not be revealed. It is highly likely that a culture consisting of both differentiated and undifferentiated cells (as revealed by the expression of markers for pluripotency and differentiation) is not stable. Since stem cells possess two opposing hallmarks, self-renewal and multi-lineage differentiation potential, the underlying signalling network, most importantly Oct4, Nanog and Sox2, needs to be tightly controlled. Probably, this network is not balanced in our rbESC cultures, which is mainly influenced by culture conditions. As shown with the experiments in 3.2.1.2, the culture conditions indeed provided some factors maintaining pluripotency. Especially, this is obvious when rbESC-5 was cultured long-term under three different conditions without faulty karyotype. Cells grown in mES medium showed the most karyotypes with normal diploid chromosome set (2n = 44). However, the mode was 44 in all

three sublines. The phenotype changed drastically when cultured in DMEM+ that does not provide pluripotent stimuli for both murine and human ESCs. This indicates the influence of extrinsic factors on maintaining pluripotency of rbESCs.

The most convenient way to culture ESCs is to use mitotically inactivated mouse embryonic fibroblasts (MEF-MITO), called feeders. In addition, there is a need to supplement the medium with LIF for mESCs and bFGF for hESCs, respectively (Fig. 56). Due to unknown signalling in rabbits, both were supplemented to rbESC medium. As shown, the downstream effectors of LIF are among others Nanog, Klf4, Tbx3 and c-myc [232,234,244,689–692]. Also, BMP4 becomes activated by LIF [243] which than activates inhibitor of differentiation genes. Contrary, BMP4 is activated during mesodermal differentiation of hESCs. Thus, the role of BMP4 remains unclear in rbESCs. Previously it was shown by Beattie *et al*. (2005) [693], that MEFs express and secrete activin into the medium that is necessary for pluripotency of hESCs [694]. In addition, Hsu *et al*. (1998) [695] found that MEFs express *gremlin* that is an inhibitor of BMP. However, the quality of feeders varies from isolation to isolation. Thus, a reliable expression and secretion of pluripotency promoting molecules could not be stably secured over longer periods which influence rbESCs pluripotent signalling.

The composition of serum has an important extrinsic effect but may vary from batch to batch. It would be worth to use a chemical defined medium. In addition, this would allow a feeder free culture as shown for hESCs [696,697]. Furthermore, then it is possible to determine if LIF and/or bFGF are needed for rabbit pluripotency (Fig. 57). In a defined medium, one can figure out which bioactive small molecules have positive effects on rbESCs. For instance, SC1 (pluripotin), that has an inhibitory effect on Erk1, was shown to support mESCs in the absence of serum, feeders and cytokines [698]. Further, the concurrent inhibition of glycogen synthase kinase 3 (GSK3, an inhibitor of Nanog [701]) and FGF4-Erk1/2 MAPK supports mESC pluripotency [699, review: 700]. In addition, Storm *et al*. (2007), Stefanovic *et al*. (2009) and Snyder *et al*. (2010) [702–704] reported that the continuous supplementation could have side effects causing differentiation. It was reported that those secondary effects lead to a high variability by the creation of heterogeneous and unstable ESC culture with fluctuating degrees of pluripotency highly similar to the findings in this thesis. Here, it would be important to elucidate the optimal concentration of LIF for rbESCs. Yang *et al*. (2009) [705] reported the derivation of mESCs of formerly refractory non-obese diabetic (NOD) mice using a defined chemical medium approach in which LIF and SC1 were used. Also, similar approaches, *e.g.* LIF in combination with inhibitors of Erk and GSK3 (referred as 2i condition) [699,706,707], were successful, also on other non-permissive strains (C57BL76, CBA) [708–710] (Fig. 56).

Interestingly, Sato *et al*. (2004) [196] found that inhibition of GSK3 maintains pluripotency in both mESCs and hESCs. In addition to LIF, the PI3K/AKT pathway is also activated by IGF1 [193,194]. This could explain the positive influence of IGF2 onto rbESCs that was seen in this work. Bendall *et al*. (2007) [711] and Brill *et al*. (2009) [712] showed that IGF and bFGF act together to maintain pluripotency. Hence, this particular combination needs to be tested on rbESCs.

Another small molecule, IQ-1 acting in the Wnt pathway was shown to maintain mESCs in feeder free conditions [713]. Burton *et al*. (2010) [714] applied successfully similar experiments on hESCs. Here, a condition free of both feeders and cytokines (including bFGF) could be achieved with the supplementation of defined chemicals [715, review]. However, Li *et al*. (2007) [716] reported that conditions using two inhibitors (2i) failed in maintaining hESCs since their pluripotency requires MEK/ERK signalling. Recently, as conclusion of the distinct species specific signalling in pluripotency, hESCs are classified as primed pluripotent, as they are slightly differentiated. In contrast, mESCs are classified as naïve pluripotent [220–222, reviews]. It was concluded, that LIF is important for the acquisition of the naïve state. Attempts by Hanna *et al*. (2010) [717] to convert hESCs to a naïve pluripotent state using 2i and LIF albeit with a constitutive expression of *Oct4* and *Klf4* were successful. On withdraw of exogenous expression, cells underwent differentiation but could be rescued by the addition of forskolin that partly activates *Klf2/4*. Experiments supplementing rbESCs with forskolin were performed within this work but cells underwent apoptosis (results not shown). Recently, Tsutsui *et al*. (2011) [718] performed a systematic analysis of various surface coatings and five small molecules in distinct concentrations (inhibitors of ROCK, MEK, GSK3, FGFR) and their combinations on hESCs. Due to the disappearance of naturally occurring naïve hESCs and also of other species, but the relative simple obtaining of mESCs, it was speculated that this phenomenon is a cause of the diapause [719]. Thus, cells have a halt in their developmental progression and it is possible to capture pluripotent cells. Apart from more simple organisms, diapause occurs only in rodents, bears, mustelids and marsupials. Accordingly, derivation of rbESCs might be hampered.

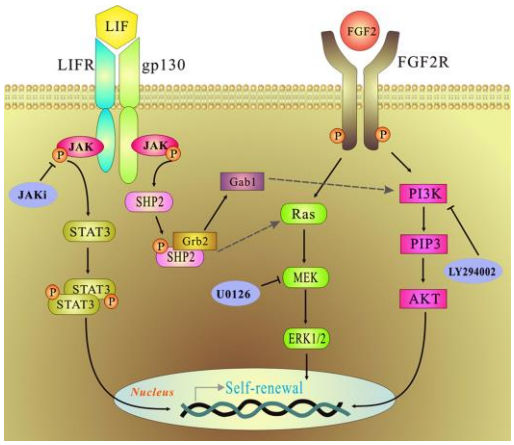

Figure 56: Signalling pathways induced by LIF and bFGF that result in self-renewal.
Also, cross interactions of the LIF pathway into bFGF pathways are indicated. Adapted from Hsieh *et al.* (2011) [720]

A further impact has the handling of ESCs especially during passaging. It was reported by Ohgushi *et al*. (2010) [721] and Chen *et al*. (2010) [722], that dissociation of mESCs to single cells has no effect on cell viability whereas hESCs undergo apoptosis when dissociated. The use of the Rho-associated protein kinase inhibitor (ROCK-i, stabilises E-cadherin) was shown to be helpful under standard conditions in rbESCs and also for hESCs [723] and monkeyESCs [1092]. In a stable culture, the cell-cell interactions inhibit Rho-ROCK signalling itself. In this condition, the addition of ROCK-i would be only needed right after passaging, when cells are dissociated and Rho-ROCK signalling becomes upregulated which then destabilises cell-cell adhesions [724–729]. In turn, Rho-ROCK signalling increases further which finally leads to a complete and irreversible loss of cell adhesions. On the other hand, supplementation of rbESCs with ROCK-i showed only positive effects on the morphology when cultured in CM and in the combination with LIF and bFGF, but not under any other condition (3.2.1.2). Also, mES medium supplemented with LIF, bFGF and ROCK-i led to differentiation of rbESCs. Since the positive feedback loop of increased Rho-ROCK signalling after dissociation and loss of cell adhesions was not observed in mESCs this could be a hint that rbESCs have a more similar signalling to mESCs than to hESCs. Recently, Kawamata and Ochiya (2010) [730] used ROCK-i to obtain and culture ratESCs. As shown by Xu *et al*. (2010) [723], the negative impact of passaging could be overcome by the use of small molecules which enhance the survival after dissociation in chemical defined medium. These molecules improve the adhesion to extracellular matrix (ECM), like matrigel or laminin but not to gelatine. Since the plates for rbESCs were covered with gelatine there could be a need for a distinct ECM substrate. It was reported by Paling *et al*. (2004) [731] and Armstrong *et al*. (2006) [732] that the increased cell-ECM interactions enhance cell survival and growth mediated by integrin signalling (Fig. 57).

In this thesis the cultivation of rbESCs in feeder-free condition was shown, although the medium was still conditioned by feeders. Xu *et al*. (2001) [733] used the same cultivation procedure for hESCs. However, for hESCs Amit *et al*. (2004) [734] used non-conditioned and serum free medium with defined factors (TGFβ, bFGF and LIF) and cultivation on fibronectin [735, review]. The supplementation of the medium with an Erk inhibitor could help to stabilize the pluripotent state in rbESCs. Nichols *et al*. (2009) [736] found that an inhibition of Erk reduces the population of Nanog-negative cells. Accordingly as found by Kunath *et al*. (2007) [737] and Stavridis *et al*. (2007) [738], a stimulation of ESCs with Erk primes them for differentiation. Since Erk becomes activated by bFGF signalling, the supplementation of rbESCs cultures could have an opposite effect as expected. In general, it was reported that the activation of oxidative pathways is linked to the induction of differentiation [739–741].

An important extrinsic factor influencing cell culture is the concentration of O_2 (Fig. 57) [1088–1090]. Wion *et al*. (2009) [742] showed that the O_2 concentration has influences on various cell functions. Recently, it was reported by Lengner *et al*. (2010) [743] that atmospheric O_2 concentration (20%) leads to X-chromosome inactivation in hESCs. As mentioned by Silva *et al*. (2008) [744], the reactivation of the X-chromosome is a further hallmark of ESCs. This could be tested in rbESCs. In this work, rbESCs were routinely cultured under atmospheric O_2 concentration. Most importantly, Hu *et al*. (2003) [745] and Covello *et al*. (2006) [746] found a direct linkage of O_2 sensing and *Oct4* regulation. Also, Yoshida *et al*. (2009) [747] reported an enhanced induction of pluripotency by low O_2. Thus, it could be that rbESCs are especially sensitive to high O_2 concentrations and should be cultivated under permanent low concentration. In a study on hESCs, 149 genes were found to be regulated differently under high and low O_2 concentrations [748,749].

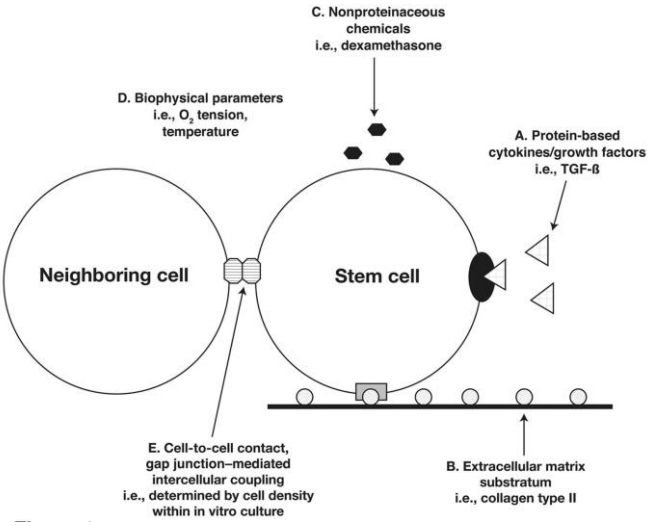

Figure 57: Extrinsic signalling that influences various cellular processes here in particular pluripotency. For instance when the neighbouring cell is differentiated, their signalling often induces differentiation in the pluripotent cell. Adapted from Heng *et al*. (2004) [750]

4.2.1.2 Plasticity of pluripotent cells

Due to the obtained results, it is speculative that rbESCs might have an unstable pluripotent state. The expression of various markers (e.g. *Oct4*, *Sox2* and *Desmin*, *Nestin*, *Hnf4α*) indicated both the presence of pluripotent and differentiated cells. The fact that not all pluripotent cells differentiated but maintained self-renewal also in high passages leads to the hypothesis of inherent plasticity of rbESCs. This is underlined by recent findings by other groups. Since the late blastocyst consists of three cell types, namely trophectoderm, hypoblast (both contributing to extraembryonic tissues [676,751; reviews]) and the epiblast, the cells are already affected by distinct cues. After implantation, pluripotent cells can still be found in the epiblast. When isolated and cultured, these cells are called EpiSC (primed ESCs) [171,172]. Nevertheless, Wei *et al*. (2005) [752] reported that those cells have distinct properties then mESCs [753, review]. For instance as shown by various groups [232,246,694,754–757], instead a requirement for LIF or BMP4, they need activin/Nodal and bFGF and instead expression of *Rex1* (*Zfp42*) and *Klf4* as markers, they express *Fgf5* and *brachyury* (*T*). By switching the media composition (supplementation with activin and bFGF [758] or inhibition of LIF/STAT3 [759]) it is possible to convert mESCs to EpiSCs (Fig. 58). Zhou *et al*. (2010) [760] used small molecules (inhibitors of LSD1, ALK5, MEK, FGFR and GSK3) for the reprogramming of EpiSCs to mESCs highlighting the huge influence of those chemicals in ESC derivation and cultivation. Previously, Chou *et al*. (2008) [761] showed that available growth factors define distinct ground states of stem cells. It would be interesting to reveal their influences on rbESCs. Due to these important differences in the signalling network the pluripotent state is subdivided into naïve ~ (ESCs) and primed pluripotency (EpiSCs) (Fig. 58). Noteworthy, as shown by Tesar *et al*. (2007) [172], Kerr *et al*. (2010) [217] and Chenoweth *et al*. (2010) [218] hESCs resemble EpiSCs very closely in terms of phenotype, culture requirements and signalling.

In addition, studies by Laslett *et al*. (2007), Hough *et al*. (2009) and Kolle *et al*. (2009) [762–764] showed that within the same population of ESCs various states exist, revealing certain plasticity in the culture. It was shown, that cells within those cultures with the highest self-renewal capacity express the highest levels of pluripotency genes. This finding underlines the hypothesis of an unstable rbESCs culture and the presence of pluripotent and differentiated cells. Accordingly, it would be necessary to elucidate the expression level of pluripotent genes in rbESCs by quantitative RT-PCR.

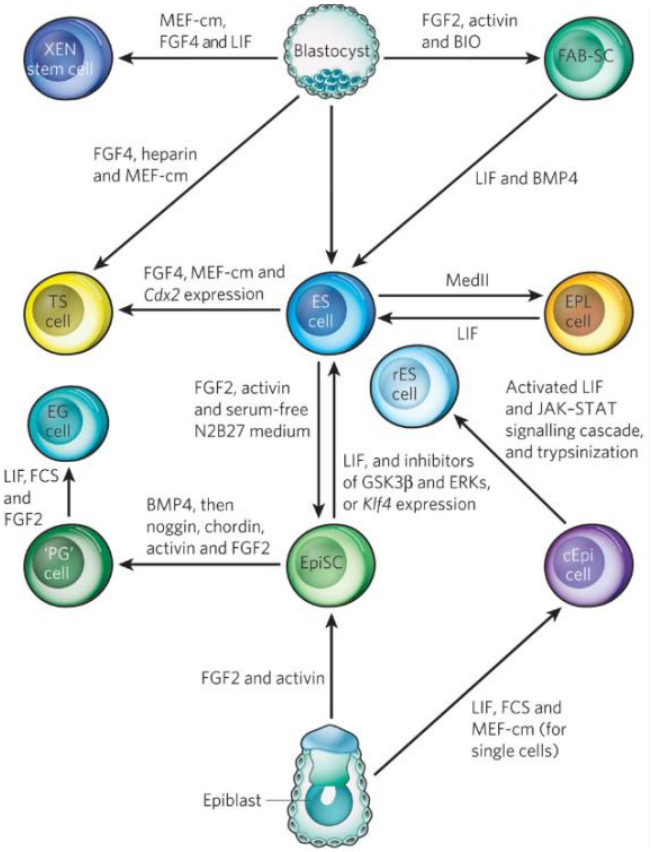

Figure 58: Plasticity of stem cells.
Summary of various factors influencing pluripotency of mESCs. Not all cell types are discussed in the text, due to irrelevance in optimisation the cultivation of rbESCs. Adapted from Pera *et al*. (2010) [223]

4.2.1.3 Pluripotent signalling network

The expression and identity of important pluripotent signalling molecules could be verified on the obtained rbESCs, including the crucial factor Oct4. Oct4 was reported by Chew *et al.* (2005) [206] to target and promote itself. Further the expression of *Nanog*, *Sox2*, *FoxD3* and *Rex1*, which are target genes of Oct4 [765–767] was demonstrated in rbESCs previously [509]. Shi *et al*. (2008) [515] characterised the rabbit gene coding for Oct4. In addition, in localisation studies thousands of sites in the genome were identified to which Oct4 binds [768–770]. The expression level of *Oct4* is very critical in the maintenance of pluripotency. Lower levels of Oct4 resulting in a trophectodermal phenotype [771], whereas elevated levels leading to differentiation into the endodermal and mesodermal lineage [772]. This finding fits to the obtained results of rbESCs. Here, the line rbESC-5 expresses markers for those both lineages (*Desmin* (mesoderm) and *Hnf4a* (endoderm)). This indicates a heterogeneous cell population consisting of differentiated cells and cells maintaining pluripotent character. However, the

expression level of Oct4 was not determined in rbESCs and needs to be confirmed to support this hypothesis. The simultaneous expression of two or more lineage associated TFs in undifferentiated stem cells is called lineage priming [773].

The TF Sox2, whose expression was also shown in rbESCs, has many of the same targets as Oct4, since both factors interact together [774,775]. Hence, many target genes possess composites of Oct4/Sox2 recognition sequences [207,776]. As shown by Ivanova *et al*. (2006) [777], a decreased level of Sox2 leads to differentiation into both trophectoderm and epiblast derived lineages; but Masui *et al*. (2007) [778] found solely a differentiation into trophectoderm. It is believed, that Sox2 stabilizes the expression of *Oct4* [778].

The third most important factor, Nanog, found also to be expressed in our rbESCs, was shown by Chen *et al*. (2008) [770] to bind composite Oct/Sox2 motifs on target genes. As reported, promoters co-bound by Oct4, Sox2 and Nanog direct the expression of signalling molecules, microRNAs and epigenetic regulators (chromatin-remodelling, histone modification) [768,769,779–781]. The epigenetic regulation in ESCs is reviewed by Bibikova *et al*. (2008) [782]. *In vivo*, Nanog is essential for the specification of the epiblast [783,784]. It has been found by Mitsui *et al*. (2003) [783] and [785] Chambers *et al.* (2003) that an overexpression of *Nanog* confers a cytokine independent self-renewal. On the other hand, a decreased or even absent level of Nanog does not terminate self-renewal. However, Chambers *et al*. (2007) [786] reported that self-renewal continues at lower efficiency and thus Nanog modulates the regulatory network. As found by Ichida *et al*. (2009) [787] and Maherali and Hochedlinger (2009) [788] the expression of *Nanog* can be upregulated by the inhibition of TGF-β. Xu *et al*. (2008) [789] reported that TGF-β can substitute for activin/Nodal in hESCs pluripotency.

However, it might be that the discussed mixed population of rbESCs is a result of initial not pure ICM due to mechanical surgery with needles. Hence, an immunosurgical method as shown by Axelrod (1984), Heins *et al*. (2004) and Chen and Melton (2007) [790–792] could result in pure isolations.

4.2.1.4 Pluripotency of rabbit cells

In 1965 Cole *et al*. (1965 [793], 1966 [794]) reported the derivation of trophoblast-like cells from rabbit blastocysts and their differentiation. One line with an epithelial phenotype showed AP activity. Later, Alliston and Pardee (1973) [795] assessed the early morphologic development of rabbit embryos. The 4.5 d blastocyst consists of approx. 278 cells of which only approx. 81 cells belong to the ICM. Twenty years later, the first report of putative rbESCs was published by Moreadith and Graves (1992 [796], 1993 [797]). Later, this group performed NT with the obtained cells [798]. Graves and Moreadith (1993) [797] reported growth in undifferentiated state

on MEF-MITOs with addition of LIF and the ability to form EBs and all three germ layers. Also, this group reported the formation of chimeras upon injection of these rbESCs into the blastocyst despite the huge mucin coat [799]. Compared to other animals, such as mice and rats, the rabbit blastocyst is surrounded by a thick mucin coat that is difficult to penetrate. Years later, Fang *et al*. (2006) [679] reported the derivation and culture of rbESCs from three different strains (New Zealand White, Chinchilla and Angora) on MEFs in serum-free medium w/o LIF but with addition of bFGF, thus sharing properties to hESCs while expressing *AP* and *Oct4*. Another group, Wang *et al*. (2008) [800], investigated the signalling pathways underlying pluripotency in their previously obtained rbESCs [680]. The morphology of those cells is very similar to those obtained in this thesis. They reported a similarity of their cells to hESCs and that pathways of TGFβ, bFGF and Wnt need to be active but BMP pathway needs to be inactive (Fig. 59). However, there is a difference in Wnt signalling that is high in rbESCs but low in hESCs where it becomes upregulated upon differentiation. bFGF activates both downstream pathways MAPK/Erk and PI3K/Akt. Therefore, they reported independency of rbESCs from LIF supplementation. Contrary to mESCs, hESCs and rbESCs of this thesis, Wang *et al*. could not detect the expression of *nodal*. Quite to the contrary, they verified the expression of *lefty*, an inhibitor of Nodal. The morphology of their obtained EBs (1200 cells/droplet) is similar to this obtained in this work with 3000 cells/droplet.

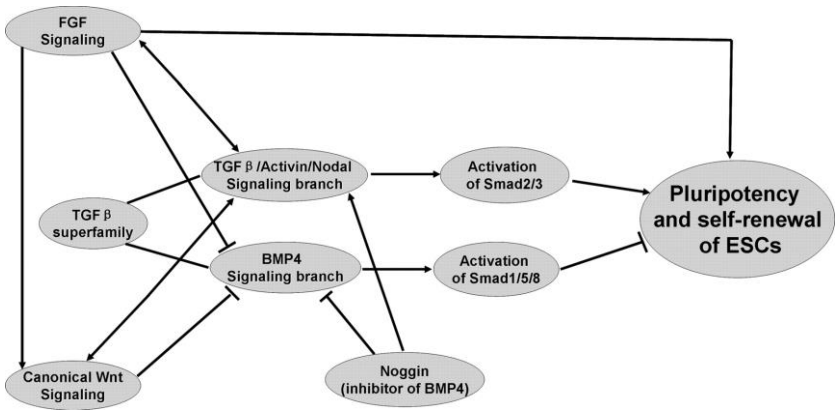

Figure 59: Suggested molecular signalling network of rbESCs obtained by Wang *et al*. (2008) [800].

A different group, Chiang *et al*. (2008) [801], cultured rabbit ICM cells on feeders in DMEM containing 20% FCS, 1% NEAA, 1% nucleoside solution, 0.1 mM 2-mercaptoethanol and 10 mg debekacin. However, one line was propagated to P14 with LIF supplementation and stained positive for AP and Oct4. They showed also expression of *AP*, *Oct4*, *Sox2*, *Nanog* and a similar morphology to hESCs [682]. Later, they reported the maintenance of rbESCs on feeders and in medium supplemented with both LIF and bFGF [720]. However, if either LIF or bFGF was added rbESCs still were pluripotent even under MEF-free conditions. Also the quantification of protein levels of Oct4 and Nanog does not show any significant variation

when increasing concentrations of LIF, bFGF or in combination of both was used. They conclude that rabbit pluripotency can be maintained at a basal level by low concentration of either LIF or bFGF, or can be reinforced by higher concentrations of each factor or both factors together. Very recently, this group reported the use of recombinant rabbit LIF (in addition to bFGF) and rabbit embryonic fibroblasts as feeder cells for the derivation and cultivation of rbESCs, but without clear findings in comparison to cultures with MEFs and human LIF [1098]. However, they conclude that bFGF is essential for rabbit pluripotency. Contrary, the group of Bösze found that LIF is essential for rbESC derivation and culture and that these cells are similar in their signalling to mESCs [802]. Nevertheless, the morphology is similar to hESCs [803]. Further, they verified the expression of *AP*, *Oct4* and *Nanog*. After EB-mediated differentiation they found fibroblasts and beating cardiomyocytes. These findings are equally to the results of this work. Recently, this group isolated rabbit pluripotency genes [804] and used them to generate iPSCs [805, review: 1099]. However, nothing is mentioned about contribution to the germ line. Also, Honda *et al*. (2008) [681] reported the establishment of rbESCs and found that bFGF maintains pluripotency of rbESCs and that signalling through activin/Nodal is necessary but LIF is dispensable [806]. They revealed the expression of *AP*, *Oct4* and *Nanog*. Further, this group used the same ROCK-i as in this work and was found to enhance cell growth. They conclude a similarity of rbESCs to hESCs. In further attempts, Honda *et al*. (2010) [807] established rb-iPSCs from both liver and stomach cells by lentiviral vectors with the human genes *c-Myc*, *Klf4*, *Sox2* and *Oct4* using both bFGF and LIF as supplement. When they used foetal and adult fibroblasts the reprogramming failed. However, established iPSCs could be cultured in the absence of LIF. They verified the endogenous expression of *c-Myc*, *Klf4*, *Sox2*, *Oct4* and *Nanog*. Very recently, Teramura *et al*. (2012) [1091] reported the derivation and culture of rbESCs on MEF-MITOs in DMEM/F12 containing 20% knockout serum replacement and bFGF. Their cells are positive for AP, Oct4, Nanog, Sox2 and SSEA-4. Further, they report hESC-like characteristics such as decency on bFGF and activin/Nodal but no effect of LIF. Also, they claim a crucial effect of ROCK-i during passaging.

Obviously, the publications of the various groups differ largely in their findings. None of the publications reporting the derivation of rabbit pluripotent cells used the ZIKA strain that was used in this work. Therefore, it could be possible that this particular strain is more refractory as the commonly used strains New Zealand and Dutch Belted. Similar observations were reported for various mice strains [705,808]. However, the large variations in culture conditions and marker expressions could be hardly explained with strain variations. Therefore,

experiments to elucidate the signalling network in developing embryos, especially in the ICM and epiblast, need to be performed to discover the required cues for rabbit pluripotency. For sure, the expression of *Oct4* is needed in true rbESCs as *Oct4* is expressed in preimplantation rabbit embryos [809–811].

As recently shown by Tang *et al*. (2010) [812], a single cell approach to elucidate the processes occurring in cells during ICM isolation and in primary culture could be applied. This method is very interesting and could be promising in understanding rabbit pluripotency.

4.2.1.5 Differentiation of pluripotent cells

The formation of EBs is usually the first step to differentiate ESCs. Martin and Evans (1975) [813] achieved the first EBs from embryonic carcinoma cells (ECCs). EBs consist of a heterogeneous mass of distinct cell types belonging to all three germ layers. To induce differentiation into the desired direction defined chemicals were added [814–821]. Since the signalling network regulating pluripotency is not absolutely understood, factors leading to guided differentiation need to be found empirically and are distinct in mESCs and hESCs [752,822–827]. The most obvious difference is BMP4 as discussed above [828, review]. To differentiate hESCs, the PI3K signalling needs to be inhibited [829]. In addition, D'Amour *et al*. (2005) [817] and McLean *et al.* (2007) [829] suggested that serum contains factors promoting pluripotency since hESC easily differentiate in the absence of serum and knockout serum replacement.

Rabbit EBs obtained in this work did not show perfect round and circular shape, but similar results were published by Mogi *et al*. (2009) [830] and Wang *et al*. (2010) [831]. Various efforts to differentiate rbESCs derived in this work into distinct cell types of each germ line resulted in a mixture of differentiated cells, not in pure populations. When the initial culture does not consist of pure pluripotent cells it is not possible to guide the differentiation process into desired directions. Also, right after differentiation the most cells underwent senescence. So it might be likely that the right cues are missing in the medium. While the directed differentiation was problematic, EB-mediated spontaneous differentiation into the three germ layers could be observed as well as unambiguously the differentiation into adipocytes (positive Oil-Red-O staining) and actively beating cardiomyocytes. Accordingly, pluripotent potential of rbESCs was proven. In addition, the expression of genes specific for each germ layer (*desmin* (mesoderm), *nestin* (ectoderm) and *hnf4α* (endoderm)) was shown by RT-PCR. As mentioned, these transcripts could be also detected in “undifferentiated” rbESCs strengthening the hypothesis of unstable pluripotent culture conditions.

4.2.1.6 Generation of rabbit chimeras

Another proof of pluripotency is the generation of chimeric animals when transplanting ECSs into donor blastocysts in which ESCs contribute to the development of the embryo and all resulting tissues including germ cells [249,832,833]. The first chimeric rabbit was reported 1974 but without the use of cultured cells [1104]. The results of this work of injections of *eGFP* expressing rbESCs into 8-cell stage rabbit embryos strongly suggests a contribution to the ICM, since the isolated and outgrown cells showed green fluorescence and PCR for *eGFP* was positive. These results indicate the presence of pluripotent cells in the original culture. The observation that not all *eGFP* positive cells (by PCR analysis) showed green fluorescence (by fluorescence microscopy) could be due to epigenetic silencing. For discussion of epigenetic silencing see 4.1.2.1 and -2. Also, Liu *et al*. (2009) [834] showed that PGK-eGFP-Neo becomes silenced in hESCs and Xia *et al*. (2007) [835] reported silencing of PGK-eGFP-Neo in hESCs and mESCs. Further, the latter group reported a silencing of *eGFP* by 55% in hESCs that is, regarding the not statistically evaluable number, similar to 45% silencing of *eGFP* in rbESCs. Finally, the first live born rabbit chimera from cultivated cells could be achieved in our group.

4.2.1.7 Improvements for the derivation of rabbit pluripotent cells

To achieve pluripotent rabbit cells, distinct other attempts could be tried. Pluripotent cells can be obtained by SCNT [836, review], cell fusion [676,837–839; reviews], the cultivation of cells in the presence of cell extracts [840–844] and the conversion of spermatogonial stem cells into germ line derived pluripotent cells [845,846].

However, the most successful possibility to obtain pluripotent rabbit cells could be the method of reprogramming [1096, review]. This induction of pluripotency of somatic cells was first shown in mouse by Takahashi and Yamanaka (2006) [181]. Remarkably, the both most important pluripotency genes *Oct4* and *Sox2* were used for this experiment, together with *c-Myc* and *Klf4*. In mESCs culture, the latter both become activated by LIF [234,244] whereas Klf4 directly regulates *Nanog* [847]. Shortly afterwards, Takahashi *et al.* (2007) [848] showed the induction of pluripotency in human somatic cells. Later, successful reprogramming was reported in cells of rhesus monkey [849], marmoset [853], rat [850,851], pig [852,1095,1103], horse [1102] and canine [854,1101]. One enhancement could be the use of transposons to efficiently deliver pluripotent inducing genes [855,856,1094,1095; review: 857]. Transposons possess the ability to get excised after successful induction. Recently, it was shown that the expression of specific microRNAs (miRNAs) can rapidly reprogram both mouse and human somatic cells with a higher efficiency than the standard induction method [1100]. miRNAs are a class of small

endogenous RNAs, that are noncoding but have crucial roles in the posttranscriptional regulation of gene expression. Nevertheless, before performing induction experiments, it is necessary to elucidate the pluripotent signalling network in rabbits. Otherwise induced cells could be lost rapidly.

However, iPSCs are not absolutely identical to ESCs as shown in experiments by Kim *et al.* (2010) [858] and Hasegawa *et al*. (2010) [859], where pluripotent mouse cells derived from blastocysts (ESCs), NT derived ESCs and iPSCs showed substantial differences in DNA methylation profiles. iPSCs still showed characteristic epigenetic marks for their original tissue, whereas NT-derived ESCs are very close to ESCs obtained from fertilised mouse embryos.

4.2.2 Multipotent cells

Multipotent stem cells (MSCs) play crucial roles in tissue homeostasis and regeneration of the adult body [860, review]. In a position paper published 2006 [275], minimal criteria for the definition of human multipotent mesenchymal stromal cells were stated. According to this paper, under standard culture conditions, MSCs must adhere onto plastic surface and, upon applying the right cues, must differentiate into osteoblasts, adipocytes and chondroblasts. Further they must express a defined set of surface molecules but must be shown to not express others, both needs to be proven be flow cytometry. These criteria were defined for the usage of human MSCs with regard to clinical applications. The first two criteria could be successfully verified for rabbit A-MSCs and BM-MSCs. The assessment of surface markers was difficult as almost no rabbit specific (primary) antibodies are available. In addition, as mentioned by Gronthos *et al*. (2001a,b) [861,862] not all surface markers are specific for MSCs. A further complication is the fact that expressed surface markers are influenced by extrinsic factors and vary between species [863, review]. In particular, the surface marker set or rbMSCs is completely unknown. Unlike ESCs, there is no standard assay to assess multipotency of MSCs *in vivo*, e.g. teratoma formation [262, review].

Since the initial isolation of MSC consist of mixed population of various cells [864] and to have a more pure culture of MSCs, they could be enriched by the use of dyes like Hoechst 33342 as shown by Goodell *et al*. (1997) [865]. Also, the dependency on bFGF supplementation to sustain proliferation and differentiation capacity as verified in this thesis is commonly seen in human [866–871], mouse [872–875], equine [877] and rabbit [876] MSCs.

4.2.2.1 Differentiation of multipotent cells

Since the multipotency of MSCs is based on trilineage potential (osteoblasts, adipocytes and chondrocytes), A-MSCs and BM-MSCs obtained in this thesis were differentiated into those three cell types. As could be expected due to their origin, A-MSCs comprised a remarkably adipogenic differentiation potential since the formation of lipid droplets was seen easily by eye. Also, the morphology changed drastically. Morphologic change was also seen in BM-MSCs and lipid droplets were verified.

As reported by Castano-Izquierdo *et al*. (2007) [878], osteogenic differentiation proceeds through three steps: proliferation, matrix maturation and finally mineralisation. The deposition of calcium is a marker for the later stages of this differentiation and was verified in this thesis by silver nitrate staining. In osteogenic differentiation, BM-MSCs revealed a much higher potential then A-MSCs that is also very likely due to their origin. Further, the morphologic change of BM-MSCs is conspicuous. On the other hand, A-MSCs did not drastically change their morphology and also silver nitrate staining failed. Also, Merkl (2009) [879] reported this missing osteogenic potential for porcine A-MSCs. This might be due to the presence of bFGF in our differentiation medium that was shown by Quarto and Longaker (2006) [872] to inhibit osteogenesis in mouse A-MSCs. However, upon withdrawal of bFGF this inhibitory effect is reversible. In addition, Malladi *et al*. (2006) [880] reported that dexamethasone, a supplement in both adipogenic and osteogenic differentiation media, inhibited osteoblast differentiation in mouse. Further, dexamethasone increases the expression of an early marker for adipogenesis in mouse A-MSCs.

After chondrogenic differentiation both A-MSC and BM-MSC stained positive for mucopolysaccharides albeit the formed pellet was dense for BM-MSCs only. Chiou *et al*. (2006) [873] reported that the supplementation with bFGF enhanced chondrogenesis of mouse A-MSCs. Thus, bFGF might improve chondrogenesis of rbA-MSCs. Because differentiations were successful in this thesis, multipotency of rabbit A- and BM-MSC was proven. To shed more light in the differentiation potential, quantification of the calcium as well as mucopolysaccharides content could be performed.

The differentiation procedures applied in this thesis were widely used as standard and based on established protocols [267,281,881–887]. As shown by Pittenger *et al*. (1999) [281] and de Ugarte *et al*. (2003) [888], for a more detailed characterisation, immunocytochemical analysis could be performed, e.g. for CD14, CD45 (haematopoietic markers) and CD29, CD44 (mesenchymal markers). Lapi *et al*. (2008) [889] characterised some specific markers that were expressed by rbBM-MSCs: *CD29*, *vimentin*, *α-smooth actin* and *desmin*, but were negative for *CD14*,

CD45, *CD90*, *MHCI*/*II* and *cytokeratin*. These results are similar to mouse and human MSCs. In 2010, Mazzetti *et al*. [890] reported the isolation and analysis of rabbit A-MSCs. However, the growth characteristics and multi-lineage potential differs among distinct isolates of MSCs [891–893] as well as in distinct strains of mice [894,895]. All MSCs used in this thesis originates from one isolation procedure. Therefore, all performed experiments are comparable. On the other hand, either negative or positive features of this particular isolate are not necessarily characteristic (or a mean representative) for all A- and BM-MSCs of rabbits. In this work, the multipotent character of the isolated rbBM-MSC was clearly proven.

4.2.2.2 Heterogeneity of mesenchymal stem cells

The heterogeneity in proliferative and differentiation capacity observed in this work between rabbit A- and BM-MSCs was also reported by others [887,896–898]. Also Zuk *et al*. (2001) [267] reported variations in the marker expression between MSCs of these both sources. In addition, heterogeneity is observed within the same isolation [899–901] and also cell clone [902–906]. In the case of A-MSCs it was shown by Jiang *et al*. (2010) [907] and Rada *et al*. (2011) [908] that the site of isolation has a huge impact on the differentiation potential which could explain the missing osteogenic potential of rbA-MSCs. Here, a further isolation might be required. All these findings are explained with the inherent plasticity of MSCs [317,909–912, reviews].

As mentioned above, an important extrinsic factor influencing cell culture is the composition of the atmosphere. Albeit having 5% CO_2, 21% O_2 and 37°C *in vitro*, the *in vivo* conditions are still different. Under physiological conditions, the O_2 concentration varies from 0.7 – 9% depending on organ and localisation [913–915, reviews]. Wion *et al*. (2009) [742], Fehrer *et al*. (2007) [916] and Krinner *et al*. (2009) [917] found that the O_2 concentration has influences on various cell functions and in particular on stem cells [1078–1082]. Krinner *et al*. [917] showed that ovine BM-MSCs improved their growth under physiological low O_2 which is similar to the results of this thesis obtained on rabbit A-MSCs and BM-MSCs. Comparable findings were reported for mouse [918], rat [919] and human MSCs [920,1083–1087].

4.2.2.3 Ageing of mesenchymal stem cells

According to published data [921, review] approx. 45 population doublings are necessary for the whole procedure beginning with the isolation of cells, until screening of targeted cells and their usage for NT. During long-term culture, Bonab *et al*. (2006) [922] and Miura *et al.* (2006) [923] reported increasing signs of cell ageing and chromosomal instability [924, review]. In this thesis, these signs were seen from the 9th passage on in both A- and BM-MSCs cultured under standard conditions since they slowed in their growth rate. A study on human MSCs by Bork

et al. (2010) [925] reported changes in methylation pattern in these higher passages. In turn, this could have negative effects during reprogramming in NT experiments. Since MSCs do not express telomerase [926], their growth capacity is limited by the Hayflick limit [927–929]. However, as found by Colter *et al*. (2000) [930], MSCs could undergo senescence due to contact inhibition. Nevertheless, Martin *et al*. (1997) [866] and Bianchi *et al*. (2003) [931] reported more than 70 population doubling for human MSCs. Digirolamo *et al*. (1999) [902] and Vacanti *et al.* (2005) [932] reported a decrease in the differentiation potential of BM-MSCs (human and porcine, respectively) after the 15th passage. All MSCs in this thesis were used in early passages for all experiments.

Since both self-renewal and proliferation capacity of MSCs declines with age of the animals [933–935,1076,1077], rabbit cells in this work were isolated from 5 weeks old rabbits. Also, with increasing age mutations due to metabolic toxins and errors in DNA replication were accumulated that could have negative effects for subsequent experiments. The observations in this thesis reveal that rbMSCs support efficiently the whole procedure necessary to generate transgenic cells, single cell cloning and NT.

4.2.3 Competence of pluripotent and multipotent rabbit stem cells for NT

Advantages of NT over microinjection are that the selection process for transgenesis precedes the obtaining of animals. Here, selection of genetic modification occurs during cell culture. In addition to random integrations, this method allows precise genetic engineering. Thus, if the donor cell was transgenic, offspring obtained after NT are 100% transgenic and production of chimeric animals is avoided. Further, the selection of the sex proceeds the generation of animals and is important for subsequent breeding.

The first mammalian ET experiments can be traced back to 1890, when Walter Heape [936] transferred rabbit embryos from one doe to another resulting in live births. Already in 1952, Briggs and King [937] reported the first cloned animals by the use of blastomeres in frogs and much later in mice [938] and sheep [939]. Blastomeres are cells of the very early embryo (up to 8 cell stage) and are still totipotent [940], but cannot be cultivated *in vitro*. Stice and Robl (1988), Collas and Robl (1990), Yang *et al*. (1992) and Chrenek *et al*. (2008) [941–944] reported initiating NT experiments in rabbits using blastomeres and cells of the morula. Skrzyszowska *et al.* (2006) [945] reported cloned chimeric rabbits by the transfer of one karyoplast into one enucleated blastomere of the 2-cell stage embryo. The low performance of rbESCs in NT experiments within this thesis might be very likely due to their unstable pluripotent character and the existence of distinct cell types within the culture (as discussed in 4.2.1.2). Therefore,

it is not clear which cell type was indeed used for NT. Du *et al.* (1995) [798] reported successful NT using putative rbESCs. They achieved a blastocyst rate of 17% of reconstructed embryos compared to 23% blastocyst rate of our rbESCs. When they used blastomeres, they achieved a rate of 31%. Chesné *et al*. [946] reported in 2002 the first cloned rabbit using somatic cells. Now, within this project, in total 18 live cloned rabbits from long-term cultured cells could be achieved, which is the highest number reported so far. Further, the first live cloned rabbit from genetically manipulated MSCs was achieved. Previously, Meng *et al*. (2009) [673] reported the highest success rate of live cloned rabbits that survived until adulthood. In that study, freshly isolated non cultured cumulus cells were used since 90% of them are naturally in the G_0/G_1 stage [947,948]. Unfortunately, these cells are not well suitable for genetic manipulations due to their poor *in vitro* proliferation [949] and resulting offspring are strictly female due to their origin. On average in mammalian cloning, only 3 – 6% of transferred cloned embryos survive to term [670, review: 950].

Since prolonged cultivation and *in vitro* manipulations like DNA transfection and drug selection could lead to genetic and epigenetic defects; the obtained results using transgenic BM-MSC are noteworthy. The first animal cloned from MSCs was reported by Kato *et al.* (2004) [951] in cattle and was later extended to further species including pigs where the successful usage of both transfected and non-transfected MSCs for NT was shown [885,952,953]. As reported for pigs [885,954,955], the use of BM-MSCs results in higher NT rates compared to fibroblasts which is similar to the results achieved with rabbit cells in our work. In those studies, the use of BM-MSCs resulted in similar cleavage rates compared to fibroblasts but to increased blastocyst rates (MSCs: 29.5%, FBs: 17.5% (Faast *et al*. (2006) [885]); MSCs: 9.9%, FBs: 2.9% (Kumar *et al*. (2007) [954]); MSCs: 18.4%, FBs: 9.5% (Jin *et al*. (2007) [955]). Further, Kumar *et al*. reported that MSC derived cloned embryos are more similar to naturally fertilised *in vivo* embryos in terms of the expression of key embryonic genes and epigenetic mark-up. Since both blastocyst rate (38% (transgenic MSCs: 55%)) and number of live born rabbits (2% (transgenic MSCs: 4%)) was higher with MSCs as with rbESCs (23% and 0, respectively) rbMSCs were chosen for subsequent targeting experiments.

In principle, it would be of great practical importance to use cells of a transgenic cloned animal for a second round of NT. Therefore, precious animals could be rescued without repeating all laborious steps in the forefront, like transfections and selection. This was also shown within this project, where two cloned transgenic rabbits were born originating from fibroblasts derived from a previously MSC cloned rabbit. Thus, it is possible to rescue cloned but possibly unviable rabbits.

4.2.3.1 Influencing factors for nuclear transfer

The efficiency of NT followed by ET is affected by arresting the oocyte at meiotic metaphase II, enucleation of the recipient oocyte, fusion of the enucleated oocyte with donor cell, activation of the reconstructed oocyte, reprogramming of donor genome, timing of ET and synchronisation of the recipient animal [956,957; reviews]. Sung *et al.* (2011) [958] reported higher fusion rates and development to morula and blastocysts in rabbits when oocytes were used from the ovary in contrast to oocytes from the oviduct. Thus, they suggest that already the origin of the oocyte has an influence on successful NT. In our experiments, oocytes were flushed from the oviduct and this might have resulted in lower efficiency. Also, Du *et al*. (2009) [959] revealed the optimal time point of oocyte collection after hormonal induction in rabbits and demonstrated an age-dependency.

Once transferred into the oocyte, the somatic nucleus needs to become quickly reprogrammed to express early developmental genes. Obviously, failures in this process result in developmental disturbances. The process of reprogramming involves about 20000 genes that need to become down regulated (somatic cell status) or up regulated (embryonic program), respectively. This involves epigenetic modifications consisting of DNA methylation, assembly of histones and its variants and the remodelling of chromatin-associated proteins (e.g. polycomb group, scaffold proteins) [960–962, reviews]. As found by Lanza *et al*. (2000) [158], Tian *et al*. (2000), Wakayama *et al*. (2000) and Betts *et al*. (2001) [963–965], the adjustment of telomere length often occurs faithfully due to reactivated telomerase in cloned embryos [966, review]. Hence, postzygotic reprogramming processes do not impair the development of NT embryos. Wakayama *et al*. (1998) [948] reported, that reprogramming is only successful in 1 – 5% of NT derived embryos, whereas in 70% abnormal reprogramming is the case and it fails in 25 – 30% of NT derived embryos.

From this arising knowledge, much has been learned about the optimal cell types to use [967,968; reviews]. An important factor for successful NT is the cell itself. During normal aging processes, Schnieke *et al*. (1997) [11] and Kühholzer *et al*. (2001) [969] found both accumulation of genetic abnormalities and epigenetic damage in cells and also during prolonged *in vitro* cultivation [970,971; reviews]. Hence, cells should be isolated from animals as early as possible and cultured with minimal passaging numbers. In general, the higher the cell's degree of developmental plasticity, the better the potential for their usability for NT [972–975, review: 976]. On the other hand, as found by Wakayama *et al*. (1998) [948], Rideout *et al*. (2000) [973] and Wakayama and Yanagimachi (1999) [977], 60 – 70% of NT embryos derived from somatic cells developed to blastocyst, but only 10 – 20% derived from ESCs. However, 10 – 20 fold more of NT

embryos in blastocyst stage derived from ESC nuclei develop to term as in the case of somatic cell derived blastocysts [948,972–974,977–982]. Overall, ESCs are more effective donors. Nevertheless, Doherty *et al*. (2000), Khosla *et al*. (2001) and Young *et al*. (2001) [983–985] reported that handling during NT and ET procedures themself could affect the development of the clone [986, review]. A further factor which influences NT efficiency is the cell cycle stage that can be controlled by starvation which was shown to enhance SCNT in rabbits by Li *et al*. (2006) [672]. Serum starvation arrests cell cycle in G_0/G_1. Campbell *et al*. (1996) [146] and Cibelli *et al*. (1998) [255] reported that only cells in G_0 and G_1 can efficiently promote development.

4.2.4 rb*hprt* knockout

As mentioned above, mice are not able to resemble the complex phenotype of Lesch-Nyhan syndrome (LNS) like overproduction of uric acid and neurobehavioral albeit the gene is conserved in humans and rodents [987,988]. Further, a lot of knowledge about LNS was obtained using cell culture models [989, review]. Hence, inconsistent results were reported [990]. An excellent animal model of LNS could elucidate relationships of cognitive development, behaviour and the involved neurologic functions including biochemistry of the brain.

4.2.4.1 Generation of targeting constructs

Since exon 3 of *hprt* is the largest exon and a lot of mutations in this exon are reported to cause LNS [991, review], the knockout of this exon was chosen. In particular, exon 3 was found to be highly conserved and to be a hotspot for mutations causing LNS [992,993]. In addition, most mutations that cause LNS result in modifications of the size of *hprt* [425].

Due to the availability of a BAC containing rb*hprt*, the PGK-Neo cassette was introduced by recombineering, a relative fast procedure to obtain the targeting construct. After linearization of BAC-rbHPRT^{Neo} a clean-up of the DNA was necessary leading to a high loss of DNA, limiting the experiments to determine best transfection methods.

4.2.4.2 Selection of *hprt*^{Neo} cells

The first hurdle to generate genetically engineered animals by cell-mediated transgenesis is the *in vitro* manipulation of the cells. It was shown within this project that the use of transgenic rbBM-MSC resulted in live born cloned animals. Therefore, rbBM-MSCs were transfected with the constructed *hprt*^{Neo} vector. By applying chemical transfection methods the exogenous DNA becomes more compact as most reagents have condensing properties. In addition, they shield the DNA to neutralise their negative charge and act as carriers to facilitate the cell entry. These complexes are able to become spontaneously endocytosed.

More advanced technologies even induce the endocytosis [994, review]. Right after, most of the internalised DNA becomes degraded. Only a small percentage reaches the nucleus. In addition, naked DNA causes cellular stress resulting in cell-cycle arrest and even apoptosis. This could explain the low efficiency seen in BAC transfections. Once successful, transfections with random integrations are not reproducible. However, with genome engineering it is possible to modify a specific area of DNA with a very high precision and is therefore reproducible. Studies by White *et al*. (2003), Walker *et al*. (2004) and Askautrud *et al*. (2009) [995–997] showed that an increase in plasmid size leads to a decrease in transfection efficiency. Thus, the uptake by the cell depends largely on the DNA size, because larger plasmids are more susceptible to degradation [998]. As found by Abrahams *et al*. (2003), Chandler *et al*. (2007) and Le Saux *et al*. (2010) [999–1001] the use of BAC could be disadvantageous since deletions and rearrangements occur frequently in large transgenes. In addition, higher amounts of naked DNA cause cellular stress (as mentioned above).

The successful HR depends on various factors; especially the cells capacity for HR and the state of the chromatin at the given locus. Since *hprt* is ubiquitously expressed, the chromatin is supposed to have an accessible euchromatin status. Due to the poor results obtained with BAC transfections, consequently a smaller plasmid containing the $hprt^{Neo}$ cassette was constructed and used for transfections. Thereby, homology was decreased to 2.8 kb (left arm, 5´) and 3.9 kb (right arm, 3´). The results were more promising and finally resulted in one putative *hprt* knockout clone out of 448 G418 resistant clones. This clone showed resistance against both G418 and 6-TG. Further, PCR analysis verified the presence of neo^R and the absence of *hprt* exon 3. During this HR event a genomic part of 14.6 kb became removed from *hprt*. This clone is now available for NT experiments.

The selection process depends on the expression of *neo* (which in fact is the *aminoglycoside phosphotransferase* that confers resistance against geneticin (G418) through a simple phosphorylation) as positive selection and in turn depends on genomic context. Therefore, the optimal concentration of G418 to select targeted cells can be distinct of that obtained in the preceding killing curve experiments. This could result in a selection pressure where random integrations were selected and the correct targeted cells might be lost. Additionally, the expression of marker genes could negatively influence cell biology. The random integration of inserted DNA molecules into the host genome occurs via micro-homologies or NHEJ both during DNA DSB repair [1003,1004; review: 1002]. To reduce random integrations by NHEJ, this mechanism could be blocked [1005] thereby enhancing targeting events. Moreover, it was reported by Arbonés *et al*. (1994), Hanson and Sedivy (1995) and Brown *et al*. (1997) [1007–

[1009] that the targeting in somatic cells is more difficult as in ESCs due to senescence, lower rates of HR but higher rates of NHEJ [1006, review].

Since the targeting of *hprt* results in its knockout, no protein is synthesised and this event can be selected by 6-TG, which is a thio-analogue of the naturally occurring purine base guanine (Fig. 60). It competes with hypoxanthine and guanine for HPRT that converts 6-TG into thioguanylphosphate (TGMP). Summarized, 6-TG acts through inhibition of purine biosynthesis by inhibiting the conversion of purine nucleotides and by incorporation into the DNA and RNA. This leads to a blockade of the synthesis and utilization of purine nucleotides. Unfortunately, the selection by 6-TG is hampered by its action on single cells only. Therefore, clones of putative targeted cells needs to become thoroughly dissociated during passaging procedure.

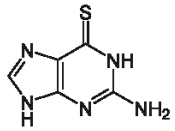

Figure 60: Chemical structure of 6-TG, an analogue of the purine base guanine.
Instead having a sulphur atom the natural purine base has an oxygen atom.

The first animal model for LNS, a mouse, was derived through injection of mutated mESCs into blastocysts by Hooper *et al*. (1987) [498]. The mESCs were randomly mutated by retroviral infection and cells were selected based on resistance to 6-TG. Almost the same experiments were carried out by Kuehn *et al*. (1987) [499]. Later in the same year, Doetschman *et al.* [142] showed the first gene targeting using *hprt*, where the mutated *hprt* was corrected in mESCs. The homology used was between 2.5 and 5 kb (endpoint of deletion on targeting vector was not known at time of publication) with a highest success rate of 2.7×10^{-6}. At the same time, Thomas and Capecchi [500] reported successful gene targeting using mESCs. Instead to repair mutated *hprt*, neo^R was introduced into *hprt* thereby replacing exon 8. Successful targeting events were discovered by G418 resistance and resistance against 6-TG. They reported that 1 out of 1000 cells was resistance against both chemicals. They used homologies of 2.8 kb (3´) and 4, 5.4 and 9.1 kb (5´). With an increase of homologous size the targeting efficiency increased. In this work, the targeting vector possessed homologous sites of 2.8 kb (5´) and 3.9 kb (3´), 6.7 kb in total. That is almost equivalent to the smallest vector of Thomas and Capecchi and might explain the low targeting efficiency. One year later, [1010] disrupted *hprt* by gene targeting in mESCs. Here, exon 3 was disrupted by introduction of *neo* using homologies of only 132 bp (5´) and 1.2 kb (3´). Selection of targeting events in cells was the same (first G418, then 6-TG) with a highest targeting efficiency of 1.6×10^{-6}. Later, Doetschman *et al*. (1988) [1011] showed germ line transmission of genetically corrected *hprt*

mESCs. There, previously randomly mutated cells were used, the mutation was identified and a corrective targeting construct with homology between 2.3 and 4.2 kb (endpoint of deletion on targeting vector was not known at time of publication) was applied. The highest targeting rate was 2.2 x 10^{-7}. Generally, the longer the homology between transgene and genomic locus, the higher was the targeting frequency [1012]. Also, genes that are highly expressed are simpler to target due to their accessibility. By targeting *hprt* in different strains of mESCs, Udy *et al*. (1997) [1013] found that the targeting frequency is inversely correlated to the cell doubling time. The targeting of *hprt* in hESCs was successful with a rate of 1.4% [1014]. This group introduced also a PGK-*Neo* cassette but in exon 1. The homologies were 7 kb (5´) and 2 kb (3´). Generally, Deng and Capecchi (1992) [1015] reported an optimal requirement of approx. 14 kb homology for efficient HR in mESCs. However, Thomas *et al*. (1992) [1016] reported a minimal requirement of 1 kb on each site of the transgene. Recently, Yang *et al*. (2009) [1017] showed the usability of the *hprt* locus for knock-in mutations in mice

4.2.4.3 Improvements for the generation of *hprt* knockout cells

Years later, the *hprt* locus is still of interest for gene targeting. Therefore, the *hprt* locus was shown to be an optimal surrogate site for gene targeting in mESCs [1018,1019]. However, Mir and Piedrahita (2004) [1020] reported that no clone at all could be obtained after targeting *hprt* in bovine foetal fibroblasts. Instead, when they applied a nuclear localisation signal (NLS), 1 out of 1 million cells was targeted. In addition, a cell cycle block in S phase by the use of thymidine increased targeting efficiency 7 fold while at the same time reducing random integrations by 54 fold. The homology was 6.5 kb (5´) and 4 kb (3´). As reported by Wilson *et al*., Ludtke *et al*. and Vacik *et al*. (1999) [1021–1023], the NLS improves the transport of the transgene vector to the nucleus. Usually, DNA molecules can pass the nuclear membrane only in M phase since the membrane stays intact during the cell cycle. In mitosis when chromatids become separated, the nuclear membrane brakes. Accordingly, exogenous DNA must wait until M-phase, but is then in the nucleus during G_1 phase when NHEJ is dominant minimizing change for HR. Wong and Capecchi (1987) [1024] and Takata *et al*. (1998) [1025] reported that HR occurs in the late S/G_2 phase before the cell enters mitosis and therefore a block with thymidine enhances HR [1026]. Difficulties in the targeting of *hprt* in fibroblasts of rhesus macaque were reported from Meehan *et al*. (2008) [1027], which were successful with cell cycle synchronisation and the inclusion of the SV40 NLS on the targeting construct. They reported a reduction of random integrations by 28 fold after synchronisation. The homology was 10.3 kb. Further, this group used 8-azaguaine (8-AG) after puromycin selection to select for *hprt* targeted cells. However, after 8-AG application they performed additionally a 6-TG

selection that survived 2625 out of 10^7 cells. Summarised, to achieve higher numbers of positively targeted rbBM-MSC, the application of thymidine to arrest the cell cycle should be done. In forefront, a NLS should be cloned onto the targeting construct when conventional electroporation or chemical transfection is used. Further, as found by Kang *et al*. (1999) [1028] targeting could be improved by the addition of SINEs at both sides of the exogenous DNA which promotes HR. Arbonés *et al*. (1994) [1007] reported that HR is much less efficient in somatic cells than in ESCs [1029,1030; reviews]. Therefore, it would be advantageous to have rbESCs to perform targeting experiments.

Although HR is a very precise genetic technology it is a very time consuming and random process that could be improved by applying site directed endonucleases, which are in principle restriction enzymes. This includes ZFNs and meganucleases. Recently, our group showed precise gene targeting by ZFNs in rabbits [1031]. Those tools recognizes sites over 12 bp providing the necessary specificity and inducing DSB which than triggers the DNA repair mechanisms [1032]. This increases the chance for HR with exogenous DNA even though NHEJ occurs at higher frequencies. Thus, the frequency of the very rare event of HR can be increased by the introduction of a DSB into a defined position within the target gene. For this ZFNs are a usable tool that allows precise knockout of genes [1033–1041]. Cathomen and Joung (2008) [1042] reported that the efficiency of knockout without additional introduction of a transgene is more than 5%. Recently, as shown by Whyte *et al*. (2011a,b) [1043,1044], knockout in pigs and genetic modification could be achieved with ZFNs. Unfortunately, the method of ZFN is very laborious in the design and creation of functional ZFNs. Often it is reported that ZFNs do not work as expected [1045–1048]. However, Doyon *et al.* (2011) [1049] showed that specificity can be increased by using heterodimers instead of homodimers.
An alternative approach for endogenous gene targeting which could be applied for both genes used in this study could be the method of transcription activator-like effector hybrid nucleases (TALENs) [1050–1053]. Although coming from plant genomics, their feasibility was shown in vertebrates [1054,1055]. Those molecules contain structural features and domains including NLS, translocation signal, activation domain and a central repeat domain responsible for DNA binding and therefore conferring specificity [1056–1058]. Compared to ZFNs, their construction is simpler and showed fewer side effects [1059–1062]. Recently, Hockemeyer *et al*. (2011) [1063] showed precise genetic modification of both human ESCs and iPSCs using TALENs. Both methods, ZFNs and TALENs, rely on HR due to the induction of DSBs that become repaired by intrinsic pathways and were designated as molecular scissors [1042,1064–1068; reviews]. In these

methods, as found by Moehle *et al*. (2007) [1038] and Hockemeyer *et al*. (2009) [1069], the size of homologous sequence needs to be only around 1 kb or less.

Another possibility to knockout rb*hprt* is by a promoter-trap vector as reported by Jasin and Berg (1988) [1070] and Sedivy and Sharp (1989) [1071]. Hereby, the selection gene (e.g. neo^R) lack its own promoter (e.g. PGK) and is introduced also by HR into the target gene. Importantly, the selection gene is only directed by the endogenous promoter and therefore only expressed if it is integrated into a gene.

To achieve a knockdown of selected target genes, the method of RNA interference could come into focus. This method uses a conserved gene regulatory process of the cell [1106–1111, reviews]. Notably, this results not in a knockout of the gene. Therefore, unwanted side effects could occur. For example, in a potential LNS model a still present minimal HPRT activity does not result in LNS but in Kelley-Seegmiller syndrome.

5 ABBREVIATIONS

6-TG	6-thioguanine
8-AG	8-azaguaine
A	adipose
aa	amino acid
AIDS	acquired immunodeficiency syndrome
BAC	bacterial artificial chromosome
bFGF	basic fibroblast growth factor
BM	bone marrow
BMP	bone morphogenic protein
CAGGs	chimeric cytomegalovirus immediate-early enhancer/modified chicken β-actin promoter/chicken β-globin intron sequence
DM	diabetes mellitus
DNA	Deoxyribonucleic acid
DSB	double strand break
EB	embryoid body
ECC	embryonic carcinoma cell
ECM	extracellular matrix
eGFP	enhanced green fluorescent protein
EpiSC	epiblast stem cell
ER	endoplasmatic reticulum
ESC	embryonic stem cell
ET	embryo transfer
FISH	fluorescence in situ hybridisation
GMP	guanosin mono phosphate
GOI	gene of interest
GSK3	glycogen synthase kinase 3
h	Human
HIV	human immunodeficiency virus
HPRT	hypoxanthine-guanine phosphoribosyl-transferase
HR	homologous recombination
ICM	inner cell mass
ICSI	Intracytoplasmic sperm injection
IGFI	insulin-like growth factor I
IMP	inosine mono phosphate
iPSC	induced pluripotent stem cell
ITR	inverted terminal repeat
Jak	Janus kinase
LIF	leukaemia inhibitory factor
LINE	long interspersed element
LNS	Lesch-Nyhan syndrome
m	mouse
MAPK	mitogen-activated protein kinase
MEF	mouse embryonic fibroblast

MEF-MITO	mitotically arrested MEFs
miRNA	mircoRNA
MSC	mesenchymal stem cell
NEAA	Non-essential amino acids
Neo	neomycin resistance
NHEJ	Non-homologous end joining
NT	nuclear transfer
o/n	over night
PB	piggyBac
PCR	polymerase chain reaction
PI3K	phosphoinositide 3-kinase
rb	rabbit
ROCK-i	Rho-associated protein kinase inhibitor
ROS	reactive oxygen species
rpm	revolutions per minute
s/n	supernatant
SB	Sleeping Beauty
SCNT	somatic cell nuclear transfer
SINE	short interspersed elements
SSEA	stage specific embryonic antigen
STAT3	signal transducer and activator of transcription 3
TALEN	transcription activator-like effector nuclease
TGMP	thioguanylphosphate
TF	transcription factor
TGF	transforming growth factor
UPR	unfolded protein response
w/o	without
wt	wild type
yr	year
ZFN	zinc finger nuclease

6 LIST OF TABLES

Table 1: PCR cycling parameters concerning to the amplifications described above. - 41 -
Table 2: PCR cycling parameters concerning to the amplifications described above. - 45 -
Table 3: Summary of all mammalian cell lines used in this thesis. - 46 -
Table 4: Summary of the microinjection experiments of SB-system with *mCherry* as transgene. - 59 -
Table 5: Summary of the microinjection experiments of SB-system with rabbit Ins^{Akita} as transgene. - 62 -
Table 6: Overview of the supplements and their combinations used to reveal the optimal conditions. - 64 -
Table 7: Summary of the morphologic results of the medium condition experiment using CM as basic medium. - 65 -
Table 8: Summary of the morphologic results of the medium condition experiment using mES medium as basic medium. - 65 -
Table 9: Complete overview of the results of the medium condition experiment. - 66 -
Table 10: Summary of counted chromosomes obtained from karyotyping of cells cultivated under stated conditions. - 67 -
Table 11: Combinations of transfection reagents. - 68 -
Table 12: Overview of the results obtained applying different reagents in different concentrations and in different combinations with distinct amounts of pPGK-eGFP1-Neo. - 69 -
Table 13: Population doubling times of rabbit BM-MSC and A-MSC cultivated under standard cell culture conditions and under reduced O_2 conditions over 9 passages. - 76 -
Table 14: Assessment of transfection efficiencies of rbBM-MSCs and A-MSCs applying different methods - 80 -
Table 15: Assessment of the potential of rbESCs, rbBM-MSCs and stably transfected rbBM-MSCs (*eGFP*) for NT - 83 -
Table 16: Assessment of the potential of rabbit fibroblasts for NT obtained from cloned *eGFP*-transgenic animals. - 83 -
Table 17: Summary of *hprt* targeting experiments using a conventional targeting vector. - 86 -
Table 18: Summary of all published microinjection experiments performed in rabbits. - 92 -

7 LIST OF FIGURES

Figure 1: Overview of different methods to achieve transgenic animals. - 2 -
Figure 2: Principle structure of the Sleeping Beauty transposon. - 5 -
Figure 3: Transposition of the Sleeping Beauty system. - 6 -
Figure 4: Early specification of cells in the blastocysts. - 8 -
Figure 5: Regulatory network of key transcription factors. - 9 -
Figure 6: Extrinsic factors maintaining pluripotency in ESCs. - 10 -
Figure 7: Occurrence of mesenchymal stem cells. - 12 -
Figure 8: Metabolites of glucose pathways that result in an increase in reactive oxygen species. - 15 -
Figure 9: Insulin action and its inhibition. - 16 -
Figure 10: Summary of the negative consequences of obesity. - 16 -
Figure 11: Amino acid sequence of preproinulin. - 17 -
Figure 12: Cellular responses (UPR) to misfolded proteins. - 18 -
Figure 13: The central role of HPRT (orange box) in the recycling of adenine and guanine (blue boxes). - 21 -
Figure 14: Structure of the rb*hprt* gene. - 22 -
Figure 15: Two PCR amplicons of rb*hprt* for subsequent cloning purposes. - 40 -
Figure 16: Two PCR amplicons of BAC-rbHPRT^{Neo} for analysing purposes. - 41 -
Figure 17: PCR amplicons of rb*Ins* for cloning purposes. - 41 -
Figure 18: Schematic draw of rabbit *insulin* and 3 x poly adenylation signal placed behind. - 55 -
Figure 19: Co-transfection of either pINS^{Akita}: pPGK-Neo (10 : 1) or pINS^{WT} : pPGK-Neo (10 : 1) into INS1E cells. - 55 -
Figure 20: Co-transfection of either pINS^{Akita} : pPGK-Neo (10 : 1) or pINS^{WT} : pPGK-Neo (10 : 1) into rbFB-1. - 56 -
Figure 21: RT-PCR for rabbit *insulin* of co-transfected INS1E cells using either pINS^{Akita} : pMACSK^{k} II (5 : 1) or pINS^{WT} : pMACSK^{k} II (5 : 1). - 57 -
Figure 22: Two vector SB-system. - 57 -
Figure 23: Verification of the functionality of SB vector system by the use of *mCherry* red fluorescent transgene in rbBM-MSC P1. - 58 -
Figure 24: Transgenic rabbit foetuses obtained by applying mCherry SB-transposon system. - 60 -
Figure 25: Location of the recognition site of the restriction enzyme BlpI on the vector pT2-SB-CAGGs-mCherry. - 60 -
Figure 26: Southern Blot analysis of DNA of the three positive foetuses and of WT as negative control. - 61 -
Figure 27: Schematic draw of pT2-SB-INS^{Akita} bearing the transposable rabbit *Ins^{Akita}* transgene and artificial 3x polyA. - 61 -
Figure 28: PCR analysis of putative transgenic rabbit embryos obtained applying SB-transposon system. - 62 -
Figure 29: Typical morphology of putative rbESCs under specific conditions of the medium composition experiment. - 66 -

Figure 30: Typical morphology of the long term medium experiment of rbESC in CM. - 67 -
Figure 31: Typical karyotype of rabbit normal diploid chromosome set after DAPI staining. - 67 -
Figure 32: Transfection of rbESC-5 P11 with the plasmid pPGK-eGFP1-Neo applying different transfection reagents, 4 distinct concentrations and each in combination with 1 and 2 µg plasmid DNA. - 69 -
Figure 33: Overview of applied conditions to differentiate rbESCs. - 70 -
Figure 34: Typical aggregates formed during EB differentiation experiments. - 71 -
Figure 35: Lipid droplets stained by Oil-Red-O in outgrown cells of attached EB-like structures. - 71 -
Figure 36: Outline of the differentiation strategy to direct differentiation into cells belonging to the three germ layers. - 72 -
Figure 37: RT-PCR analysis of differentiation markers. - 73 -
Figure 38: Assessment of the contribution of rbESCs to the developing rabbit embryo. - 74 -
Figure 39: Typical morphology of rabbit BM-MSC and A-MSC under standard cell culture conditions and under reduced O_2 conditions each at P1 and P9. - 75 -
Figure 40: Growth curves obtained from data collected during the culture of rabbit BM-MSC and A-MSC under standard cell culture conditions and under reduced O_2 conditions over 9 passages. - 75 -
Figure 41: Colony forming assay of rbBM-MSC and rbA-MSC. - 76 -
Figure 42: Dependency of rbMSCs on the supplementation of bFGF as verified on BM-MSC. - 77 -
Figure 43: Multipotency of rbMSCs. BM-MSCs and A-MSCs cultured under conditions inducing adipogenic differentiation. - 77 -
Figure 44: Multipotency of rbMSCs. BM-MSCs and A-MSCs cultured under conditions inducing osteogenic differentiation. - 78 -
Figure 45: Multipotency of rbMSCs. - 78 -
Figure 46: Multipotency of rbMSCs. - 78 -
Figure 47: Transfection of rbBM-MSCs and A-MSCs using pCAGGs-mCherry-Neo. - 80 -
Figure 48: Transfection of rbBM-MSCs with vector BAC-mCherry-Neo applying different methods. - 82 -
Figure 49: Amplification of two parts of rb*hprt* for subsequent cloning. - 84 -
Figure 50: pl452-rbHPRT. - 84 -
Figure 51: Structure of rb$hprt^{Neo}$ located on a BAC after successful recombineering thereby decreasing the overall size of rb*hprt*. - 84 -
Figure 52: Structure of the targeting vector prbHPRT^{Neo}. - 85 -
Figure 53: Overview of the applied selection strategy. - 86 -
Figure 54: PCR analysis of rbBM-MSC colonies transfected with prbHPRT^{Neo} that were resistant against both G418 and 6-TG. - 87 -
Figure 55: Overview of current strategies to restore the natural adaptive insulin providing function. - 99 -
Figure 56: Signalling pathways induced by LIF and bFGF that result in self-renewal. - 104 -
Figure 57: Extrinsic signalling that influences various cellular processes here in particular pluripotency. - 105 -

Figure 58: Plasticity of stem cells. - 107 -
Figure 59: Suggested molecular signalling network of rbESCs obtained by Wang *et al*. (2008) [800]. - 109 -
Figure 60: Chemical structure of 6-TG, an analogue of the purine base guanine. - 121 -
Figure 61: Schematic draw of the annealing of the primer pair SB-Cherry. - 133 -

8 APPENDIX

This chapter gives a detailed description of the construction of vectors and its verification by detailed restriction digests. However, data are not shown.

8.1 Construction of rabbit *insulin* expression vectors

In a first step, rabbit *insulin* was cloned stepwise. The promoter region was amplified using primer pair rbIns-5´region (2.1.14.1) resulting in a 1187 bp fragment, whose correctness was verified by two restriction digests (PvuII: 554 bp + 633 bp, NcoI: 236 bp + 924 bp). The successful ligation (4161 bp) of this fragment into the cloning vector pjet1.2 was verified by three restriction digests (SmaI: 614 bp + 3547 bp, SacI: 592 bp + 3569 bp, SwaI: 1780 bp + 2381 bp). The ligated fragment was sequenced with the oligonucleotide pJET1.2 sequencing primer-fwd.

The transcription unit was amplified using oligonucleotides rbIns-ex1-fwd and rbIns-ex3-rev resulting in a 824 bp fragment, whose correctness was verified by two restriction digests (SacI: 335 bp + 489 bp, EcoNI: 247 bp + 577 bp). The successful ligation (3798 bp) of this fragment into the cloning vector pjet1.2 was verified by colony PCR and four restriction digests (SacI/PmeI: 883 bp + 2915 bp or 728 bp + 3070 bp, EcoNI/HindIII: 831 bp + 2967 bp or 377 bp + 3421 bp; HaeII: 67 bp + 79 bp +370 bp + 417 bp + 704 bp + 2250 bp, NcoI: 744 bp + 3076 bp). The ligated fragment was sequenced with the oligonucleotide pjet1.2 sequencing primer-rev.

In order to insert the desired Akita mutation, the transition of guanine to adenine at position 303, the Quick Change II-E Site-Directed Mutagenesis kit was used. After transformation, positive colonies were identified by colony PCR and two restriction digests (SacI/PmeI and EcoNI/HindIII). The inserted transition was proved by sequencing with oligonucleotide rbIns-Mut-seq.

In the next step, the two parts of the *insulin* gene, promoter and mutated transcription unit (Ins^{Akita}) (for control vector non-mutated transcription unit (*Ins*)), were combined. For this, promoter bearing vector was digested with restriction endonucleases EcoNI and HindIII (1283 bp + 2898 bp) and transcription unit bearing vector with NotI-HF and EcoNI (288 bp + 3532 bp). In following steps, both underlined fragments were ligated together and proper ligation (4821 bp) was verified by four restriction digests (SwaI: 2381 bp + 2440 bp, RsaI: 769 bp + 1331 bp + 2692 bp, HaeII: 79 bp + 282 bp + 417 bp + 704 bp + 2969 bp, HinfI: 65 bp + 75 bp + 396 bp + 400 bp + 519 bp + 531 bp + 1295 bp).

In a final cloning step, a poly adenylation signal was added to both *insulin* expression vectors. For this, the vectors of the previous step were linearized with restriction endonuclease HindIII, the vector pBluescript-3xpA (4613 bp) was digested with restriction endonucleases XhoI and EcoRI-HF (3956 bp + 657 bp) and the underlined fragment was ligated to the first mentioned vector. The final vectors (5470 bp) were verified by seven restriction digests (SacI: 592 bp + 1153 bp +3725 bp, HincII: 1141 bp + 4329 bp, PstI: 27 bp + 133 bp + 312 bp + 415 bp + 543 bp + 700 bp + 3340 bp, HaeII: 79 bp + 282 bp + 370 bp + 417 bp + 1353 bp + 2969 bp, RsaI: 796 bp + 1333 bp + 3349 bp, NcoI: 744 bp + 962 bp + 3772 bp, PvuII: 60 bp + 584 bp + 1050 bp + 1179 bp + 2605 bp). Finally, the vectors were subjected to sequencing. Here, oligonucleotides rbIns-pA-fwd, pjet1.2 Sequencing Primer-fwd and –rev were used. Hence, $pINS^{Akita}$ and $pINS^{WT}$ have been constructed.

8.2 Construction of Sleeping Beauty transposon system

To prepare SB system vectors, the transposase *SB100* was subcloned. For this, *SB100 transposase* cassette (1731 bp) was cut out of the received vector carrying SB100 (4984 bp) by restriction digest with NotI and SacII. The obtained fragment was verified by EcoRI restriction digest (641 bp + 1090 bp). Then, the correct *SB100* cassette was subcloned into pCAGGseGFP of which the *eGFP* cassette was cut out by restriction digest with NotI and SalI. The correctness of the resulting transposase expression vector pCAGGsSB100 (5819 bp) was verified by restriction digests with BlpI/HindIII (252 bp + 617 bp + 1281 bp + 3669 bp), DraI (19 bp + 261 bp + 692 bp + 1772 bp + 3075 bp), HaeII (36 bp + 43 bp +114 bp + 126 bp + 354 bp + 370 bp + 2359 bp + 2417 bp) and HinfI (65 bp + 75 bp + 396 bp + 517 bp + 577 bp + 1217 bp + 1386 bp + 1586 bp).

To flank the gen of interest with SB-IR, the vector pT2BDS3 (7644 bp) was modified. For this, the vector was digested with BglII and XhoI to remove unnecessary sequences between IRs, resulting in a 3304 bp fragment. Also, the vector pSL1180 Amersham (3422 bp), containing a superpolylinker, was digested with MscI to release the superpolylinker (279 bp) which was then ligated into pT2BDS3. The resulting pT2BDS3-polylinker (3583 bp) was verified by restriction digest with SacI (343 bp + 3240 bp or 586 bp + 2997 bp).

Afterwards, the first GOI, *CAGGs-mCherry*, was cloned into the superpolylinker of pT2BDS3. For this, the *CAGGs*-mCherry cassette of pCAGGs-mCherry (5546 bp) was cut out by restriction digest with HindIII and SalI (3030 bp). This fragment was subcloned into linearized pT2BDS3-polylinker resulting in the vector pT2-SB-CAGGs-mCherry (6693 bp),

which was verified by restriction digests with NdeI (2842 bp + 3851), XbaI (463 bp + 2682 bp + 3548 bp) and BglII/SalI (64 bp + 973 bp + 2660 bp + 2996 bp) and sequencing.
After successful generation of mCherry positive rabbits, the *Ins*^{Akita} cassette including 3 x polyA was cloned into the superpolylinker of pT2BDS3. For this, pINS^{Akita} was restriction digested with PmeI/SbfI. The resulting fragment (2559 bp) was ligated into the target vector pT2-SB-polyinker (linearized by restriction digest with EcoRV (3583 bp)). This resulted in the vector pT2-SB-INS^{Akita} (6154 bp), which was verified by restriction digests with BamHI (357 bp + 905 bp + 1910 bp + 2982 bp), EcoRI/BsrGI (357 bp + 5797 bp) and BlpI/HindIII (22 bp + 193 bp + 324 bp + 353 bp + 567 bp + 653 bp + 1102 bp + 2940 bp) and sequencing.

8.3 Generation of transgenic rabbits carrying mCherry

In this chapter, details for the verification of the obtained positive PCR bands are given. From the recovered foetuses during the generation of *mCherry* transgenic rabbits genomic DNA was isolated and PCR with primer pair SB-Cherry was performed to verify the integration of *CAGGsmCherry*. The correct identity of the obtained PCR products was proven by restriction digests (Fig. 61) with BstXI (222 bp + 772 bp) and BstEII (171 bp + 191 bp + 642 bp) (data not shown).

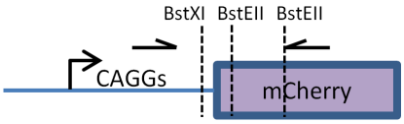

Figure 61: Schematic draw of the annealing of the primer pair SB-Cherry.
The obtained PCR products were restriction digested separately with BstXI and BstEII.

8.4 Mutagenesis of a bacterial artificial chromosome

The following experimental steps were part of the Bachelor-thesis of Ala El Din Samara: To provide homologous sites for the recombineering process, part of intron 1 with exon 2 (478 bp) and exon 4 with part of intron 4 (476 bp) were amplified by PCR both from BAC-rb*hprt* using oligonucleotides designed with restriction sites (rbHPRT-exon2-EcoRI-fwd, rbHPRT-exon2-NheI-rev, rbHPRT-exon4-BamHI-rev and rbHPRT-exon4-NotI-rev) (Fig. 49, 3.2.4.1). Each PCR product was ligated into pjet1.2/blunt. Correct vectors (3467 bp (exon 2) and 3461 bp (exon 4)) were verified by restriction digests with BglII (539 bp + 2937 bp) and EcoRI/NheI (487 bp + 2974 bp), both for exon 2, or BglII (533 bp + 2928 bp) and BamHI/NotI (45 bp + 476 bp + 2940 bp), and these both for exon 4. The ligated PCR products were cut out of the cloning vectors by restriction digests with EcoRI and NheI (exon 2)

or BamHI and NotI (exon 4). The cloning vector pl452 (4823 bp) was digested with BamHI and NotI resulting in a 4804 bp backbone in which the cassette exon 4 (476 bp) was ligated 3′ of the PGK-Neo-pA cassette. Correct integration of exon 4 into pl452 was verified by restriction digests with BamHI/NotI (476 bp + 4804 bp) and BsaAI (1642 bp + 3638 bp).
The resulting cloning vector pl452-exon4 (5280 bp) was digested with EcoRI and NheI resulting in a 5171 bp backbone in which the cassette exon 2 (487 bp) was ligated 5′ of the PGK-Neo-pA cassette. Correct integration of exon 4 into pl452 (5658 bp) was verified by restriction digests with EcoRI/NheI (487 bp + 5171 bp) and PscI (640 bp + 5018 bp).
The final construct pl452-rbHPRT was then subjected to sequencing with oligonucleotides rbHPRT-exon2-fwd, rbHPRT-exon2-rev, rbHPRT-exon4-fwd and rbHPRT-exon4-rev. Here, the work of the Bachelor thesis ends.
To get rid of the backbone of pl452-rbHPRT for recombineering, this plasmid was digested with BstXI and SalI. Since the expected fragments would have a similar size (2778 bp + 2880 bp), the plasmid was further digested with BsaI, resulting in three bands: 2778 bp + 1508 bp + 1372 bp. The isolated rbHPRT-ex2-PGK-Neo-pA-ex4 cassette (2778 bp) was transferred by transformation into recombineering-competent *E. coli* SW106 and selected by ampicillin and chloramphenicol. Successful recombineering was verified by PCR analysis, whereby one fragment (2002 bp) was amplified with a primerpair (Intron1-PGK) binding in intron 1 of rbHPRT (sequence not on pl452-rbHPRT) and in the PGK promoter. The 2nd fragment (2000 bp) was amplified with a primerpair (pA-intron4) binding in the pA and in intron 4 (sequence not on pl452-rbHPRT). Both reactions resulted in a positive band on the agarose gel. Hence, the artificial cassette introduced into the rabbit *hprt* gene has a size of 1743 bp.

8.5 Construction of a rabbit *hprt* targeting construct

To construct a conventional targeting vector for rabbit *hprt*, BAC-rbHPRT^{Neo} was restriction digested by KpnI. The correctness of the obtained fragment (9508 bp) was verified by restriction digest (NcoI: 571 bp + 1289 bp + 1640 bp + 3019 bp + 3380 bp) before ligation into restriction digested (KpnI) vector pBluescript SK+ (2691 bp, control restriction digest with DdeI: 166 bp + 409 bp + 540 bp + 771 bp + 1075 bp).
The resulting targeting vector, prbHPRT^{Neo} was subjected to sequencing using oligonucleotides T3 and T7 provided by the sequencing company. Additionally, this vector was sequenced completely in the cassette supposed for targeting using oligonucleotides HPRT-3′-site-a-rev, HPRT-3′-site-b-rev, HPRT-5′-site-a-fwd, HPRT-51 fwd and 73 rev,

HPRT-51 fwd and 73 rev-b, HPRT-51 fwd and 73 rev-c, HPRT-51-fwd, HPRT-51-b-fwd, HPRT-51-rev, HPRT-51-b-rev, HPRT-51-c-rev, HPRT-73-fwd, HPRT-73-b-fwd, HPRT-73-rev.

9 LITERATURE

1. Gordon, J. W., Scangos, G. A., Plotkin, D. J., Barbosa, J. A. & Ruddle, F. H. Genetic transformation of mouse embryos by microinjection of purified DNA. *Proc. Natl. Acad. Sci. U.S.A* **77**, 7380–7384 (1980).
2. Gordon, J. W. & Ruddle, F. H. Integration and stable germ line transmission of genes injected into mouse pronuclei. *Science* **214**, 1244–1246 (1981).
3. Selden, R., Springman, K., Hondele, J., Meyer, J., Winnacker, E.-L., Kräußlich, H., Brem, G., Brenig, B., Goodman, H. M., Graf, F. & Kruff, B. Production of transgenic mice, rabbits and pigs by microinjection into pronuclei. *Reprod Domest Anim* **20**, 251–252 (1985).
4. Hammer, R. E., Pursel, V. G., Rexroad, C. E., Wall, R. J., Bolt, D. J., Ebert, K. M., Palmiter, R. D. & Brinster, R. L. Production of transgenic rabbits, sheep and pigs by microinjection. *Nature* **315**, 680–683 (1985).
5. Krimpenfort, P., Rademakers, A., Eyestone, W., van der Schans, A., van den Broek, S., Kooiman, P., Kootwijk, E., Platenburg, G., Pieper, F. & Strijker, R. Generation of transgenic dairy cattle using 'in vitro' embryo production. *Biotechnology (N.Y.)* **9**, 844–847 (1991).
6. Stacey, A., Schnieke, A., Kerr, M., Scott, A., McKee, C., Cottingham, I., Binas, B., Wilde, C. & Colman, A. Lactation is disrupted by alpha-lactalbumin deficiency and can be restored by human alpha-lactalbumin gene replacement in mice. *Proc. Natl. Acad. Sci. U.S.A* **92**, 2835–2839 (1995).
7. Crepso, J., Blaya, C., Crespo, A. & Aliño, S. F. Long-term expression of the human alpha1-antitrypsin gene in mice employing anionic and cationic liposome vectors. *Biochem. Pharmacol* **51**, 1309–1314 (1996).
8. Gay, E., Seurin, D., Babajko, S., Doublier, S., Cazillis, M. & Binoux, M. Liver-specific expression of human insulin-like growth factor binding protein-1 in transgenic mice: repercussions on reproduction, ante- and perinatal mortality and postnatal growth. *Endocrinology* **138**, 2937–2947 (1997).
9. Wright, G., Carver, A., Cottom, D., Reeves, D., Scott, A., Simons, P., Wilmut, I., Garner, I. & Colman, A. High level expression of active human alpha-1-antitrypsin in the milk of transgenic sheep. *Biotechnology (N.Y.)* **9**, 830–834 (1991).
10. Spencer, L. T., Humphries, J. E. & Brantly, M. L. Antibody response to aerosolized transgenic human alpha1-antitrypsin. *N. Engl. J. Med* **352**, 2030–2031 (2005).
11. Schnieke, A. E., Kind, A. J., Ritchie, W. A., Mycock, K., Scott, A. R., Ritchie, M., Wilmut, I., Colman, A. & Campbell, K. H. Human factor IX transgenic sheep produced by transfer of nuclei from transfected fetal fibroblasts. *Science* **278**, 2130–2133 (1997).
12. Kuroiwa, Y., Kasinathan, P., Choi, Y. J., Naeem, R., Tomizuka, K., Sullivan, E. J., Knott, J. G., Duteau, A., Goldsby, R. A., Osborne, B. A., Ishida, I. & Robl, J. M. Cloned transchromosomic calves producing human immunoglobulin. *Nat. Biotechnol* **20**, 889–894 (2002).
13. Song, G. & Han, J. Y. Avian biomodels for use as pharmaceutical bioreactors and for studying human diseases. *Ann. N. Y. Acad. Sci* **1229**, 69–75 (2011).
14. Yang, B., Wang, J., Tang, B., Liu, Y., Guo, C., Yang, P., Yu, T., Li, R., Zhao, J., Zhang, L., Dai, Y. & Li, N. Characterization of bioactive recombinant human lysozyme expressed in milk of cloned transgenic cattle. *PLoS ONE* **6**, e17593 (2011).
15. Houdebine, L.-M. Production of pharmaceutical proteins by transgenic animals. *Comparative Immunology, Microbiology and Infectious Diseases* **32**, 107–121 (2009).
16. Weiss, J. *Tierpflege in Forschung und Klinik. 86 Tabellen* (Enke, Stuttgart, 2008).
17. Strömqvist, M., Houdebine, M., Andersson, J. O., Edlund, A., Johansson, T., Viglietta, C., Puissant, C. & Hansson, L. Recombinant human extracellular superoxide dismutase produced in milk of transgenic rabbits. *Transgenic Res* **6**, 271–278 (1997).
18. Yamamoto, T., Bishop, R. W., Brown, M. S., Goldstein, J. L. & Russell, D. W. Deletion in cysteine-rich region of LDL receptor impedes transport to cell surface in WHHL rabbit. *Science* **232**, 1230–1237 (1986).
19. La Ville, A., Turner, P. R., Pittilo, R. M., Martini, S., Marenah, C. B., Rowles, P. M., Morris, G., Thomson, G. A., Woolf, N. & Lewis, B. Hereditary hyperlipidemia in the rabbit due to overproduction of lipoproteins. I. Biochemical studies. *Arteriosclerosis* **7**, 105–112 (1987).
20. Shiomi, M. & Ito, T. The Watanabe heritable hyperlipidemic (WHHL) rabbit, its characteristics and history of development: a tribute to the late Dr. Yoshio Watanabe. *Atherosclerosis* **207**, 1–7 (2009).
21. Wakeman, A. J. ON THE HEXON BASES OF LIVER TISSUE UNDER NORMAL AND CERTAIN PATHOLOGICAL CONDITIONS. *J. Exp. Med* **7**, 292–304 (1905).
22. Graur, D., Duret, L. & Gouy, M. Phylogenetic position of the order Lagomorpha (rabbits, hares and allies). *Nature* **379**, 333–335 (1996).
23. Reyes, A., Gissi, C., Pesole, G., Catzeflis, F. M. & Saccone, C. Where do rodents fit? Evidence from the complete mitochondrial genome of Sciurus vulgaris. *Mol. Biol. Evol.* **17**, 979–983 (2000).
24. Fan, J. & Watanabe, T. Transgenic rabbits as therapeutic protein bioreactors and human disease models. *Pharmacol. Ther* **99**, 261–282 (2003).

25. Palmiter, R. D., Brinster, R. L., Hammer, R. E., Trumbauer, M. E., Rosenfeld, M. G., Birnberg, N. C. & Evans, R. M. Dramatic growth of mice that develop from eggs microinjected with metallothionein-growth hormone fusion genes. *Nature* **300**, 611–615 (1982).
26. Pinkert, C. A., Galbreath, E. J., Yang, C. W. & Striker, L. J. Liver, renal and subcutaneous histopathology in PEPCK-bGH transgenic pigs. *Transgenic Res* **3**, 401–405 (1994).
27. Costa, C., Solanes, G., Visa, J. & Bosch, F. Transgenic rabbits overexpressing growth hormone develop acromegaly and diabetes mellitus. *FASEB J* **12**, 1455–1460 (1998).
28. Tardiff, J. C., Factor, S. M., Tompkins, B. D., Hewett, T. E., Palmer, B. M., Moore, R. L., Schwartz, S., Robbins, J. & Leinwand, L. A. A truncated cardiac troponin T molecule in transgenic mice suggests multiple cellular mechanisms for familial hypertrophic cardiomyopathy. *J. Clin. Invest* **101**, 2800–2811 (1998).
29. Marian, A. J., Wu, Y., Lim, D. S., McCluggage, M., Youker, K., Yu, Q. T., Brugada, R., DeMayo, F., Quinones, M. & Roberts, R. A transgenic rabbit model for human hypertrophic cardiomyopathy. *J. Clin. Invest* **104**, 1683–1692 (1999).
30. Patel, R., Nagueh, S. F., Tsybouleva, N., Abdellatif, M., Lutucuta, S., Kopelen, H. A., Quinones, M. A., Zoghbi, W. A., Entman, M. L., Roberts, R. & Marian, A. J. Simvastatin induces regression of cardiac hypertrophy and fibrosis and improves cardiac function in a transgenic rabbit model of human hypertrophic cardiomyopathy. *Circulation* **104**, 317–324 (2001).
31. Senthil, V., Chen, S. N., Tsybouleva, N., Halder, T., Nagueh, S. F., Willerson, J. T., Roberts, R. & Marian, A. J. Prevention of cardiac hypertrophy by atorvastatin in a transgenic rabbit model of human hypertrophic cardiomyopathy. *Circ. Res* **97**, 285–292 (2005).
32. Sanbe, A., James, J., Tuzcu, V., Nas, S., Martin, L., Gulick, J., Osinska, H., Sakthivel, S., Klevitsky, R., Ginsburg, K. S., Bers, D. M., Zinman, B., Lakatta, E. G. & Robbins, J. Transgenic rabbit model for human troponin I-based hypertrophic cardiomyopathy. *Circulation* **111**, 2330–2338 (2005).
33. Manabe, Y. C., Dannenberg, A. M., Tyagi, S. K., Hatem, C. L., Yoder, M., Woolwine, S. C., Zook, B. C., Pitt, M. L. M. & Bishai, W. R. Different strains of Mycobacterium tuberculosis cause various spectrums of disease in the rabbit model of tuberculosis. *Infect. Immun* **71**, 6004–6011 (2003).
34. Dorman, S. E., Hatem, C. L., Tyagi, S., Aird, K., Lopez-Molina, J., Pitt, M. L. M., Zook, B. C., Dannenberg, A. M., Bishai, W. R. & Manabe, Y. C. Susceptibility to tuberculosis: clues from studies with inbred and outbred New Zealand White rabbits. *Infect. Immun* **72**, 1700–1705 (2004).
35. Scott, C. P., Kumar, N., Bishai, W. R. & Manabe, Y. C. Short report: modulation of Mycobacterium tuberculosis infection by Plasmodium in the murine model. *Am. J. Trop. Med. Hyg* **70**, 144–148 (2004).
36. Yamamura, Y., Kotani, M., Chowdhury, M. I., Yamamoto, N., Yamaguchi, K., Karasuyama, H., Katsura, Y. & Miyasaka, M. Infection of human CD4+ rabbit cells with HIV-1: the possibility of the rabbit as a model for HIV-1 infection. *Int. Immunol* **3**, 1183–1187 (1991).
37. Snyder, B. W., Vitale, J., Milos, P., Gosselin, J., Gillespie, F., Ebert, K., Hague, B. F., Kindt, T. J., Wadsworth, S. & Leibowitz, P. Developmental and tissue-specific expression of human CD4 in transgenic rabbits. *Mol. Reprod. Dev* **40**, 419–428 (1995).
38. Dunn, C. S., Mehtali, M., Houdebine, L. M., Gut, J. P., Kirn, A. & Aubertin, A. M. Human immunodeficiency virus type 1 infection of human CD4-transgenic rabbits. *J. Gen. Virol* **76 (Pt 6)**, 1327–1336 (1995).
39. Leno, M., Hague, B. F., Teller, R. & Kindt, T. J. HIV-1 mediates rapid apoptosis of lymphocytes from human CD4 transgenic but not normal rabbits. *Virology* **213**, 450–454 (1995).
40. Speck, R. F., Penn, M. L., Wimmer, J., Esser, U., Hague, B. F., Kindt, T. J., Atchison, R. E. & Goldsmith, M. A. Rabbit cells expressing human CD4 and human CCR5 are highly permissive for human immunodeficiency virus type 1 infection. *J. Virol* **72**, 5728–5734 (1998).
41. Knight, K. L., Spieker-Polet, H., Kazdin, D. S. & Oi, V. T. Transgenic rabbits with lymphocytic leukemia induced by the c-myc oncogene fused with the immunoglobulin heavy chain enhancer. *Proc. Natl. Acad. Sci. U.S.A* **85**, 3130–3134 (1988).
42. Peng, X., Olson, R. O., Christian, C. B., Lang, C. M. & Kreider, J. W. Papillomas and carcinomas in transgenic rabbits carrying EJ-ras DNA and cottontail rabbit papillomavirus DNA. *J. Virol* **67**, 1698–1701 (1993).
43. Sethupathi, P., Spieker-Polet, H., Polet, H., Yam, P. C., Tunyaplin, C. & Knight, K. L. Lymphoid and non-lymphoid tumors in E kappa-myc transgenic rabbits. *Leukemia* **8**, 2144–2155 (1994).
44. Peng, X., Griffith, J. W. & Lang, C. M. Reinitiated expression of EJras transgene in targeted epidermal cells of transgenic rabbits by cottontail rabbit papillomavirus infection. *Cancer Lett* **171**, 193–200 (2001).
45. van den Hout, J. M., Reuser, A. J., Klerk, J. B. de, Arts, W. F., Smeitink, J. A. & van der Ploeg, A. T. Enzyme therapy for pompe disease with recombinant human alpha-glucosidase from rabbit milk. *J. Inherit. Metab. Dis* **24**, 266–274 (2001).
46. Bosze, Z., Hiripi, L., Carnwath, J. W. & Niemann, H. The transgenic rabbit as model for human diseases and as a source of biologically active recombinant proteins. *Transgenic Res* **12**, 541–553 (2003).

47. Bühler, T. A., Bruyère, T., Went, D. F., Stranzinger, G. & Bürki, K. Rabbit beta-casein promoter directs secretion of human interleukin-2 into the milk of transgenic rabbits. *Biotechnology (N.Y.)* **8**, 140–143 (1990).
48. Bijvoet, A. G., van Hirtum, H., Kroos, M. A., van de Kamp, E. H., Schoneveld, O., Visser, P., Brakenhoff, J. P., Weggeman, M., van Corven, E. J., van der Ploeg, A. T. & Reuser, A. J. Human acid alpha-glucosidase from rabbit milk has therapeutic effect in mice with glycogen storage disease type II. *Hum. Mol. Genet* **8**, 2145–2153 (1999).
49. Hiripi, L., Makovics, F., Halter, R., Baranyi, M., Paul, D., Carnwath, J. W., Bösze, Z. & Niemann, H. Expression of active human blood clotting factor VIII in mammary gland of transgenic rabbits. *DNA Cell Biol* **22**, 41–45 (2003).
50. Koles, K., van Berkel, P. H. C., Pieper, F. R., Nuijens, J. H., Mannesse, M. L. M., Vliegenthart, J. F. G. & Kamerling, J. P. N- and O-glycans of recombinant human C1 inhibitor expressed in the milk of transgenic rabbits. *Glycobiology* **14**, 51–64 (2004).
51. Grosse-Hovest, L., Müller, S., Minoia, R., Wolf, E., Zakhartchenko, V., Wenigerkind, H., Lassnig, C., Besenfelder, U., Müller, M., Lytton, S. D., Jung, G. & Brem, G. Cloned transgenic farm animals produce a bispecific antibody for T cell-mediated tumor cell killing. *Proc. Natl. Acad. Sci. U.S.A* **101**, 6858–6863 (2004).
52. Soler, E., Le Saux, A., Guinut, F., Passet, B., Cohen, R., Merle, C., Charpilienne, A., Fourgeux, C., Sorel, V., Piriou, A., Schwartz-Cornil, I., Cohen, J. & Houdebine, L.-M. Production of two vaccinating recombinant rotavirus proteins in the milk of transgenic rabbits. *Transgenic Res* **14**, 833–844 (2005).
53. Houdebine, L. M. The production of pharmaceutical proteins from the milk of transgenic animals. *Reprod. Nutr. Dev* **35**, 609–617 (1995).
54. Dove, A. Milking the genome for profit. *Nat. Biotechnol* **18**, 1045–1048 (2000).
55. Buelow, R. & van Schooten, W. The future of antibody therapy. *Ernst Schering Found Symp Proc*, 83–106 (2006).
56. Zabetian, M., Tahmooresp, M. & Hosseini, K. The Applications of Transgenic Rabbits in Agriculture and Biomedicine. *J. of Animal and Veterinary Advances* **10**, 780–790 (2011).
57. Wolf, E., Schernthaner, W., Zakhartchenko, V., Prelle, K., Stojkovic, M. & Brem, G. Transgenic technology in farm animals--progress and perspectives. *Exp. Physiol.* **85**, 615–625 (2000).
58. Niemann, H. & Kues, W. A. Application of transgenesis in livestock for agriculture and biomedicine. *Anim. Reprod. Sci.* **79**, 291–317 (2003).
59. Tesson, L., Cozzi, J., Ménoret, S., Rémy, S., Usal, C., Fraichard, A. & Anegon, I. Transgenic modifications of the rat genome. *Transgenic Res.* **14**, 531–546 (2005).
60. Robl, J. M., Wang, Z., Kasinathan, P. & Kuroiwa, Y. Transgenic animal production and animal biotechnology. *Theriogenology* **67**, 127–133 (2007).
61. Henikoff, S. Conspiracy of silence among repeated transgenes. *Bioessays* **20**, 532–535 (1998).
62. Geurts, A. M., Collier, L. S., Geurts, J. L., Oseth, L. L., Bell, M. L., Mu, D., Lucito, R., Godbout, S. A., Green, L. E., Lowe, S. W., Hirsch, B. A., Leinwand, L. A. & Largaespada, D. A. Gene mutations and genomic rearrangements in the mouse as a result of transposon mobilization from chromosomal concatemers. *PLoS Genet.* **2**, e156 (2006).
63. Wall, R. J., Hyman, P., Kerr, D., Pintado, B. & Wells, K. Transgenic animal technology. *J. Androl.* **18**, 236–239 (1997).
64. Schröder, A. R. W., Shinn, P., Chen, H., Berry, C., Ecker, J. R. & Bushman, F. HIV-1 integration in the human genome favors active genes and local hotspots. *Cell* **110**, 521–529 (2002).
65. Baum, C., Kustikova, O., Modlich, U., Li, Z. & Fehse, B. Mutagenesis and oncogenesis by chromosomal insertion of gene transfer vectors. *Hum. Gene Ther.* **17**, 253–263 (2006).
66. Mátés, L., Chuah, M. K. L., Belay, E., Jerchow, B., Manoj, N., Acosta-Sanchez, A., Grzela, D. P., Schmitt, A., Becker, K., Matrai, J., Ma, L., Samara-Kuko, E., Gysemans, C., Pryputniewicz, D., Miskey, C., Fletcher, B., VandenDriessche, T., Ivics, Z. & Izsvák, Z. Molecular evolution of a novel hyperactive Sleeping Beauty transposase enables robust stable gene transfer in vertebrates. *Nat. Genet* **41**, 753–761 (2009).
67. Lander, E. S., Linton, L. M., Birren, B., Nusbaum, C., Zody, M. C., Baldwin, J., Devon, K., Dewar, K., Doyle, M., FitzHugh, W., Funke, R., Gage, D., Harris, K., Heaford, A., Howland, J., Kann, L., Lehoczky, J., LeVine, R., McEwan, P., McKernan, K., Meldrim, J., Mesirov, J. P., Miranda, C., Morris, W., Naylor, J., Raymond, C., Rosetti, M., Santos, R., Sheridan, A., Sougnez, C., Stange-Thomann, N., Stojanovic, N., Subramanian, A., Wyman, D., Rogers, J., Sulston, J., Ainscough, R., Beck, S., Bentley, D., Burton, J., Clee, C., Carter, N., Coulson, A., Deadman, R., Deloukas, P., Dunham, A., Dunham, I., Durbin, R., French, L., Grafham, D., Gregory, S., Hubbard, T., Humphray, S., Hunt, A., Jones, M., Lloyd, C., McMurray, A., Matthews, L., Mercer, S., Milne, S., Mullikin, J. C., Mungall, A., Plumb, R., Ross, M., Shownkeen, R., Sims, S., Waterston, R. H., Wilson, R. K., Hillier, L. W., McPherson, J. D., Marra, M. A., Mardis, E. R., Fulton, L. A., Chinwalla, A. T., Pepin, K. H., Gish, W. R., Chissoe, S. L., Wendl, M. C., Delehaunty, K. D., Miner, T. L., Delehaunty, A., Kramer, J. B., Cook, L. L., Fulton, R. S., Johnson, D. L., Minx, P. J., Clifton, S. W., Hawkins, T., Branscomb, E., Predki, P., Richardson, P., Wenning, S., Slezak, T., Doggett, N., Cheng,

J. F., Olsen, A., Lucas, S., Elkin, C., Uberbacher, E., Frazier, M., Gibbs, R. A., Muzny, D. M., Scherer, S. E., Bouck, J. B., Sodergren, E. J., Worley, K. C., Rives, C. M., Gorrell, J. H., Metzker, M. L., Naylor, S. L., Kucherlapati, R. S., Nelson, D. L., Weinstock, G. M., Sakaki, Y., Fujiyama, A., Hattori, M., Yada, T., Toyoda, A., Itoh, T., Kawagoe, C., Watanabe, H., Totoki, Y., Taylor, T., Weissenbach, J., Heilig, R., Saurin, W., Artiguenave, F., Brottier, P., Bruls, T., Pelletier, E., Robert, C., Wincker, P., Smith, D. R., Doucette-Stamm, L., Rubenfield, M., Weinstock, K., Lee, H. M., Dubois, J., Rosenthal, A., Platzer, M., Nyakatura, G., Taudien, S., Rump, A., Yang, H., Yu, J., Wang, J., Huang, G., Gu, J., Hood, L., Rowen, L., Madan, A., Qin, S., Davis, R. W., Federspiel, N. A., Abola, A. P., Proctor, M. J., Myers, R. M., Schmutz, J., Dickson, M., Grimwood, J., Cox, D. R., Olson, M. V., Kaul, R., Shimizu, N., Kawasaki, K., Minoshima, S., Evans, G. A., Athanasiou, M., Schultz, R., Roe, B. A., Chen, F., Pan, H., Ramser, J., Lehrach, H., Reinhardt, R., McCombie, W. R., La Bastide, M. de, Dedhia, N., Blöcker, H., Hornischer, K., Nordsiek, G., Agarwala, R., Aravind, L., Bailey, J. A., Bateman, A., Batzoglou, S., Birney, E., Bork, P., Brown, D. G., Burge, C. B., Cerutti, L., Chen, H. C., Church, D., Clamp, M., Copley, R. R., Doerks, T., Eddy, S. R., Eichler, E. E., Furey, T. S., Galagan, J., Gilbert, J. G., Harmon, C., Hayashizaki, Y., Haussler, D., Hermjakob, H., Hokamp, K., Jang, W., Johnson, L. S., Jones, T. A., Kasif, S., Kaspryzk, A., Kennedy, S., Kent, W. J., Kitts, P., Koonin, E. V., Korf, I., Kulp, D., Lancet, D., Lowe, T. M., McLysaght, A., Mikkelsen, T., Moran, J. V., Mulder, N., Pollara, V. J., Ponting, C. P., Schuler, G., Schultz, J., Slater, G., Smit, A. F., Stupka, E., Szustakowski, J., Thierry-Mieg, D., Thierry-Mieg, J., Wagner, L., Wallis, J., Wheeler, R., Williams, A., Wolf, Y. I., Wolfe, K. H., Yang, S. P., Yeh, R. F., Collins, F., Guyer, M. S., Peterson, J., Felsenfeld, A., Wetterstrand, K. A., Patrinos, A., Morgan, M. J., Jong, P. de, Catanese, J. J., Osoegawa, K., Shizuya, H., Choi, S., Chen, Y. J. & Szustakowki, J. Initial sequencing and analysis of the human genome. *Nature* **409**, 860–921 (2001).

68. Venter, J. C., Adams, M. D., Myers, E. W., Li, P. W., Mural, R. J., Sutton, G. G., Smith, H. O., Yandell, M., Evans, C. A., Holt, R. A., Gocayne, J. D., Amanatides, P., Ballew, R. M., Huson, D. H., Wortman, J. R., Zhang, Q., Kodira, C. D., Zheng, X. H., Chen, L., Skupski, M., Subramanian, G., Thomas, P. D., Zhang, J., Gabor Miklos, G. L., Nelson, C., Broder, S., Clark, A. G., Nadeau, J., McKusick, V. A., Zinder, N., Levine, A. J., Roberts, R. J., Simon, M., Slayman, C., Hunkapiller, M., Bolanos, R., Delcher, A., Dew, I., Fasulo, D., Flanigan, M., Florea, L., Halpern, A., Hannenhalli, S., Kravitz, S., Levy, S., Mobarry, C., Reinert, K., Remington, K., Abu-Threideh, J., Beasley, E., Biddick, K., Bonazzi, V., Brandon, R., Cargill, M., Chandramouliswaran, I., Charlab, R., Chaturvedi, K., Deng, Z., Di Francesco, V., Dunn, P., Eilbeck, K., Evangelista, C., Gabrielian, A. E., Gan, W., Ge, W., Gong, F., Gu, Z., Guan, P., Heiman, T. J., Higgins, M. E., Ji, R. R., Ke, Z., Ketchum, K. A., Lai, Z., Lei, Y., Li, Z., Li, J., Liang, Y., Lin, X., Lu, F., Merkulov, G. V., Milshina, N., Moore, H. M., Naik, A. K., Narayan, V. A., Neelam, B., Nusskern, D., Rusch, D. B., Salzberg, S., Shao, W., Shue, B., Sun, J., Wang, Z., Wang, A., Wang, X., Wang, J., Wei, M., Wides, R., Xiao, C., Yan, C., Yao, A., Ye, J., Zhan, M., Zhang, W., Zhang, H., Zhao, Q., Zheng, L., Zhong, F., Zhong, W., Zhu, S., Zhao, S., Gilbert, D., Baumhueter, S., Spier, G., Carter, C., Cravchik, A., Woodage, T., Ali, F., An, H., Awe, A., Baldwin, D., Baden, H., Barnstead, M., Barrow, I., Beeson, K., Busam, D., Carver, A., Center, A., Cheng, M. L., Curry, L., Danaher, S., Davenport, L., Desilets, R., Dietz, S., Dodson, K., Doup, L., Ferriera, S., Garg, N., Gluecksmann, A., Hart, B., Haynes, J., Haynes, C., Heiner, C., Hladun, S., Hostin, D., Houck, J., Howland, T., Ibegwam, C., Johnson, J., Kalush, F., Kline, L., Koduru, S., Love, A., Mann, F., May, D., McCawley, S., McIntosh, T., McMullen, I., Moy, M., Moy, L., Murphy, B., Nelson, K., Pfannkoch, C., Pratts, E., Puri, V., Qureshi, H., Reardon, M., Rodriguez, R., Rogers, Y. H., Romblad, D., Ruhfel, B., Scott, R., Sitter, C., Smallwood, M., Stewart, E., Strong, R., Suh, E., Thomas, R., Tint, N. N., Tse, S., Vech, C., Wang, G., Wetter, J., Williams, S., Williams, M., Windsor, S., Winn-Deen, E., Wolfe, K., Zaveri, J., Zaveri, K., Abril, J. F., Guigó, R., Campbell, M. J., Sjolander, K. V., Karlak, B., Kejariwal, A., Mi, H., Lazareva, B., Hatton, T., Narechania, A., Diemer, K., Muruganujan, A., Guo, N., Sato, S., Bafna, V., Istrail, S., Lippert, R., Schwartz, R., Walenz, B., Yooseph, S., Allen, D., Basu, A., Baxendale, J., Blick, L., Caminha, M., Carnes-Stine, J., Caulk, P., Chiang, Y. H., Coyne, M., Dahlke, C., Mays, A., Dombroski, M., Donnelly, M., Ely, D., Esparham, S., Fosler, C., Gire, H., Glanowski, S., Glasser, K., Glodek, A., Gorokhov, M., Graham, K., Gropman, B., Harris, M., Heil, J., Henderson, S., Hoover, J., Jennings, D., Jordan, C., Jordan, J., Kasha, J., Kagan, L., Kraft, C., Levitsky, A., Lewis, M., Liu, X., Lopez, J., Ma, D., Majoros, W., McDaniel, J., Murphy, S., Newman, M., Nguyen, T., Nguyen, N., Nodell, M., Pan, S., Peck, J., Peterson, M., Rowe, W., Sanders, R., Scott, J., Simpson, M., Smith, T., Sprague, A., Stockwell, T., Turner, R., Venter, E., Wang, M., Wen, M., Wu, D., Wu, M., Xia, A., Zandieh, A. & Zhu, X. The sequence of the human genome. *Science* **291**, 1304–1351 (2001).
69. Feschotte, C. & Pritham, E. J. DNA Transposons and the Evolution of Eukaryotic Genomes. *Annu. Rev. Genet.* **41**, 331–68 (2007).
70. Claeys Bouuaert, C. & Chalmers, R. M. Gene therapy vectors: the prospects and potentials of the cut-and-paste transposons. *Genetica* **138**, 473–484 (2010).
71. Rushforth, A. M., Saari, B. & Anderson, P. Site-selected insertion of the transposon Tc1 into a Caenorhabditis elegans myosin light chain gene. *Mol. Cell. Biol* **13**, 902–910 (1993).

72. Zwaal, R. R., Broeks, A., van Meurs, J., Groenen, J. T. & Plasterk, R. H. Target-selected gene inactivation in Caenorhabditis elegans by using a frozen transposon insertion mutant bank. *Proc. Natl. Acad. Sci. U.S.A* **90**, 7431–7435 (1993).
73. Bessereau, J. L., Wright, A., Williams, D. C., Schuske, K., Davis, M. W. & Jorgensen, E. M. Mobilization of a Drosophila transposon in the Caenorhabditis elegans germ line. *Nature* **413**, 70–74 (2001).
74. Sasakura, Y., Awazu, S., Chiba, S. & Satoh, N. Germ-line transgenesis of the Tc1/mariner superfamily transposon Minos in Ciona intestinalis. *Proc. Natl. Acad. Sci. U.S.A* **100**, 7726–7730 (2003).
75. Cooley, L., Kelley, R. & Spradling, A. Insertional mutagenesis of the Drosophila genome with single P elements. *Science* **239**, 1121–1128 (1988).
76. Thibault, S. T., Singer, M. A., Miyazaki, W. Y., Milash, B., Dompe, N. A., Singh, C. M., Buchholz, R., Demsky, M., Fawcett, R., Francis-Lang, H. L., Ryner, L., Cheung, L. M., Chong, A., Erickson, C., Fisher, W. W., Greer, K., Hartouni, S. R., Howie, E., Jakkula, L., Joo, D., Killpack, K., Laufer, A., Mazzotta, J., Smith, R. D., Stevens, L. M., Stuber, C., Tan, L. R., Ventura, R., Woo, A., Zakrajsek, I., Zhao, L., Chen, F., Swimmer, C., Kopczynski, C., Duyk, G., Winberg, M. L. & Margolis, J. A complementary transposon tool kit for Drosophila melanogaster using P and piggyBac. *Nat. Genet* **36**, 283–287 (2004).
77. Kawakami, K., Shima, A. & Kawakami, N. Identification of a functional transposase of the Tol2 element, an Ac-like element from the Japanese medaka fish, and its transposition in the zebrafish germ lineage. *Proc. Natl. Acad. Sci. U.S.A* **97**, 11403–11408 (2000).
78. Hamlet, M. R. J., Yergeau, D. A., Kuliyev, E., Takeda, M., Taira, M., Kawakami, K. & Mead, P. E. Tol2 transposon-mediated transgenesis in Xenopus tropicalis. *Genesis* **44**, 438–445 (2006).
79. Sinzelle, L., Vallin, J., Coen, L., Chesneau, A., Du Pasquier, D., Pollet, N., Demeneix, B. & Mazabraud, A. Generation of trangenic Xenopus laevis using the Sleeping Beauty transposon system. *Transgenic Res* **15**, 751–760 (2006).
80. Dupuy, A. J., Clark, K., Carlson, C. M., Fritz, S., Davidson, A. E., Markley, K. M., Finley, K., Fletcher, C. F., Ekker, S. C., Hackett, P. B., Horn, S. & Largaespada, D. A. Mammalian germ-line transgenesis by transposition. *Proc. Natl. Acad. Sci. U.S.A* **99**, 4495–4499 (2002).
81. Drabek, D., Zagoraiou, L., deWit, T., an Langeveld, Roumpaki, C., Mamalaki, C., Savakis, C. & Grosveld, F. Transposition of the Drosophila hydei Minos transposon in the mouse germ line. *Genomics* **81**, 108–111 (2003).
82. Ding, S., Wu, X., Li, G., Han, M., Zhuang, Y. & Xu, T. Efficient transposition of the piggyBac (PB) transposon in mammalian cells and mice. *Cell* **122**, 473–483 (2005).
83. An, W., Han, J. S., Wheelan, S. J., Davis, E. S., Coombes, C. E., Ye, P., Triplett, C. & Boeke, J. D. Active retrotransposition by a synthetic L1 element in mice. *Proc. Natl. Acad. Sci. U.S.A* **103**, 18662–18667 (2006).
84. Jang, C.-W. & Behringer, R. R. Transposon-mediated transgenesis in rats. *CSH Protoc* **2007**, pdb.prot4866 (2007).
85. Kitada, K., Ishishita, S., Tosaka, K., Takahashi, R.-i., Ueda, M., Keng, V. W., Horie, K. & Takeda, J. Transposon-tagged mutagenesis in the rat. *Nat. Methods* **4**, 131–133 (2007).
86. Miskey, C., Izsvák, Z., Plasterk, R. H. & Ivics, Z. The Frog Prince: a reconstructed transposon from Rana pipiens with high transpositional activity in vertebrate cells. *Nucleic Acids Res* **31**, 6873–6881 (2003).
87. Han, J. S. & Boeke, J. D. A highly active synthetic mammalian retrotransposon. *Nature* **429**, 314–318 (2004).
88. Miskey, C., Papp, B., Mátés, L., Sinzelle, L., Keller, H., Izsvák, Z. & Ivics, Z. The ancient mariner sails again: transposition of the human Hsmar1 element by a reconstructed transposase and activities of the SETMAR protein on transposon ends. *Mol. Cell. Biol* **27**, 4589–4600 (2007).
89. Doak, T. G., Doerder, F. P., Jahn, C. L. & Herrick, G. A proposed superfamily of transposase genes: transposon-like elements in ciliated protozoa and a common "D35E" motif. *Proc. Natl. Acad. Sci. U.S.A* **91**, 942–946 (1994).
90. Ivics, Z., Izsvak, Z., Minter, A. & Hackett, P. B. Identification of functional domains and evolution of Tc1-like transposable elements. *Proc. Natl. Acad. Sci. U.S.A* **93**, 5008–5013 (1996).
91. Ivics, Z., Hackett, P. B., Plasterk, R. H. & Izsvák, Z. Molecular reconstruction of Sleeping Beauty, a Tc1-like transposon from fish, and its transposition in human cells. *Cell* **91**, 501–510 (1997).
92. Radice, A. D., Bugaj, B., Fitch, D. H. & Emmons, S. W. Widespread occurrence of the Tc1 transposon family: Tc1-like transposons from teleost fish. *Mol. Gen. Genet* **244**, 606–612 (1994).
93. Ivics, Z., Li, M. A., Mátés, L., Boeke, J. D., Nagy, A., Bradley, A. & Izsvák, Z. Transposon-mediated genome manipulation in vertebrates. *Nat. Methods* **6**, 415–422 (2009).
94. Izsvák, Z., Chuah, M. K. L., VandenDriessche, T. & Ivics, Z. Efficient stable gene transfer into human cells by the Sleeping Beauty transposon vectors. *Methods* **49**, 287–297 (2009).
95. Plasterk, R. H. Molecular mechanisms of transposition and its control. *Cell* **74**, 781–786 (1993).
96. Plasterk, R. H., Izsvák, Z. & Ivics, Z. Resident aliens: the Tc1/mariner superfamily of transposable elements. *Trends Genet* **15**, 326–332 (1999).

97. Vigdal, T. J., Kaufman, C. D., Izsvák, Z., Voytas, D. F. & Ivics, Z. Common physical properties of DNA affecting target site selection of sleeping beauty and other Tc1/mariner transposable elements. *J. Mol. Biol* **323**, 441–452 (2002).
98. Liu, G., Geurts, A. M., Yae, K., Srinivasan, A. R., Fahrenkrug, S. C., Largaespada, D. A., Takeda, J., Horie, K., Olson, W. K. & Hackett, P. B. Target-site preferences of Sleeping Beauty transposons. *J. Mol. Biol* **346**, 161–173 (2005).
99. Geurts, A. M., Hackett, C. S., Bell, J. B., Bergemann, T. L., Collier, L. S., Carlson, C. M., Largaespada, D. A. & Hackett, P. B. Structure-based prediction of insertion-site preferences of transposons into chromosomes. *Nucleic Acids Res.* **34**, 2803–2811 (2006).
100. Yant, S. R., Wu, X., Huang, Y., Garrison, B., Burgess, S. M. & Kay, M. A. High-resolution genome-wide mapping of transposon integration in mammals. *Mol. Cell. Biol* **25**, 2085–2094 (2005).
101. Yant, S. R. & Kay, M. A. Nonhomologous-end-joining factors regulate DNA repair fidelity during Sleeping Beauty element transposition in mammalian cells. *Mol. Cell. Biol.* **23**, 8505–8518 (2003).
102. Liu, G., Aronovich, E. L., Cui, Z., Whitley, C. B. & Hackett, P. B. Excision of Sleeping Beauty transposons: parameters and applications to gene therapy. *J Gene Med* **6**, 574–583 (2004).
103. Izsvák, Z., Stüwe, E. E., Fiedler, D., Katzer, A., Jeggo, P. A. & Ivics, Z. Healing the wounds inflicted by sleeping beauty transposition by double-strand break repair in mammalian somatic cells. *Mol. Cell* **13**, 279–290 (2004).
104. Prof. Perry Hackett. Generic diagram of the sub-domains of Sleeping Beauty transposase. Developmental Biology and Genetics, Department of Genetics, Cell Biology and Development, University of Minnesota, 1445 Gortner Avenue, St. Paul, MN 55108-1095, USA. under Creative Commons 3.0 License. http://en.wikipedia.org/wiki/File:SBTS2.png (19 March 2012).
105. Cui, Z., Geurts, A. M., Liu, G., Kaufman, C. D. & Hackett, P. B. Structure-function analysis of the inverted terminal repeats of the sleeping beauty transposon. *J. Mol. Biol* **318**, 1221–1235 (2002).
106. Izsvák, Z., Ivics, Z. & Plasterk, R. H. Sleeping Beauty, a wide host-range transposon vector for genetic transformation in vertebrates. *J. Mol. Biol* **302**, 93–102 (2000).
107. Davidson, A. E., Gratsch, T. E., Morell, M. H., O'Shea, K. S. & Krull, C. E. Use of the Sleeping Beauty Transposon System for Stable Gene Expression in Mouse Embryonic Stem Cells. *Cold Spring Harbor Protocols* **2009**, pdb.prot5270 (2009).
108. Geurts, A. M., Yang, Y., Clark, K. J., Liu, G., Cui, Z., Dupuy, A. J., Bell, J. B., Largaespada, D. A. & Hackett, P. B. Gene transfer into genomes of human cells by the sleeping beauty transposon system. *Mol. Ther* **8**, 108–117 (2003).
109. Zayed, H., Izsvák, Z., Walisko, O. & Ivics, Z. Development of hyperactive sleeping beauty transposon vectors by mutational analysis. *Mol. Ther* **9**, 292–304 (2004).
110. Yant, S. R., Park, J., Huang, Y., Mikkelsen, J. G. & Kay, M. A. Mutational analysis of the N-terminal DNA-binding domain of sleeping beauty transposase: critical residues for DNA binding and hyperactivity in mammalian cells. *Mol. Cell. Biol* **24**, 9239–9247 (2004).
111. Baus, J., Liu, L., Heggestad, A. D., Sanz, S. & Fletcher, B. S. Hyperactive transposase mutants of the Sleeping Beauty transposon. *Mol. Ther* **12**, 1148–1156 (2005).
112. Grabundzija, I., Irgang, M., Mátés, L., Belay, E., Matrai, J., Gogol-Döring, A., Kawakami, K., Chen, W., Ruiz, P., Chuah, M. K. L., VandenDriessche, T., Izsvák, Z. & Ivics, Z. Comparative analysis of transposable element vector systems in human cells. *Mol. Ther* **18**, 1200–1209 (2010).
113. Dupuy, A. J., Fritz, S. & Largaespada, D. A. Transposition and gene disruption in the male germline of the mouse. *Genesis* **30**, 82–88 (2001).
114. Horie, K., Yusa, K., Yae, K., Odajima, J., Fischer, S. E. J., Keng, V. W., Hayakawa, T., Mizuno, S., Kondoh, G., Ijiri, T., Matsuda, Y., Plasterk, R. H. A. & Takeda, J. Characterization of Sleeping Beauty transposition and its application to genetic screening in mice. *Mol. Cell. Biol* **23**, 9189–9207 (2003).
115. Ivics, Z. & Izsvák, Z. A whole lotta jumpin' goin' on: new transposon tools for vertebrate functional genomics. *Trends Genet* **21**, 8–11 (2005).
116. Keng, V. W., Yae, K., Hayakawa, T., Mizuno, S., Uno, Y., Yusa, K., Kokubu, C., Kinoshita, T., Akagi, K., Jenkins, N. A., Copeland, N. G., Horie, K. & Takeda, J. Region-specific saturation germline mutagenesis in mice using the Sleeping Beauty transposon system. *Nat. Methods* **2**, 763–769 (2005).
117. Carlson, C. M. & Largaespada, D. A. Insertional mutagenesis in mice: new perspectives and tools. *Nat. Rev. Genet* **6**, 568–580 (2005).
118. Jacob, H. J., Lazar, J., Dwinell, M. R., Moreno, C. & Geurts, A. M. Gene targeting in the rat: advances and opportunities. *Trends Genet* **26**, 510–518 (2010).
119. Dupuy, A. J. Transposon-based screens for cancer gene discovery in mouse models. *Semin. Cancer Biol* **20**, 261–268 (2010).
120. Harris, J. W., Strong, D. D., Amoui, M., Baylink, D. J. & Lau, K.-H. W. Construction of a Tc1-like transposon Sleeping Beauty-based gene transfer plasmid vector for generation of stable transgenic mammalian cell clones. *Anal. Biochem.* **310**, 15–26 (2002).

121. Belur, L. R., Frandsen, J. L., Dupuy, A. J., Ingbar, D. H., Largaespada, D. A., Hackett, P. B. & Scott McIvor, R. Gene insertion and long-term expression in lung mediated by the Sleeping Beauty transposon system. *Mol. Ther.* **8**, 501–507 (2003).
122. Ohlfest, J. R., Frandsen, J. L., Fritz, S., Lobitz, P. D., Perkinson, S. G., Clark, K. J., Nelsestuen, G., Key, N. S., McIvor, R. S., Hackett, P. B. & Largaespada, D. A. Phenotypic correction and long-term expression of factor VIII in hemophilic mice by immunotolerization and nonviral gene transfer using the Sleeping Beauty transposon system. *Blood* **105**, 2691–2698 (2005).
123. Huang, X., Wilber, A. C., Bao, L., Tuong, D., Tolar, J., Orchard, P. J., Levine, B. L., June, C. H., McIvor, R. S., Blazar, B. R. & Zhou, X. Stable gene transfer and expression in human primary T cells by the Sleeping Beauty transposon system. *Blood* **107**, 483–491 (2006).
124. Xue, X., Huang, X., Nodland, S. E., Mátés, L., Ma, L., Izsvák, Z., Ivics, Z., LeBien, T. W., McIvor, R. S., Wagner, J. E. & Zhou, X. Stable gene transfer and expression in cord blood-derived CD34+ hematopoietic stem and progenitor cells by a hyperactive Sleeping Beauty transposon system. *Blood* **114**, 1319–1330 (2009).
125. Wilson, M. H., Coates, C. J. & George, A. L. PiggyBac transposon-mediated gene transfer in human cells. *Mol. Ther* **15**, 139–145 (2007).
126. Clark, K. J., Carlson, D. F., Leaver, M. J., Foster, L. K. & Fahrenkrug, S. C. Passport, a native Tc1 transposon from flatfish, is functionally active in vertebrate cells. *Nucleic Acids Res* **37**, 1239–1247 (2009).
127. Emelyanov, A., Gao, Y., Naqvi, N. I. & Parinov, S. Trans-kingdom transposition of the maize dissociation element. *Genetics* **174**, 1095–1104 (2006).
128. Kühholzer, B. & Prather, R. S. Advances in livestock nuclear transfer. *Proc. Soc. Exp. Biol. Med.* **224**, 240–245 (2000).
129. Campbell, K. H. S. A background to nuclear transfer and its applications in agriculture and human therapeutic medicine. *J. Anat.* **200**, 267–275 (2002).
130. Wakayama, T. Development of novel intracytoplasmic sperm injection and somatic cell nuclear transfer techniques for animal reproduction. *Anim. Sci. J.* **82**, 8–16 (2011).
131. Peterson, A. & Cross, D. Mouse chimeras and genetic rescue of mosaic muscle. *Adv. Exp. Med. Biol.* **280**, 173–185 (1990).
132. Ueno, H. & Weissman, I. L. The origin and fate of yolk sac hematopoiesis: application of chimera analyses to developmental studies. *Int. J. Dev. Biol.* **54**, 1019–1031 (2010).
133. Brinster, R. L. The effect of cells transferred into the mouse blastocyst on subsequent development. *J. Exp. Med* **140**, 1049–1056 (1974).
134. Papaioannou, V. E., McBurney, M. W., Gardner, R. L. & Evans, M. J. Fate of teratocarcinoma cells injected into early mouse embryos. *Nature* **258**, 70–73 (1975).
135. Mintz, B. & Illmensee, K. Normal genetically mosaic mice produced from malignant teratocarcinoma cells. *Proc. Natl. Acad. Sci. U.S.A* **72**, 3585–3589 (1975).
136. Melton, D. W. Gene targeting in the mouse. *Bioessays* **16**, 633–638 (1994).
137. Smithies, O., Koralewski, M. A., Song, K. Y. & Kucherlapati, R. S. Homologous recombination with DNA introduced into mammalian cells. *Cold Spring Harb. Symp. Quant. Biol* **49**, 161–170 (1984).
138. Folger, K., Thomas, K. & Capecchi, M. R. Analysis of homologous recombination in cultured mammalian cells. *Cold Spring Harb. Symp. Quant. Biol* **49**, 123–138 (1984).
139. Evans, M. J., Bradley, A., Kuehn, M. R. & Robertson, E. J. The ability of EK cells to form chimeras after selection of clones in G418 and some observations on the integration of retroviral vector proviral DNA into EK cells. *Cold Spring Harb. Symp. Quant. Biol* **50**, 685–689 (1985).
140. Lovell-Badge, R. H., Bygrave, A. E., Bradley, A., Robertson, E., Evans, M. J. & Cheah, K. S. Transformation of embryonic stem cells with the human type-II collagen gene and its expression in chimeric mice. *Cold Spring Harb. Symp. Quant. Biol* **50**, 707–711 (1985).
141. Robertson, E., Bradley, A., Kuehn, M. & Evans, M. Germ-line transmission of genes introduced into cultured pluripotential cells by retroviral vector. *Nature* **323**, 445–448 (1986).
142. Doetschman, T., Gregg, R. G., Maeda, N., Hooper, M. L., Melton, D. W., Thompson, S. & Smithies, O. Targetted correction of a mutant HPRT gene in mouse embryonic stem cells. *Nature* **330**, 576–578 (1987).
143. Smithies, O. Turning pages (Nobel lecture). *Chembiochem* **9**, 1342–1359 (2008).
144. Capecchi, M. R. The making of a scientist II (Nobel Lecture). *Chembiochem* **9**, 1530–1543 (2008).
145. Smithies, O., Gregg, R. G., Boggs, S. S., Koralewski, M. A. & Kucherlapati, R. S. Insertion of DNA sequences into the human chromosomal beta-globin locus by homologous recombination. *Nature* **317**, 230–234 (1985).
146. Campbell, K. H., McWhir, J., Ritchie, W. A. & Wilmut, I. Sheep cloned by nuclear transfer from a cultured cell line. *Nature* **380**, 64–66 (1996).
147. Wilmut, I., Schnieke, A. E., McWhir, J., Kind, A. J. & Campbell, K. H. Viable offspring derived from fetal and adult mammalian cells. *Nature* **385**, 810–813 (1997).
148. Wadman, M. Cloning special: Dolly: a decade on. *Nature* **445**, 800–801 (2007).

149. McCreath, K. J., Howcroft, J., Campbell, K. H., Colman, A., Schnieke, A. E. & Kind, A. J. Production of gene-targeted sheep by nuclear transfer from cultured somatic cells. *Nature* **405**, 1066–1069 (2000).
150. Rogers, C. S., Stoltz, D. A., Meyerholz, D. K., Ostedgaard, L. S., Rokhlina, T., Taft, P. J., Rogan, M. P., Pezzulo, A. A., Karp, P. H., Itani, O. A., Kabel, A. C., Wohlford-Lenane, C. L., Davis, G. J., Hanfland, R. A., Smith, T. L., Samuel, M., Wax, D., Murphy, C. N., Rieke, A., Whitworth, K., Uc, A., Starner, T. D., Brogden, K. A., Shilyansky, J., McCray, P. B., Zabner, J., Prather, R. S. & Welsh, M. J. Disruption of the CFTR gene produces a model of cystic fibrosis in newborn pigs. *Science* **321**, 1837–1841 (2008).
151. Dai, Y., Vaught, T. D., Boone, J., Chen, S.-H., Phelps, C. J., Ball, S., Monahan, J. A., Jobst, P. M., McCreath, K. J., Lamborn, A. E., Cowell-Lucero, J. L., Wells, K. D., Colman, A., Polejaeva, I. A. & Ayares, D. L. Targeted disruption of the alpha1,3-galactosyltransferase gene in cloned pigs. *Nat. Biotechnol* **20**, 251–255 (2002).
152. Lai, L., Kolber-Simonds, D., Park, K.-W., Cheong, H.-T., Greenstein, J. L., Im, G.-S., Samuel, M., Bonk, A., Rieke, A., Day, B. N., Murphy, C. N., Carter, D. B., Hawley, R. J. & Prather, R. S. Production of alpha-1,3-galactosyltransferase knockout pigs by nuclear transfer cloning. *Science* **295**, 1089–1092 (2002).
153. Kues, W. A. & Niemann, H. The contribution of farm animals to human health. *Trends Biotechnol* **22**, 286–294 (2004).
154. Kawarasaki, T., Uchiyama, K., Hirao, A., Azuma, S., Otake, M., Shibata, M., Tsuchiya, S., Enosawa, S., Takeuchi, K., Konno, K., Hakamata, Y., Yoshino, H., Wakai, T., Ookawara, S., Tanaka, H., Kobayashi, E. & Murakami, T. Profile of new green fluorescent protein transgenic Jinhua pigs as an imaging source. *J Biomed Opt* **14**, 54017.
155. Cho, S.-K., Hwang, K.-C., Choi, Y.-J., Bui, H.-T., van Nguyen, T., Park, C., Kim, J.-H. & Kim, J.-H. Production of transgenic pigs harboring the human erythropoietin (hEPO) gene using somatic cell nuclear transfer. *J. Reprod. Dev* **55**, 128–136 (2009).
156. Umeyama, K., Watanabe, M., Saito, H., Kurome, M., Tohi, S., Matsunari, H., Miki, K. & Nagashima, H. Dominant-negative mutant hepatocyte nuclear factor 1alpha induces diabetes in transgenic-cloned pigs. *Transgenic Res* **18**, 697–706 (2009).
157. Hill, J. R., Roussel, A. J., Cibelli, J. B., Edwards, J. F., Hooper, N. L., Miller, M. W., Thompson, J. A., Looney, C. R., Westhusin, M. E., Robl, J. M. & Stice, S. L. Clinical and pathologic features of cloned transgenic calves and fetuses (13 case studies). *Theriogenology* **51**, 1451–1465 (1999).
158. Lanza, R. P., Cibelli, J. B., Blackwell, C., Cristofalo, V. J., Francis, M. K., Baerlocher, G. M., Mak, J., Schertzer, M., Chavez, E. A., Sawyer, N., Lansdorp, P. M. & West, M. D. Extension of cell life-span and telomere length in animals cloned from senescent somatic cells. *Science* **288**, 665–669 (2000).
159. Sousa, P. A. de, King, T., Harkness, L., Young, L. E., Walker, S. K. & Wilmut, I. Evaluation of gestational deficiencies in cloned sheep fetuses and placentae. *Biol. Reprod* **65**, 23–30 (2001).
160. Young, L. E., Sinclair, K. D. & Wilmut, I. Large offspring syndrome in cattle and sheep. *Rev. Reprod* **3**, 155–163 (1998).
161. Dinnyes, A. & Szmolenszky, A. Animal cloning by nuclear transfer: state-of-the-art and future perspectives. *Acta Biochim. Pol.* **52**, 585–588 (2005).
162. Rideout III, W. M. Nuclear Cloning and Epigenetic Reprogramming of the Genome. *Science* **293**, 1093–1098 (2001).
163. Stevens, L. C. & Little, C. C. Spontaneous Testicular Teratomas in an Inbred Strain of Mice. *Proc. Natl. Acad. Sci. U.S.A* **40**, 1080–1087 (1954).
164. Evans, M. Origin of mouse embryonal carcinoma cells and the possibility of their direct isolation into tissue culture. *J. Reprod. Fertil* **62**, 625–631 (1981).
165. Martin, G. R. Isolation of a pluripotent cell line from early mouse embryos cultured in medium conditioned by teratocarcinoma stem cells. *Proc. Natl. Acad. Sci. U.S.A* **78**, 7634–7638 (1981).
166. Evans, M. J. & Kaufman, M. H. Establishment in culture of pluripotential cells from mouse embryos. *Nature* **292**, 154–156 (1981).
167. Bradley, A., Evans, M., Kaufman, M. H. & Robertson, E. Formation of germ-line chimaeras from embryo-derived teratocarcinoma cell lines. *Nature* **309**, 255–256 (1984).
168. Thomson, J. A., Itskovitz-Eldor, J., Shapiro, S. S., Waknitz, M. A., Swiergiel, J. J., Marshall, V. S. & Jones, J. M. Embryonic stem cell lines derived from human blastocysts. *Science* **282**, 1145–1147 (1998).
169. Brook, F. A. & Gardner, R. L. The origin and efficient derivation of embryonic stem cells in the mouse. *Proc. Natl. Acad. Sci. U.S.A* **94**, 5709–5712 (1997).
170. Kanatsu-Shinohara, M., Inoue, K., Lee, J., Yoshimoto, M., Ogonuki, N., Miki, H., Baba, S., Kato, T., Kazuki, Y., Toyokuni, S., Toyoshima, M., Niwa, O., Oshimura, M., Heike, T., Nakahata, T., Ishino, F., Ogura, A. & Shinohara, T. Generation of pluripotent stem cells from neonatal mouse testis. *Cell* **119**, 1001–1012 (2004).
171. Brons, I. G. M., Smithers, L. E., Trotter, M. W. B., Rugg-Gunn, P., Sun, B., Chuva Sousa Lopes, S. M. de, Howlett, S. K., Clarkson, A., Ahrlund-Richter, L., Pedersen, R. A. & Vallier, L. Derivation of pluripotent epiblast stem cells from mammalian embryos. *Nature* **448**, 191–195 (2007).

172. Tesar, P. J., Chenoweth, J. G., Brook, F. A., Davies, T. J., Evans, E. P., Mack, D. L., Gardner, R. L. & McKay, R. D. G. New cell lines from mouse epiblast share defining features with human embryonic stem cells. *Nature* **448**, 196–199 (2007).
173. Leitch, H. G., Blair, K., Mansfield, W., Ayetey, H., Humphreys, P., Nichols, J., Surani, M. A. & Smith, A. Embryonic germ cells from mice and rats exhibit properties consistent with a generic pluripotent ground state. *Development* **137**, 2279–2287 (2010).
174. Kakegawa, R., Teramura, T., Takehara, T., Anzai, M., Mitani, T., Matsumoto, K., Saeki, K., Sagawa, N., Fukuda, K. & Hosoi, Y. Isolation and culture of rabbit primordial germ cells. *J. Reprod. Dev* **54**, 352–357 (2008).
175. Stevens, L. C. The biology of teratomas including evidence indicating their origin form primordial germ cells. *Annee Biol* **1**, 585–610 (1962).
176. Stevens, L. C. Origin of testicular teratomas from primordial germ cells in mice. *J. Natl. Cancer Inst* **38**, 549–552 (1967).
177. Finch, B. W. & Ephrussi, B. Retention of multiple developmental potentialities by cells of a mouse testicular teratocarcinoma during prolonged culture in vitro and their extinction upon hybridization with cells of permanent lines. *Proc. Natl. Acad. Sci. U.S.A* **57**, 615–621 (1967).
178. Martin, G. R. & Evans, M. J. The morphology and growth of a pluripotent teratocarcinoma cell line and its derivatives in tissue culture. *Cell* **2**, 163–172 (1974).
179. Kleinsmith, L. J. & Pierce, G. B. Multipotentiality of single embryonal carcinoma cells. *Cancer Res* **24**, 1544–1551 (1964).
180. Evans, M. Discovering pluripotency: 30 years of mouse embryonic stem cells. *Nat. Rev. Mol. Cell Biol* **12**, 680–686 (2011).
181. Takahashi, K. & Yamanaka, S. Induction of pluripotent stem cells from mouse embryonic and adult fibroblast cultures by defined factors. *Cell* **126**, 663–676 (2006).
182. Aasen, T., Raya, A., Barrero, M. J., Garreta, E., Consiglio, A., Gonzalez, F., Vassena, R., Bilić, J., Pekarik, V., Tiscornia, G., Edel, M., Boué, S. & Izpisúa Belmonte, J. C. Efficient and rapid generation of induced pluripotent stem cells from human keratinocytes. *Nat. Biotechnol* **26**, 1276–1284 (2008).
183. Loh, Y.-H., Agarwal, S., Park, I.-H., Urbach, A., Huo, H., Heffner, G. C., Kim, K., Miller, J. D., Ng, K. & Daley, G. Q. Generation of induced pluripotent stem cells from human blood. *Blood* **113**, 5476–5479 (2009).
184. Kim, J. B., Sebastiano, V., Wu, G., Araúzo-Bravo, M. J., Sasse, P., Gentile, L., Ko, K., Ruau, D., Ehrich, M., van den Boom, D., Meyer, J., Hübner, K., Bernemann, C., Ortmeier, C., Zenke, M., Fleischmann, B. K., Zaehres, H. & Schöler, H. R. Oct4-induced pluripotency in adult neural stem cells. *Cell* **136**, 411–419 (2009).
185. Abujarour, R. & Ding, S. Induced pluripotent stem cells free of exogenous reprogramming factors. *Genome Biol* **10**, 220 (2009).
186. Zhou, H. & Ding, S. Evolution of induced pluripotent stem cell technology. *Curr. Opin. Hematol* **17**, 276–280 (2010).
187. Zhou, H., Wu, S., Joo, J. Y., Zhu, S., Han, D. W., Lin, T., Trauger, S., Bien, G., Yao, S., Zhu, Y., Siuzdak, G., Schöler, H. R., Duan, L. & Ding, S. Generation of induced pluripotent stem cells using recombinant proteins. *Cell Stem Cell* **4**, 381–384 (2009).
188. Vallier, L., Alexander, M. & Pedersen, R. A. Activin/Nodal and FGF pathways cooperate to maintain pluripotency of human embryonic stem cells. *J. Cell. Sci* **118**, 4495–4509 (2005).
189. Greber, B., Lehrach, H. & Adjaye, J. Fibroblast growth factor 2 modulates transforming growth factor beta signaling in mouse embryonic fibroblasts and human ESCs (hESCs) to support hESC self-renewal. *Stem Cells* **25**, 455–464 (2007).
190. Massagué, J. TGF-beta signal transduction. *Annu. Rev. Biochem* **67**, 753–791 (1998).
191. Valdimarsdottir, G. & Mummery, C. Functions of the TGFbeta superfamily in human embryonic stem cells. *APMIS* **113**, 773–789 (2005).
192. Greber, B., Wu, G., Bernemann, C., Joo, J. Y., Han, D. W., Ko, K., Tapia, N., Sabour, D., Sterneckert, J., Tesar, P. & Schöler, H. R. Conserved and divergent roles of FGF signaling in mouse epiblast stem cells and human embryonic stem cells. *Cell Stem Cell* **6**, 215–226 (2010).
193. Alessi, D. R., Andjelkovic, M., Caudwell, B., Cron, P., Morrice, N., Cohen, P. & Hemmings, B. A. Mechanism of activation of protein kinase B by insulin and IGF-1. *EMBO J* **15**, 6541–6551 (1996).
194. Rubin, R., Arzumanyan, A., Soliera, A. R., Ross, B., Peruzzi, F. & Prisco, M. Insulin receptor substrate (IRS)-1 regulates murine embryonic stem (mES) cells self-renewal. *J. Cell. Physiol* **213**, 445–453 (2007).
195. Kielman, M. F., Rindapää, M., Gaspar, C., van Poppel, N., Breukel, C., van Leeuwen, S., Taketo, M. M., Roberts, S., Smits, R. & Fodde, R. Apc modulates embryonic stem-cell differentiation by controlling the dosage of beta-catenin signaling. *Nat. Genet* **32**, 594–605 (2002).
196. Sato, N., Meijer, L., Skaltsounis, L., Greengard, P. & Brivanlou, A. H. Maintenance of pluripotency in human and mouse embryonic stem cells through activation of Wnt signaling by a pharmacological GSK-3-specific inhibitor. *Nat. Med* **10**, 55–63 (2004).

197. Hao, J., Li, T.-G., Qi, X., Zhao, D.-F. & Zhao, G.-Q. WNT/beta-catenin pathway up-regulates Stat3 and converges on LIF to prevent differentiation of mouse embryonic stem cells. *Dev. Biol* **290**, 81–91 (2006).
198. Cole, M. F., Johnstone, S. E., Newman, J. J., Kagey, M. H. & Young, R. A. Tcf3 is an integral component of the core regulatory circuitry of embryonic stem cells. *Genes Dev* **22**, 746–755 (2008).
199. Logan, C. Y. & Nusse, R. The Wnt signaling pathway in development and disease. *Annu. Rev. Cell Dev. Biol* **20**, 781–810 (2004).
200. Willert, K. & Jones, K. A. Wnt signaling: is the party in the nucleus? *Genes Dev* **20**, 1394–1404 (2006).
201. Clevers, H. Wnt/beta-catenin signaling in development and disease. *Cell* **127**, 469–480 (2006).
202. Dravid, G., Ye, Z., Hammond, H., Chen, G., Pyle, A., Donovan, P., Yu, X. & Cheng, L. Defining the role of Wnt/beta-catenin signaling in the survival, proliferation, and self-renewal of human embryonic stem cells. *Stem Cells* **23**, 1489–1501 (2005).
203. Ogawa, K., Nishinakamura, R., Iwamatsu, Y., Shimosato, D. & Niwa, H. Synergistic action of Wnt and LIF in maintaining pluripotency of mouse ES cells. *Biochem. Biophys. Res. Commun* **343**, 159–166 (2006).
204. Takao, Y., Yokota, T. & Koide, H. Beta-catenin up-regulates Nanog expression through interaction with Oct-3/4 in embryonic stem cells. *Biochem. Biophys. Res. Commun* **353**, 699–705 (2007).
205. Vallier, L., Mendjan, S., Brown, S., Chng, Z., Teo, A., Smithers, L. E., Trotter, M. W. B., Cho, C. H.-H., Martinez, A., Rugg-Gunn, P., Brons, G. & Pedersen, R. A. Activin/Nodal signalling maintains pluripotency by controlling Nanog expression. *Development* **136**, 1339–1349 (2009).
206. Chew, J.-L., Loh, Y.-H., Zhang, W., Chen, X., Tam, W.-L., Yeap, L.-S., Li, P., Ang, Y.-S., Lim, B., Robson, P. & Ng, H.-H. Reciprocal transcriptional regulation of Pou5f1 and Sox2 via the Oct4/Sox2 complex in embryonic stem cells. *Mol. Cell. Biol* **25**, 6031–6046 (2005).
207. Kuroda, T., Tada, M., Kubota, H., Kimura, H., Hatano, S.-y., Suemori, H., Nakatsuji, N. & Tada, T. Octamer and Sox elements are required for transcriptional cis regulation of Nanog gene expression. *Mol. Cell. Biol* **25**, 2475–2485 (2005).
208. Okumura-Nakanishi, S., Saito, M., Niwa, H. & Ishikawa, F. Oct-3/4 and Sox2 regulate Oct-3/4 gene in embryonic stem cells. *J. Biol. Chem* **280**, 5307–5317 (2005).
209. Rodda, D. J., Chew, J.-L., Lim, L.-H., Loh, Y.-H., Wang, B., Ng, H.-H. & Robson, P. Transcriptional regulation of nanog by OCT4 and SOX2. *J. Biol. Chem* **280**, 24731–24737 (2005).
210. Chambers, I. & Tomlinson, S. R. The transcriptional foundation of pluripotency. *Development* **136**, 2311–2322 (2009).
211. Wang, J., Rao, S., Chu, J., Shen, X., Levasseur, D. N., Theunissen, T. W. & Orkin, S. H. A protein interaction network for pluripotency of embryonic stem cells. *Nature* **444**, 364–368 (2006).
212. Jiang, J., Chan, Y.-S., Loh, Y.-H., Cai, J., Tong, G.-Q., Lim, C.-A., Robson, P., Zhong, S. & Ng, H.-H. A core Klf circuitry regulates self-renewal of embryonic stem cells. *Nat. Cell Biol* **10**, 353–360 (2008).
213. van den Berg, D. L. C., Snoek, T., Mullin, N. P., Yates, A., Bezstarosti, K., Demmers, J., Chambers, I. & Poot, R. A. An Oct4-centered protein interaction network in embryonic stem cells. *Cell Stem Cell* **6**, 369–381 (2010).
214. Pardo, M., Lang, B., Yu, L., Prosser, H., Bradley, A., Babu, M. M. & Choudhary, J. An expanded Oct4 interaction network: implications for stem cell biology, development, and disease. *Cell Stem Cell* **6**, 382–395 (2010).
215. Wray, J., Kalkan, T. & Smith, A. G. The ground state of pluripotency. *Biochem. Soc. Trans* **38**, 1027–1032 (2010).
216. Pan, G. & Thomson, J. A. Nanog and transcriptional networks in embryonic stem cell pluripotency. *Cell Res.* **17**, 42–49 (2007).
217. Kerr, C. L. & Cheng, L. Multiple, interconvertible states of human pluripotent stem cells. *Cell Stem Cell* **6**, 497–499 (2010).
218. Chenoweth, J. G., McKay, R. D. G. & Tesar, P. J. Epiblast stem cells contribute new insight into pluripotency and gastrulation. *Dev. Growth Differ* **52**, 293–301 (2010).
219. Jacob, F. Mouse teratocarcinoma and embryonic antigens. *Immunol. Rev* **33**, 3–32 (1977).
220. Nichols, J. & Smith, A. Naive and primed pluripotent states. *Cell Stem Cell* **4**, 487–492 (2009).
221. Buecker, C. & Geijsen, N. Different flavors of pluripotency, molecular mechanisms, and practical implications. *Cell Stem Cell* **7**, 559–564 (2010).
222. Hanna, J. H., Saha, K. & Jaenisch, R. Pluripotency and cellular reprogramming: facts, hypotheses, unresolved issues. *Cell* **143**, 508–525 (2010).
223. Pera, M. F. & Tam, P. P. L. Extrinsic regulation of pluripotent stem cells. *Nature* **465**, 713–720 (2010).
224. Tomida, M., Yamamoto-Yamaguchi, Y. & Hozumi, M. Purification of a factor inducing differentiation of mouse myeloid leukemic M1 cells from conditioned medium of mouse fibroblast L929 cells. *J. Biol. Chem* **259**, 10978–10982 (1984).
225. Gearing, D. P., Gough, N. M., King, J. A., Hilton, D. J., Nicola, N. A., Simpson, R. J., Nice, E. C., Kelso, A. & Metcalf, D. Molecular cloning and expression of cDNA encoding a murine myeloid leukaemia inhibitory factor (LIF). *EMBO J* **6**, 3995–4002 (1987).

226. Moreau, J. F., Bonneville, M., Godard, A., Gascan, H., Gruart, V., Moore, M. A. & Soulillou, J. P. Characterization of a factor produced by human T cell clones exhibiting eosinophil-activating and burst-promoting activities. *J. Immunol* **138**, 3844–3849 (1987).
227. Smith, A. G., Heath, J. K., Donaldson, D. D., Wong, G. G., Moreau, J., Stahl, M. & Rogers, D. Inhibition of pluripotential embryonic stem cell differentiation by purified polypeptides. *Nature* **336**, 688–690 (1988).
228. Godard, A., Gascan, H., Naulet, J., Peyrat, M. A., Jacques, Y., Soulillou, J. P. & Moreau, J. F. Biochemical characterization and purification of HILDA, a human lymphokine active on eosinophils and bone marrow cells. *Blood* **71**, 1618–1623 (1988).
229. Moreau, J. F., Donaldson, D. D., Bennett, F., Witek-Giannotti, J., Clark, S. C. & Wong, G. G. Leukaemia inhibitory factor is identical to the myeloid growth factor human interleukin for DA cells. *Nature* **336**, 690–692 (1988).
230. Williams, R. L., Hilton, D. J., Pease, S., Willson, T. A., Stewart, C. L., Gearing, D. P., Wagner, E. F., Metcalf, D., Nicola, N. A. & Gough, N. M. Myeloid leukaemia inhibitory factor maintains the developmental potential of embryonic stem cells. *Nature* **336**, 684–687 (1988).
231. Smith, A. G., Nichols, J., Robertson, M. & Rathjen, P. D. Differentiation inhibiting activity (DIA/LIF) and mouse development. *Dev. Biol* **151**, 339–351 (1992).
232. Niwa, H., Burdon, T., Chambers, I. & Smith, A. Self-renewal of pluripotent embryonic stem cells is mediated via activation of STAT3. *Genes Dev* **12**, 2048–2060 (1998).
233. Matsuda, T., Nakamura, T., Nakao, K., Arai, T., Katsuki, M., Heike, T. & Yokota, T. STAT3 activation is sufficient to maintain an undifferentiated state of mouse embryonic stem cells. *EMBO J* **18**, 4261–4269 (1999).
234. Cartwright, P., McLean, C., Sheppard, A., Rivett, D., Jones, K. & Dalton, S. LIF/STAT3 controls ES cell self-renewal and pluripotency by a Myc-dependent mechanism. *Development* **132**, 885–896 (2005).
235. Hall, J., Guo, G., Wray, J., Eyres, I., Nichols, J., Grotewold, L., Morfopoulou, S., Humphreys, P., Mansfield, W., Walker, R., Tomlinson, S. & Smith, A. Oct4 and LIF/Stat3 additively induce Krüppel factors to sustain embryonic stem cell self-renewal. *Cell Stem Cell* **5**, 597–609 (2009).
236. Heinrich, P. C., Behrmann, I., Müller-Newen, G., Schaper, F. & Graeve, L. Interleukin-6-type cytokine signalling through the gp130/Jak/STAT pathway. *Biochem. J* **334 (Pt 2)**, 297–314 (1998).
237. Levy, D. E. & Darnell, J. E. Stats: transcriptional control and biological impact. *Nat. Rev. Mol. Cell Biol* **3**, 651–662 (2002).
238. Heinrich, P. C., Behrmann, I., Haan, S., Hermanns, H. M., Müller-Newen, G. & Schaper, F. Principles of interleukin (IL)-6-type cytokine signalling and its regulation. *Biochem. J* **374**, 1–20 (2003).
239. Murray, P. J. The JAK-STAT signaling pathway: input and output integration. *J. Immunol* **178**, 2623–2629 (2007).
240. Watanabe, S., Umehara, H., Murayama, K., Okabe, M., Kimura, T. & Nakano, T. Activation of Akt signaling is sufficient to maintain pluripotency in mouse and primate embryonic stem cells. *Oncogene* **25**, 2697–2707 (2006).
241. Burdon, T., Stracey, C., Chambers, I., Nichols, J. & Smith, A. Suppression of SHP-2 and ERK signalling promotes self-renewal of mouse embryonic stem cells. *Dev. Biol* **210**, 30–43 (1999).
242. Kidder, B. L., Yang, J. & Palmer, S. Stat3 and c-Myc genome-wide promoter occupancy in embryonic stem cells. *PLoS ONE* **3**, e3932 (2008).
243. Ying, Q. L., Nichols, J., Chambers, I. & Smith, A. BMP induction of Id proteins suppresses differentiation and sustains embryonic stem cell self-renewal in collaboration with STAT3. *Cell* **115**, 281–292 (2003).
244. Bourillot, P.-Y., Aksoy, I., Schreiber, V., Wianny, F., Schulz, H., Hummel, O., Hubner, N. & Savatier, P. Novel STAT3 target genes exert distinct roles in the inhibition of mesoderm and endoderm differentiation in cooperation with Nanog. *Stem Cells* **27**, 1760–1771 (2009).
245. Hollnagel, A., Oehlmann, V., Heymer, J., Rüther, U. & Nordheim, A. Id genes are direct targets of bone morphogenetic protein induction in embryonic stem cells. *J. Biol. Chem* **274**, 19838–19845 (1999).
246. Qi, X., Li, T.-G., Hao, J., Hu, J., Wang, J., Simmons, H., Miura, S., Mishina, Y. & Zhao, G.-Q. BMP4 supports self-renewal of embryonic stem cells by inhibiting mitogen-activated protein kinase pathways. *Proc. Natl. Acad. Sci. U.S.A* **101**, 6027–6032 (2004).
247. Johansson, B. M. & Wiles, M. V. Evidence for involvement of activin A and bone morphogenetic protein 4 in mammalian mesoderm and hematopoietic development. *Mol. Cell. Biol* **15**, 141–151 (1995).
248. Monteiro, R. M., Sousa Lopes, S. M. C. de, Korchynskyi, O., Dijke, P. ten & Mummery, C. L. Spatio-temporal activation of Smad1 and Smad5 in vivo: monitoring transcriptional activity of Smad proteins. *J. Cell. Sci* **117**, 4653–4663 (2004).
249. Nagy, A., Gócza, E., Diaz, E. M., Prideaux, V. R., Iványi, E., Markkula, M. & Rossant, J. Embryonic stem cells alone are able to support fetal development in the mouse. *Development* **110**, 815–821 (1990).
250. Kuijk, E. W., Chuva Sousa Lopes, S. M. de, Geijsen, N., Macklon, N. & Roelen, B. A. J. The different shades of mammalian pluripotent stem cells. *Hum. Reprod. Update* **17**, 254–271 (2011).

251. Buehr, M., Meek, S., Blair, K., Yang, J., Ure, J., Silva, J., McLay, R., Hall, J., Ying, Q.-L. & Smith, A. Capture of authentic embryonic stem cells from rat blastocysts. *Cell* **135**, 1287–1298 (2008).
252. Li, P., Tong, C., Mehrian-Shai, R., Jia, L., Wu, N., Yan, Y., Maxson, R. E., Schulze, E. N., Song, H., Hsieh, C.-L., Pera, M. F. & Ying, Q.-L. Germline competent embryonic stem cells derived from rat blastocysts. *Cell* **135**, 1299–1310 (2008).
253. Yadav, P. S., Kues, W. A., Herrmann, D., Carnwath, J. W. & Niemann, H. Bovine ICM derived cells express the Oct4 ortholog. *Mol. Reprod. Dev* **72**, 182–190 (2005).
254. Shim, H., Gutiérrez-Adán, A., Chen, L. R., BonDurant, R. H., Behboodi, E. & Anderson, G. B. Isolation of pluripotent stem cells from cultured porcine primordial germ cells. *Biol. Reprod* **57**, 1089–1095 (1997).
255. Cibelli, J. B., Stice, S. L., Golueke, P. J., Kane, J. J., Jerry, J., Blackwell, C., Ponce León, F. A. de & Robl, J. M. Transgenic bovine chimeric offspring produced from somatic cell-derived stem-like cells. *Nat. Biotechnol* **16**, 642–646 (1998).
256. Maximow, A. A. Über experimentelle Erzeugung von Knochenmarks-gewebe. *Anatomischer Anzeiger*, 24–38 (1906).
257. Maximow, A. A. Untersuchungen über Blut und Bindegewebe. III. Die embryonale Histogenese des Knochenmarks der Saugetiere. *Archiv für mikroskopische Anatomie*, 1–113 (1910).
258. Becker, A. J., McCulloch, E. A. & Till, J. E. Cytological demonstration of the clonal nature of spleen colonies derived from transplanted mouse marrow cells. *Nature* **197**, 452–454 (1963).
259. Siminovitch, L., McCulloch, E. A. & Till, J. E. The distribution of colony-forming cells among spleen colonies. *J. Cell. Physiol* **62**, 327–336 (1963).
260. Jackson, W. M., Nesti, L. J. & Tuan, R. S. Potential therapeutic applications of muscle-derived mesenchymal stem and progenitor cells. *Expert Opin Biol Ther* **10**, 505–517 (2010).
261. Zou, Z., Zhang, Y., Hao, L., Wang, F., Liu, D., Su, Y. & Sun, H. More insight into mesenchymal stem cells and their effects inside the body. *Expert Opin Biol Ther* **10**, 215–230 (2010).
262. Nombela-Arrieta, C., Ritz, J. & Silberstein, L. E. The elusive nature and function of mesenchymal stem cells. *Nat Rev Mol Cell Biol* **12**, 126–131 (2011).
263. Viero Nora, C. C., Camassola, M., Bellagamba, B., Ikuta, N., Christoff, A. P., Meirelles, L. d. S., Ayres, R., Margis, R. & Nardi, N. B. Molecular Analysis of the Differentiation Potential of Murine Mesenchymal Stem Cells from Tissues of Endodermal or Mesodermal Origin. *Stem Cells and Development*, 111122101822008 (2011).
264. Friedenstein, A. J., Piatetzky-Shapiro, I. I. & Petrakova, K. V. Osteogenesis in transplants of bone marrow cells. *J Embryol Exp Morphol* **16**, 381–390 (1966).
265. Friedenstein, A. J., Deriglasova, U. F., Kulagina, N. N., Panasuk, A. F., Rudakowa, S. F., Luriá, E. A. & Ruadkow, I. A. Precursors for fibroblasts in different populations of hematopoietic cells as detected by the in vitro colony assay method. *Exp. Hematol* **2**, 83–92 (1974).
266. Khan, M. A. Glycolytic type I white muscle fibres lack butyrylcholinesterase activity at acetylcholinergic end plates. *Cytobios* **26**, 167–173 (1979).
267. Zuk, P. A., Zhu, M., Mizuno, H., Huang, J., Futrell, J. W., Katz, A. J., Benhaim, P., Lorenz, H. P. & Hedrick, M. H. Multilineage cells from human adipose tissue: implications for cell-based therapies. *Tissue Eng* **7**, 211–228 (2001).
268. Zuk, P. A., Zhu, M., Ashjian, P., Ugarte, D. A. de, Huang, J. I., Mizuno, H., Alfonso, Z. C., Fraser, J. K., Benhaim, P. & Hedrick, M. H. Human adipose tissue is a source of multipotent stem cells. *Mol. Biol. Cell* **13**, 4279–4295 (2002).
269. Gimble, J. M., Katz, A. J. & Bunnell, B. A. Adipose-derived stem cells for regenerative medicine. *Circ. Res* **100**, 1249–1260 (2007).
270. Werts, E. D., DeGowin, R. L., Knapp, S. K. & Gibson, D. P. Characterization of marrow stromal (fibroblastoid) cells and their association with erythropoiesis. *Exp. Hematol* **8**, 423–433 (1980).
271. Simmons, P. J. & Torok-Storb, B. Identification of stromal cell precursors in human bone marrow by a novel monoclonal antibody, STRO-1. *Blood* **78**, 55–62 (1991).
272. Quirici, N., Soligo, D., Bossolasco, P., Servida, F., Lumini, C. & Deliliers, G. L. Isolation of bone marrow mesenchymal stem cells by anti-nerve growth factor receptor antibodies. *Exp. Hematol* **30**, 783–791 (2002).
273. Gronthos, S., Zannettino, A. C. W., Hay, S. J., Shi, S., Graves, S. E., Kortesidis, A. & Simmons, P. J. Molecular and cellular characterisation of highly purified stromal stem cells derived from human bone marrow. *J. Cell. Sci* **116**, 1827–1835 (2003).
274. Jones, E. A., English, A., Kinsey, S. E., Straszynski, L., Emery, P., Ponchel, F. & McGonagle, D. Optimization of a flow cytometry-based protocol for detection and phenotypic characterization of multipotent mesenchymal stromal cells from human bone marrow. *Cytometry B Clin Cytom* **70**, 391–399 (2006).

275. Dominici, M., Le Blanc, K., Mueller, I., Slaper-Cortenbach, I., Marini, F., Krause, D., Deans, R., Keating, A., Prockop, D. & Horwitz, E. Minimal criteria for defining multipotent mesenchymal stromal cells. The International Society for Cellular Therapy position statement. *Cytotherapy* **8**, 315–317 (2006).
276. Gang, E. J., Bosnakovski, D., Figueiredo, C. A., Visser, J. W. & Perlingeiro, R. C. R. SSEA-4 identifies mesenchymal stem cells from bone marrow. *Blood* **109**, 1743–1751 (2007).
277. Bühring, H.-J., Battula, V. L., Treml, S., Schewe, B., Kanz, L. & Vogel, W. Novel markers for the prospective isolation of human MSC. *Ann. N. Y. Acad. Sci* **1106**, 262–271 (2007).
278. Battula, V. L., Treml, S., Bareiss, P. M., Gieseke, F., Roelofs, H., Zwart, P. de, Müller, I., Schewe, B., Skutella, T., Fibbe, W. E., Kanz, L. & Bühring, H.-J. Isolation of functionally distinct mesenchymal stem cell subsets using antibodies against CD56, CD271, and mesenchymal stem cell antigen-1. *Haematologica* **94**, 173–184 (2009).
279. Ashton, B. A., Allen, T. D., Howlett, C. R., Eaglesom, C. C., Hattori, A. & Owen, M. Formation of bone and cartilage by marrow stromal cells in diffusion chambers in vivo. *Clin. Orthop. Relat. Res*, 294–307 (1980).
280. Haynesworth, S. E., Goshima, J., Goldberg, V. M. & Caplan, A. I. Characterization of cells with osteogenic potential from human marrow. *Bone* **13**, 81–88 (1992).
281. Pittenger, M. F., Mackay, A. M., Beck, S. C., Jaiswal, R. K., Douglas, R., Mosca, J. D., Moorman, M. A., Simonetti, D. W., Craig, S. & Marshak, D. R. Multilineage potential of adult human mesenchymal stem cells. *Science* **284**, 143–147 (1999).
282. Friedenstein, A. J., Gorskaja, J. F. & Kulagina, N. N. Fibroblast precursors in normal and irradiated mouse hematopoietic organs. *Exp. Hematol* **4**, 267–274 (1976).
283. Piersma, A. H., Brockbank, K. G., Ploemacher, R. E., van Vliet, E., Brakel-van Peer, K. M. & Visser, P. J. Characterization of fibroblastic stromal cells from murine bone marrow. *Exp. Hematol* **13**, 237–243 (1985).
284. Friedenstein, A. J., Chailakhyan, R. K., Latsinik, N. V., Panasyuk, A. F. & Keiliss-Borok, I. V. Stromal cells responsible for transferring the microenvironment of the hemopoietic tissues. Cloning in vitro and retransplantation in vivo. *Transplantation* **17**, 331–340 (1974).
285. Tavassoli, M. & Crosby, W. H. Transplantation of marrow to extramedullary sites. *Science* **161**, 54–56 (1968).
286. Li, F., Wang, X. & Niyibizi, C. Bone marrow stromal cells contribute to bone formation following infusion into femoral cavities of a mouse model of osteogenesis imperfecta. *Bone* **47**, 546–555 (2010).
287. Arthur, A., Rychkov, G., Shi, S., Koblar, S. A. & Gronthos, S. Adult human dental pulp stem cells differentiate toward functionally active neurons under appropriate environmental cues. *Stem Cells* **26**, 1787–1795 (2008).
288. Wakitani, S., Saito, T. & Caplan, A. I. Myogenic cells derived from rat bone marrow mesenchymal stem cells exposed to 5-azacytidine. *Muscle Nerve* **18**, 1417–1426 (1995).
289. Makino, S., Fukuda, K., Miyoshi, S., Konishi, F., Kodama, H., Pan, J., Sano, M., Takahashi, T., Hori, S., Abe, H., Hata, J., Umezawa, A. & Ogawa, S. Cardiomyocytes can be generated from marrow stromal cells in vitro. *J. Clin. Invest* **103**, 697–705 (1999).
290. Phinney, D. G. & Prockop, D. J. Concise review: mesenchymal stem/multipotent stromal cells: the state of transdifferentiation and modes of tissue repair--current views. *Stem Cells* **25**, 2896–2902 (2007).
291. Oswald, J., Boxberger, S., Jørgensen, B., Feldmann, S., Ehninger, G., Bornhäuser, M. & Werner, C. Mesenchymal stem cells can be differentiated into endothelial cells in vitro. *Stem Cells* **22**, 377–384 (2004).
292. Sato, Y., Araki, H., Kato, J., Nakamura, K., Kawano, Y., Kobune, M., Sato, T., Miyanishi, K., Takayama, T., Takahashi, M., Takimoto, R., Iyama, S., Matsunaga, T., Ohtani, S., Matsuura, A., Hamada, H. & Niitsu, Y. Human mesenchymal stem cells xenografted directly to rat liver are differentiated into human hepatocytes without fusion. *Blood* **106**, 756–763 (2005).
293. Snykers, S., Kock, J. de, Rogiers, V. & Vanhaecke, T. In vitro differentiation of embryonic and adult stem cells into hepatocytes: state of the art. *Stem Cells* **27**, 577–605 (2009).
294. Ju, S., Teng, G.-J., Lu, H., Jin, J., Zhang, Y., Zhang, A. & Ni, Y. In vivo differentiation of magnetically labeled mesenchymal stem cells into hepatocytes for cell therapy to repair damaged liver. *Invest Radiol* **45**, 625–633 (2010).
295. Sun, Y., Chen, L., Hou, X.-g., Hou, W.-k., Dong, J.-j., Sun, L., Tang, K.-x., Wang, B., Song, J., Li, H. & Wang, K.-x. Differentiation of bone marrow-derived mesenchymal stem cells from diabetic patients into insulin-producing cells in vitro. *Chin. Med. J* **120**, 771–776 (2007).
296. Davani, B., Ariely, S., Ikonomou, L., Oron, Y. & Gershengorn, M. C. Human islet-derived precursor cells can cycle between epithelial clusters and mesenchymal phenotypes. *J. Cell. Mol. Med* **13**, 2570–2581 (2009).
297. Hoogduijn, M. J., Popp, F., Verbeek, R., Masoodi, M., Nicolaou, A., Baan, C. & Dahlke, M.-H. The immunomodulatory properties of mesenchymal stem cells and their use for immunotherapy. *Int. Immunopharmacol* **10**, 1496–1500 (2010).

298. Chen, P.-M., Yen, M.-L., Liu, K.-J., Sytwu, H.-K. & Yen, B.-L. Immunomodulatory properties of human adult and fetal multipotent mesenchymal stem cells. *J. Biomed. Sci* **18**, 49 (2011).
299. Raaijmakers, M. H. G. P., Mukherjee, S., Guo, S., Zhang, S., Kobayashi, T., Schoonmaker, J. A., Ebert, B. L., Al-Shahrour, F., Hasserjian, R. P., Scadden, E. O., Aung, Z., Matza, M., Merkenschlager, M., Lin, C., Rommens, J. M. & Scadden, D. T. Bone progenitor dysfunction induces myelodysplasia and secondary leukaemia. *Nature* **464**, 852–857 (2010).
300. Caplan, A. I. The mesengenic process. *Clin Plast Surg* **21**, 429–435 (1994).
301. Prockop, D. J. Marrow stromal cells as stem cells for nonhematopoietic tissues. *Science* **276**, 71–74 (1997).
302. Zhang, J., Niu, C., Ye, L., Huang, H., He, X., Tong, W.-G., Ross, J., Haug, J., Johnson, T., Feng, J. Q., Harris, S., Wiedemann, L. M., Mishina, Y. & Li, L. Identification of the haematopoietic stem cell niche and control of the niche size. *Nature* **425**, 836–841 (2003).
303. Sacchetti, B., Funari, A., Michienzi, S., Di Cesare, S., Piersanti, S., Saggio, I., Tagliafico, E., Ferrari, S., Robey, P. G., Riminucci, M. & Bianco, P. Self-renewing osteoprogenitors in bone marrow sinusoids can organize a hematopoietic microenvironment. *Cell* **131**, 324–336 (2007).
304. Méndez-Ferrer, S., Michurina, T. V., Ferraro, F., Mazloom, A. R., Macarthur, B. D., Lira, S. A., Scadden, D. T., Ma'ayan, A., Enikolopov, G. N. & Frenette, P. S. Mesenchymal and haematopoietic stem cells form a unique bone marrow niche. *Nature* **466**, 829–834 (2010).
305. Caplan, A. I. Mesenchymal stem cells. *J. Orthop. Res* **9**, 641–650 (1991).
306. Kopen, G. C., Prockop, D. J. & Phinney, D. G. Marrow stromal cells migrate throughout forebrain and cerebellum, and they differentiate into astrocytes after injection into neonatal mouse brains. *Proc. Natl. Acad. Sci. U.S.A* **96**, 10711–10716 (1999).
307. Woodbury, D., Schwarz, E. J., Prockop, D. J. & Black, I. B. Adult rat and human bone marrow stromal cells differentiate into neurons. *J. Neurosci. Res* **61**, 364–370 (2000).
308. Hermann, A., Gastl, R., Liebau, S., Popa, M. O., Fiedler, J., Boehm, B. O., Maisel, M., Lerche, H., Schwarz, J., Brenner, R. & Storch, A. Efficient generation of neural stem cell-like cells from adult human bone marrow stromal cells. *J. Cell. Sci* **117**, 4411–4422 (2004).
309. Toma, C., Pittenger, M. F., Cahill, K. S., Byrne, B. J. & Kessler, P. D. Human mesenchymal stem cells differentiate to a cardiomyocyte phenotype in the adult murine heart. *Circulation* **105**, 93–98 (2002).
310. Xu, W., Zhang, X., Qian, H., Zhu, W., Sun, X., Hu, J., Zhou, H. & Chen, Y. Mesenchymal stem cells from adult human bone marrow differentiate into a cardiomyocyte phenotype in vitro. *Exp. Biol. Med. (Maywood)* **229**, 623–631 (2004).
311. Maltman, D. J., Hardy, S. A. & Przyborski, S. A. Role of mesenchymal stem cells in neurogenesis and nervous system repair. *Neurochem. Int* **59**, 347–356 (2011).
312. Vassalli, G. & Moccetti, T. Cardiac repair with allogeneic mesenchymal stem cells after myocardial infarction. *Swiss Med Wkly* **141**, w13209 (2011).
313. Zannettino, A. C. W., Paton, S., Arthur, A., Khor, F., Itescu, S., Gimble, J. M. & Gronthos, S. Multipotential human adipose-derived stromal stem cells exhibit a perivascular phenotype in vitro and in vivo. *J. Cell. Physiol* **214**, 413–421 (2008).
314. Traktuev, D. O., Merfeld-Clauss, S., Li, J., Kolonin, M., Arap, W., Pasqualini, R., Johnstone, B. H. & March, K. L. A population of multipotent CD34-positive adipose stromal cells share pericyte and mesenchymal surface markers, reside in a periendothelial location, and stabilize endothelial networks. *Circ. Res* **102**, 77–85 (2008).
315. Lin, G., Garcia, M., Ning, H., Banie, L., Guo, Y.-L., Lue, T. F. & Lin, C.-S. Defining stem and progenitor cells within adipose tissue. *Stem Cells Dev* **17**, 1053–1063 (2008).
316. Zimmerlin, L., Donnenberg, V. S., Pfeifer, M. E., Meyer, E. M., Péault, B., Rubin, J. P. & Donnenberg, A. D. Stromal vascular progenitors in adult human adipose tissue. *Cytometry A* **77**, 22–30 (2010).
317. Baer, P. C. Adipose-derived stem cells and their potential to differentiate into the epithelial lineage. *Stem Cells Dev* **20**, 1805–1816 (2011).
318. Ugarte, D. A. de, Morizono, K., Elbarbary, A., Alfonso, Z., Zuk, P. A., Zhu, M., Dragoo, J. L., Ashjian, P., Thomas, B., Benhaim, P., Chen, I., Fraser, J. & Hedrick, M. H. Comparison of multi-lineage cells from human adipose tissue and bone marrow. *Cells Tissues Organs (Print)* **174**, 101–109 (2003).
319. Caplan, A. I. Adult mesenchymal stem cells for tissue engineering versus regenerative medicine. *J. Cell. Physiol* **213**, 341–347 (2007).
320. Aust, L., Devlin, B., Foster, S. J., Halvorsen, Y. D. C., Hicok, K., Du Laney, T., Sen, A., Willingmyre, G. D. & Gimble, J. M. Yield of human adipose-derived adult stem cells from liposuction aspirates. *Cytotherapy* **6**, 7–14 (2004).
321. Oedayrajsingh-Varma, M. J., van Ham, S. M., Knippenberg, M., Helder, M. N., Klein-Nulend, J., Schouten, T. E., Ritt, M. J. P. F. & van Milligen, F. J. Adipose tissue-derived mesenchymal stem cell yield and growth characteristics are affected by the tissue-harvesting procedure. *Cytotherapy* **8**, 166–177 (2006).
322. Fraser, J. K., Zhu, M., Wulur, I. & Alfonso, Z. Adipose-derived stem cells. *Methods Mol. Biol* **449**, 59–67 (2008).

323. The Lancet. The diabetes pandemic. *The Lancet* **378**, 99 (2011).
324. Danaei, G., Finucane, M. M., Lu, Y., Singh, G. M., Cowan, M. J., Paciorek, C. J., Lin, J. K., Farzadfar, F., Khang, Y.-H., Stevens, G. A., Rao, M., Ali, M. K., Riley, L. M., Robinson, C. A. & Ezzati, M. National, regional, and global trends in fasting plasma glucose and diabetes prevalence since 1980: systematic analysis of health examination surveys and epidemiological studies with 370 country-years and 2·7 million participants. *The Lancet* **378**, 31–40 (2011).
325. Birch, L. L., Parker, L. & Burns, A. C. *Early childhood obesity prevention policies* (National Academies Press, Washington, D.C, 2011).
326. Ogden, C. L., Carroll, M. D., Kit, B. K. & Flegal, K. M. Prevalence of Obesity and Trends in Body Mass Index Among US Children and Adolescents, 1999-2010. *JAMA: The Journal of the American Medical Association* **307**, 483–490 (2012).
327. Flegal, K. M., Carroll, M. D., Kit, B. K. & Ogden, C. L. Prevalence of Obesity and Trends in the Distribution of Body Mass Index Among US Adults, 1999-2010. *JAMA: The Journal of the American Medical Association* **307**, 491–497 (2012).
328. Rubin, R. R. & Peyrot, M. Quality of life and diabetes. *Diabetes Metab. Res. Rev.* **15**, 205–218 (1999).
329. American Diabetes Association. Diagnosis and classification of diabetes mellitus. *Diabetes Care* **27 Suppl 1**, S5-S10 (2004).
330. Aronson, D. Hyperglycemia and the pathobiology of diabetic complications. *Adv Cardiol* **45**, 1–16 (2008).
331. Laakso, M. Hyperglycemia and cardiovascular disease in type 2 diabetes. *Diabetes* **48**, 937–942 (1999).
332. Aronson, D. & Rayfield, E. J. How hyperglycemia promotes atherosclerosis: molecular mechanisms. *Cardiovasc Diabetol* **1**, 1 (2002).
333. Mokdad, A. H., Ford, E. S., Bowman, B. A., Dietz, W. H., Vinicor, F., Bales, V. S. & Marks, J. S. Prevalence of obesity, diabetes, and obesity-related health risk factors, 2001. *JAMA* **289**, 76–79 (2003).
334. Reaven, G. M. The insulin resistance syndrome: definition and dietary approaches to treatment. *Annu. Rev. Nutr* **25**, 391–406 (2005).
335. Das, U. N. Obesity: genes, brain, gut, and environment. *Nutrition* **26**, 459–473 (2010).
336. Facchini, F. S., Hua, N., Abbasi, F. & Reaven, G. M. Insulin resistance as a predictor of age-related diseases. *J. Clin. Endocrinol. Metab.* **86**, 3574–3578 (2001).
337. Stumvoll, M., Goldstein, B. J. & van Haeften, T. W. Type 2 diabetes: principles of pathogenesis and therapy. *Lancet* **365**, 1333–1346 (2005).
338. Hamilton, M. T., Hamilton, D. G. & Zderic, T. W. Role of low energy expenditure and sitting in obesity, metabolic syndrome, type 2 diabetes, and cardiovascular disease. *Diabetes* **56**, 2655–2667 (2007).
339. Boitard, C., Efendic, S., Ferrannini, E., Henquin, J.-C., Steiner, D. F. & Cerasi, E. A tale of two cousins: type 1 and type 2 diabetes. *Diabetes* **54 Suppl 2**, S1-3 (2005).
340. Molven, A., Ringdal, M., Nordbø, A. M., Raeder, H., Støy, J., Lipkind, G. M., Steiner, D. F., Philipson, L. H., Bergmann, I., Aarskog, D., Undlien, D. E., Joner, G., Søvik, O., Bell, G. I. & Njølstad, P. R. Mutations in the insulin gene can cause MODY and autoantibody-negative type 1 diabetes. *Diabetes* **57**, 1131–1135 (2008).
341. Weiss, M. A. Proinsulin and the genetics of diabetes mellitus. *J. Biol. Chem.* **284**, 19159–19163 (2009).
342. Eberhard, D., Kragl, M. & Lammert, E. 'Giving and taking': endothelial and beta-cells in the islets of Langerhans. *Trends Endocrinol. Metab* **21**, 457–463 (2010).
343. Pugliese, A., Zeller, M., Fernandez, A., Zalcberg, L. J., Bartlett, R. J., Ricordi, C., Pietropaolo, M., Eisenbarth, G. S., Bennett, S. T. & Patel, D. D. The insulin gene is transcribed in the human thymus and transcription levels correlated with allelic variation at the INS VNTR-IDDM2 susceptibility locus for type 1 diabetes. *Nat. Genet.* **15**, 293–297 (1997).
344. Vafiadis, P., Bennett, S. T., Todd, J. A., Nadeau, J., Grabs, R., Goodyer, C. G., Wickramasinghe, S., Colle, E. & Polychronakos, C. Insulin expression in human thymus is modulated by INS VNTR alleles at the IDDM2 locus. *Nat. Genet.* **15**, 289–292 (1997).
345. Devaskar, S. U., Giddings, S. J., Rajakumar, P. A., Carnaghi, L. R., Menon, R. K. & Zahm, D. S. Insulin gene expression and insulin synthesis in mammalian neuronal cells. *J. Biol. Chem.* **269**, 8445–8454 (1994).
346. Cunha, D. A., Carneiro, E. M., Alves, M. C. de, Jorge, A. G., Sousa, S. M. de, Boschero, A. C., Saad, M. J. A., Velloso, L. A. & Rocha, E. M. Insulin secretion by rat lacrimal glands: effects of systemic and local variables. *Am. J. Physiol. Endocrinol. Metab.* **289**, E768-75 (2005).
347. Vallejo, G., Mead, P. M., Gaynor, D. H., Devlin, J. T. & Robbins, D. C. Characterization of immunoreactive insulin in human saliva: evidence against production in situ. *Diabetologia* **27**, 437–440 (1984).
348. Kojima, H., Fujimiya, M., Matsumura, K., Nakahara, T., Hara, M. & Chan, L. Extrapancreatic insulin-producing cells in multiple organs in diabetes. *Proc. Natl. Acad. Sci. U.S.A.* **101**, 2458–2463 (2004).
349. Redmon, J. B., Towle, H. C. & Robertson, R. P. Regulation of human insulin gene transcription by glucose, epinephrine, and somatostatin. *Diabetes* **43**, 546–551 (1994).

350. Regazzi, R., Verchere, C. B., Halban, P. A. & Polonsky, K. S. Insulin production: from gene to granule. *Diabetologia* **40 Suppl 3**, B33-8 (1997).
351. Ashcroft, S. J. & Ashcroft, F. M. The sulfonylurea receptor. *Biochim. Biophys. Acta* **1175**, 45–59 (1992).
352. Henquin, J. C., Gembal, M., Detimary, P., Gao, Z. Y., Warnotte, C. & Gilon, P. Multisite control of insulin release by glucose. *Diabete Metab* **20**, 132–137 (1994).
353. Newgard, C. B. & McGarry, J. D. Metabolic coupling factors in pancreatic beta-cell signal transduction. *Annu. Rev. Biochem* **64**, 689–719 (1995).
354. Prentki, M., Tornheim, K. & Corkey, B. E. Signal transduction mechanisms in nutrient-induced insulin secretion. *Diabetologia* **40 Suppl 2**, S32-41 (1997).
355. Matschinsky, F. M., Glaser, B. & Magnuson, M. A. Pancreatic beta-cell glucokinase: closing the gap between theoretical concepts and experimental realities. *Diabetes* **47**, 307–315 (1998).
356. Gepts, W. Pathologic anatomy of the pancreas in juvenile diabetes mellitus. *Diabetes* **14**, 619–633 (1965).
357. Notkins, A. L. & Lernmark, A. Autoimmune type 1 diabetes: resolved and unresolved issues. *J. Clin. Invest.* **108**, 1247–1252 (2001).
358. Petrone, A., Galgani, A., Spoletini, M., Alemanno, I., Di Cola, S., Bassotti, G., Picardi, A., Manfrini, S., Osborn, J., Pozzilli, P. & Buzzetti, R. Residual insulin secretion at diagnosis of type 1 diabetes is independently associated with both, age of onset and HLA genotype. *Diabetes Metab. Res. Rev.* **21**, 271–275 (2005).
359. Saltiel, A. R. & Kahn, C. R. Insulin signalling and the regulation of glucose and lipid metabolism. *Nature* **414**, 799–806 (2001).
360. Xu, B., Hu, S.-Q., Chu, Y.-C., Huang, K., Nakagawa, S. H., Whittaker, J., Katsoyannis, P. G. & Weiss, M. A. Diabetes-associated mutations in insulin: consecutive residues in the B chain contact distinct domains of the insulin receptor. *Biochemistry* **43**, 8356–8372 (2004).
361. Schenk, S., Saberi, M. & Olefsky, J. M. Insulin sensitivity: modulation by nutrients and inflammation. *J. Clin. Invest* **118**, 2992–3002 (2008).
362. Kaiser, N., Leibowitz, G. & Nesher, R. Glucotoxicity and beta-cell failure in type 2 diabetes mellitus. *J. Pediatr. Endocrinol. Metab* **16**, 5–22 (2003).
363. Brownlee, M. The pathobiology of diabetic complications: a unifying mechanism. *Diabetes* **54**, 1615–1625 (2005).
364. Houstis, N., Rosen, E. D. & Lander, E. S. Reactive oxygen species have a causal role in multiple forms of insulin resistance. *Nature* **440**, 944–948 (2006).
365. Robertson, R. P. Chronic oxidative stress as a central mechanism for glucose toxicity in pancreatic islet beta cells in diabetes. *J. Biol. Chem* **279**, 42351–42354 (2004).
366. Martínez, J. A. Mitochondrial oxidative stress and inflammation: an slalom to obesity and insulin resistance. *J. Physiol. Biochem.* **62**, 303–306 (2006).
367. Luca, C. de & Olefsky, J. M. Inflammation and insulin resistance. *FEBS Lett.* **582**, 97–105 (2008).
368. Tiedge, M., Lortz, S., Drinkgern, J. & Lenzen, S. Relation between antioxidant enzyme gene expression and antioxidative defense status of insulin-producing cells. *Diabetes* **46**, 1733–1742 (1997).
369. Parillo, M. & Riccardi, G. Diet composition and the risk of type 2 diabetes: epidemiological and clinical evidence. *Br. J. Nutr* **92**, 7–19 (2004).
370. Briaud, I., Harmon, J. S., Kelpe, C. L., Segu, V. B. & Poitout, V. Lipotoxicity of the pancreatic beta-cell is associated with glucose-dependent esterification of fatty acids into neutral lipids. *Diabetes* **50**, 315–321 (2001).
371. Unger, R. H. Lipotoxic diseases. *Annu. Rev. Med.* **53**, 319–336 (2002).
372. Shoelson, S. E., Herrero, L. & Naaz, A. Obesity, inflammation, and insulin resistance. *Gastroenterology* **132**, 2169–2180 (2007).
373. Cnop, M. Fatty acids and glucolipotoxicity in the pathogenesis of Type 2 diabetes. *Biochem. Soc. Trans.* **36**, 348–352 (2008).
374. Milagro, F. I., Campión, J. & Martínez, J. A. Weight gain induced by high-fat feeding involves increased liver oxidative stress. *Obesity (Silver Spring)* **14**, 1118–1123 (2006).
375. Sikharulidze, M. D., Dzhanashiia, N. G., Sanikidze, T. V. & Gogeshvili, S. G. [The role of oxidative stress in pathogenesis of obesity]. *Georgian Med News*, 123–126 (2006).
376. Dahlman, I., Forsgren, M., Sjögren, A., Nordström, E. A., Kaaman, M., Näslund, E., Attersand, A. & Arner, P. Downregulation of electron transport chain genes in visceral adipose tissue in type 2 diabetes independent of obesity and possibly involving tumor necrosis factor-alpha. *Diabetes* **55**, 1792–1799 (2006).
377. Liu, K., Paterson, A. J., Chin, E. & Kudlow, J. E. Glucose stimulates protein modification by O-linked GlcNAc in pancreatic beta cells: linkage of O-linked GlcNAc to beta cell death. *Proc. Natl. Acad. Sci. U.S.A.* **97**, 2820–2825 (2000).

378. Biarnés, M., Montolio, M., Nacher, V., Raurell, M., Soler, J. & Montanya, E. Beta-cell death and mass in syngeneically transplanted islets exposed to short- and long-term hyperglycemia. *Diabetes* **51**, 66–72 (2002).
379. Hu, F. B., Stampfer, M. J., Solomon, C. G., Liu, S., Willett, W. C., Speizer, F. E., Nathan, D. M. & Manson, J. E. The impact of diabetes mellitus on mortality from all causes and coronary heart disease in women: 20 years of follow-up. *Arch. Intern. Med.* **161**, 1717–1723 (2001).
380. Franco, O. H., Steyerberg, E. W., Hu, F. B., Mackenbach, J. & Nusselder, W. Associations of diabetes mellitus with total life expectancy and life expectancy with and without cardiovascular disease. *Arch. Intern. Med.* **167**, 1145–1151 (2007).
381. Shapiro, A. M., Lakey, J. R., Ryan, E. A., Korbutt, G. S., Toth, E., Warnock, G. L., Kneteman, N. M. & Rajotte, R. V. Islet transplantation in seven patients with type 1 diabetes mellitus using a glucocorticoid-free immunosuppressive regimen. *N. Engl. J. Med.* **343**, 230–238 (2000).
382. Mohanakumar, T., Narayanan, K., Desai, N., Ramachandran, S., Shenoy, S., Jendrisak, M., Susskind, B. M., Olack, B., Benshoff, N., Phelan, D. L., Brennan, D. C., Fernandez, L. A., Odorico, J. S. & Polonsky, K. S. A significant role for histocompatibility in human islet transplantation. *Transplantation* **82**, 180–187 (2006).
383. Cardani, R., Pileggi, A., Ricordi, C., Gomez, C., Baidal, D. A., Ponte, G. G., Mineo, D., Faradji, R. N., Froud, T., Ciancio, G., Esquenazi, V., Burke, G. W., Selvaggi, G., Miller, J., Kenyon, N. S. & Alejandro, R. Allosensitization of islet allograft recipients. *Transplantation* **84**, 1413–1427 (2007).
384. Campbell, P. M., Senior, P. A., Salam, A., Labranche, K., Bigam, D. L., Kneteman, N. M., Imes, S., Halpin, A., Ryan, E. A. & Shapiro, A. M. J. High risk of sensitization after failed islet transplantation. *Am. J. Transplant.* **7**, 2311–2317 (2007).
385. Ryan, E. A., Paty, B. W., Senior, P. A., Bigam, D., Alfadhli, E., Kneteman, N. M., Lakey, J. R. T. & Shapiro, A. M. J. Five-year follow-up after clinical islet transplantation. *Diabetes* **54**, 2060–2069 (2005).
386. Bosi, E., Braghi, S., Maffi, P., Scirpoli, M., Bertuzzi, F., Pozza, G., Secchi, A. & Bonifacio, E. Autoantibody response to islet transplantation in type 1 diabetes. *Diabetes* **50**, 2464–2471 (2001).
387. Huurman, V. A. L., Hilbrands, R., Pinkse, G. G. M., Gillard, P., Duinkerken, G., van de Linde, P., van der Meer-Prins, P. M. W., Versteeg-van der Voort Maarschalk, M. F. J., Verbeeck, K., Alizadeh, B. Z., Mathieu, C., Gorus, F. K., Roelen, D. L., Claas, F. H. J., Keymeulen, B., Pipeleers, D. G. & Roep, B. O. Cellular islet autoimmunity associates with clinical outcome of islet cell transplantation. *PLoS ONE* **3**, e2435 (2008).
388. Ryan, E. A., Lakey, J. R. T., Paty, B. W., Imes, S., Korbutt, G. S., Kneteman, N. M., Bigam, D., Rajotte, R. V. & Shapiro, A. M. J. Successful islet transplantation: continued insulin reserve provides long-term glycemic control. *Diabetes* **51**, 2148–2157 (2002).
389. Bugger, H. & Abel, E. D. Rodent models of diabetic cardiomyopathy. *Dis Model Mech* **2**, 454–466 (2009).
390. Yoshioka, M., Kayo, T., Ikeda, T. & Koizumi, A. A novel locus, Mody4, distal to D7Mit189 on chromosome 7 determines early-onset NIDDM in nonobese C57BL/6 (Akita) mutant mice. *Diabetes* **46**, 887–894 (1997).
391. Wang, J., Takeuchi, T., Tanaka, S., Kubo, S. K., Kayo, T., Lu, D., Takata, K., Koizumi, A. & Izumi, T. A mutation in the insulin 2 gene induces diabetes with severe pancreatic beta-cell dysfunction in the Mody mouse. *J. Clin. Invest.* **103**, 27–37 (1999).
392. Støy, J., Edghill, E. L., Flanagan, S. E., Ye, H., Paz, V. P., Pluzhnikov, A., Below, J. E., Hayes, M. G., Cox, N. J., Lipkind, G. M., Lipton, R. B., Greeley, S. A. W., Patch, A.-M., Ellard, S., Steiner, D. F., Hattersley, A. T., Philipson, L. H. & Bell, G. I. Insulin gene mutations as a cause of permanent neonatal diabetes. *Proc. Natl. Acad. Sci. U.S.A.* **104**, 15040–15044 (2007).
393. Hodish, I., Liu, M., Rajpal, G., Larkin, D., Holz, R. W., Adams, A., Liu, L. & Arvan, P. Misfolded proinsulin affects bystander proinsulin in neonatal diabetes. *J. Biol. Chem.* **285**, 685–694 (2010).
394. Izumi, T., Yokota-Hashimoto, H., Zhao, S., Wang, J., Halban, P. A. & Takeuchi, T. Dominant negative pathogenesis by mutant proinsulin in the Akita diabetic mouse. *Diabetes* **52**, 409–416 (2003).
395. Allen, J. R., Nguyen, L. X., Sargent, K. E. G., Lipson, K. L., Hackett, A. & Urano, F. High ER stress in beta-cells stimulates intracellular degradation of misfolded insulin. *Biochem. Biophys. Res. Commun.* **324**, 166–170 (2004).
396. Lipson, K. L., Fonseca, S. G., Ishigaki, S., Nguyen, L. X., Foss, E., Bortell, R., Rossini, A. A. & Urano, F. Regulation of insulin biosynthesis in pancreatic beta cells by an endoplasmic reticulum-resident protein kinase IRE1. *Cell Metab.* **4**, 245–254 (2006).
397. Liu, M., Hodish, I., Rhodes, C. J. & Arvan, P. Proinsulin maturation, misfolding, and proteotoxicity. *Proc. Natl. Acad. Sci. U.S.A.* **104**, 15841–15846 (2007).
398. Kopito, R. R. ER quality control: the cytoplasmic connection. *Cell* **88**, 427–430 (1997).
399. Kaufman, R. J. Stress signaling from the lumen of the endoplasmic reticulum: coordination of gene transcriptional and translational controls. *Genes Dev.* **13**, 1211–1233 (1999).

400. Zhang, K. & Kaufman, R. J. Protein folding in the endoplasmic reticulum and the unfolded protein response. *Handb Exp Pharmacol*, 69–91 (2006).
401. Schröder, M. The unfolded protein response. *Mol. Biotechnol.* **34**, 279–290 (2006).
402. Ron, D. Proteotoxicity in the endoplasmic reticulum: lessons from the Akita diabetic mouse. *J. Clin. Invest.* **109**, 443–445 (2002).
403. Oyadomari, S., Araki, E. & Mori, M. Endoplasmic reticulum stress-mediated apoptosis in pancreatic beta-cells. *Apoptosis* **7**, 335–345 (2002).
404. Araki, E., Oyadomari, S. & Mori, M. Endoplasmic reticulum stress and diabetes mellitus. *Intern. Med.* **42**, 7–14 (2003).
405. Shen, X., Zhang, K. & Kaufman, R. J. The unfolded protein response--a stress signaling pathway of the endoplasmic reticulum. *J. Chem. Neuroanat.* **28**, 79–92 (2004).
406. Schröder, M. & Kaufman, R. J. The mammalian unfolded protein response. *Annu. Rev. Biochem.* **74**, 739–789 (2005).
407. Zhang, K. & Kaufman, R. J. The unfolded protein response: a stress signaling pathway critical for health and disease. *Neurology* **66**, S102-9 (2006).
408. Wu, J. & Kaufman, R. J. From acute ER stress to physiological roles of the Unfolded Protein Response. *Cell Death Differ.* **13**, 374–384 (2006).
409. Malhotra, J. D. & Kaufman, R. J. The endoplasmic reticulum and the unfolded protein response. *Semin. Cell Dev. Biol.* **18**, 716–731 (2007).
410. Fonseca, S. G., Burcin, M., Gromada, J. & Urano, F. Endoplasmic reticulum stress in beta-cells and development of diabetes. *Curr Opin Pharmacol* **9**, 763–770 (2009).
411. Rees, D. A. & Alcolado, J. C. Animal models of diabetes mellitus. *Diabet. Med.* **22**, 359–370 (2005).
412. Wang, J., Wan, R., Mo, Y., Zhang, Q., Sherwood, L. C. & Chien, S. Creating a Long-Term Diabetic Rabbit Model. *Experimental Diabetes Research* **2010**, 1–10 (2010).
413. Hoefnagel, D., Andrew, E. D., Mireault, N. G. & Berndt, W. O. Hereditary choreoathetosis, self-mutilation and hyperuricemia in young males. *N. Engl. J. Med* **273**, 130–135 (1965).
414. Catel, W. & Schmidt, J. Über familiäre gichtische Diathese in Verbindung mit zerebralen und renalen Symptomen bei einem Kleinkind. [On familial gouty diathesis associated with cerebral and renal symptoms in a small child]. *Dtsch. Med. Wochenschr* **84**, 2145–2147 (1959).
415. Riley, I. D. Gout and Cerebral Palsy in a Three-year-old Boy. *Arch. Dis. Child.* **35**, 293–295 (1960).
416. Lesch, M. & Nyhan, W. L. A familial disorder of uric acid metabolism and central nervous system function. *Am. J. Med* **36**, 561–570 (1964).
417. Seegmiller, J. E., Rosenbloom, F. M. & Kelley, W. N. Enzyme Defect Associated with a Sex-Linked Human Neurological Disorder and Excessive Purine Synthesis. *Science* **155**, 1682–1684 (1967).
418. NYHAN, W. L., Pesek, J., Sweetman, L., Carpenter, D. G. & Carter, C. H. Genetics of an X-Linked Disorder of Uric Acid Metabolism and Cerebral Function. *Pediatr Res* **1**, 5–13 (1967).
419. Sweetman, L. & NYHAN, W. L. Excretion of hypoxanthine and xanthine in a genetic disease of purine metabolism. *Nature* **215**, 859–860 (1967).
420. Yang, T. P., Patel, P. I., Chinault, A. C., Stout, J. T., Jackson, L. G., Hildebrand, B. M. & Caskey, C. T. Molecular evidence for new mutation at the hprt locus in Lesch-Nyhan patients. *Nature* **310**, 412–414 (1984).
421. Davidson, B. L., Tarlé, S. A., van Antwerp, M., Gibbs, D. A., Watts, R. W., Kelley, W. N. & Palella, T. D. Identification of 17 independent mutations responsible for human hypoxanthine-guanine phosphoribosyltransferase (HPRT) deficiency. *Am. J. Hum. Genet* **48**, 951–958 (1991).
422. Tarlé, S. A., Davidson, B. L., Wu, V. C., Zidar, F. J., Seegmiller, J. E., Kelley, W. N. & Palella, T. D. Determination of the mutations responsible for the Lesch-Nyhan syndrome in 17 subjects. *Genomics* **10**, 499–501 (1991).
423. Sege-Peterson, K., Chambers, J., Page, T., Jones, O. W. & NYHAN, W. L. Characterization of mutations in phenotypic variants of hypoxanthine phosphoribosyltransferase deficiency. *Hum. Mol. Genet* **1**, 427–432 (1992).
424. Mak, B. S., Chi, C. S., Tsai, C. R., Lee, W. J. & Lin, H. Y. New mutations of the HPRT gene in Lesch-Nyhan syndrome. *Pediatr. Neurol.* **23**, 332–335 (2000).
425. Torres, R. J., Mateos, F. A., Molano, J., Gathoff, B. S., O'Neill, J. P., Gundel, R. M., Trombley, L. & Puig, J. G. Molecular basis of hypoxanthine-guanine phosphoribosyltransferase deficiency in thirteen Spanish families. *Hum. Mutat.* **15**, 383 (2000).
426. Jinnah, H. A., Harris, J. C., Nyhan, W. L. & O'Neill, J. P. The spectrum of mutations causing HPRT deficiency: an update. *Nucleosides Nucleotides Nucleic Acids* **23**, 1153–1160 (2004).
427. Nyhan, W. L. Lesch-Nyhan disease. *Nucleosides Nucleotides Nucleic Acids* **27**, 559–563 (2008).
428. Kim, S. H., Moores, J. C., David, D., Respess, J. G., Jolly, D. J. & Friedmann, T. The organization of the human HPRT gene. *Nucleic Acids Res.* **14**, 3103–3118 (1986).
429. Patel, P. I., Framson, P. E., Caskey, C. T. & Chinault, A. C. Fine structure of the human hypoxanthine phosphoribosyltransferase gene. *Mol. Cell. Biol.* **6**, 393–403 (1986).

430. Davidson, J. D. & WinteR, T. S. Purine nucleotide pyrophosphorylases in 6-mercaptopurine-sensitive and -resistant human leukemias. *Cancer Res* **24**, 261–267 (1964).
431. NYHAN, W. L., Sweetman, L., Carpenter, D. G., Carter, C. H. & HOEFNAGEL, D. Effects of azathiprine in a disorder of uric acid metabolism and cerebral function. *J. Pediatr* **72**, 111–118 (1968).
432. Kelley, W. N., Greene, M. L., Rosenbloom, F. M., Henderson, J. F. & Seegmiller, J. E. Hypoxanthine-guanine phosphoribosyltransferase deficiency in gout. *Ann. Intern. Med* **70**, 155–206 (1969).
433. Greene, M. L. Clinical features of patients with the "partial" deficiency of the X-linked uricaciduria enzyme. *Arch. Intern. Med* **130**, 193–198 (1972).
434. Emmerson, B. T. & Thompson, L. The spectrum of hypoxanthine-guanine phosphoribosyltransferase deficiency. *Q. J. Med* **42**, 423–440 (1973).
435. Page, T. & Nyhan, W. L. The spectrum of HPRT deficiency: an update. *Adv. Exp. Med. Biol* **253**, 129–133 (1989).
436. Melton, D. W., Konecki, D. S., Brennand, J. & Caskey, C. T. Structure, expression, and mutation of the hypoxanthine phosphoribosyltransferase gene. *Proc. Natl. Acad. Sci. U.S.A.* **81**, 2147–2151 (1984).
437. Melton, D. W., McEwan, C., McKie, A. B. & Reid, A. M. Expression of the mouse HPRT gene: deletional analysis of the promoter region of an X-chromosome linked housekeeping gene. *Cell* **44**, 319–328 (1986).
438. Puig, J. G., Jiménez, M. L., Mateos, F. A. & Fox, I. H. Adenine nucleotide turnover in hypoxanthine-guanine phosphoribosyl-transferase deficiency: evidence for an increased contribution of purine biosynthesis de novo. *Metab. Clin. Exp* **38**, 410–418 (1989).
439. Zoref-Shani, E., Bromberg, Y., Brosh, S., Sidi, Y. & Sperling, O. Characterization of the alterations in purine nucleotide metabolism in hypoxanthine-guanine phosphoribosyltransferase-deficient rat neuroma cell line. *J. Neurochem* **61**, 457–463 (1993).
440. Michener, W. M. Hyperuricemia and mental retardation with athetosis and self-mutilation. *Am. J. Dis. Child* **113**, 195–206 (1967).
441. Partington, M. W. & Hennen, B. K. The Lesch-Nyhan syndrome: self-destructive biting, mental retardation, neurological disorder and hyperuricaemia. *Dev Med Child Neurol* **9**, 563–572 (1967).
442. Benke, P. J., Herrick, N., Smitten, L., Aradine, C., Laessig, R. & Wolcott, G. J. Adenine and folic acid in the Lesch-Nyhan syndrome. *Pediatr. Res* **7**, 729–738 (1973).
443. Wortmann, R. L. & Fox, I. H. Limited value of uric acid to creatinine ratios in estimating uric acid excretion. *Ann. Intern. Med* **93**, 822–825 (1980).
444. Puliyel, J. M. & Kumar, M. Lesch Nyhan syndrome. *Indian Pediatr* **21**, 251–252 (1984).
445. Dizmang, L. H. & Cheatham, C. F. The Lesch-Nyhan syndrome. *Am J Psychiatry* **127**, 671–677 (1970).
446. NYHAN, W. L. Clinical features of the Lesch-Nyhan syndrome. *Arch. Intern. Med* **130**, 186–192 (1972).
447. Mizuno, T. I. & Yugari, Y. Letter: Self mutilation in Lesch-Nyhan syndrome. *Lancet* **1**, 761 (1974).
448. NYHAN, W. L. Behavior in the Lesch--Nyhan syndrome. *J Autism Child Schizophr* **6**, 235–252 (1976).
449. Christie, R., Bay, C., Kaufman, I. A., Bakay, B., Borden, M. & NYHAN, W. L. Lesch-Nyhan disease: clinical experience with nineteen patients. *Dev Med Child Neurol* **24**, 293–306 (1982).
450. Watts, R. W., Spellacy, E., Gibbs, D. A., Allsop, J., McKeran, R. O. & Slavin, G. E. Clinical, post-mortem, biochemical and therapeutic observations on the Lesch-Nyhan syndrome with particular reference to the Neurological manifestations. *Q. J. Med* **51**, 43–78 (1982).
451. Mizuno, T. Long-term follow-up of ten patients with Lesch-Nyhan syndrome. *Neuropediatrics* **17**, 158–161 (1986).
452. Anderson, L. T. & Ernst, M. Self-injury in Lesch-Nyhan disease. *J Autism Dev Disord* **24**, 67–81 (1994).
453. Hunter, T. C., Melancon, S. B., Dallaire, L., Taft, S., Skopek, T. R., Albertini, R. J. & O'Neill, J. P. Germinal HPRT splice donor site mutation results in multiple RNA splicing products in T-lymphocyte cultures. *Somat. Cell Mol. Genet* **22**, 145–150 (1996).
454. Schretlen, D. J., Ward, J., Meyer, S. M., Yun, J., Puig, J. G., Nyhan, W. L., Jinnah, H. A. & Harris, J. C. Behavioral aspects of Lesch-Nyhan disease and its variants. *Dev Med Child Neurol* **47**, 673–677 (2005).
455. Jinnah, H. A., Visser, J. E., Harris, J. C., Verdu, A., Larovere, L., Ceballos-Picot, I., Gonzalez-Alegre, P., Neychev, V., Torres, R. J., Dulac, O., Desguerre, I., Schretlen, D. J., Robey, K. L., Barabas, G., Bloem, B. R., Nyhan, W., Kremer, R. de, Eddey, G. E., Puig, J. G. & Reich, S. G. Delineation of the motor disorder of Lesch-Nyhan disease. *Brain* **129**, 1201–1217 (2006).
456. Preston, R. An error in the code: what can a rare disorder tell us about human behavior? *New Yorker*, 30–36 (2007).
457. Scherzer, A. L. & Ilson, J. B. Normal intelligence in the Lesch-Nyhan syndrome. *Pediatrics* **44**, 116–120 (1969).
458. Bakay, B., Nissinen, E., Sweetman, L., Francke, U. & NYHAN, W. L. Utilization of purines by an HPRT variant in an intelligent, nonmutilative patient with features of the Lesch-Nyhan syndrome. *Pediatr. Res* **13**, 1365–1370 (1979).

459. Schretlen, D. J., Harris, J. C., Park, K. S., Jinnah, H. A. & del Pozo, N. O. Neurocognitive functioning in Lesch-Nyhan disease and partial hypoxanthine-guanine phosphoribosyltransferase deficiency. *J Int Neuropsychol Soc* **7**, 805–812 (2001).
460. Di Chiara, G., Camba, R. & SPano, P. F. Evidence for Inhibition by Brain Serotonin of Mouse Killing Behaviour in Rats. *Nature* **233**, 272–273 (1971).
461. Nyhan, W. L., Johnson, H. G., Kaufman, I. A. & Jones, K. L. Serotonergic approaches to the modification of behavior in the Lesch-Nyhan Syndrome. *Appl Res Ment Retard* **1**, 25–40 (1980).
462. Lloyd, K. G., Hornykiewicz, O., Davidson, L., Shannak, K., Farley, I., Goldstein, M., Shibuya, M., Kelley, W. N. & Fox, I. H. Biochemical evidence of dysfunction of brain neurotransmitters in the Lesch-Nyhan syndrome. *N. Engl. J. Med* **305**, 1106–1111 (1981).
463. Silverstein, F. S., Johnston, M. V., Hutchinson, R. J. & Edwards, N. L. Lesch-Nyhan syndrome: CSF neurotransmitter abnormalities. *Neurology* **35**, 907–911 (1985).
464. Jankovic, J., Caskey, T. C., Stout, J. T. & Butler, I. J. Lesch-Nyhan syndrome: a study of motor behavior and cerebrospinal fluid neurotransmitters. *Ann. Neurol* **23**, 466–469 (1988).
465. Curto, R., Voit, E. O. & Cascante, M. Analysis of abnormalities in purine metabolism leading to gout and to neurological dysfunctions in man. *Biochem. J* **329 (Pt 3)**, 477–487 (1998).
466. Visser, J. E., Bär, P. R. & Jinnah, H. A. Lesch-Nyhan disease and the basal ganglia. *Brain Res. Brain Res. Rev* **32**, 449–475 (2000).
467. Sculley, D. G., Dawson, P. A., Emmerson, B. T. & Gordon, R. B. A review of the molecular basis of hypoxanthine-guanine phosphoribosyltransferase (HPRT) deficiency. *Hum. Genet.* **90**, 195–207 (1992).
468. Harris, J. C., Lee, R. R., Jinnah, H. A., Wong, D. F., Yaster, M. & Bryan, R. N. Craniocerebral magnetic resonance imaging measurement and findings in Lesch-Nyhan syndrome. *Arch. Neurol* **55**, 547–553 (1998).
469. Proctor, P. & McGinness, J. E. Levodopa side-effects and the Lesch-Nyhan syndrome. *Lancet* **2**, 1367 (1970).
470. Nyhan, W. L. Dopamine function in Lesch-Nyhan disease. *Environ. Health Perspect* **108 Suppl 3**, 409–411 (2000).
471. Visser, J. E., Smith, D. W., Moy, S. S., Breese, G. R., Friedmann, T., Rothstein, J. D. & Jinnah, H. A. Oxidative stress and dopamine deficiency in a genetic mouse model of Lesch-Nyhan disease. *Brain Res. Dev. Brain Res* **133**, 127–139 (2002).
472. Ceballos-Picot, I., Mockel, L., Potier, M.-C., Dauphinot, L., Shirley, T. L., Torero-Ibad, R., Fuchs, J. & Jinnah, H. A. Hypoxanthine-guanine phosphoribosyl transferase regulates early developmental programming of dopamine neurons: implications for Lesch-Nyhan disease pathogenesis. *Hum. Mol. Genet* **18**, 2317–2327 (2009).
473. Niznik, H. B. Dopamine receptors: molecular structure and function. *Mol. Cell. Endocrinol* **54**, 1–22 (1987).
474. Freissmuth, M., Casey, P. J. & Gilman, A. G. G proteins control diverse pathways of transmembrane signaling. *FASEB J* **3**, 2125–2131 (1989).
475. Neer, E. J. Heterotrimeric G proteins: organizers of transmembrane signals. *Cell* **80**, 249–257 (1995).
476. Beal, M. F. Aging, energy, and oxidative stress in neurodegenerative diseases. *Ann. Neurol* **38**, 357–366 (1995).
477. Yeh, J., Zheng, S. & Howard, B. D. Impaired differentiation of HPRT-deficient dopaminergic neurons: a possible mechanism underlying neuronal dysfunction in Lesch-Nyhan syndrome. *J. Neurosci. Res* **53**, 78–85 (1998).
478. Rosenbloom, F. M., Kelley, W. N., Miller, J., Henderson, J. F. & Seegmiller, J. E. Inherited disorder of purine metabolism. Correlation between central nervous system dysfunction and biochemical defects. *JAMA* **202**, 175–177 (1967).
479. Rijksen, G., Staal, G. E., van der Vlist, M. J., Beemer, F. a., Troost, J., Gutensohn, W., van Laarhoven, J. P. & Bruyn, C. H. de. Partial hypoxanthine-guanine phosphoribosyl transferase deficiency with full expression of the Lesch-Nyhan syndrome. *Hum. Genet* **57**, 39–47 (1981).
480. Thorpe, W. P. The Lesch-Nyhan syndrome. *Enzyme* **12**, 129–142 (1971).
481. Skolnick, P., Marangos, P. J., Goodwin, F. K., Edwards, M. & Paul, S. Identification of inosine and hypoxanthine as endogenous inhibitors of [3H] diazepam binding in the central nervous system. *Life Sci* **23**, 1473–1480 (1978).
482. Norstrand, I. F. Lesch-Nyhan syndrome. *N. Engl. J. Med* **306**, 1368 (1982).
483. Palmour, R. M., Heshka, T. W. & Ervin, F. R. Hypoxanthine accumulation and dopamine depletion in Lesch-Nyhan disease. *Adv. Exp. Med. Biol* **253**, 165–172 (1989).
484. NYHAN, W. L. The recognition of Lesch-Nyhan syndrome as an inborn error of purine metabolism. *J. Inherit. Metab. Dis* **20**, 171–178 (1997).
485. Scriver, C. R. *The metabolic and molecular bases of inherited disease* (McGraw-Hill, New York [etc.], op. 2001).

486. Gregorio, L. de, Jinnah, H. A., Harris, J. C., Nyhan, W. L., Schretlen, D. J., Trombley, L. M. & O'Neill, J. P. Lesch-Nyhan disease in a female with a clinically normal monozygotic twin. *Mol. Genet. Metab* **85**, 70–77 (2005).
487. Torres, R. J. & Puig, J. G. Hypoxanthine-guanine phosophoribosyltransferase (HPRT) deficiency: Lesch-Nyhan syndrome. *Orphanet J Rare Dis* **2**, 48 (2007).
488. Breese, G. R. & Traylor, T. D. Developmental characteristics of brain catecholamines and tyrosine hydroxylase in the rat: effects of 6-hydroxydopamine. *Br. J. Pharmacol* **44**, 210–222 (1972).
489. Breese, G. R., Baumeister, A. A., McCown, T. J., Emerick, S. G., Frye, G. D. & Mueller, R. A. Neonatal-6-hydroxydopamine treatment: model of susceptibility for self-mutilation in the Lesch-Nyhan syndrome. *Pharmacol. Biochem. Behav* **21**, 459–461 (1984).
490. Breese, G. R., Baumeister, A. A., McCown, T. J., Emerick, S. G., Frye, G. D., Crotty, K. & Mueller, R. A. Behavioral differences between neonatal and adult 6-hydroxydopamine-treated rats to dopamine agonists: relevance to neurological symptoms in clinical syndromes with reduced brain dopamine. *J. Pharmacol. Exp. Ther* **231**, 343–354 (1984).
491. Breese, G. R., Criswell, H. E. & Mueller, R. A. Evidence that lack of brain dopamine during development can increase the susceptibility for aggression and self-injurious behavior by influencing D1-dopamine receptor function. *Prog. Neuropsychopharmacol. Biol. Psychiatry* **14**, S65-80 (1990).
492. Breese, G. R., Criswell, H. E., Duncan, G. E. & Mueller, R. A. A dopamine deficiency model of Lesch-Nyhan disease--the neonatal-6-OHDA-lesioned rat. *Brain Res. Bull* **25**, 477–484 (1990).
493. Stodgell, C. J., Loupe, P. S., Schroeder, S. R. & Tessel, R. E. Cross-sensitization between footshock stress and apomorphine on self-injurious behavior and neostriatal catecholamines in a rat model of Lesch-Nyhan syndrome. *Brain Res* **783**, 10–18 (1998).
494. Breese, G. R., Criswell, H. E., Johnson, K. B., O'Callaghan, J. P., Duncan, G. E., Jensen, K. F., Simson, P. E. & Mueller, R. A. Neonatal destruction of dopaminergic neurons. *Neurotoxicology* **15**, 149–159 (1994).
495. Breese, G. R., Criswell, H. E., Duncan, G. E., Moy, S. S., Johnson, K. B., Wong, D. F. & Mueller, R. A. Model for reduced brain dopamine in Lesch-Nyhan syndrome and the mentally retarded: Neurobiology of neonatal-6-hydroxydopamine-lesioned rats. *Ment. Retard. Dev. Disabil. Res. Rev* **1**, 111–119 (1995).
496. Breese, G. R., Knapp, D. J., Criswell, H. E., Moy, S. S., Papadeas, S. T. & Blake, B. L. The neonate-6-hydroxydopamine-lesioned rat: a model for clinical neuroscience and neurobiological principles. *Brain Res. Brain Res. Rev* **48**, 57–73 (2005).
497. Jolly, D. J., Okayama, H., Berg, P., Esty, A. C., Filpula, D., Bohlen, P., Johnson, G. G., Shively, J. E., Hunkapillar, T. & Friedmann, T. Isolation and characterization of a full-length expressible cDNA for human hypoxanthine phosphoribosyl transferase. *Proc. Natl. Acad. Sci. U.S.A* **80**, 477–481 (1983).
498. Hooper, M., Hardy, K., Handyside, A., Hunter, S. & Monk, M. HPRT-deficient (Lesch-Nyhan) mouse embryos derived from germline colonization by cultured cells. *Nature* **326**, 292–295 (1987).
499. Kuehn, M. R., Bradley, A., Robertson, E. J. & Evans, M. J. A potential animal model for Lesch-Nyhan syndrome through introduction of HPRT mutations into mice. *Nature* **326**, 295–298 (1987).
500. Thomas, K. R. & Capecchi, M. R. Site-directed mutagenesis by gene targeting in mouse embryo-derived stem cells. *Cell* **51**, 503–512 (1987).
501. Finger, S., Heavens, R. P., Sirinathsinghji, D. J., Kuehn, M. R. & Dunnett, S. B. Behavioral and neurochemical evaluation of a transgenic mouse model of Lesch-Nyhan syndrome. *J. Neurol. Sci.* **86**, 203–213 (1988).
502. Dunnett, S. B., Sirinathsinghji, D. J., Heavens, R., Rogers, D. C. & Kuehn, M. R. Monoamine deficiency in a transgenic (Hprt-) mouse model of Lesch-Nyhan syndrome. *Brain Res.* **501**, 401–406 (1989).
503. Jinnah, H. A., Gage, F. H. & Friedmann, T. Amphetamine-induced behavioral phenotype in a hypoxanthine-guanine phosphoribosyltransferase-deficient mouse model of Lesch-Nyhan syndrome. *Behav. Neurosci* **105**, 1004–1012 (1991).
504. Williamson, D. J., Hooper, M. L. & Melton, D. W. Mouse models of hypoxanthine phosphoribosyltransferase deficiency. *J. Inherit. Metab. Dis.* **15**, 665–673 (1992).
505. Jinnah, H. A., Langlais, P. J. & Friedmann, T. Functional analysis of brain dopamine systems in a genetic mouse model of Lesch-Nyhan syndrome. *J. Pharmacol. Exp. Ther* **263**, 596–607 (1992).
506. Engle, S. J., Womer, D. E., Davies, P. M., Boivin, G., Sahota, A., Simmonds, H. A., Stambrook, P. J. & Tischfield, J. A. HPRT-APRT-deficient mice are not a model for lesch-nyhan syndrome. *Hum. Mol. Genet.* **5**, 1607–1610 (1996).
507. Shi, J., Cai, D., Chen, X. & Sheng, H. Cloning of rabbit HPRT gene using the recombineering system. *Acta Biochim. Biophys. Sin. (Shanghai)* **39**, 591–598 (2007).
508. Paul, B., Cloninger, C., Felton, M., Khachatoorian, R. & Metzenberg, S. A nonalkaline method for isolating sequencing-ready plasmids. *Anal. Biochem.* **377**, 218–222 (2008).
509. Richter, T. R. *Isolation and characterization of a putative rabbit embryonic stem cell line. Master-thesis* (2008).
510. Bain, G., Kitchens, D., Yao, M., Huettner, J. E. & Gottlieb, D. I. Embryonic stem cells express neuronal properties in vitro. *Dev. Biol.* **168**, 342–357 (1995).

511. Burdsal, C. A., Flannery, M. L. & Pedersen, R. A. FGF-2 alters the fate of mouse epiblast from ectoderm to mesoderm in vitro. *Dev. Biol.* **198**, 231–244 (1998).
512. Loebel, D. A., Watson, C. M., Young, R. de & Tam, P. P. Lineage choice and differentiation in mouse embryos and embryonic stem cells. *Developmental Biology* **264**, 1–14 (2003).
513. Schuldiner, M., Yanuka, O., Itskovitz-Eldor, J., Melton, D. A. & Benvenisty, N. Effects of eight growth factors on the differentiation of cells derived from human embryonic stem cells. *Proc. Natl. Acad. Sci. U.S.A.* **97**, 11307–11312 (2000).
514. Takeda, J., Seino, S. & Bell, G. I. Human Oct3 gene family: cDNA sequences, alternative splicing, gene organization, chromosomal location, and expression at low levels in adult tissues. *Nucleic Acids Res.* **20**, 4613–4620 (1992).
515. Shi, J. J., Cai, D. H., Chen, X. J. & Sheng, H. Z. Cloning and characterization of the rabbit POU5F1 gene. *DNA Seq.* **19**, 56–61 (2008).
516. Zakhartchenko, V., Flisikowska, T., Li, S., Richter, T., Wieland, H., Durkovic, M., Rottmann, O., Kessler, B., Gungor, T., Brem, G., Kind, A., Wolf, E. & Schnieke, A. Cell-Mediated Transgenesis in Rabbits: Chimeric and Nuclear Transfer Animals. *Biology of Reproduction* **84**, 229–237 (2011).
517. Izsvák, Z. & Ivics, Z. Sleeping beauty transposition: biology and applications for molecular therapy. *Mol. Ther* **9**, 147–156 (2004).
518. Hackett, P. B., Ekker, S. C., Largaespada, D. A. & McIvor, R. S. Sleeping beauty transposon-mediated gene therapy for prolonged expression. *Adv. Genet* **54**, 189–232 (2005).
519. Aronovich, E. L., McIvor, R. S. & Hackett, P. B. The Sleeping Beauty transposon system: a non-viral vector for gene therapy. *Human Molecular Genetics* **20**, R14 (2011).
520. Aronovich, E. L., Bell, J. B., Belur, L. R., Gunther, R., Koniar, B., Erickson, D. C. C., Schachern, P. A., Matise, I., McIvor, R. S., Whitley, C. B. & Hackett, P. B. Prolonged expression of a lysosomal enzyme in mouse liver after Sleeping Beauty transposon-mediated gene delivery: implications for non-viral gene therapy of mucopolysaccharidoses. *J Gene Med* **9**, 403–415 (2007).
521. Aronovich, E. L., Bell, J. B., Khan, S. A., Belur, L. R., Gunther, R., Koniar, B., Schachern, P. A., Parker, J. B., Carlson, C. S., Whitley, C. B., McIvor, R. S., Gupta, P. & Hackett, P. B. Systemic correction of storage disease in MPS I NOD/SCID mice using the sleeping beauty transposon system. *Mol. Ther* **17**, 1136–1144 (2009).
522. Wang, W., Lin, C., Lu, D., Ning, Z., Cox, T., Melvin, D., Wang, X., Bradley, A. & Liu, P. Chromosomal transposition of PiggyBac in mouse embryonic stem cells. *Proc. Natl. Acad. Sci. U.S.A* **105**, 9290–9295 (2008).
523. Hackett, P. B., Largaespada, D. A. & Cooper, L. J. N. A transposon and transposase system for human application. *Mol. Ther* **18**, 674–683 (2010).
524. Mikkelsen, J. G., Yant, S. R., Meuse, L., Huang, Z., Xu, H. & Kay, M. A. Helper-Independent Sleeping Beauty transposon-transposase vectors for efficient nonviral gene delivery and persistent gene expression in vivo. *Mol. Ther.* **8**, 654–665 (2003).
525. Converse, A. D., Belur, L. R., Gori, J. L., Liu, G., Amaya, F., Aguilar-Cordova, E., Hackett, P. B. & McIvor, R. S. Counterselection and co-delivery of transposon and transposase functions for Sleeping Beauty-mediated transposition in cultured mammalian cells. *Biosci. Rep.* **24**, 577–594 (2004).
526. Liang, Q., Kong, J., Stalker, J. & Bradley, A. Chromosomal mobilization and reintegration of Sleeping Beauty and PiggyBac transposons. *Genesis* **47**, 404–408 (2009).
527. Izsvák, Z., Fröhlich, J., Grabundzija, I., Shirley, J. R., Powell, H. M., Chapman, K. M., Ivics, Z. & Hamra, F. K. Generating knockout rats by transposon mutagenesis in spermatogonial stem cells. *Nat. Methods* **7**, 443–445 (2010).
528. Garrison, B. S., Yant, S. R., Mikkelsen, J. G. & Kay, M. A. Postintegrative gene silencing within the Sleeping Beauty transposition system. *Mol. Cell. Biol.* **27**, 8824–8833 (2007).
529. Wilber, A., Linehan, J. L., Tian, X., Woll, P. S., Morris, J. K., Belur, L. R., McIvor, R. S. & Kaufman, D. S. Efficient and stable transgene expression in human embryonic stem cells using transposon-mediated gene transfer. *Stem Cells* **25**, 2919–2927 (2007).
530. Limonta, J. M., Castro, F. O., Martínez, R., Puentes, P., Ramos, B., Aguilar, A., Lleonart, R. L. & La Fuente, J. de. Transgenic rabbits as bioreactors for the production of human growth hormone. *J. Biotechnol.* **40**, 49–58 (1995).
531. Spieker-Polet, H., Sethupathi, P., Yam, P. C. & Knight, K. L. Rabbit monoclonal antibodies: generating a fusion partner to produce rabbit-rabbit hybridomas. *Proc. Natl. Acad. Sci. U.S.A.* **92**, 9348–9352 (1995).
532. Aigner, B., Besenfelder, U., Seregi, J., Frenyo, L. V., Sahin-Toth, T. & Brem, G. Expression of the murine wild-type tyrosinase gene in transgenic rabbits. *Transgenic Res.* **5**, 405–411 (1996).
533. Duverger, N., Viglietta, C., Berthou, L., Emmanuel, F., Tailleux, A., Parmentier-Nihoul, L., Laine, B., Fievet, C., Castro, G., Fruchart, J. C., Houbebine, L. M. & Denèfie, P. Transgenic rabbits expressing human apolipoprotein A-I in the liver. *Arterioscler. Thromb. Vasc. Biol* **16**, 1424–1429 (1996).
534. Hoeg, J. M., Vaisman, B. L., Demosky, S. J., Meyn, S. M., Talley, G. D., Hoyt, R. F., Feldman, S., Bérard, A. M., Sakai, N., Wood, D., Brousseau, M. E., Marcovina, S., Brewer, H. B. & Santamarina-Fojo, S.

Lecithin:cholesterol acyltransferase overexpression generates hyperalpha-lipoproteinemia and a nonatherogenic lipoprotein pattern in transgenic rabbits. *J. Biol. Chem.* **271**, 4396–4402 (1996).
535. Peng, X., Griffith, J. W., Han, R., Lang, C. M. & Kreider, J. W. Development of keratoacanthomas and squamous cell carcinomas in transgenic rabbits with targeted expression of EJras oncogene in epidermis. *Am. J. Pathol* **155**, 315–324 (1999).
536. Hirabayashi, M., Takahashi, R., Ito, K., Kashiwazaki, N., Hirao, M., Hirasawa, K., Hochi, S. & Ueda, M. A comparative study on the integration of exogenous DNA into mouse, rat, rabbit, and pig genomes. *Exp. Anim.* **50**, 125–131 (2001).
537. Bodó, S., Gócza, E., Révay, T., Hiripi, L., Carstea, B., Kovács, A., Bodrogi, L. & Bösze, Z. Production of transgenic chimeric rabbits and transmission of the transgene through the germline. *Mol. Reprod. Dev.* **68**, 435–440 (2004).
538. Chrenek, P., Vasicek, D., Makarevich, A. V., Jurcik, R., Suvegova, K., Parkanyi, V., Bauer, M., Rafay, J., Batorova, A. & Paleyanda, R. K. Increased transgene integration efficiency upon microinjection of DNA into both pronuclei of rabbit embryos. *Transgenic Res.* **14**, 417–428 (2005).
539. Kondo, M., Sakai, T., Komeima, K., Kurimoto, Y., Ueno, S., Nishizawa, Y., Usukura, J., Fujikado, T., Tano, Y. & Terasaki, H. Generation of a transgenic rabbit model of retinal degeneration. *Invest. Ophthalmol. Vis. Sci* **50**, 1371–1377 (2009).
540. Davidson, A. E., Balciunas, D., Mohn, D., Shaffer, J., Hermanson, S., Sivasubbu, S., Cliff, M. P., Hackett, P. B. & Ekker, S. C. Efficient gene delivery and gene expression in zebrafish using the Sleeping Beauty transposon. *Dev. Biol* **263**, 191–202 (2003).
541. Grabher, C., Henrich, T., Sasado, T., Arenz, A., Wittbrodt, J. & Furutani-Seiki, M. Transposon-mediated enhancer trapping in medaka. *Gene* **322**, 57–66 (2003).
542. Hermanson, S., Davidson, A. E., Sivasubbu, S., Balciunas, D. & Ekker, S. C. Sleeping Beauty transposon for efficient gene delivery. *Methods Cell Biol* **77**, 349–362 (2004).
543. Carlson, C. M., Frandsen, J. L., Kirchhof, N., McIvor, R. S. & Largaespada, D. A. Somatic integration of an oncogene-harboring Sleeping Beauty transposon models liver tumor development in the mouse. *Proc. Natl. Acad. Sci. U.S.A* **102**, 17059–17064 (2005).
544. Luo, G., Ivics, Z., Izsvák, Z. & Bradley, A. Chromosomal transposition of a Tc1/mariner-like element in mouse embryonic stem cells. *Proc. Natl. Acad. Sci. U.S.A* **95**, 10769–10773 (1998).
545. Fischer, S. E., Wienholds, E. & Plasterk, R. H. Regulated transposition of a fish transposon in the mouse germ line. *Proc. Natl. Acad. Sci. U.S.A* **98**, 6759–6764 (2001).
546. Carlson, C. M., Dupuy, A. J., Fritz, S., Roberg-Perez, K. J., Fletcher, C. F. & Largaespada, D. A. Transposon mutagenesis of the mouse germline. *Genetics* **165**, 243–256 (2003).
547. Kues, W. A., Schwinzer, R., Wirth, D., Verhoeyen, E., Lemme, E., Herrmann, D., Barg-Kues, B., Hauser, H., Wonigeit, K. & Niemann, H. Epigenetic silencing and tissue independent expression of a novel tetracycline inducible system in double-transgenic pigs. *FASEB J* **20**, 1200–1202 (2006).
548. Hackett, C. S., Geurts, A. M. & Hackett, P. B. Predicting preferential DNA vector insertion sites: implications for functional genomics and gene therapy. *Genome Biol* **8 Suppl 1**, S12 (2007).
549. Brinster, R. L., Chen, H. Y., Trumbauer, M. E., Yagle, M. K. & Palmiter, R. D. Factors affecting the efficiency of introducing foreign DNA into mice by microinjecting eggs. *Proc. Natl. Acad. Sci. U.S.A* **82**, 4438–4442 (1985).
550. Towbin, B. D., Meister, P. & Gasser, S. M. The nuclear envelope--a scaffold for silencing? *Curr. Opin. Genet. Dev* **19**, 180–186 (2009).
551. Wako, T. & Fukui, K. Higher organization and histone modification of the plant nucleus and chromosome. *Cytogenet. Genome Res* **129**, 55–63 (2010).
552. Mátés, L., Izsvák, Z. & Ivics, Z. Technology transfer from worms and flies to vertebrates: transposition-based genome manipulations and their future perspectives. *Genome Biol* **8 Suppl 1**, S1 (2007).
553. Thurman, R. E., Rynes, E., Humbert, R., Vierstra, J., Maurano, M. T., Haugen, E., Sheffield, N. C., Stergachis, A. B., Wang, H., Vernot, B., Garg, K., John, S., Sandstrom, R., Bates, D., Boatman, L., Canfield, T. K., Diegel, M., Dunn, D., Ebersol, A. K., Frum, T., Giste, E., Johnson, A. K., Johnson, E. M., Kutyavin, T., Lajoie, B., Lee, B.-K., Lee, K., London, D., Lotakis, D., Neph, S., Neri, F., Nguyen, E. D., Qu, H., Reynolds, A. P., Roach, V., Safi, A., Sanchez, M. E., Sanyal, A., Shafer, A., Simon, J. M., Song, L., Vong, S., Weaver, M., Yan, Y., Zhang, Z., Zhang, Z., Lenhard, B., Tewari, M., Dorschner, M. O., Hansen, R. S., Navas, P. A., Stamatoyannopoulos, G., Iyer, V. R., Lieb, J. D., Sunyaev, S. R., Akey, J. M., Sabo, P. J., Kaul, R., Furey, T. S., Dekker, J., Crawford, G. E. & Stamatoyannopoulos, J. A. The accessible chromatin landscape of the human genome. *Nature* **489**, 75–82 (2012).
554. Bernstein, B. E., Birney, E., Dunham, I., Green, E. D., Gunter, C. & Snyder, M. An integrated encyclopedia of DNA elements in the human genome. *Nature* **489**, 57–74 (2012).
555. Devon, R. S., Porteous, D. J. & Brookes, A. J. Splinkerettes--improved vectorettes for greater efficiency in PCR walking. *Nucleic Acids Res.* **23**, 1644–1645 (1995).

556. Mikkers, H., Allen, J., Knipscheer, P., Romeijn, L., Hart, A., Vink, E., Berns, A. & Romeyn, L. High-throughput retroviral tagging to identify components of specific signaling pathways in cancer. *Nat. Genet.* **32**, 153–159 (2002).
557. Largaespada, D. A. & Collier, L. S. Transposon-mediated mutagenesis in somatic cells: identification of transposon-genomic DNA junctions. *Methods Mol. Biol.* **435**, 95–108 (2008).
558. Uren, A. G., Mikkers, H., Kool, J., van der Weyden, L., Lund, A. H., Wilson, C. H., Rance, R., Jonkers, J., van Lohuizen, M., Berns, A. & Adams, D. J. A high-throughput splinkerette-PCR method for the isolation and sequencing of retroviral insertion sites. *Nat Protoc* **4**, 789–798 (2009).
559. Kitada, K., Keng, V. W., Takeda, J. & Horie, K. Generating mutant rats using the Sleeping Beauty transposon system. *Methods* **49**, 236–242 (2009).
560. Liu, Y. G. & Whittier, R. F. Thermal asymmetric interlaced PCR: automatable amplification and sequencing of insert end fragments from P1 and YAC clones for chromosome walking. *Genomics* **25**, 674–681 (1995).
561. Liu, Y.-G. & Chen, Y. High-efficiency thermal asymmetric interlaced PCR for amplification of unknown flanking sequences. *BioTechniques* **43**, 649-50, 652, 654 passim (2007).
562. Liang, Z., Breman, A. M., Grimes, B. R. & Rosen, E. D. Identifying and genotyping transgene integration loci. *Transgenic Res* **17**, 979–983 (2008).
563. Yant, S. R., Meuse, L., Chiu, W., Ivics, Z., Izsvak, Z. & Kay, M. A. Somatic integration and long-term transgene expression in normal and haemophilic mice using a DNA transposon system. *Nat. Genet.* **25**, 35–41 (2000).
564. Sumiyama, K., Kawakami, K. & Yagita, K. A simple and highly efficient transgenesis method in mice with the Tol2 transposon system and cytoplasmic microinjection. *Genomics* **95**, 306–311 (2010).
565. Garrels, W., Mátés, L., Holler, S., Dalda, A., Taylor, U., Petersen, B., Niemann, H., Izsvák, Z., Ivics, Z. & Kues, W. A. Germline transgenic pigs by Sleeping Beauty transposition in porcine zygotes and targeted integration in the pig genome. *PLoS ONE* **6**, e23573 (2011).
566. Yusa, K., Takeda, J. & Horie, K. Enhancement of Sleeping Beauty transposition by CpG methylation: possible role of heterochromatin formation. *Mol. Cell. Biol.* **24**, 4004–4018 (2004).
567. Park, C. W., Kren, B. T., Largaespada, D. A. & Steer, C. J. DNA methylation of Sleeping Beauty with transposition into the mouse genome. *Genes Cells* **10**, 763–776 (2005).
568. Ikeda, R., Kokubu, C., Yusa, K., Keng, V. W., Horie, K. & Takeda, J. Sleeping beauty transposase has an affinity for heterochromatin conformation. *Mol. Cell. Biol.* **27**, 1665–1676 (2007).
569. Carlson, D. F., Geurts, A. M., Garbe, J. R., Park, C.-W., Rangel-Filho, A., O'Grady, S. M., Jacob, H. J., Steer, C. J., Largaespada, D. A. & Fahrenkrug, S. C. Efficient mammalian germline transgenesis by cis-enhanced Sleeping Beauty transposition. *Transgenic Res.* **20**, 29–45 (2011).
570. Pikaart, M. J., Recillas-Targa, F. & Felsenfeld, G. Loss of transcriptional activity of a transgene is accompanied by DNA methylation and histone deacetylation and is prevented by insulators. *Genes Dev.* **12**, 2852–2862 (1998).
571. Recillas-Targa, F., Valadez-Graham, V. & Farrell, C. M. Prospects and implications of using chromatin insulators in gene therapy and transgenesis. *Bioessays* **26**, 796–807 (2004).
572. Blackwood, E. M. & Kadonaga, J. T. Going the distance: a current view of enhancer action. *Science* **281**, 60–63 (1998).
573. Zohar, M., Mesika, A. & Reich, Z. Analysis of genetic control elements in eukaryotes: transcriptional activity or nuclear hitchhiking? *Bioessays* **23**, 1176–1179 (2001).
574. West, A. G., Gaszner, M. & Felsenfeld, G. Insulators: many functions, many mechanisms. *Genes Dev.* **16**, 271–288 (2002).
575. Rister, J. & Desplan, C. Deciphering the genome's regulatory code: the many languages of DNA. *Bioessays* **32**, 381–384 (2010).
576. Robertson, G., Garrick, D., Wu, W., Kearns, M., Martin, D. & Whitelaw, E. Position-dependent variegation of globin transgene expression in mice. *Proc. Natl. Acad. Sci. U.S.A.* **92**, 5371–5375 (1995).
577. Giraldo, P., Rival-Gervier, S., Houdebine, L.-M. & Montoliu, L. The potential benefits of insulators on heterologous constructs in transgenic animals. *Transgenic Res* **12**, 751–755 (2003).
578. van Keuren, M. L., Gavrilina, G. B., Filipiak, W. E., Zeidler, M. G. & Saunders, T. L. Generating transgenic mice from bacterial artificial chromosomes: transgenesis efficiency, integration and expression outcomes. *Transgenic Res* **18**, 769–785 (2009).
579. Burgess-Beusse, B., Farrell, C., Gaszner, M., Litt, M., Mutskov, V., Recillas-Targa, F., Simpson, M., West, A. & Felsenfeld, G. The insulation of genes from external enhancers and silencing chromatin. *Proc. Natl. Acad. Sci. U.S.A.* **99 Suppl 4**, 16433–16437 (2002).
580. Walisko, O., Schorn, A., Rolfs, F., Devaraj, A., Miskey, C., Izsvák, Z. & Ivics, Z. Transcriptional activities of the Sleeping Beauty transposon and shielding its genetic cargo with insulators. *Mol. Ther.* **16**, 359–369 (2008).

581. Dalsgaard, T., Moldt, B., Sharma, N., Wolf, G., Schmitz, A., Pedersen, F. S. & Mikkelsen, J. G. Shielding of sleeping beauty DNA transposon-delivered transgene cassettes by heterologous insulators in early embryonal cells. *Mol. Ther.* **17**, 121–130 (2009).
582. Ammar, I., Izsvák, Z. & Ivics, Z. The Sleeping Beauty transposon toolbox. *Methods Mol. Biol.* **859**, 229–240 (2012).
583. Wilson, M. H., Kaminski, J. M. & George, A. L. Functional zinc finger/sleeping beauty transposase chimeras exhibit attenuated overproduction inhibition. *FEBS Lett.* **579**, 6205–6209 (2005).
584. Gallardo-Gálvez, J. B., Méndez, T., Béjar, J. & Alvarez, M. C. Endogenous transposases affect differently Sleeping Beauty and Frog Prince transposons in fish cells. *Mar. Biotechnol.* **13**, 695–705 (2011).
585. Bellen, H. J., Levis, R. W., He, Y., Carlson, J. W., Evans-Holm, M., Bae, E., Kim, J., Metaxakis, A., Savakis, C., Schulze, K. L., Hoskins, R. A. & Spradling, A. C. The Drosophila gene disruption project: progress using transposons with distinctive site specificities. *Genetics* **188**, 731–743 (2011).
586. Urasaki, A., Morvan, G. & Kawakami, K. Functional dissection of the Tol2 transposable element identified the minimal cis-sequence and a highly repetitive sequence in the subterminal region essential for transposition. *Genetics* **174**, 639–649 (2006).
587. Clark, K. J., Carlson, D. F. & Fahrenkrug, S. C. Pigs taking wing with transposons and recombinases. *Genome Biol* **8 Suppl 1**, S13 (2007).
588. Wu, S. C.-Y., Meir, Y.-J. J., Coates, C. J., Handler, A. M., Pelczar, P., Moisyadi, S. & Kaminski, J. M. piggyBac is a flexible and highly active transposon as compared to sleeping beauty, Tol2, and Mos1 in mammalian cells. *Proc. Natl. Acad. Sci. U.S.A.* **103**, 15008–15013 (2006).
589. Balciunas, D., Wangensteen, K. J., Wilber, A., Bell, J., Geurts, A., Sivasubbu, S., Wang, X., Hackett, P. B., Largaespada, D. A., McIvor, R. S. & Ekker, S. C. Harnessing a high cargo-capacity transposon for genetic applications in vertebrates. *PLoS Genet* **2**, e169 (2006).
590. Koga, A., Higashide, I., Hori, H., Wakamatsu, Y., Kyono-Hamaguchi, Y. & Hamaguchi, S. The Tol1 element of medaka fish is transposed with only terminal regions and can deliver large DNA fragments into the chromosomes. *J. Hum. Genet* **52**, 1026–1030 (2007).
591. Suster, M. L., Sumiyama, K. & Kawakami, K. Transposon-mediated BAC transgenesis in zebrafish and mice. *BMC Genomics* **10**, 477 (2009).
592. Cadiñanos, J. & Bradley, A. Generation of an inducible and optimized piggyBac transposon system. *Nucleic Acids Res* **35**, e87 (2007).
593. Dupuy, A. J., Rogers, L. M., Kim, J., Nannapaneni, K., Starr, T. K., Liu, P., Largaespada, D. A., Scheetz, T. E., Jenkins, N. A. & Copeland, N. G. A modified sleeping beauty transposon system that can be used to model a wide variety of human cancers in mice. *Cancer Res.* **69**, 8150–8156 (2009).
594. Mathis, D., Vence, L. & Benoist, C. beta-Cell death during progression to diabetes. *Nature* **414**, 792–798 (2001).
595. Soares, M. B., Schon, E., Henderson, A., Karathanasis, S. K., Cate, R., Zeitlin, S., Chirgwin, J. & Efstratiadis, A. RNA-mediated gene duplication: the rat preproinsulin I gene is a functional retroposon. *Mol. Cell. Biol.* **5**, 2090–2103 (1985).
596. Draznin, B. & LeRoith, D. *Molecular biology of diabetes* (Humana Press, Totowa, N.J, 1994).
597. Odagiri, H., Wang, J. & German, M. S. Function of the human insulin promoter in primary cultured islet cells. *J. Biol. Chem.* **271**, 1909–1915 (1996).
598. Hay, C. W. & Docherty, K. Comparative analysis of insulin gene promoters: implications for diabetes research. *Diabetes* **55**, 3201–3213 (2006).
599. Bell, G. I., Pictet, R. L., Rutter, W. J., Cordell, B., Tischer, E. & Goodman, H. M. Sequence of the human insulin gene. *Nature* **284**, 26–32 (1980).
600. Hong, E.-G., Jung, D. Y., Ko, H. J., Zhang, Z., Ma, Z., Jun, J. Y., Kim, J. H., Sumner, A. D., Vary, T. C., Gardner, T. W., Bronson, S. K. & Kim, J. K. Nonobese, insulin-deficient Ins2Akita mice develop type 2 diabetes phenotypes including insulin resistance and cardiac remodeling. *Am. J. Physiol. Endocrinol. Metab.* **293**, E1687-96 (2007).
601. Herbach, N., Rathkolb, B., Kemter, E., Pichl, L., Klaften, M., Angelis, M. H. de, Halban, P. A., Wolf, E., Aigner, B. & Wanke, R. Dominant-negative effects of a novel mutated Ins2 allele causes early-onset diabetes and severe beta-cell loss in Munich Ins2C95S mutant mice. *Diabetes* **56**, 1268–1276 (2007).
602. Louet, J.-F., LeMay, C. & Mauvais-Jarvis, F. Antidiabetic actions of estrogen: insight from human and genetic mouse models. *Curr Atheroscler Rep* **6**, 180–185 (2004).
603. Edghill, E. L., Flanagan, S. E., Patch, A.-M., Boustred, C., Parrish, A., Shields, B., Shepherd, M. H., Hussain, K., Kapoor, R. R., Malecki, M., MacDonald, M. J., Støy, J., Steiner, D. F., Philipson, L. H., Bell, G. I., Hattersley, A. T. & Ellard, S. Insulin mutation screening in 1,044 patients with diabetes: mutations in the INS gene are a common cause of neonatal diabetes but a rare cause of diabetes diagnosed in childhood or adulthood. *Diabetes* **57**, 1034–1042 (2008).
604. Wollheim, C. B., Meda, P. & Halban, P. A. Establishment and culture of insulin-secreting beta cell lines. *Meth. Enzymol* **192**, 223–235 (1990).

605. Wollheim, C. B., Meda, P. & Halban, P. A. Isolation of pancreatic islets and primary culture of the intact microorgans or of dispersed islet cells. *Meth. Enzymol* **192**, 188–223 (1990).
606. Asfari, M., Janjic, D., Meda, P., Li, G., Halban, P. A. & Wollheim, C. B. Establishment of 2-mercaptoethanol-dependent differentiated insulin-secreting cell lines. *Endocrinology* **130**, 167–178 (1992).
607. Brun, T., Roche, E., Kim, K. H. & Prentki, M. Glucose regulates acetyl-CoA carboxylase gene expression in a pancreatic beta-cell line (INS-1). *J. Biol. Chem* **268**, 18905–18911 (1993).
608. Susini, S., Roche, E., Prentki, M. & Schlegel, W. Glucose and glucoincretin peptides synergize to induce c-fos, c-jun, junB, zif-268, and nur-77 gene expression in pancreatic beta(INS-1) cells. *FASEB J* **12**, 1173–1182 (1998).
609. Araki, E., Oyadomari, S. & Mori, M. Impact of endoplasmic reticulum stress pathway on pancreatic beta-cells and diabetes mellitus. *Exp. Biol. Med. (Maywood)* **228**, 1213–1217 (2003).
610. Hartley, T., Siva, M., Lai, E., Teodoro, T., Zhang, L. & Volchuk, A. Endoplasmic reticulum stress response in an INS-1 pancreatic beta-cell line with inducible expression of a folding-deficient proinsulin. *BMC Cell Biol.* **11**, 59 (2010).
611. Liu, M., Ramos-Castañeda, J. & Arvan, P. Role of the connecting peptide in insulin biosynthesis. *J. Biol. Chem.* **278**, 14798–14805 (2003).
612. Zhang, B.-y., Liu, M. & Arvan, P. Behavior in the eukaryotic secretory pathway of insulin-containing fusion proteins and single-chain insulins bearing various B-chain mutations. *J. Biol. Chem.* **278**, 3687–3693 (2003).
613. Liu, M., Li, Y., Cavener, D. & Arvan, P. Proinsulin disulfide maturation and misfolding in the endoplasmic reticulum. *J. Biol. Chem.* **280**, 13209–13212 (2005).
614. Ohtsubo, K., Chen, M. Z., Olefsky, J. M. & Marth, J. D. Pathway to diabetes through attenuation of pancreatic beta cell glycosylation and glucose transport. *Nat Med* **17**, 1067–1075 (2011).
615. Zhang, X.-j., Chinkes, D. L., Aarsland, A., Herndon, D. N. & Wolfe, R. R. Lipid metabolism in diet-induced obese rabbits is similar to that of obese humans. *J. Nutr.* **138**, 515–518 (2008).
616. Milner, R. D. Plasma and tissue insulin concentrations in foetal and postnatal rabbits. *J. Endocrinol.* **43**, 119–124 (1969).
617. Metzger, P. & Brachet, E. The rabbit during the last third of gestation. Data concerning the whole fetus, its diaphragm and brown adipose tissue. *Biol. Neonate* **33**, 297–303 (1978).
618. Milner, R. D. The secretion of insulin from foetal and postnatal rabbit pancreas in vitro in response to various substances. *J. Endocrinol.* **44**, 267–272 (1969).
619. Milner, R. D., Leach, R. N., Ashworth, M. A., Cser, A. & Jack, P. M. Development of pathways of insulin secretion in the rabbit. *J. Endocrinol.* **64**, 349–361 (1975).
620. Fletcher, J. M., Falconer, J. & Bassett, J. M. The relationship of body and placental weight to plasma levels of insulin and other hormones during development in fetal rabbits. *Diabetologia* **23**, 124–130 (1982).
621. Palmer, J. P., Fleming, G. A., Greenbaum, C. J., Herold, K. C., Jansa, L. D., Kolb, H., Lachin, J. M., Polonsky, K. S., Pozzilli, P., Skyler, J. S. & Steffes, M. W. C-peptide is the appropriate outcome measure for type 1 diabetes clinical trials to preserve beta-cell function: report of an ADA workshop, 21-22 October 2001. *Diabetes* **53**, 250–264 (2004).
622. Righettoni, M., Tricoli, A. & Pratsinis, S. E. Si:WO(3) Sensors for highly selective detection of acetone for easy diagnosis of diabetes by breath analysis. *Anal. Chem.* **82**, 3581–3587 (2010).
623. Gossen, M. & Bujard, H. Tight control of gene expression in mammalian cells by tetracycline-responsive promoters. *Proc. Natl. Acad. Sci. U.S.A.* **89**, 5547–5551 (1992).
624. Furth, P. A., St Onge, L., Böger, H., Gruss, P., Gossen, M., Kistner, A., Bujard, H. & Hennighausen, L. Temporal control of gene expression in transgenic mice by a tetracycline-responsive promoter. *Proc. Natl. Acad. Sci. U.S.A.* **91**, 9302–9306 (1994).
625. Gossen, M., Freundlieb, S., Bender, G., Müller, G., Hillen, W. & Bujard, H. Transcriptional activation by tetracyclines in mammalian cells. *Science* **268**, 1766–1769 (1995).
626. Schultze, N., Burki, Y., Lang, Y., Certa, U. & Bluethmann, H. Efficient control of gene expression by single step integration of the tetracycline system in transgenic mice. *Nat. Biotechnol.* **14**, 499–503 (1996).
627. Stieger, K., Belbellaa, B., Le Guiner, C., Moullier, P. & Rolling, F. In vivo gene regulation using tetracycline-regulatable systems. *Adv. Drug Deliv. Rev.* **61**, 527–541 (2009).
628. Bonner-Weir, S. & Sharma, A. Pancreatic stem cells. *J. Pathol.* **197**, 519–526 (2002).
629. Passweg, J. & Tyndall, A. Autologous stem cell transplantation in autoimmune diseases. *Semin. Hematol* **44**, 278–285 (2007).
630. Nelson, J. L., Torrez, R., Louie, F. M., Choe, O. S., Storb, R. & Sullivan, K. M. Pre-existing autoimmune disease in patients with long-term survival after allogeneic bone marrow transplantation. *J Rheumatol Suppl* **48**, 23–29 (1997).
631. Lampeter, E. F., McCann, S. R. & Kolb, H. Transfer of diabetes type 1 by bone-marrow transplantation. *Lancet* **351**, 568–569 (1998).
632. Kang, E. M., Zickler, P. P., Burns, S., Langemeijer, S. M., Brenner, S., Phang, O. A., Patterson, N., Harlan, D. & Tisdale, J. F. Hematopoietic stem cell transplantation prevents diabetes in NOD mice but does

not contribute to significant islet cell regeneration once disease is established. *Exp. Hematol* **33**, 699–705 (2005).
633. Voltarelli, J. C., Couri, C. E. B., Stracieri, A. B. P. L., Oliveira, M. C., Moraes, D. A., Pieroni, F., Coutinho, M., Malmegrim, K. C. R., Foss-Freitas, M. C., Simões, B. P., Foss, M. C., Squiers, E. & Burt, R. K. Autologous nonmyeloablative hematopoietic stem cell transplantation in newly diagnosed type 1 diabetes mellitus. *JAMA* **297**, 1568–1576 (2007).
634. Couri, C. E. B., Oliveira, M. C. B., Stracieri, A. B. P. L., Moraes, D. A., Pieroni, F., Barros, G. M. N., Madeira, M. I. A., Malmegrim, K. C. R., Foss-Freitas, M. C., Simões, B. P., Martinez, E. Z., Foss, M. C., Burt, R. K. & Voltarelli, J. C. C-peptide levels and insulin independence following autologous nonmyeloablative hematopoietic stem cell transplantation in newly diagnosed type 1 diabetes mellitus. *JAMA* **301**, 1573–1579 (2009).
635. Ryan, E. A., Lakey, J. R., Rajotte, R. V., Korbutt, G. S., Kin, T., Imes, S., Rabinovitch, A., Elliott, J. F., Bigam, D., Kneteman, N. M., Warnock, G. L., Larsen, I. & Shapiro, A. M. Clinical outcomes and insulin secretion after islet transplantation with the Edmonton protocol. *Diabetes* **50**, 710–719 (2001).
636. Bigam, D. L. & Am Shapiro, J. Pancreatic Transplantation: Beta Cell Replacement. *Curr Treat Options Gastroenterol* **7**, 329–341 (2004).
637. Shapiro, A. M. J., Ricordi, C., Hering, B. J., Auchincloss, H., Lindblad, R., Robertson, R. P., Secchi, A., Brendel, M. D., Berney, T., Brennan, D. C., Cagliero, E., Alejandro, R., Ryan, E. A., DiMercurio, B., Morel, P., Polonsky, K. S., Reems, J.-A., Bretzel, R. G., Bertuzzi, F., Froud, T., Kandaswamy, R., Sutherland, D. E. R., Eisenbarth, G., Segal, M., Preiksaitis, J., Korbutt, G. S., Barton, F. B., Viviano, L., Seyfert-Margolis, V., Bluestone, J. & Lakey, J. R. T. International trial of the Edmonton protocol for islet transplantation. *N. Engl. J. Med.* **355**, 1318–1330 (2006).
638. Shapiro, A. M. J., Nanji, S. A. & Lakey, J. R. T. Clinical islet transplant: current and future directions towards tolerance. *Immunol. Rev.* **196**, 219–236 (2003).
639. Ricordi, C. & Strom, T. B. Clinical islet transplantation: advances and immunological challenges. *Nat. Rev. Immunol.* **4**, 259–268 (2004).
640. Shapiro, A. M. J., Lakey, J. R. T., Paty, B. W., Senior, P. A., Bigam, D. L. & Ryan, E. A. Strategic opportunities in clinical islet transplantation. *Transplantation* **79**, 1304–1307 (2005).
641. Fiorina, P., Shapiro, A. M. J., Ricordi, C. & Secchi, A. The clinical impact of islet transplantation. *Am. J. Transplant.* **8**, 1990–1997 (2008).
642. CITR Research Group. 2007 update on allogeneic islet transplantation from the Collaborative Islet Transplant Registry (CITR). *Cell Transplant* **18**, 753–767 (2009).
643. Mattsson, G., Jansson, L. & Carlsson, P.-O. Decreased vascular density in mouse pancreatic islets after transplantation. *Diabetes* **51**, 1362–1366 (2002).
644. Zhang, N., Richter, A., Suriawinata, J., Harbaran, S., Altomonte, J., Cong, L., Zhang, H., Song, K., Meseck, M., Bromberg, J. & Dong, H. Elevated vascular endothelial growth factor production in islets improves islet graft vascularization. *Diabetes* **53**, 963–970 (2004).
645. Lai, Y., Schneider, D., Kidszun, A., Hauck-Schmalenberger, I., Breier, G., Brandhorst, D., Brandhorst, H., Iken, M., Brendel, M. D., Bretzel, R. G. & Linn, T. Vascular endothelial growth factor increases functional beta-cell mass by improvement of angiogenesis of isolated human and murine pancreatic islets. *Transplantation* **79**, 1530–1536 (2005).
646. Su, D., Zhang, N., He, J., Qu, S., Slusher, S., Bottino, R., Bertera, S., Bromberg, J. & Dong, H. H. Angiopoietin-1 production in islets improves islet engraftment and protects islets from cytokine-induced apoptosis. *Diabetes* **56**, 2274–2283 (2007).
647. Miao, G., Mace, J., Kirby, M., Hopper, A., Peverini, R., Chinnock, R., Shapiro, J. & Hathout, E. In vitro and in vivo improvement of islet survival following treatment with nerve growth factor. *Transplantation* **81**, 519–524 (2006).
648. Sordi, V. & Piemonti, L. Mesenchymal stem cells as feeder cells for pancreatic islet transplants. *Rev Diabet Stud* **7**, 132–143 (2010).
649. Berman, D. M., Willman, M. A., Han, D., Kleiner, G., Kenyon, N. M., Cabrera, O., Karl, J. A., Wiseman, R. W., O'Connor, D. H., Bartholomew, A. M. & Kenyon, N. S. Mesenchymal stem cells enhance allogeneic islet engraftment in nonhuman primates. *Diabetes* **59**, 2558–2568 (2010).
650. Olerud, J., Kanaykina, N., Vasylovska, S., Vasilovska, S., King, D., Sandberg, M., Jansson, L. & Kozlova, E. N. Neural crest stem cells increase beta cell proliferation and improve islet function in co-transplanted murine pancreatic islets. *Diabetologia* **52**, 2594–2601 (2009).
651. Frank, A. M., Barker, C. F. & Markmann, J. F. Comparison of whole organ pancreas and isolated islet transplantation for type 1 diabetes. *Adv Surg* **39**, 137–163 (2005).
652. Ricordi, C. Islet transplantation: a brave new world. *Diabetes* **52**, 1595–1603 (2003).
653. Froud, T., Ricordi, C., Baidal, D. A., Hafiz, M. M., Ponte, G., Cure, P., Pileggi, A., Poggioli, R., Ichii, H., Khan, A., Ferreira, J. V., Pugliese, A., Esquenazi, V. V., Kenyon, N. S. & Alejandro, R. Islet transplantation in type 1 diabetes mellitus using cultured islets and steroid-free immunosuppression: Miami experience. *Am. J. Transplant.* **5**, 2037–2046 (2005).

654. Voltarelli, J. C. & Couri, C. E. B. Stem cell transplantation for type 1 diabetes mellitus. *Diabetol Metab Syndr* **1**, 4 (2009).
655. Couri, C. E. B. & Voltarelli, J. C. Autologous stem cell transplantation for early type 1 diabetes mellitus. *Autoimmunity* **41**, 666–672 (2008).
656. Raikwar, S. P. & Zavazava, N. Spontaneous in vivo differentiation of embryonic stem cell-derived pancreatic endoderm-like cells corrects hyperglycemia in diabetic mice. *Transplantation* **91**, 11–20 (2011).
657. Zhou, Q., Brown, J., Kanarek, A., Rajagopal, J. & Melton, D. A. In vivo reprogramming of adult pancreatic exocrine cells to beta-cells. *Nature* **455**, 627–632 (2008).
658. Timper, K., Seboek, D., Eberhardt, M., Linscheid, P., Christ-Crain, M., Keller, U., Müller, B. & Zulewski, H. Human adipose tissue-derived mesenchymal stem cells differentiate into insulin, somatostatin, and glucagon expressing cells. *Biochem. Biophys. Res. Commun* **341**, 1135–1140 (2006).
659. Gao, F., Wu, D.-q., Hu, Y.-h. & Jin, G.-x. Extracellular matrix gel is necessary for in vitro cultivation of insulin producing cells from human umbilical cord blood derived mesenchymal stem cells. *Chin. Med. J* **121**, 811–818 (2008).
660. Lee, J., Han, D.-J. & Kim, S.-C. In vitro differentiation of human adipose tissue-derived stem cells into cells with pancreatic phenotype by regenerating pancreas extract. *Biochem. Biophys. Res. Commun* **375**, 547–551 (2008).
661. Okura, H., Komoda, H., Fumimoto, Y., Lee, C.-M., Nishida, T., Sawa, Y. & Matsuyama, A. Transdifferentiation of human adipose tissue-derived stromal cells into insulin-producing clusters. *J Artif Organs* **12**, 123–130 (2009).
662. Chandra, V., G, S., Phadnis, S., Nair, P. D. & Bhonde, R. R. Generation of pancreatic hormone-expressing islet-like cell aggregates from murine adipose tissue-derived stem cells. *Stem Cells* **27**, 1941–1953 (2009).
663. Lin, G., Wang, G., Liu, G., Yang, L.-J., Chang, L.-J., Lue, T. F. & Lin, C.-S. Treatment of type 1 diabetes with adipose tissue-derived stem cells expressing pancreatic duodenal homeobox 1. *Stem Cells Dev* **18**, 1399–1406 (2009).
664. Kajiyama, H., Hamazaki, T. S., Tokuhara, M., Masui, S., Okabayashi, K., Ohnuma, K., Yabe, S., Yasuda, K., Ishiura, S., Okochi, H. & Asashima, M. Pdx1-transfected adipose tissue-derived stem cells differentiate into insulin-producing cells in vivo and reduce hyperglycemia in diabetic mice. *Int. J. Dev. Biol* **54**, 699–705 (2010).
665. Amariglio, N., Hirshberg, A., Scheithauer, B. W., Cohen, Y., Loewenthal, R., Trakhtenbrot, L., Paz, N., Koren-Michowitz, M., Waldman, D., Leider-Trejo, L., Toren, A., Constantini, S. & Rechavi, G. Donor-derived brain tumor following neural stem cell transplantation in an ataxia telangiectasia patient. *PLoS Med.* **6**, e1000029 (2009).
666. Thirabanjasak, D., Tantiwongse, K. & Thorner, P. S. Angiomyeloproliferative lesions following autologous stem cell therapy. *J. Am. Soc. Nephrol.* **21**, 1218–1222 (2010).
667. Bhatia, M., Elefanty, A. G., Fisher, S. J., Patient, R., Schlaeger, T. & Snyder, E. Y. (eds) *Current Protocols in Stem Cell Biology* (John Wiley & Sons, Inc, Hoboken, NJ, USA, 2007).
668. Fahn, S. Description of Parkinson's disease as a clinical syndrome. *Ann. N. Y. Acad. Sci.* **991**, 1–14 (2003).
669. Hardy, J., Cai, H., Cookson, M. R., Gwinn-Hardy, K. & Singleton, A. Genetics of Parkinson's disease and parkinsonism. *Ann. Neurol.* **60**, 389–398 (2006).
670. Petersen, B., Lucas-Hahn, A., Oropeza, M., Hornen, N., Lemme, E., Hassel, P., Queisser, A.-L. & Niemann, H. Development and validation of a highly efficient protocol of porcine somatic cloning using preovulatory embryo transfer in peripubertal gilts. *Cloning Stem Cells* **10**, 355–362 (2008).
671. Mendicino, M., Ramsoondar, J., Phelps, C., Vaught, T., Ball, S., LeRoith, T., Monahan, J., Chen, S., Dandro, A., Boone, J., Jobst, P., Vance, A., Wertz, N., Bergman, Z., Sun, X.-Z., Polejaeva, I., Butler, J., Dai, Y., Ayares, D. & Wells, K. Generation of antibody- and B cell-deficient pigs by targeted disruption of the J-region gene segment of the heavy chain locus. *Transgenic Res* **20**, 625–641 (2011).
672. Li, S., Chen, X., Fang, Z., Shi, J. & Sheng, H. Z. Rabbits generated from fibroblasts through nuclear transfer. *Reproduction* **131**, 1085–1090 (2006).
673. Meng, Q., Polgar, Z., Liu, J. & Dinnyes, A. Live birth of somatic cell-cloned rabbits following trichostatin A treatment and cotransfer of parthenogenetic embryos. *Cloning Stem Cells* **11**, 203–208 (2009).
674. Li, S., Guo, Y., Shi, J., Yin, C., Xing, F., Xu, L., Zhang, C., Liu, T., Li, Y., Li, H., Du, L. & Chen, X. Transgene expression of enhanced green fluorescent protein in cloned rabbits generated from in vitro-transfected adult fibroblasts. *Transgenic Res* **18**, 227–235 (2009).
675. van de Velde, H., Cauffman, G., Tournaye, H., Devroey, P. & Liebaers, I. The four blastomeres of a 4-cell stage human embryo are able to develop individually into blastocysts with inner cell mass and trophectoderm. *Hum. Reprod* **23**, 1742–1747 (2008).
676. Do, J. T. & Schöler, H. R. Cell-cell fusion as a means to establish pluripotency. *Ernst Schering Res. Found. Workshop*, 35–45 (2006).

677. Mitalipov, S. & Wolf, D. Totipotency, pluripotency and nuclear reprogramming. *Adv. Biochem. Eng. Biotechnol* **114**, 185–199 (2009).
678. Smith, K. P., Luong, M. X. & Stein, G. S. Pluripotency: toward a gold standard for human ES and iPS cells. *J. Cell. Physiol* **220**, 21–29 (2009).
679. Fang, Z. F., Gai, H., Huang, Y. Z., Li, S. G., Chen, X. J., Shi, J. J., Wu, L., Liu, A., Xu, P. & Sheng, H. Z. Rabbit embryonic stem cell lines derived from fertilized, parthenogenetic or somatic cell nuclear transfer embryos. *Exp. Cell Res* **312**, 3669–3682 (2006).
680. Wang, S., Tang, X., Niu, Y., Chen, H., Li, B., Li, T., Zhang, X., Hu, Z., Zhou, Q. & Ji, W. Generation and characterization of rabbit embryonic stem cells. *Stem Cells* **25**, 481–489 (2007).
681. Honda, A., Hirose, M., Inoue, K., Ogonuki, N., Miki, H., Shimozawa, N., Hatori, M., Shimizu, N., Murata, T., Hirose, M., Katayama, K., Wakisaka, N., Miyoshi, H., Yokoyama, K. K., Sankai, T. & Ogura, A. Stable embryonic stem cell lines in rabbits: potential small animal models for human research. *Reprod. Biomed. Online* **17**, 706–715 (2008).
682. Intawicha, P., Ou, Y.-W., Lo, N.-W., Zhang, S.-C., Chen, Y.-Z., Lin, T.-A., Su, H.-L., Guu, H.-F., Chen, M.-J., Lee, K.-H., Chiu, Y.-T. & Ju, J.-C. Characterization of embryonic stem cell lines derived from New Zealand white rabbit embryos. *Cloning Stem Cells* **11**, 27–38 (2009).
683. Malaver-Ortega, L. F., Sumer, H., Liu, J. & Verma, P. J. The state of the art for pluripotent stem cells derivation in domestic ungulates. *Theriogenology* (2012).
684. Hall, V. J., Kristensen, M., Rasmussen, M. A., Ujhelly, O., Dinnyés, A. & Hyttel, P. Temporal Repression of Endogenous Pluripotency Genes during Reprogramming of Porcine Induced Pluripotent Stem Cells. *Cellular reprogramming* (2012).
685. Maruotti, J., Muñoz, M., Degrelle, S. A., Gómez, E., Louet, C., Monforte, C. D., Longchamp, P. H. de, Brochard, V., Hue, I., Caamaño, J. N. & Jouneau, A. Efficient derivation of bovine embryonic stem cells needs more than active core pluripotency factors. *Mol Reprod Dev.* **79**, 461-477 (2012).
686. Khodadadi, K., Sumer, H., Pashaiasl, M., Lim, S., Williamson, M. & Verma, P. J. Induction of Pluripotency in Adult Equine Fibroblasts without c-MYC. *Stem Cells Int* **2012**, 429160 (2012).
687. Ye, S., Tan, L., Yang, R., Fang, B., Qu, S., Schulze, E. N., Song, H., Ying, Q. & Li, P. Pleiotropy of Glycogen Synthase Kinase-3 Inhibition by CHIR99021 Promotes Self-Renewal of Embryonic Stem Cells from Refractory Mouse Strains. *PLoS ONE* **7**, e35892 (2012).
688. Sharma, M., Kumar, R., Dubey, P. K., Verma, O. P., Nath, A., Saikumar, G. & Sharma, G. T. Expression and quantification of Oct-4 gene in blastocyst and embryonic stem cells derived from in vitro produced buffalo embryos. *In Vitro Cell. Dev. Biol. Anim.* **48**, 229–235 (2012).
689. Nichols, J., Chambers, I., Taga, T. & Smith, A. Physiological rationale for responsiveness of mouse embryonic stem cells to gp130 cytokines. *Development* **128**, 2333–2339 (2001).
690. Li, Y., McClintick, J., Zhong, L., Edenberg, H. J., Yoder, M. C. & Chan, R. J. Murine embryonic stem cell differentiation is promoted by SOCS-3 and inhibited by the zinc finger transcription factor Klf4. *Blood* **105**, 635–637 (2005).
691. Bechard, M. & Dalton, S. Subcellular localization of glycogen synthase kinase 3beta controls embryonic stem cell self-renewal. *Mol. Cell. Biol* **29**, 2092–2104 (2009).
692. Niwa, H., Ogawa, K., Shimosato, D. & Adachi, K. A parallel circuit of LIF signalling pathways maintains pluripotency of mouse ES cells. *Nature* **460**, 118–122 (2009).
693. Beattie, G. M., Lopez, A. D., Bucay, N., Hinton, A., Firpo, M. T., King, C. C. & Hayek, A. Activin A maintains pluripotency of human embryonic stem cells in the absence of feeder layers. *Stem Cells* **23**, 489–495 (2005).
694. James, D., Levine, A. J., Besser, D. & Hemmati-Brivanlou, A. TGFbeta/activin/nodal signaling is necessary for the maintenance of pluripotency in human embryonic stem cells. *Development* **132**, 1273–1282 (2005).
695. Hsu, D. R., Economides, A. N., Wang, X., Eimon, P. M. & Harland, R. M. The Xenopus dorsalizing factor Gremlin identifies a novel family of secreted proteins that antagonize BMP activities. *Mol. Cell* **1**, 673–683 (1998).
696. Carpenter, M. K., Rosler, E. S., Fisk, G. J., Brandenberger, R., Ares, X., Miura, T., Lucero, M. & Rao, M. S. Properties of four human embryonic stem cell lines maintained in a feeder-free culture system. *Dev. Dyn* **229**, 243–258 (2004).
697. Rosler, E. S., Fisk, G. J., Ares, X., Irving, J., Miura, T., Rao, M. S. & Carpenter, M. K. Long-term culture of human embryonic stem cells in feeder-free conditions. *Dev. Dyn* **229**, 259–274 (2004).
698. Chen, S., Do, J. T., Zhang, Q., Yao, S., Yan, F., Peters, E. C., Schöler, H. R., Schultz, P. G. & Ding, S. Self-renewal of embryonic stem cells by a small molecule. *Proc. Natl. Acad. Sci. U.S.A* **103**, 17266–17271 (2006).
699. Ying, Q.-L., Wray, J., Nichols, J., Batlle-Morera, L., Doble, B., Woodgett, J., Cohen, P. & Smith, A. The ground state of embryonic stem cell self-renewal. *Nature* **453**, 519–523 (2008).
700. Lanner, F. & Rossant, J. The role of FGF/Erk signaling in pluripotent cells. *Development* **137**, 3351–3360 (2010).

701. Storm, M. P., Bone, H. K., Beck, C. G., Bourillot, P.-Y., Schreiber, V., Damiano, T., Nelson, A., Savatier, P. & Welham, M. J. Regulation of Nanog expression by phosphoinositide 3-kinase-dependent signaling in murine embryonic stem cells. *J. Biol. Chem* **282**, 6265–6273 (2007).
702. Yuan, H., Corbi, N., Basilico, C. & Dailey, L. Developmental-specific activity of the FGF-4 enhancer requires the synergistic action of Sox2 and Oct-3. *Genes Dev* **9**, 2635–2645 (1995).
703. Stefanovic, S., Abboud, N., Désilets, S., Nury, D., Cowan, C. & Pucéat, M. Interplay of Oct4 with Sox2 and Sox17: a molecular switch from stem cell pluripotency to specifying a cardiac fate. *J. Cell Biol* **186**, 665–673 (2009).
704. Snyder, M., Huang, X.-Y. & Zhang, J. J. Stat3 directly controls the expression of Tbx5, Nkx2.5, and GATA4 and is essential for cardiomyocyte differentiation of P19CL6 cells. *J. Biol. Chem* **285**, 23639–23646 (2010).
705. Yang, W., Wei, W., Shi, C., Zhu, J., Ying, W., Shen, Y., Ye, X., Fang, L., Duo, S., Che, J., Shen, H., Ding, S. & Deng, H. Pluripotin combined with leukemia inhibitory factor greatly promotes the derivation of embryonic stem cell lines from refractory strains. *Stem Cells* **27**, 383–389 (2009).
706. Hanna, J., Markoulaki, S., Mitalipova, M., Cheng, A. W., Cassady, J. P., Staerk, J., Carey, B. W., Lengner, C. J., Foreman, R., Love, J., Gao, Q., Kim, J. & Jaenisch, R. Metastable pluripotent states in NOD-mouse-derived ESCs. *Cell Stem Cell* **4**, 513–524 (2009).
707. Nichols, J., Jones, K., Phillips, J. M., Newland, S. A., Roode, M., Mansfield, W., Smith, A. & Cooke, A. Validated germline-competent embryonic stem cell lines from nonobese diabetic mice. *Nat. Med* **15**, 814–818 (2009).
708. Buehr, M. & Smith, A. Genesis of embryonic stem cells. *Philos. Trans. R. Soc. Lond., B, Biol. Sci* **358**, 1397-402; discussion 1402 (2003).
709. Batlle-Morera, L., Smith, A. & Nichols, J. Parameters influencing derivation of embryonic stem cells from murine embryos. *Genesis* **46**, 758–767 (2008).
710. Kiyonari, H., Kaneko, M., Abe, S.-i. & Aizawa, S. Three inhibitors of FGF receptor, ERK, and GSK3 establishes germline-competent embryonic stem cells of C57BL/6N mouse strain with high efficiency and stability. *Genesis* **48**, 317–327 (2010).
711. Bendall, S. C., Stewart, M. H., Menendez, P., George, D., Vijayaragavan, K., Werbowetski-Ogilvie, T., Ramos-Mejia, V., Rouleau, A., Yang, J., Bossé, M., Lajoie, G. & Bhatia, M. IGF and FGF cooperatively establish the regulatory stem cell niche of pluripotent human cells in vitro. *Nature* **448**, 1015–1021 (2007).
712. Brill, L. M., Xiong, W., Lee, K.-B., Ficarro, S. B., Crain, A., Xu, Y., Terskikh, A., Snyder, E. Y. & Ding, S. Phosphoproteomic analysis of human embryonic stem cells. *Cell Stem Cell* **5**, 204–213 (2009).
713. Miyabayashi, T., Teo, J.-L., Yamamoto, M., McMillan, M., Nguyen, C. & Kahn, M. Wnt/beta-catenin/CBP signaling maintains long-term murine embryonic stem cell pluripotency. *Proc. Natl. Acad. Sci. U.S.A* **104**, 5668–5673 (2007).
714. Burton, P., Adams, D. R., Abraham, A., Allcock, R. W., Jiang, Z., McCahill, A., Gilmour, J., McAbney, J., Kaupisch, A., Kane, N. M., Baillie, G. S., Baker, A. H., Milligan, G., Houslay, M. D. & Mountford, J. C. Erythro-9-(2-hydroxy-3-nonyl)adenine (EHNA) blocks differentiation and maintains the expression of pluripotency markers in human embryonic stem cells. *Biochem. J* **432**, 575–584 (2010).
715. Burton, P., Adams, D. R., Abraham, A., Allcock, R. W., Jiang, Z., McCahill, A., Gilmour, J., McAbney, J., Kane, N. M., Baillie, G. S., McKenzie, F. R., Baker, A. H., Houslay, M. D., Mountford, J. C. & Milligan, G. Identification and characterization of small-molecule ligands that maintain pluripotency of human embryonic stem cells. *Biochem. Soc. Trans* **38**, 1058–1061 (2010).
716. Li, J., Wang, G., Wang, C., Zhao, Y., Zhang, H., Tan, Z., Song, Z., Ding, M. & Deng, H. MEK/ERK signaling contributes to the maintenance of human embryonic stem cell self-renewal. *Differentiation* **75**, 299–307 (2007).
717. Hanna, J., Cheng, A. W., Saha, K., Kim, J., Lengner, C. J., Soldner, F., Cassady, J. P., Muffat, J., Carey, B. W. & Jaenisch, R. Human embryonic stem cells with biological and epigenetic characteristics similar to those of mouse ESCs. *Proc. Natl. Acad. Sci. U.S.A* **107**, 9222–9227 (2010).
718. Tsutsui, H., Valamehr, B., Hindoyan, A., Qiao, R., Ding, X., Guo, S., Witte, O. N., Liu, X., Ho, C.-M. & Wu, H. An optimized small molecule inhibitor cocktail supports long-term maintenance of human embryonic stem cells. *Nat Commun* **2**, 167 (2011).
719. Nichols, J. & Smith, A. The origin and identity of embryonic stem cells. *Development* **138**, 3–8 (2011).
720. Hsieh, Y.-C., Intawicha, P., Lee, K.-H., Chiu, Y.-T., Lo, N.-W. & Ju, J.-C. LIF and FGF cooperatively support stemness of rabbit embryonic stem cells derived from parthenogenetically activated embryos. *Cell Reprogram* **13**, 241–255 (2011).
721. Ohgushi, M., Matsumura, M., Eiraku, M., Murakami, K., Aramaki, T., Nishiyama, A., Muguruma, K., Nakano, T., Suga, H., Ueno, M., Ishizaki, T., Suemori, H., Narumiya, S., Niwa, H. & Sasai, Y. Molecular pathway and cell state responsible for dissociation-induced apoptosis in human pluripotent stem cells. *Cell Stem Cell* **7**, 225–239 (2010).
722. Chen, G., Hou, Z., Gulbranson, D. R. & Thomson, J. A. Actin-myosin contractility is responsible for the reduced viability of dissociated human embryonic stem cells. *Cell Stem Cell* **7**, 240–248 (2010).

723. Xu, Y., Zhu, X., Hahm, H. S., Wei, W., Hao, E., Hayek, A. & Ding, S. Revealing a core signaling regulatory mechanism for pluripotent stem cell survival and self-renewal by small molecules. *Proc. Natl. Acad. Sci. U.S.A* **107**, 8129–8134 (2010).
724. Anderson, S. C., Stone, C., Tkach, L. & SundarRaj, N. Rho and Rho-kinase (ROCK) signaling in adherens and gap junction assembly in corneal epithelium. *Invest. Ophthalmol. Vis. Sci.* **43**, 978–986 (2002).
725. Sturge, J., Wienke, D. & Isacke, C. M. Endosomes generate localized Rho-ROCK-MLC2-based contractile signals via Endo180 to promote adhesion disassembly. *J. Cell Biol.* **175**, 337–347 (2006).
726. Watanabe, K., Ueno, M., Kamiya, D., Nishiyama, A., Matsumura, M., Wataya, T., Takahashi, J. B., Nishikawa, S., Nishikawa, S.-i., Muguruma, K. & Sasai, Y. A ROCK inhibitor permits survival of dissociated human embryonic stem cells. *Nat. Biotechnol.* **25**, 681–686 (2007).
727. Gauthaman, K., Fong, C.-Y. & Bongso, A. Effect of ROCK inhibitor Y-27632 on normal and variant human embryonic stem cells (hESCs) in vitro: its benefits in hESC expansion. *Stem Cell Rev* **6**, 86–95 (2010).
728. Ichikawa, H., Yoshie, S., Shirasawa, S., Yokoyama, T., Yue, F., Tomotsune, D. & Sasaki, K. Freeze-thawing single human embryonic stem cells induce e-cadherin and actin filament network disruption via g13 signaling. *Cryo Letters* **32**, 516–524 (2011).
729. Zhang, L., Valdez, J. M., Zhang, B., Wei, L., Chang, J. & Xin, L. ROCK inhibitor Y-27632 suppresses dissociation-induced apoptosis of murine prostate stem/progenitor cells and increases their cloning efficiency. *PLoS ONE* **6**, e18271 (2011).
730. Kawamata, M. & Ochiya, T. Generation of genetically modified rats from embryonic stem cells. *Proc. Natl. Acad. Sci. U.S.A* **107**, 14223–14228 (2010).
731. Paling, N. R. D., Wheadon, H., Bone, H. K. & Welham, M. J. Regulation of embryonic stem cell self-renewal by phosphoinositide 3-kinase-dependent signaling. *J. Biol. Chem* **279**, 48063–48070 (2004).
732. Armstrong, L., Hughes, O., Yung, S., Hyslop, L., Stewart, R., Wappler, I., Peters, H., Walter, T., Stojkovic, P., Evans, J., Stojkovic, M. & Lako, M. The role of PI3K/AKT, MAPK/ERK and NFkappabeta signalling in the maintenance of human embryonic stem cell pluripotency and viability highlighted by transcriptional profiling and functional analysis. *Hum. Mol. Genet* **15**, 1894–1913 (2006).
733. Xu, C., Inokuma, M. S., Denham, J., Golds, K., Kundu, P., Gold, J. D. & Carpenter, M. K. Feeder-free growth of undifferentiated human embryonic stem cells. *Nat. Biotechnol* **19**, 971–974 (2001).
734. Amit, M., Shariki, C., Margulets, V. & Itskovitz-Eldor, J. Feeder layer- and serum-free culture of human embryonic stem cells. *Biol. Reprod* **70**, 837–845 (2004).
735. Hoffman, L. M. & Carpenter, M. K. Characterization and culture of human embryonic stem cells. *Nat Biotechnol* **23**, 699–708 (2005).
736. Nichols, J., Silva, J., Roode, M. & Smith, A. Suppression of Erk signalling promotes ground state pluripotency in the mouse embryo. *Development* **136**, 3215–3222 (2009).
737. Kunath, T., Saba-El-Leil, M. K., Almousailleakh, M., Wray, J., Meloche, S. & Smith, A. FGF stimulation of the Erk1/2 signalling cascade triggers transition of pluripotent embryonic stem cells from self-renewal to lineage commitment. *Development* **134**, 2895–2902 (2007).
738. Stavridis, M. P., Lunn, J. S., Collins, B. J. & Storey, K. G. A discrete period of FGF-induced Erk1/2 signalling is required for vertebrate neural specification. *Development* **134**, 2889–2894 (2007).
739. Ezashi, T., Das, P. & Roberts, R. M. Low O2 tensions and the prevention of differentiation of hES cells. *Proc. Natl. Acad. Sci. U.S.A* **102**, 4783–4788 (2005).
740. Lin, Q., Lee, Y.-J. & Yun, Z. Differentiation arrest by hypoxia. *J. Biol. Chem* **281**, 30678–30683 (2006).
741. Tsatmali, M., Walcott, E. C. & Crossin, K. L. Newborn neurons acquire high levels of reactive oxygen species and increased mitochondrial proteins upon differentiation from progenitors. *Brain Res* **1040**, 137–150 (2005).
742. Wion, D., Christen, T., Barbier, E. L. & Coles, J. A. PO(2) matters in stem cell culture. *Cell Stem Cell* **5**, 242–243 (2009).
743. Lengner, C. J., Gimelbrant, A. A., Erwin, J. A., Cheng, A. W., Guenther, M. G., Welstead, G. G., Alagappan, R., Frampton, G. M., Xu, P., Muffat, J., Santagata, S., Powers, D., Barrett, C. B., Young, R. A., Lee, J. T., Jaenisch, R. & Mitalipova, M. Derivation of pre-X inactivation human embryonic stem cells under physiological oxygen concentrations. *Cell* **141**, 872–883 (2010).
744. Silva, J., Barrandon, O., Nichols, J., Kawaguchi, J., Theunissen, T. W. & Smith, A. Promotion of reprogramming to ground state pluripotency by signal inhibition. *PLoS Biol* **6**, e253 (2008).
745. Hu, C.-J., Wang, L.-Y., Chodosh, L. A., Keith, B. & Simon, M. C. Differential roles of hypoxia-inducible factor 1alpha (HIF-1alpha) and HIF-2alpha in hypoxic gene regulation. *Mol. Cell. Biol* **23**, 9361–9374 (2003).
746. Covello, K. L., Kehler, J., Yu, H., Gordan, J. D., Arsham, A. M., Hu, C.-J., Labosky, P. A., Simon, M. C. & Keith, B. HIF-2alpha regulates Oct-4: effects of hypoxia on stem cell function, embryonic development, and tumor growth. *Genes Dev* **20**, 557–570 (2006).

747. Yoshida, Y., Takahashi, K., Okita, K., Ichisaka, T. & Yamanaka, S. Hypoxia enhances the generation of induced pluripotent stem cells. *Cell Stem Cell* **5**, 237–241 (2009).
748. Westfall, S. D., Sachdev, S., Das, P., Hearne, L. B., Hannink, M., Roberts, R. M. & Ezashi, T. Identification of oxygen-sensitive transcriptional programs in human embryonic stem cells. *Stem Cells Dev* **17**, 869–881 (2008).
749. Forsyth, N. R., Kay, A., Hampson, K., Downing, A., Talbot, R. & McWhir, J. Transcriptome alterations due to physiological normoxic (2% O2) culture of human embryonic stem cells. *Regen Med* **3**, 817–833 (2008).
750. Heng, B. C., Cao, T. & Lee, E. H. Directing stem cell differentiation into the chondrogenic lineage in vitro. *Stem Cells* **22**, 1152–1167 (2004).
751. Miguel, M. P. de, Fuentes-Julián, S. & Alcaina, Y. Pluripotent stem cells: origin, maintenance and induction. *Stem Cell Rev* **6**, 633–649 (2010).
752. Wei, C. L., Miura, T., Robson, P., Lim, S.-K., Xu, X.-Q., Lee, M. Y.-C., Gupta, S., Stanton, L., Luo, Y., Schmitt, J., Thies, S., Wang, W., Khrebtukova, I., Zhou, D., Liu, E. T., Ruan, Y. J., Rao, M. & Lim, B. Transcriptome profiling of human and murine ESCs identifies divergent paths required to maintain the stem cell state. *Stem Cells* **23**, 166–185 (2005).
753. Ohtsuka, S. & Dalton, S. Molecular and biological properties of pluripotent embryonic stem cells. *Gene Ther* **15**, 74–81 (2008).
754. Zhou, X., Sasaki, H., Lowe, L., Hogan, B. L. & Kuehn, M. R. Nodal is a novel TGF-beta-like gene expressed in the mouse node during gastrulation. *Nature* **361**, 543–547 (1993).
755. Xu, R.-H., Peck, R. M., Li, D. S., Feng, X., Ludwig, T. & Thomson, J. A. Basic FGF and suppression of BMP signaling sustain undifferentiated proliferation of human ES cells. *Nat. Methods* **2**, 185–190 (2005).
756. Levenstein, M. E., Ludwig, T. E., Xu, R.-H., Llanas, R. A., VanDenHeuvel-Kramer, K., Manning, D. & Thomson, J. A. Basic fibroblast growth factor support of human embryonic stem cell self-renewal. *Stem Cells* **24**, 568–574 (2006).
757. Xiao, L., Yuan, X. & Sharkis, S. J. Activin A maintains self-renewal and regulates fibroblast growth factor, Wnt, and bone morphogenic protein pathways in human embryonic stem cells. *Stem Cells* **24**, 1476–1486 (2006).
758. Guo, G., Yang, J., Nichols, J., Hall, J. S., Eyres, I., Mansfield, W. & Smith, A. Klf4 reverts developmentally programmed restriction of ground state pluripotency. *Development* **136**, 1063–1069 (2009).
759. Greber, B., Lehrach, H. & Adjaye, J. Control of early fate decisions in human ES cells by distinct states of TGFbeta pathway activity. *Stem Cells Dev* **17**, 1065–1077 (2008).
760. Zhou, H., Li, W., Zhu, S., Joo, J. Y., Do, J. T., Xiong, W., Kim, J. B., Zhang, K., Schöler, H. R. & Ding, S. Conversion of mouse epiblast stem cells to an earlier pluripotency state by small molecules. *J. Biol. Chem* **285**, 29676–29680 (2010).
761. Chou, Y.-F., Chen, H.-H., Eijpe, M., Yabuuchi, A., Chenoweth, J. G., Tesar, P., Lu, J., McKay, R. D. G. & Geijsen, N. The growth factor environment defines distinct pluripotent ground states in novel blastocyst-derived stem cells. *Cell* **135**, 449–461 (2008).
762. Laslett, A. L., Grimmond, S., Gardiner, B., Stamp, L., Lin, A., Hawes, S. M., Wormald, S., Nikolic-Paterson, D., Haylock, D. & Pera, M. F. Transcriptional analysis of early lineage commitment in human embryonic stem cells. *BMC Dev. Biol* **7**, 12 (2007).
763. Hough, S. R., Laslett, A. L., Grimmond, S. B., Kolle, G. & Pera, M. F. A continuum of cell states spans pluripotency and lineage commitment in human embryonic stem cells. *PLoS ONE* **4**, e7708 (2009).
764. Kolle, G., Ho, M., Zhou, Q., Chy, H. S., Krishnan, K., Cloonan, N., Bertoncello, I., Laslett, A. L. & Grimmond, S. M. Identification of human embryonic stem cell surface markers by combined membrane-polysome translation state array analysis and immunotranscriptional profiling. *Stem Cells* **27**, 2446–2456 (2009).
765. Ben-Shushan, E., Thompson, J. R., Gudas, L. J. & Bergman, Y. Rex-1, a gene encoding a transcription factor expressed in the early embryo, is regulated via Oct-3/4 and Oct-6 binding to an octamer site and a novel protein, Rox-1, binding to an adjacent site. *Mol. Cell. Biol* **18**, 1866–1878 (1998).
766. Catena, R., Tiveron, C., Ronchi, A., Porta, S., Ferri, A., Tatangelo, L., Cavallaro, M., Favaro, R., Ottolenghi, S., Reinbold, R., Schöler, H. & Nicolis, S. K. Conserved POU binding DNA sites in the Sox2 upstream enhancer regulate gene expression in embryonic and neural stem cells. *J. Biol. Chem* **279**, 41846–41857 (2004).
767. van den Berg, D. L. C., Zhang, W., Yates, A., Engelen, E., Takacs, K., Bezstarosti, K., Demmers, J., Chambers, I. & Poot, R. A. Estrogen-related receptor beta interacts with Oct4 to positively regulate Nanog gene expression. *Mol. Cell. Biol* **28**, 5986–5995 (2008).
768. Boyer, L. A., Lee, T. I., Cole, M. F., Johnstone, S. E., Levine, S. S., Zucker, J. P., Guenther, M. G., Kumar, R. M., Murray, H. L., Jenner, R. G., Gifford, D. K., Melton, D. A., Jaenisch, R. & Young, R. A. Core transcriptional regulatory circuitry in human embryonic stem cells. *Cell* **122**, 947–956 (2005).
769. Loh, Y.-H., Wu, Q., Chew, J.-L., Vega, V. B., Zhang, W., Chen, X., Bourque, G., George, J., Leong, B., Liu, J., Wong, K.-Y., Sung, K. W., Lee, C. W. H., Zhao, X.-D., Chiu, K.-P., Lipovich, L., Kuznetsov, V. A.,

Robson, P., Stanton, L. W., Wei, C.-L., Ruan, Y., Lim, B. & Ng, H.-H. The Oct4 and Nanog transcription network regulates pluripotency in mouse embryonic stem cells. *Nat. Genet* **38**, 431–440 (2006).
770. Chen, X., Xu, H., Yuan, P., Fang, F., Huss, M., Vega, V. B., Wong, E., Orlov, Y. L., Zhang, W., Jiang, J., Loh, Y.-H., Yeo, H. C., Yeo, Z. X., Narang, V., Govindarajan, K. R., Leong, B., Shahab, A., Ruan, Y., Bourque, G., Sung, W.-K., Clarke, N. D., Wei, C.-L. & Ng, H.-H. Integration of external signaling pathways with the core transcriptional network in embryonic stem cells. *Cell* **133**, 1106–1117 (2008).
771. Nichols, J., Zevnik, B., Anastassiadis, K., Niwa, H., Klewe-Nebenius, D., Chambers, I., Schöler, H. & Smith, A. Formation of pluripotent stem cells in the mammalian embryo depends on the POU transcription factor Oct4. *Cell* **95**, 379–391 (1998).
772. Niwa, H., Miyazaki, J. & Smith, A. G. Quantitative expression of Oct-3/4 defines differentiation, dedifferentiation or self-renewal of ES cells. *Nat. Genet* **24**, 372–376 (2000).
773. Hu, M., Krause, D., Greaves, M., Sharkis, S., Dexter, M., Heyworth, C. & Enver, T. Multilineage gene expression precedes commitment in the hemopoietic system. *Genes Dev* **11**, 774–785 (1997).
774. Ambrosetti, D. C., Basilico, C. & Dailey, L. Synergistic activation of the fibroblast growth factor 4 enhancer by Sox2 and Oct-3 depends on protein-protein interactions facilitated by a specific spatial arrangement of factor binding sites. *Mol. Cell. Biol* **17**, 6321–6329 (1997).
775. Ambrosetti, D. C., Schöler, H. R., Dailey, L. & Basilico, C. Modulation of the activity of multiple transcriptional activation domains by the DNA binding domains mediates the synergistic action of Sox2 and Oct-3 on the fibroblast growth factor-4 enhancer. *J. Biol. Chem* **275**, 23387–23397 (2000).
776. Williams, D. C., Cai, M. & Clore, G. M. Molecular basis for synergistic transcriptional activation by Oct1 and Sox2 revealed from the solution structure of the 42-kDa Oct1.Sox2.Hoxb1-DNA ternary transcription factor complex. *J. Biol. Chem* **279**, 1449–1457 (2004).
777. Ivanova, N., Dobrin, R., Lu, R., Kotenko, I., Levorse, J., DeCoste, C., Schafer, X., Lun, Y. & Lemischka, I. R. Dissecting self-renewal in stem cells with RNA interference. *Nature* **442**, 533–538 (2006).
778. Masui, S., Nakatake, Y., Toyooka, Y., Shimosato, D., Yagi, R., Takahashi, K., Okochi, H., Okuda, A., Matoba, R., Sharov, A. A., Ko, M. S. H. & Niwa, H. Pluripotency governed by Sox2 via regulation of Oct3/4 expression in mouse embryonic stem cells. *Nat. Cell Biol* **9**, 625–635 (2007).
779. Liang, J., Wan, M., Zhang, Y., Gu, P., Xin, H., Jung, S. Y., Qin, J., Wong, J., Cooney, A. J., Liu, D. & Songyang, Z. Nanog and Oct4 associate with unique transcriptional repression complexes in embryonic stem cells. *Nat. Cell Biol* **10**, 731–739 (2008).
780. Ho, L., Jothi, R., Ronan, J. L., Cui, K., Zhao, K. & Crabtree, G. R. An embryonic stem cell chromatin remodeling complex, esBAF, is an essential component of the core pluripotency transcriptional network. *Proc. Natl. Acad. Sci. U.S.A* **106**, 5187–5191 (2009).
781. Kidder, B. L., Palmer, S. & Knott, J. G. SWI/SNF-Brg1 regulates self-renewal and occupies core pluripotency-related genes in embryonic stem cells. *Stem Cells* **27**, 317–328 (2009).
782. Bibikova, M., Laurent, L. C., Ren, B., Loring, J. F. & Fan, J.-B. Unraveling epigenetic regulation in embryonic stem cells. *Cell Stem Cell* **2**, 123–134 (2008).
783. Mitsui, K., Tokuzawa, Y., Itoh, H., Segawa, K., Murakami, M., Takahashi, K., Maruyama, M., Maeda, M. & Yamanaka, S. The homeoprotein Nanog is required for maintenance of pluripotency in mouse epiblast and ES cells. *Cell* **113**, 631–642 (2003).
784. Silva, J., Nichols, J., Theunissen, T. W., Guo, G., van Oosten, A. L., Barrandon, O., Wray, J., Yamanaka, S., Chambers, I. & Smith, A. Nanog is the gateway to the pluripotent ground state. *Cell* **138**, 722–737 (2009).
785. Chambers, I., Colby, D., Robertson, M., Nichols, J., Lee, S., Tweedie, S. & Smith, A. Functional expression cloning of Nanog, a pluripotency sustaining factor in embryonic stem cells. *Cell* **113**, 643–655 (2003).
786. Chambers, I., Silva, J., Colby, D., Nichols, J., Nijmeijer, B., Robertson, M., Vrana, J., Jones, K., Grotewold, L. & Smith, A. Nanog safeguards pluripotency and mediates germline development. *Nature* **450**, 1230–1234 (2007).
787. Ichida, J. K., Blanchard, J., Lam, K., Son, E. Y., Chung, J. E., Egli, D., Loh, K. M., Carter, A. C., Di Giorgio, F. P., Koszka, K., Huangfu, D., Akutsu, H., Liu, D. R., Rubin, L. L. & Eggan, K. A small-molecule inhibitor of tgf-Beta signaling replaces sox2 in reprogramming by inducing nanog. *Cell Stem Cell* **5**, 491–503 (2009).
788. Maherali, N. & Hochedlinger, K. Tgfbeta signal inhibition cooperates in the induction of iPSCs and replaces Sox2 and cMyc. *Curr. Biol* **19**, 1718–1723 (2009).
789. Xu, R.-H., Sampsell-Barron, T. L., Gu, F., Root, S., Peck, R. M., Pan, G., Yu, J., Antosiewicz-Bourget, J., Tian, S., Stewart, R. & Thomson, J. A. NANOG is a direct target of TGFbeta/activin-mediated SMAD signaling in human ESCs. *Cell Stem Cell* **3**, 196–206 (2008).
790. Axelrod, H. R. Embryonic stem cell lines derived from blastocysts by a simplified technique. *Dev. Biol.* **101**, 225–228 (1984).

791. Heins, N., Englund, M. C. O., Sjöblom, C., Dahl, U., Tonning, A., Bergh, C., Lindahl, A., Hanson, C. & Semb, H. Derivation, characterization, and differentiation of human embryonic stem cells. *Stem Cells* **22**, 367–376 (2004).
792. Chen, A. E. & Melton, D. A. Derivation of human embryonic stem cells by immunosurgery. *J Vis Exp*, 574 (2007).
793. Cole, R. J., Edwards, R. G. & Paul, J. Cytodifferentiation in cell colonies and cell strains derived from cleaving ova and blastocysts of the rabbit. *Exp. Cell Res.* **37**, 501–504 (1965).
794. Cole, R. J., Edwards, R. G. & Paul, J. Cytodifferentiation and embryogenesis in cell colonies and tissue cultures derived from ova and blastocysts of the rabbit. *Dev. Biol.* **13**, 385–407 (1966).
795. Alliston, C. W. & Pardee, N. R. Variability of embryonic development in the rabbit at 19 to 168 hours after mating. *Lab. Anim. Sci.* **23**, 665–670 (1973).
796. Moreadith, R. W. & Graves, K. H. Derivation of pluripotential embryonic stem cells from the rabbit. *Trans. Assoc. Am. Physicians* **105**, 197–203 (1992).
797. Graves, K. H. & Moreadith, R. W. Derivation and characterization of putative pluripotential embryonic stem cells from preimplantation rabbit embryos. *Mol. Reprod. Dev.* **36**, 424–433 (1993).
798. Du, F., Giles, J. R., Foote, R. H., Graves, K. H., Yang, X. & Moreadith, R. W. Nuclear transfer of putative rabbit embryonic stem cells leads to normal blastocyst development. *J. Reprod. Fertil.* **104**, 219–223 (1995).
799. Schoonjans, L., Albright, G. M., Li, J. L., Collen, D. & Moreadith, R. W. Pluripotential rabbit embryonic stem (ES) cells are capable of forming overt coat color chimeras following injection into blastocysts. *Mol. Reprod. Dev.* **45**, 439–443 (1996).
800. Wang, S., Shen, Y., Yuan, X., Chen, K., Guo, X., Chen, Y., Niu, Y., Li, J., Xu, R.-H., Yan, X., Zhou, Q. & Ji, W. Dissecting signaling pathways that govern self-renewal of rabbit embryonic stem cells. *J. Biol. Chem.* **283**, 35929–35940 (2008).
801. Chiang, S.-K., Chang, H.-H., Ou, Y.-W., Intawicha, P., Cheng, S.-P., Chen, L.-R., Lee, K.-H., Giles, J. & Ju, J.-C. Successful induction of antisera against rabbit embryos for isolation of the ICM and putative embryonic stem cells. *Reprod. Domest. Anim.* **43**, 181–188 (2008).
802. Catunda, A. P., Gócza, E., Carstea, B. V., Hiripi, L., Hayes, H., Rogel-Gaillard, C., Bertaud, M. & Bosze, Z. Characterization, chromosomal assignment, and role of LIFR in early embryogenesis and stem cell establishment of rabbits. *Cloning Stem Cells* **10**, 523–534 (2008).
803. Gócza, E. Program and abstracts of the 6th Transgenic Technology Meeting (TT2005). *Transgenic Res* **14**, 483–529 (2005).
804. Tancos, Z., Ujhelly, O., Pirity, M. K. & Dinnyes, A. 223 isolation of rabbit pluripotency genes to generate rabbit induced pluripotent stem cells. *Reprod. Fertil. Dev.* **24**, 223–224 (2011).
805. Dinnyes, A., Pirity, M. K., Gocza, E., Osteil, P., Daniel, N., Tancos, Z., Polgar, Z., Maraghechi, P., Ujhelly, O., Nemes, C., Stout, T., Tapponnier, Y., Bosze, Z., Jouneau, A., Afanassieff, M. & Savatier, P. Generation of rabbit pluripotent stem cell lines. *Reprod. Fertil. Dev.* **24**, 286 (2012).
806. Honda, A., Hirose, M. & Ogura, A. Basic FGF and Activin/Nodal but not LIF signaling sustain undifferentiated status of rabbit embryonic stem cells. *Exp. Cell Res.* **315**, 2033–2042 (2009).
807. Honda, A., Hirose, M., Hatori, M., Matoba, S., Miyoshi, H., Inoue, K. & Ogura, A. Generation of induced pluripotent stem cells in rabbits: potential experimental models for human regenerative medicine. *J. Biol. Chem.* **285**, 31362–31369 (2010).
808. Lodge, P., McWhir, J., Gallagher, E. & Sang, H. Increased gp130 signaling in combination with inhibition of the MEK/ERK pathway facilitates embryonic stem cell isolation from normally refractory murine CBA blastocysts. *Cloning Stem Cells* **7**, 2–7 (2005).
809. Mamo, S., Gal, A. B., Polgar, Z. & Dinnyes, A. Expression profiles of the pluripotency marker gene POU5F1 and validation of reference genes in rabbit oocytes and preimplantation stage embryos. *BMC Mol. Biol.* **9**, 67 (2008).
810. Kobolak, J., Kiss, K., Polgar, Z., Mamo, S., Rogel-Gaillard, C., Tancos, Z., Bock, I., Baji, A. G., Tar, K., Pirity, M. K. & Dinnyes, A. Promoter analysis of the rabbit POU5F1 gene and its expression in preimplantation stage embryos. *BMC Mol. Biol.* **10**, 88 (2009).
811. Chen, C.-H., Chang, W.-F., Liu, C.-C., Su, H.-Y., Shyue, S.-K., Cheng, W. T. K., Chen, Y. E., Wu, S.-C., Du, F., Sung, L.-Y. & Xu, J. Spatial and temporal distribution of Oct-4 and acetylated H4K5 in rabbit embryos. *Reproductive biomedicine online* (2012).
812. Tang, F., Barbacioru, C., Bao, S., Lee, C., Nordman, E., Wang, X., Lao, K. & Surani, M. A. Tracing the derivation of embryonic stem cells from the inner cell mass by single-cell RNA-Seq analysis. *Cell Stem Cell* **6**, 468–478 (2010).
813. Martin, G. R. & Evans, M. J. Differentiation of clonal lines of teratocarcinoma cells: formation of embryoid bodies in vitro. *Proc. Natl. Acad. Sci. U.S.A* **72**, 1441–1445 (1975).
814. Ying, Q.-L., Stavridis, M., Griffiths, D., Li, M. & Smith, A. Conversion of embryonic stem cells into neuroectodermal precursors in adherent monoculture. *Nat. Biotechnol* **21**, 183–186 (2003).

815. Ding, S., Wu, T. Y. H., Brinker, A., Peters, E. C., Hur, W., Gray, N. S. & Schultz, P. G. Synthetic small molecules that control stem cell fate. *Proc. Natl. Acad. Sci. U.S.A* **100**, 7632–7637 (2003).
816. Wu, X., Ding, S., Ding, Q., Gray, N. S. & Schultz, P. G. Small molecules that induce cardiomyogenesis in embryonic stem cells. *J. Am. Chem. Soc* **126**, 1590–1591 (2004).
817. D'Amour, K. A., Agulnick, A. D., Eliazer, S., Kelly, O. G., Kroon, E. & Baetge, E. E. Efficient differentiation of human embryonic stem cells to definitive endoderm. *Nat. Biotechnol* **23**, 1534–1541 (2005).
818. Laflamme, M. A., Chen, K. Y., Naumova, A. V., Muskheli, V., Fugate, J. A., Dupras, S. K., Reinecke, H., Xu, C., Hassanipour, M., Police, S., O'Sullivan, C., Collins, L., Chen, Y., Minami, E., Gill, E. A., Ueno, S., Yuan, C., Gold, J. & Murry, C. E. Cardiomyocytes derived from human embryonic stem cells in pro-survival factors enhance function of infarcted rat hearts. *Nat. Biotechnol* **25**, 1015–1024 (2007).
819. Zhu, S., Wurdak, H., Wang, J., Lyssiotis, C. A., Peters, E. C., Cho, C. Y., Wu, X. & Schultz, P. G. A small molecule primes embryonic stem cells for differentiation. *Cell Stem Cell* **4**, 416–426 (2009).
820. Chen, S., Borowiak, M., Fox, J. L., Maehr, R., Osafune, K., Davidow, L., Lam, K., Peng, L. F., Schreiber, S. L., Rubin, L. L. & Melton, D. A small molecule that directs differentiation of human ESCs into the pancreatic lineage. *Nat. Chem. Biol* **5**, 258–265 (2009).
821. Borowiak, M., Maehr, R., Chen, S., Chen, A. E., Tang, W., Fox, J. L., Schreiber, S. L. & Melton, D. A. Small molecules efficiently direct endodermal differentiation of mouse and human embryonic stem cells. *Cell Stem Cell* **4**, 348–358 (2009).
822. Kramer, J., Hegert, C., Guan, K., Wobus, A. M., Müller, P. K. & Rohwedel, J. Embryonic stem cell-derived chondrogenic differentiation in vitro: activation by BMP-2 and BMP-4. *Mech. Dev* **92**, 193–205 (2000).
823. Levenberg, S., Golub, J. S., Amit, M., Itskovitz-Eldor, J. & Langer, R. Endothelial cells derived from human embryonic stem cells. *Proc. Natl. Acad. Sci. U.S.A* **99**, 4391–4396 (2002).
824. Pera, M. F., Filipczyk, A. A., Hawes, S. M. & Laslett, A. L. Isolation, characterization, and differentiation of human embryonic stem cells. *Meth. Enzymol* **365**, 429–446 (2003).
825. Bhattacharya, B., Miura, T., Brandenberger, R., Mejido, J., Luo, Y., Yang, A. X., Joshi, B. H., Ginis, I., Thies, R. S., Amit, M., Lyons, I., Condie, B. G., Itskovitz-Eldor, J., Rao, M. S. & Puri, R. K. Gene expression in human embryonic stem cell lines: unique molecular signature. *Blood* **103**, 2956–2964 (2004).
826. Ginis, I., Luo, Y., Miura, T., Thies, S., Brandenberger, R., Gerecht-Nir, S., Amit, M., Hoke, A., Carpenter, M. K., Itskovitz-Eldor, J. & Rao, M. S. Differences between human and mouse embryonic stem cells. *Dev. Biol* **269**, 360–380 (2004).
827. Brandenberger, R., Wei, H., Zhang, S., Lei, S., Murage, J., Fisk, G. J., Li, Y., Xu, C., Fang, R., Guegler, K., Rao, M. S., Mandalam, R., Lebkowski, J. & Stanton, L. W. Transcriptome characterization elucidates signaling networks that control human ES cell growth and differentiation. *Nat. Biotechnol* **22**, 707–716 (2004).
828. Zhang, J. & Li, L. BMP signaling and stem cell regulation. *Dev. Biol* **284**, 1–11 (2005).
829. McLean, A. B., D'Amour, K. A., Jones, K. L., Krishnamoorthy, M., Kulik, M. J., Reynolds, D. M., Sheppard, A. M., Liu, H., Xu, Y., Baetge, E. E. & Dalton, S. Activin a efficiently specifies definitive endoderm from human embryonic stem cells only when phosphatidylinositol 3-kinase signaling is suppressed. *Stem Cells* **25**, 29–38 (2007).
830. Mogi, A., Ichikawa, H., Matsumoto, C., Hieda, T., Tomotsune, D., Sakaki, S., Yamada, S. & Sasaki, K. The method of mouse embryoid body establishment affects structure and developmental gene expression. *Tissue Cell* **41**, 79–84 (2009).
831. Wang, T., Mao, F., Lai, W., Li, W., Yu, W., Wang, Z., Zhang, L., Zhang, J., Niu, J., Zhang, X., Lahn, B. T. & Xiang, A. Multiple mesodermal lineage differentiation of Apodemus sylvaticus embryonic stem cells in vitro. *BMC Cell Biol* **11**, 42 (2010).
832. Beddington, R. S. & Robertson, E. J. An assessment of the developmental potential of embryonic stem cells in the midgestation mouse embryo. *Development* **105**, 733–737 (1989).
833. Rossant, J. Stem cells from the Mammalian blastocyst. *Stem Cells* **19**, 477–482 (2001).
834. Liu, J., Jones, K. L., Sumer, H. & Verma, P. J. Stable transgene expression in human embryonic stem cells after simple chemical transfection. *Mol. Reprod. Dev.* **76**, 580–586 (2009).
835. Xia, X., Zhang, Y., Zieth, C. R. & Zhang, S.-C. Transgenes delivered by lentiviral vector are suppressed in human embryonic stem cells in a promoter-dependent manner. *Stem Cells Dev.* **16**, 167–176 (2007).
836. Surani, M. A. Reprogramming of genome function through epigenetic inheritance. *Nature* **414**, 122–128 (2001).
837. Do, J. T. & Schöler, H. R. Nuclei of embryonic stem cells reprogram somatic cells. *Stem Cells* **22**, 941–949 (2004).
838. Do, J. T., Han, D. W. & Schöler, H. R. Reprogramming somatic gene activity by fusion with pluripotent cells. *Stem Cell Rev* **2**, 257–264 (2006).
839. Do, J. T. & Schöler, H. R. Cell fusion-induced reprogramming. *Methods Mol. Biol* **636**, 179–190 (2010).

840. Kikyo, N., Wade, P. A., Guschin, D., Ge, H. & Wolffe, A. P. Active remodeling of somatic nuclei in egg cytoplasm by the nucleosomal ATPase ISWI. *Science* **289**, 2360–2362 (2000).
841. Hansis, C., Barreto, G., Maltry, N. & Niehrs, C. Nuclear reprogramming of human somatic cells by xenopus egg extract requires BRG1. *Curr. Biol* **14**, 1475–1480 (2004).
842. Taranger, C. K., Noer, A., Sørensen, A. L., Håkelien, A.-M., Boquest, A. C. & Collas, P. Induction of dedifferentiation, genomewide transcriptional programming, and epigenetic reprogramming by extracts of carcinoma and embryonic stem cells. *Mol. Biol. Cell* **16**, 5719–5735 (2005).
843. Xu, Y.-N., Guan, N., Wang, Z.-D., Shan, Z.-Y., Shen, J.-L., Zhang, Q.-H., Jin, L.-H. & Lei, L. ES cell extract-induced expression of pluripotent factors in somatic cells. *Anat Rec (Hoboken)* **292**, 1229–1234 (2009).
844. Miyamoto, K., Tsukiyama, T., Yang, Y., Li, N., Minami, N., Yamada, M. & Imai, H. Cell-free extracts from mammalian oocytes partially induce nuclear reprogramming in somatic cells. *Biol. Reprod* **80**, 935–943 (2009).
845. Ko, K., Tapia, N., Wu, G., Kim, J. B., Bravo, M. J. A., Sasse, P., Glaser, T., Ruau, D., Han, D. W., Greber, B., Hausdörfer, K., Sebastiano, V., Stehling, M., Fleischmann, B. K., Brüstle, O., Zenke, M. & Schöler, H. R. Induction of pluripotency in adult unipotent germline stem cells. *Cell Stem Cell* **5**, 87–96 (2009).
846. Ko, K., Araúzo-Bravo, M. J., Kim, J., Stehling, M. & Schöler, H. R. Conversion of adult mouse unipotent germline stem cells into pluripotent stem cells. *Nat Protoc* **5**, 921–928 (2010).
847. Chan, K. K.-K., Zhang, J., Chia, N.-Y., Chan, Y.-S., Sim, H. S., Tan, K. S., Oh, S. K.-W., Ng, H.-H. & Choo, A. B.-H. KLF4 and PBX1 directly regulate NANOG expression in human embryonic stem cells. *Stem Cells* **27**, 2114–2125 (2009).
848. Takahashi, K., Tanabe, K., Ohnuki, M., Narita, M., Ichisaka, T., Tomoda, K. & Yamanaka, S. Induction of pluripotent stem cells from adult human fibroblasts by defined factors. *Cell* **131**, 861–872 (2007).
849. Liu, H., Zhu, F., Yong, J., Zhang, P., Hou, P., Li, H., Jiang, W., Cai, J., Liu, M., Cui, K., Qu, X., Xiang, T., Lu, D., Chi, X., Gao, G., Ji, W., Ding, M. & Deng, H. Generation of induced pluripotent stem cells from adult rhesus monkey fibroblasts. *Cell Stem Cell* **3**, 587–590 (2008).
850. Li, W., Wei, W., Zhu, S., Zhu, J., Shi, Y., Lin, T., Hao, E., Hayek, A., Deng, H. & Ding, S. Generation of rat and human induced pluripotent stem cells by combining genetic reprogramming and chemical inhibitors. *Cell Stem Cell* **4**, 16–19 (2009).
851. Liao, J., Cui, C., Chen, S., Ren, J., Chen, J., Gao, Y., Li, H., Jia, N., Cheng, L., Xiao, H. & Xiao, L. Generation of induced pluripotent stem cell lines from adult rat cells. *Cell Stem Cell* **4**, 11–15 (2009).
852. Wu, Z., Chen, J., Ren, J., Bao, L., Liao, J., Cui, C., Rao, L., Li, H., Gu, Y., Dai, H., Zhu, H., Teng, X., Cheng, L. & Xiao, L. Generation of pig induced pluripotent stem cells with a drug-inducible system. *J Mol Cell Biol* **1**, 46–54 (2009).
853. Tomioka, I., Maeda, T., Shimada, H., Kawai, K., Okada, Y., Igarashi, H., Oiwa, R., Iwasaki, T., Aoki, M., Kimura, T., Shiozawa, S., Shinohara, H., Suemizu, H., Sasaki, E. & Okano, H. Generating induced pluripotent stem cells from common marmoset (Callithrix jacchus) fetal liver cells using defined factors, including Lin28. *Genes Cells* **15**, 959–969 (2010).
854. Shimada, H., Nakada, A., Hashimoto, Y., Shigeno, K., Shionoya, Y. & Nakamura, T. Generation of canine induced pluripotent stem cells by retroviral transduction and chemical inhibitors. *Mol. Reprod. Dev* **77**, 2 (2010).
855. Woltjen, K., Michael, I. P., Mohseni, P., Desai, R., Mileikovsky, M., Hämäläinen, R., Cowling, R., Wang, W., Liu, P., Gertsenstein, M., Kaji, K., Sung, H.-K. & Nagy, A. piggyBac transposition reprograms fibroblasts to induced pluripotent stem cells. *Nature* **458**, 766–770 (2009).
856. Yusa, K., Rad, R., Takeda, J. & Bradley, A. Generation of transgene-free induced pluripotent mouse stem cells by the piggyBac transposon. *Nat. Methods* **6**, 363–369 (2009).
857. VandenDriessche, T., Ivics, Z., Izsvák, Z. & Chuah, M. K. L. Emerging potential of transposons for gene therapy and generation of induced pluripotent stem cells. *Blood* **114**, 1461–1468 (2009).
858. Kim, K., Doi, A., Wen, B., Ng, K., Zhao, R., Cahan, P., Kim, J., Aryee, M. J., Ji, H., Ehrlich, L. I. R., Yabuuchi, A., Takeuchi, A., Cunniff, K. C., Hongguang, H., McKinney-Freeman, S., Naveiras, O., Yoon, T. J., Irizarry, R. A., Jung, N., Seita, J., Hanna, J., Murakami, P., Jaenisch, R., Weissleder, R., Orkin, S. H., Weissman, I. L., Feinberg, A. P. & Daley, G. Q. Epigenetic memory in induced pluripotent stem cells. *Nature* **467**, 285–290 (2010).
859. Hasegawa, K., Zhang, P., Wei, Z., Pomeroy, J. E., Lu, W. & Pera, M. F. Comparison of reprogramming efficiency between transduction of reprogramming factors, cell-cell fusion, and cytoplast fusion. *Stem Cells* **28**, 1338–1348 (2010).
860. Slotkin, T. A., Seidler, F. J., Kavlock, R. J. & Gray, J. A. Fetal dexamethasone exposure accelerates development of renal function: relationship to dose, cell differentiation and growth inhibition. *J. Dev. Physiol* **17**, 55–61 (1992).
861. Gronthos, S., Simmons, P. J., Graves, S. E. & Robey, P. G. Integrin-mediated interactions between human bone marrow stromal precursor cells and the extracellular matrix. *Bone* **28**, 174–181 (2001).

862. Gronthos, S., Franklin, D. M., Leddy, H. A., Robey, P. G., Storms, R. W. & Gimble, J. M. Surface protein characterization of human adipose tissue-derived stromal cells. *J. Cell. Physiol* **189**, 54–63 (2001).
863. Chamberlain, G., Fox, J., Ashton, B. & Middleton, J. Concise review: mesenchymal stem cells: their phenotype, differentiation capacity, immunological features, and potential for homing. *Stem Cells* **25**, 2739–2749 (2007).
864. Lodie, T. A., Blickarz, C. E., Devarakonda, T. J., He, C., Dash, A. B., Clarke, J., Gleneck, K., Shihabuddin, L. & Tubo, R. Systematic analysis of reportedly distinct populations of multipotent bone marrow-derived stem cells reveals a lack of distinction. *Tissue Eng.* **8**, 739–751 (2002).
865. Goodell, M. A., Rosenzweig, M., Kim, H., Marks, D. F., DeMaria, M., Paradis, G., Grupp, S. A., Sieff, C. A., Mulligan, R. C. & Johnson, R. P. Dye efflux studies suggest that hematopoietic stem cells expressing low or undetectable levels of CD34 antigen exist in multiple species. *Nat. Med* **3**, 1337–1345 (1997).
866. Martin, I., Muraglia, A., Campanile, G., Cancedda, R. & Quarto, R. Fibroblast growth factor-2 supports ex vivo expansion and maintenance of osteogenic precursors from human bone marrow. *Endocrinology* **138**, 4456–4462 (1997).
867. van den Bos, C., Mosca, J. D., Winkles, J., Kerrigan, L., Burgess, W. H. & Marshak, D. R. Human mesenchymal stem cells respond to fibroblast growth factors. *Hum. Cell* **10**, 45–50 (1997).
868. Solchaga, L. A., Penick, K., Porter, J. D., Goldberg, V. M., Caplan, A. I. & Welter, J. F. FGF-2 enhances the mitotic and chondrogenic potentials of human adult bone marrow-derived mesenchymal stem cells. *J. Cell. Physiol.* **203**, 398–409 (2005).
869. Sotiropoulou, P. A., Perez, S. A., Salagianni, M., Baxevanis, C. N. & Papamichail, M. Characterization of the optimal culture conditions for clinical scale production of human mesenchymal stem cells. *Stem Cells* **24**, 462–471 (2006).
870. Ito, T., Sawada, R., Fujiwara, Y., Seyama, Y. & Tsuchiya, T. FGF-2 suppresses cellular senescence of human mesenchymal stem cells by down-regulation of TGF-beta2. *Biochem. Biophys. Res. Commun.* **359**, 108–114 (2007).
871. Lee, S.-Y., Lim, J., Khang, G., Son, Y., Choung, P.-H., Kang, S.-S., Chun, S. Y., Shin, H.-I., Kim, S.-Y. & Park, E. K. Enhanced ex vivo expansion of human adipose tissue-derived mesenchymal stromal cells by fibroblast growth factor-2 and dexamethasone. *Tissue Eng Part A* **15**, 2491–2499 (2009).
872. Quarto, N. & Longaker, M. T. FGF-2 inhibits osteogenesis in mouse adipose tissue-derived stromal cells and sustains their proliferative and osteogenic potential state. *Tissue Eng.* **12**, 1405–1418 (2006).
873. Chiou, M., Xu, Y. & Longaker, M. T. Mitogenic and chondrogenic effects of fibroblast growth factor-2 in adipose-derived mesenchymal cells. *Biochem. Biophys. Res. Commun.* **343**, 644–652 (2006).
874. Ou, G., Charles, L., Matton, S., Rodner, C., Hurley, M., Kuhn, L. & Gronowicz, G. Fibroblast growth factor-2 stimulates the proliferation of mesenchyme-derived progenitor cells from aging mouse and human bone. *J. Gerontol. A Biol. Sci. Med. Sci.* **65**, 1051–1059 (2010).
875. Mojsilović, S., Krstić, A., Ilić, V., Okić-Đorđević, I., Kocić, J., Trivanović, D., Santibañez, J. F., Jovčić, G. & Bugarski, D. IL-17 and FGF signaling involved in mouse mesenchymal stem cell proliferation. *Cell Tissue Res.* **346**, 305–316 (2011).
876. Tsutsumi, S., Shimazu, A., Miyazaki, K., Pan, H., Koike, C., Yoshida, E., Takagishi, K. & Kato, Y. Retention of multilineage differentiation potential of mesenchymal cells during proliferation in response to FGF. *Biochem. Biophys. Res. Commun.* **288**, 413–419 (2001).
877. Stewart, A. A., Byron, C. R., Pondenis, H. & Stewart, M. C. Effect of fibroblast growth factor-2 on equine mesenchymal stem cell monolayer expansion and chondrogenesis. *Am. J. Vet. Res.* **68**, 941–945 (2007).
878. Castano-Izquierdo, H., Alvarez-Barreto, J., van den Dolder, J., Jansen, J. A., Mikos, A. G. & Sikavitsas, V. I. Pre-culture period of mesenchymal stem cells in osteogenic media influences their in vivo bone forming potential. *J Biomed Mater Res A* **82**, 129–138 (2007).
879. Merkl, C. *RNA Interference in livestock Knockdown of the porcine whey protein Beta-Lactoglobulin and the tumor suppressor protein p53* (München, 2009).
880. Malladi, P., Xu, Y., Yang, G. P. & Longaker, M. T. Functions of vitamin D, retinoic acid, and dexamethasone in mouse adipose-derived mesenchymal cells. *Tissue Eng.* **12**, 2031–2040 (2006).
881. Pereira, R. F., Halford, K. W., O'Hara, M. D., Leeper, D. B., Sokolov, B. P., Pollard, M. D., Bagasra, O. & Prockop, D. J. Cultured adherent cells from marrow can serve as long-lasting precursor cells for bone, cartilage, and lung in irradiated mice. *Proc. Natl. Acad. Sci. U.S.A* **92**, 4857–4861 (1995).
882. Jaiswal, N., Haynesworth, S. E., Caplan, A. I. & Bruder, S. P. Osteogenic differentiation of purified, culture-expanded human mesenchymal stem cells in vitro. *J. Cell. Biochem* **64**, 295–312 (1997).
883. Mackay, A. M., Beck, S. C., Murphy, J. M., Barry, F. P., Chichester, C. O. & Pittenger, M. F. Chondrogenic differentiation of cultured human mesenchymal stem cells from marrow. *Tissue Eng* **4**, 415–428 (1998).
884. Johnstone, B., Hering, T. M., Caplan, A. I., Goldberg, V. M. & Yoo, J. U. In vitro chondrogenesis of bone marrow-derived mesenchymal progenitor cells. *Exp. Cell Res* **238**, 265–272 (1998).

885. Faast, R., Harrison, S. J., Beebe, L. F. S., McIlfatrick, S. M., Ashman, R. J. & Nottle, M. B. Use of adult mesenchymal stem cells isolated from bone marrow and blood for somatic cell nuclear transfer in pigs. *Cloning Stem Cells* **8**, 166–173 (2006).
886. Derfoul, A., Perkins, G. L., Hall, D. J. & Tuan, R. S. Glucocorticoids promote chondrogenic differentiation of adult human mesenchymal stem cells by enhancing expression of cartilage extracellular matrix genes. *Stem Cells* **24**, 1487–1495 (2006).
887. Zhu, Y., Liu, T., Song, K., Fan, X., Ma, X. & Cui, Z. Adipose-derived stem cell: a better stem cell than BMSC. *Cell Biochem. Funct* **26**, 664–675 (2008).
888. Ugarte, D. A. de, Alfonso, Z., Zuk, P. A., Elbarbary, A., Zhu, M., Ashjian, P., Benhaim, P., Hedrick, M. H. & Fraser, J. K. Differential expression of stem cell mobilization-associated molecules on multi-lineage cells from adipose tissue and bone marrow. *Immunol. Lett* **89**, 267–270 (2003).
889. Lapi, S., Nocchi, F., Lamanna, R., Passeri, S., Iorio, M., Paolicchi, A., Urciuoli, P., Coli, A., Abramo, F., Miragliotta, V., Giannessi, E., Stornelli, M. R., Vanacore, R., Stampacchia, G., Pisani, G., Borghetti, L. & Scatena, F. Different media and supplements modulate the clonogenic and expansion properties of rabbit bone marrow mesenchymal stem cells. *BMC Res Notes* **1**, 53 (2008).
890. Mazzetti, M. P. V., Oliveira, I. S., Miranda-Ferreira, R., Fauaz, G., Ribeiro, C. N., Gomes, P. O., Pontes, P., Ferreira, A. T. & Eça, L. P. Qualitative and quantitative analysis of rabbit's fat mesenchymal stem cells. *Acta Cir Bras* **25**, 24–27 (2010).
891. Phinney, D. G., Kopen, G., Righter, W., Webster, S., Tremain, N. & Prockop, D. J. Donor variation in the growth properties and osteogenic potential of human marrow stromal cells. *J. Cell. Biochem* **75**, 424–436 (1999).
892. Muraglia, A., Cancedda, R. & Quarto, R. Clonal mesenchymal progenitors from human bone marrow differentiate in vitro according to a hierarchical model. *J. Cell. Sci* **113 (Pt 7)**, 1161–1166 (2000).
893. Russell, K. C., Phinney, D. G., Lacey, M. R., Barrilleaux, B. L., Meyertholen, K. E. & O'Connor, K. C. In vitro high-capacity assay to quantify the clonal heterogeneity in trilineage potential of mesenchymal stem cells reveals a complex hierarchy of lineage commitment. *Stem Cells* **28**, 788–798 (2010).
894. Phinney, D. G., Kopen, G., Isaacson, R. L. & Prockop, D. J. Plastic adherent stromal cells from the bone marrow of commonly used strains of inbred mice: variations in yield, growth, and differentiation. *J. Cell. Biochem* **72**, 570–585 (1999).
895. Peister, A., Mellad, J. A., Larson, B. L., Hall, B. M., Gibson, L. F. & Prockop, D. J. Adult stem cells from bone marrow (MSCs) isolated from different strains of inbred mice vary in surface epitopes, rates of proliferation, and differentiation potential. *Blood* **103**, 1662–1668 (2004).
896. Kuznetsov, S. A., Krebsbach, P. H., Satomura, K., Kerr, J., Riminucci, M., Benayahu, D. & Robey, P. G. Single-colony derived strains of human marrow stromal fibroblasts form bone after transplantation in vivo. *J. Bone Miner. Res* **12**, 1335–1347 (1997).
897. Colter, D. C., Sekiya, I. & Prockop, D. J. Identification of a subpopulation of rapidly self-renewing and multipotential adult stem cells in colonies of human marrow stromal cells. *Proc. Natl. Acad. Sci. U.S.A* **98**, 7841–7845 (2001).
898. Sakaguchi, Y., Sekiya, I., Yagishita, K. & Muneta, T. Comparison of human stem cells derived from various mesenchymal tissues: superiority of synovium as a cell source. *Arthritis Rheum* **52**, 2521–2529 (2005).
899. Zipori, D., Duksin, D., Tamir, M., Argaman, A., Toledo, J. & Malik, Z. Cultured mouse marrow stromal cell lines. II. Distinct subtypes differing in morphology, collagen types, myelopoietic factors, and leukemic cell growth modulating activities. *J. Cell. Physiol* **122**, 81–90 (1985).
900. Tremain, N., Korkko, J., Ibberson, D., Kopen, G. C., DiGirolamo, C. & Phinney, D. G. MicroSAGE analysis of 2,353 expressed genes in a single cell-derived colony of undifferentiated human mesenchymal stem cells reveals mRNAs of multiple cell lineages. *Stem Cells* **19**, 408–418 (2001).
901. Wagner, W., Feldmann, R. E., Seckinger, A., Maurer, M. H., Wein, F., Blake, J., Krause, U., Kalenka, A., Bürgers, H. F., Saffrich, R., Wuchter, P., Kuschinsky, W. & Ho, A. D. The heterogeneity of human mesenchymal stem cell preparations--evidence from simultaneous analysis of proteomes and transcriptomes. *Exp. Hematol* **34**, 536–548 (2006).
902. Digirolamo, C. M., Stokes, D., Colter, D., Phinney, D. G., Class, R. & Prockop, D. J. Propagation and senescence of human marrow stromal cells in culture: a simple colony-forming assay identifies samples with the greatest potential to propagate and differentiate. *Br. J. Haematol* **107**, 275–281 (1999).
903. Guilak, F., Lott, K. E., Awad, H. A., Cao, Q., Hicok, K. C., Fermor, B. & Gimble, J. M. Clonal analysis of the differentiation potential of human adipose-derived adult stem cells. *J. Cell. Physiol* **206**, 229–237 (2006).
904. Anjos-Afonso, F. & Bonnet, D. Nonhematopoietic/endothelial SSEA-1+ cells define the most primitive progenitors in the adult murine bone marrow mesenchymal compartment. *Blood* **109**, 1298–1306 (2007).
905. Ylöstalo, J., Bazhanov, N. & Prockop, D. J. Reversible commitment to differentiation by human multipotent stromal cells in single-cell-derived colonies. *Exp. Hematol* **36**, 1390–1402 (2008).

906. Sengers, B. G., Dawson, J. I. & Oreffo, R. O. C. Characterisation of human bone marrow stromal cell heterogeneity for skeletal regeneration strategies using a two-stage colony assay and computational modelling. *Bone* **46**, 496–503 (2010).
907. Jiang, T., Liu, W., Lv, X., Sun, H., Zhang, L., Liu, Y., Zhang, W. J., Cao, Y. & Zhou, G. Potent in vitro chondrogenesis of CD105 enriched human adipose-derived stem cells. *Biomaterials* **31**, 3564–3571 (2010).
908. Rada, T., Reis, R. L. & Gomes, M. E. Distinct stem cells subpopulations isolated from human adipose tissue exhibit different chondrogenic and osteogenic differentiation potential. *Stem Cell Rev* **7**, 64–76 (2011).
909. Loeffler, M. & Roeder, I. Tissue stem cells: definition, plasticity, heterogeneity, self-organization and models--a conceptual approach. *Cells Tissues Organs (Print)* **171**, 8–26 (2002).
910. Zipori, D. The nature of stem cells: state rather than entity. *Nat. Rev. Genet* **5**, 873–878 (2004).
911. Zipori, D. The stem state: mesenchymal plasticity as a paradigm. *Curr Stem Cell Res Ther* **1**, 95–102 (2006).
912. Galliot, B. & Ghila, L. Cell plasticity in homeostasis and regeneration. *Mol. Reprod. Dev* **77**, 837–855 (2010).
913. Csete, M. Oxygen in the cultivation of stem cells. *Ann. N. Y. Acad. Sci* **1049**, 1–8 (2005).
914. Simon, M. C. & Keith, B. The role of oxygen availability in embryonic development and stem cell function. *Nat. Rev. Mol. Cell Biol* **9**, 285–296 (2008).
915. Lin, Q., Kim, Y., Alarcon, R. M. & Yun, Z. Oxygen and Cell Fate Decisions. *Gene Regul Syst Bio* **2**, 43–51 (2008).
916. Fehrer, C., Brunauer, R., Laschober, G., Unterluggauer, H., Reitinger, S., Kloss, F., Gülly, C., Gassner, R. & Lepperdinger, G. Reduced oxygen tension attenuates differentiation capacity of human mesenchymal stem cells and prolongs their lifespan. *Aging Cell* **6**, 745–757 (2007).
917. Krinner, A., Zscharnack, M., Bader, A., Drasdo, D. & Galle, J. Impact of oxygen environment on mesenchymal stem cell expansion and chondrogenic differentiation. *Cell Prolif* **42**, 471–484 (2009).
918. Ren, H., Cao, Y., Zhao, Q., Li, J., Zhou, C., Liao, L., Jia, M., Zhao, Q., Cai, H., Han, Z. C., Yang, R., Chen, G. & Zhao, R. C. Proliferation and differentiation of bone marrow stromal cells under hypoxic conditions. *Biochem. Biophys. Res. Commun* **347**, 12–21 (2006).
919. Lennon, D. P., Edmison, J. M. & Caplan, A. I. Cultivation of rat marrow-derived mesenchymal stem cells in reduced oxygen tension: effects on in vitro and in vivo osteochondrogenesis. *J. Cell. Physiol* **187**, 345–355 (2001).
920. D'Ippolito, G., Diabira, S., Howard, G. A., Roos, B. A. & Schiller, P. C. Low oxygen tension inhibits osteogenic differentiation and enhances stemness of human MIAMI cells. *Bone* **39**, 513–522 (2006).
921. Clark, A. J., Burl, S., Denning, C. & Dickinson, P. Gene targeting in livestock: a preview. *Transgenic Res.* **9**, 263–275 (2000).
922. Bonab, M. M., Alimoghaddam, K., Talebian, F., Ghaffari, S. H., Ghavamzadeh, A. & Nikbin, B. Aging of mesenchymal stem cell in vitro. *BMC Cell Biol* **7**, 14 (2006).
923. Miura, M., Miura, Y., Padilla-Nash, H. M., Molinolo, A. A., Fu, B., Patel, V., Seo, B.-M., Sonoyama, W., Zheng, J. J., Baker, C. C., Chen, W., Ried, T. & Shi, S. Accumulated chromosomal instability in murine bone marrow mesenchymal stem cells leads to malignant transformation. *Stem Cells* **24**, 1095–1103 (2006).
924. Wagner, W., Ho, A. D. & Zenke, M. Different facets of aging in human mesenchymal stem cells. *Tissue Eng Part B Rev* **16**, 445–453 (2010).
925. Bork, S., Pfister, S., Witt, H., Horn, P., Korn, B., Ho, A. D. & Wagner, W. DNA methylation pattern changes upon long-term culture and aging of human mesenchymal stromal cells. *Aging Cell* **9**, 54–63 (2010).
926. Bernardo, M. E., Zaffaroni, N., Novara, F., Cometa, A. M., Avanzini, M. A., Moretta, A., Montagna, D., Maccario, R., Villa, R., Daidone, M. G., Zuffardi, O. & Locatelli, F. Human bone marrow derived mesenchymal stem cells do not undergo transformation after long-term in vitro culture and do not exhibit telomere maintenance mechanisms. *Cancer Res* **67**, 9142–9149 (2007).
927. HAYFLICK, L. & MOORHEAD, P. S. The serial cultivation of human diploid cell strains. *Exp. Cell Res.* **25**, 585–621 (1961).
928. Hayflick, L. & Moorhead, P. S. The serial cultivation of human diploid cell strains. *Exp. Cell Res.* **25**, 585–621 (1961).
929. Hayflick, L. The limited in vitro lifetime of human diploid cell strains. *Exp. Cell Res.* **37**, 614–636 (1965).
930. Colter, D. C., Class, R., Digirolamo, C. M. & Prockop, D. J. Rapid expansion of recycling stem cells in cultures of plastic-adherent cells from human bone marrow. *Proc. Natl. Acad. Sci. U.S.A* **97**, 3213–3218 (2000).
931. Bianchi, G., Banfi, A., Mastrogiacomo, M., Notaro, R., Luzzatto, L., Cancedda, R. & Quarto, R. Ex vivo enrichment of mesenchymal cell progenitors by fibroblast growth factor 2. *Exp. Cell Res.* **287**, 98–105 (2003).
932. Vacanti, V., Kong, E., Suzuki, G., Sato, K., Canty, J. M. & Lee, T. Phenotypic changes of adult porcine mesenchymal stem cells induced by prolonged passaging in culture. *J. Cell. Physiol* **205**, 194–201 (2005).

933. McCulloch, C. A., Strugurescu, M., Hughes, F., Melcher, A. H. & Aubin, J. E. Osteogenic progenitor cells in rat bone marrow stromal populations exhibit self-renewal in culture. *Blood* **77**, 1906–1911 (1991).
934. Quarto, R., Thomas, D. & Liang, C. T. Bone progenitor cell deficits and the age-associated decline in bone repair capacity. *Calcif. Tissue Int.* **56**, 123–129 (1995).
935. D'Ippolito, G., Schiller, P. C., Ricordi, C., Roos, B. A. & Howard, G. A. Age-related osteogenic potential of mesenchymal stromal stem cells from human vertebral bone marrow. *J. Bone Miner. Res.* **14**, 1115–1122 (1999).
936. Heape, W. Preliminary Note on the Transplantation and Growth of Mammalian Ova within a Uterine Foster-Mother. *Proceedings of the Royal Society of London* **48**, 457–458 (1890).
937. Briggs, R. & King, T. J. Transplantation of Living Nuclei From Blastula Cells into Enucleated Frogs' Eggs. *Proc. Natl. Acad. Sci. U.S.A* **38**, 455–463 (1952).
938. McGrath, J. & Solter, D. Nuclear transplantation in mouse embryos. *J. Exp. Zool.* **228**, 355–362 (1983).
939. Willadsen, S. M. Nuclear transplantation in sheep embryos. *Nature* **320**, 63–65 (1986).
940. Tarkowski, A. K. & Wróblewska, J. Development of blastomeres of mouse eggs isolated at the 4- and 8-cell stage. *J Embryol Exp Morphol* **18**, 155–180 (1967).
941. Stice, S. L. & Robl, J. M. Nuclear reprogramming in nuclear transplant rabbit embryos. *Biol. Reprod* **39**, 657–664 (1988).
942. Collas, P. & Robl, J. M. Factors affecting the efficiency of nuclear transplantation in the rabbit embryo. *Biol. Reprod* **43**, 877–884 (1990).
943. Yang, X., Jiang, S., Kovács, A. & Foote, R. H. Nuclear totipotency of cultured rabbit morulae to support full-term development following nuclear transfer. *Biol. Reprod* **47**, 636–643 (1992).
944. Chrenek, P., Makarevich, A. V., Bauer, M. & Jurcik, R. Developmental rate and allocation of transgenic cells in rabbit chimeric embryos. *Zygote* **16**, 87–91 (2008).
945. Skrzyszowska, M., Smorag, Z., Słomski, R., Katska-Ksiazkiewicz, L., Kalak, R., Michalak, E., Wielgus, K., Lehmann, J., Lipiński, D., Szalata, M., Pławski, A., Samiec, M., Jura, J., Gajda, B., Ryńska, B. & Pieńkowski, M. Generation of transgenic rabbits by the novel technique of chimeric somatic cell cloning. *Biol. Reprod.* **74**, 1114–1120 (2006).
946. Chesné, P., Adenot, P. G., Viglietta, C., Baratte, M., Boulanger, L. & Renard, J.-P. Cloned rabbits produced by nuclear transfer from adult somatic cells. *Nat. Biotechnol* **20**, 366–369 (2002).
947. Schuetz, A. W., Whittingham, D. G. & Snowden, R. Alterations in the cell cycle of mouse cumulus granulosa cells during expansion and mucification in vivo and in vitro. *Reprod. Fertil. Dev.* **8**, 935–943 (1996).
948. Wakayama, T., Perry, A. C., Zuccotti, M., Johnson, K. R. & Yanagimachi, R. Full-term development of mice from enucleated oocytes injected with cumulus cell nuclei. *Nature* **394**, 369–374 (1998).
949. Dinnyés, A., Dai, Y., Barber, M., Liu, L., Xu, J., Zhou, P. & Yang, X. Development of cloned embryos from adult rabbit fibroblasts: effect of activation treatment and donor cell preparation. *Biol. Reprod* **64**, 257–263 (2001).
950. Fulka, J. & Fulka, H. Somatic cell nuclear transfer (SCNT) in mammals: the cytoplast and its reprogramming activities. *Adv. Exp. Med. Biol* **591**, 93–102 (2007).
951. Kato, Y., Imabayashi, H., Mori, T., Tani, T., Taniguchi, M., Higashi, M., Matsumoto, M., Umezawa, A. & Tsunoda, Y. Nuclear transfer of adult bone marrow mesenchymal stem cells: developmental totipotency of tissue-specific stem cells from an adult mammal. *Biol. Reprod* **70**, 415–418 (2004).
952. Colleoni, S., Donofrio, G., Lagutina, I., Duchi, R., Galli, C. & Lazzari, G. Establishment, differentiation, electroporation, viral transduction, and nuclear transfer of bovine and porcine mesenchymal stem cells. *Cloning Stem Cells* **7**, 154–166 (2005).
953. Bosch, P., Pratt, S. L. & Stice, S. L. Isolation, characterization, gene modification, and nuclear reprogramming of porcine mesenchymal stem cells. *Biol. Reprod* **74**, 46–57 (2006).
954. Kumar, B. M., Jin, H.-F., Kim, J.-G., Ock, S.-A., Hong, Y., Balasubramanian, S., Choe, S.-Y. & Rho, G.-J. Differential gene expression patterns in porcine nuclear transfer embryos reconstructed with fetal fibroblasts and mesenchymal stem cells. *Dev. Dyn* **236**, 435–446 (2007).
955. Jin, H.-F., Kumar, B. M., Kim, J.-G., Song, H.-J., Jeong, Y.-J., Cho, S.-K., Balasubramanian, S., Choe, S.-Y. & Rho, G.-J. Enhanced development of porcine embryos cloned from bone marrow mesenchymal stem cells. *Int. J. Dev. Biol* **51**, 85–90 (2007).
956. Shi, W., Zakhartchenko, V. & Wolf, E. Epigenetic reprogramming in mammalian nuclear transfer. *Differentiation* **71**, 91–113 (2003).
957. Edwards, J. L., Schrick, F. N., McCracken, M. D., van Amstel, S. R., Hopkins, F. M., Welborn, M. G. & Davies, C. J. Cloning adult farm animals: a review of the possibilities and problems associated with somatic cell nuclear transfer. *Am. J. Reprod. Immunol.* **50**, 113–123 (2003).
958. Sung, L.-Y., Chen, C.-H., Xu, J., Lin, T.-A., Su, H.-Y., Chang, W.-F., Liu, C.-C., Sung, Y.-S., Cheng, W. T. K., Zhang, J., Tian, X. C., Ju, J.-C., Chen, Y. E., Wu, S.-C. & Du, F. Follicular oocytes better support development in rabbit cloning than oviductal oocytes. *Cell Reprogram* **13**, 503–512 (2011).

959. Du, F., Xu, J., Zhang, J., Gao, S., Carter, M. G., He, C., Sung, L.-Y., Chaubal, S., Fissore, R. A., Tian, X. C., Yang, X. & Chen, Y. E. Beneficial effect of young oocytes for rabbit somatic cell nuclear transfer. *Cloning Stem Cells* **11**, 131–140 (2009).
960. Jaenisch, R. DNA methylation and imprinting: why bother? *Trends Genet* **13**, 323–329 (1997).
961. Cezar, G. G. Epigenetic reprogramming of cloned animals. *Cloning Stem Cells* **5**, 165–180 (2003).
962. Niemann, H., Tian, X. C., King, W. A. & Lee, R. S. F. Epigenetic reprogramming in embryonic and foetal development upon somatic cell nuclear transfer cloning. *Reproduction* **135**, 151–163 (2008).
963. Tian, X. C., Xu, J. & Yang, X. Normal telomere lengths found in cloned cattle. *Nat. Genet* **26**, 272–273 (2000).
964. Wakayama, T., Shinkai, Y., Tamashiro, K. L., Niida, H., Blanchard, D. C., Blanchard, R. J., Ogura, A., Tanemura, K., Tachibana, M., Perry, A. C., Colgan, D. F., Mombaerts, P. & Yanagimachi, R. Cloning of mice to six generations. *Nature* **407**, 318–319 (2000).
965. Betts, D., Bordignon, V., Hill, J., Winger, Q., Westhusin, M., Smith, L. & King, W. Reprogramming of telomerase activity and rebuilding of telomere length in cloned cattle. *Proc. Natl. Acad. Sci. U.S.A* **98**, 1077–1082 (2001).
966. Yang, X. & Tian, X. C. Cloning adult animals - what is the genetic age of the clones? *Cloning* **2**, 123–128 (2000).
967. Jaenisch, R., Eggan, K., Humpherys, D., Rideout, W. & Hochedlinger, K. Nuclear cloning, stem cells, and genomic reprogramming. *Cloning Stem Cells* **4**, 389–396 (2002).
968. Oback, B. & Wells, D. Practical aspects of donor cell selection for nuclear cloning. *Cloning Stem Cells* **4**, 169–174 (2002).
969. Kühholzer, B., Hawley, R. J., Lai, L., Kolber-Simonds, D. & Prather, R. S. Clonal lines of transgenic fibroblast cells derived from the same fetus result in different development when used for nuclear transfer in pigs. *Biol. Reprod* **64**, 1695–1698 (2001).
970. Gurdon, J. B. & Colman, A. The future of cloning. *Nature* **402**, 743–746 (1999).
971. DePinho, R. A. The age of cancer. *Nature* **408**, 248–254 (2000).
972. Wakayama, T., Rodriguez, I., Perry, A. C., Yanagimachi, R. & Mombaerts, P. Mice cloned from embryonic stem cells. *Proc. Natl. Acad. Sci. U.S.A* **96**, 14984–14989 (1999).
973. Rideout, W. M., Wakayama, T., Wutz, A., Eggan, K., Jackson-Grusby, L., Dausman, J., Yanagimachi, R. & Jaenisch, R. Generation of mice from wild-type and targeted ES cells by nuclear cloning. *Nat. Genet* **24**, 109–110 (2000).
974. Eggan, K., Akutsu, H., Loring, J., Jackson-Grusby, L., Klemm, M., Rideout, W. M., Yanagimachi, R. & Jaenisch, R. Hybrid vigor, fetal overgrowth, and viability of mice derived by nuclear cloning and tetraploid embryo complementation. *Proc. Natl. Acad. Sci. U.S.A* **98**, 6209–6214 (2001).
975. Eggan, K., Rode, A., Jentsch, I., Samuel, C., Hennek, T., Tintrup, H., Zevnik, B., Erwin, J., Loring, J., Jackson-Grusby, L., Speicher, M. R., Kuehn, R. & Jaenisch, R. Male and female mice derived from the same embryonic stem cell clone by tetraploid embryo complementation. *Nat. Biotechnol* **20**, 455–459 (2002).
976. Oback, B. & Wells, D. N. Donor cell differentiation, reprogramming, and cloning efficiency: elusive or illusive correlation? *Mol. Reprod. Dev* **74**, 646–654 (2007).
977. Wakayama, T. & Yanagimachi, R. Cloning of male mice from adult tail-tip cells. *Nat. Genet* **22**, 127–128 (1999).
978. Wells, D. N., Misica, P. M. & Tervit, H. R. Production of cloned calves following nuclear transfer with cultured adult mural granulosa cells. *Biol. Reprod* **60**, 996–1005 (1999).
979. Kato, Y., Tani, T. & Tsunoda, Y. Cloning of calves from various somatic cell types of male and female adult, newborn and fetal cows. *J. Reprod. Fertil* **120**, 231–237 (2000).
980. Polejaeva, I. A., Chen, S. H., Vaught, T. D., Page, R. L., Mullins, J., Ball, S., Dai, Y., Boone, J., Walker, S., Ayares, D. L., Colman, A. & Campbell, K. H. Cloned pigs produced by nuclear transfer from adult somatic cells. *Nature* **407**, 86–90 (2000).
981. Keefer, C. L., Baldassarre, H., Keyston, R., Wang, B., Bhatia, B., Bilodeau, A. S., Zhou, J. F., Leduc, M., Downey, B. R., Lazaris, A. & Karatzas, C. N. Generation of dwarf goat (Capra hircus) clones following nuclear transfer with transfected and nontransfected fetal fibroblasts and in vitro-matured oocytes. *Biol. Reprod* **64**, 849–856 (2001).
982. Zou, X., Chen, Y., Wang, Y., Luo, J., Zhang, Q., Zhang, X., Yang, Y., Ju, H., Shen, Y., Lao, W., Xu, S. & Du, M. Production of cloned goats from enucleated oocytes injected with cumulus cell nuclei or fused with cumulus cells. *Cloning* **3**, 31–37 (2001).
983. Doherty, A. S., Mann, M. R., Tremblay, K. D., Bartolomei, M. S. & Schultz, R. M. Differential effects of culture on imprinted H19 expression in the preimplantation mouse embryo. *Biol. Reprod* **62**, 1526–1535 (2000).
984. Khosla, S., Dean, W., Brown, D., Reik, W. & Feil, R. Culture of preimplantation mouse embryos affects fetal development and the expression of imprinted genes. *Biol. Reprod* **64**, 918–926 (2001).

985. Young, L. E., Fernandes, K., McEvoy, T. G., Butterwith, S. C., Gutierrez, C. G., Carolan, C., Broadbent, P. J., Robinson, J. J., Wilmut, I. & Sinclair, K. D. Epigenetic change in IGF2R is associated with fetal overgrowth after sheep embryo culture. *Nat. Genet* **27**, 153–154 (2001).
986. Khosla, S., Dean, W., Reik, W. & Feil, R. Culture of preimplantation embryos and its long-term effects on gene expression and phenotype. *Hum. Reprod. Update* **7**, 419–427 (2001).
987. Konecki, D. S., Brennand, J., Fuscoe, J. C., Caskey, C. T. & Chinault, A. C. Hypoxanthine-guanine phosphoribosyltransferase genes of mouse and Chinese hamster: construction and sequence analysis of cDNA recombinants. *Nucleic Acids Res.* **10**, 6763–6775 (1982).
988. Jinnah, H. A., Jones, M. D., Wojcik, B. E., Rothstein, J. D., Hess, E. J., Friedmann, T. & Breese, G. R. Influence of age and strain on striatal dopamine loss in a genetic mouse model of Lesch-Nyhan disease. *J. Neurochem.* **72**, 225–229 (1999).
989. Jinnah, H. A. Lesch-Nyhan disease: from mechanism to model and back again. *Disease Models and Mechanisms* **2**, 116–121 (2009).
990. Shirley, T. L., Lewers, J. C., Egami, K., Majumdar, A., Kelly, M., Ceballos-Picot, I., Seidman, M. M. & Jinnah, H. A. A human neuronal tissue culture model for Lesch-Nyhan disease. *J. Neurochem* **101**, 841–853 (2007).
991. Jinnah, H. A., Gregorio, L. de, Harris, J. C., NYHAN, W. L. & O'Neill, J. P. The spectrum of inherited mutations causing HPRT deficiency: 75 new cases and a review of 196 previously reported cases. *Mutat. Res* **463**, 309–326 (2000).
992. Bouwens-Rombouts, A. G., van den Boogaard, M. J., Puig, J. G., Mateos, F. A., Hennekam, R. C. & Tilanus, M. G. Identification of two new nucleotide mutations (HPRTUtrecht and HPRTMadrid) in exon 3 of the human hypoxanthine-guanine phosphoribosyltransferase (HPRT) gene. *Hum. Genet.* **91**, 451–454 (1993).
993. Cariello, N. F. & Skopek, T. R. Analysis of mutations occurring at the human hprt locus. *J. Mol. Biol.* **231**, 41–57 (1993).
994. Jiang, H.-L., Kim, T.-H., Kim, Y.-K., Park, I.-Y., Cho, M.-H. & Cho, C.-S. Efficient gene delivery using chitosan-polyethylenimine hybrid systems. *Biomed Mater* **3**, 25013 (2008).
995. White, R. E., Wade-Martins, R., Hart, S. L., Frampton, J., Huey, B., Desai-Mehta, A., Cerosaletti, K. M., Concannon, P. & James, M. R. Functional delivery of large genomic DNA to human cells with a peptide-lipid vector. *J Gene Med* **5**, 883–892 (2003).
996. Walker, W. E., Porteous, D. J. & Boyd, A. C. The effects of plasmid copy number and sequence context upon transfection efficiency. *J Control Release* **94**, 245–252 (2004).
997. Askautrud, H. A., Gjernes, E., Størvold, G. L., Lindeberg, M. M., Thorsen, J., Prydz, H. & Frengen, E. Regulated expression of a transgene introduced on an oriP/EBNA-1 PAC shuttle vector into human cells. *BMC Biotechnol.* **9**, 88 (2009).
998. McLenachan, S., Sarsero, J. P. & Ioannou, P. A. Flow-cytometric analysis of mouse embryonic stem cell lipofection using small and large DNA constructs. *Genomics* **89**, 708–720 (2007).
999. Abrahams, B. S., Chong, A. C. O., Nisha, M., Milette, D., Brewster, D. A., Berry, M. L., Muratkhodjaev, F., Mai, S., Rajcan-Separovic, E. & Simpson, E. M. Metaphase FISHing of transgenic mice recommended: FISH and SKY define BAC-mediated balanced translocation. *Genesis* **36**, 134–141 (2003).
1000. Chandler, K. J., Chandler, R. L., Broeckelmann, E. M., Hou, Y., Southard-Smith, E. M. & Mortlock, D. P. Relevance of BAC transgene copy number in mice: transgene copy number variation across multiple transgenic lines and correlations with transgene integrity and expression. *Mamm. Genome* **18**, 693–708 (2007).
1001. Le Saux, A., Houdebine, L.-M. & Jolivet, G. Chromosome integration of BAC (bacterial artificial chromosome): evidence of multiple rearrangements. *Transgenic Res* **19**, 923–931 (2010).
1002. Bishop, J. O. Chromosomal insertion of foreign DNA. *Reprod. Nutr. Dev* **36**, 607–618 (1996).
1003. Würtele, H., Little, K. C. E. & Chartrand, P. Illegitimate DNA integration in mammalian cells. *Gene Ther* **10**, 1791–1799 (2003).
1004. Kamisugi, Y., Schlink, K., Rensing, S. A., Schween, G., Stackelberg, M. von, Cuming, A. C., Reski, R. & Cove, D. J. The mechanism of gene targeting in Physcomitrella patens: homologous recombination, concatenation and multiple integration. *Nucleic Acids Res* **34**, 6205–6214 (2006).
1005. Iiizumi, S., Kurosawa, A., So, S., Ishii, Y., Chikaraishi, Y., Ishii, A., Koyama, H. & Adachi, N. Impact of non-homologous end-joining deficiency on random and targeted DNA integration: implications for gene targeting. *Nucleic Acids Res.* **36**, 6333–6342 (2008).
1006. Waldman, A. S. Targeted homologous recombination in mammalian cells. *Crit. Rev. Oncol. Hematol.* **12**, 49–64 (1992).
1007. Arbonés, M. L., Austin, H. A., Capon, D. J. & Greenburg, G. Gene targeting in normal somatic cells: inactivation of the interferon-gamma receptor in myoblasts. *Nat. Genet.* **6**, 90–97 (1994).
1008. Hanson, K. D. & Sedivy, J. M. Analysis of biological selections for high-efficiency gene targeting. *Mol. Cell. Biol.* **15**, 45–51 (1995).

1009. Brown, J. P., Wei, W. & Sedivy, J. M. Bypass of senescence after disruption of p21CIP1/WAF1 gene in normal diploid human fibroblasts. *Science* **277**, 831–834 (1997).
1010. Doetschman, T., Maeda, N. & Smithies, O. Targeted mutation of the Hprt gene in mouse embryonic stem cells. *Proc. Natl. Acad. Sci. U.S.A.* **85**, 8583–8587 (1988).
1011. Thompson, S., Clarke, A. R., Pow, A. M., Hooper, M. L. & Melton, D. W. Germ line transmission and expression of a corrected HPRT gene produced by gene targeting in embryonic stem cells. *Cell* **56**, 313–321 (1989).
1012. Hasty, P., Rivera-Pérez, J. & Bradley, A. The length of homology required for gene targeting in embryonic stem cells. *Mol. Cell. Biol.* **11**, 5586–5591 (1991).
1013. Udy, G. B., Parkes, B. D. & Wells, D. N. ES cell cycle rates affect gene targeting frequencies. *Exp. Cell Res.* **231**, 296–301 (1997).
1014. Sakurai, K., Shimoji, M., Tahimic, C. G. T., Aiba, K., Kawase, E., Hasegawa, K., Amagai, Y., Suemori, H. & Nakatsuji, N. Efficient integration of transgenes into a defined locus in human embryonic stem cells. *Nucleic Acids Res.* **38**, e96 (2010).
1015. Deng, C. & Capecchi, M. R. Reexamination of gene targeting frequency as a function of the extent of homology between the targeting vector and the target locus. *Mol. Cell. Biol.* **12**, 3365–3371 (1992).
1016. Thomas, K. R., Deng, C. & Capecchi, M. R. High-fidelity gene targeting in embryonic stem cells by using sequence replacement vectors. *Mol. Cell. Biol.* **12**, 2919–2923 (1992).
1017. Yang, G. S., Banks, K. G., Bonaguro, R. J., Wilson, G., Dreolini, L., Leeuw, C. N. de, Liu, L., Swanson, D. J., Goldowitz, D., Holt, R. A. & Simpson, E. M. Next generation tools for high-throughput promoter and expression analysis employing single-copy knock-ins at the Hprt1 locus. *Genomics* **93**, 196–204 (2009).
1018. Guillot, P. V., Liu, L., Kuivenhoven, J. A., Guan, J., Rosenberg, R. D. & Aird, W. C. Targeting of human eNOS promoter to the Hprt locus of mice leads to tissue-restricted transgene expression. *Physiol. Genomics* **2**, 77–83 (2000).
1019. Heaney, J. D., Rettew, A. N. & Bronson, S. K. Tissue-specific expression of a BAC transgene targeted to the Hprt locus in mouse embryonic stem cells. *Genomics* **83**, 1072–1082 (2004).
1020. Mir, B. & Piedrahita, J. A. Nuclear localization signal and cell synchrony enhance gene targeting efficiency in primary fetal fibroblasts. *Nucleic Acids Res.* **32**, e25 (2004).
1021. Wilson, G. L., Dean, B. S., Wang, G. & Dean, D. A. Nuclear import of plasmid DNA in digitonin-permeabilized cells requires both cytoplasmic factors and specific DNA sequences. *J. Biol. Chem.* **274**, 22025–22032 (1999).
1022. Ludtke, J. J., Zhang, G., Sebestyén, M. G. & Wolff, J. A. A nuclear localization signal can enhance both the nuclear transport and expression of 1 kb DNA. *J. Cell. Sci.* **112 (Pt 12)**, 2033–2041 (1999).
1023. Vacik, J., Dean, B. S., Zimmer, W. E. & Dean, D. A. Cell-specific nuclear import of plasmid DNA. *Gene Ther.* **6**, 1006–1014 (1999).
1024. Wong, E. A. & Capecchi, M. R. Homologous recombination between coinjected DNA sequences peaks in early to mid-S phase. *Mol. Cell. Biol.* **7**, 2294–2295 (1987).
1025. Takata, M., Sasaki, M. S., Sonoda, E., Morrison, C., Hashimoto, M., Utsumi, H., Yamaguchi-Iwai, Y., Shinohara, A. & Takeda, S. Homologous recombination and non-homologous end-joining pathways of DNA double-strand break repair have overlapping roles in the maintenance of chromosomal integrity in vertebrate cells. *EMBO J.* **17**, 5497–5508 (1998).
1026. Lundin, C., Erixon, K., Arnaudeau, C., Schultz, N., Jenssen, D., Meuth, M. & Helleday, T. Different roles for nonhomologous end joining and homologous recombination following replication arrest in mammalian cells. *Mol. Cell. Biol.* **22**, 5869–5878 (2002).
1027. Meehan, D. T., Zink, M. A., Mahlen, M., Nelson, M., Sanger, W. G., Mitalipov, S. M., Wolf, D. P., Ouellette, M. M. & Norgren, R. B. Gene targeting in adult rhesus macaque fibroblasts. *BMC Biotechnol.* **8**, 31 (2008).
1028. Kang, Y. K., Park, J. S., Lee, C. S., Yeom, Y. I., Chung, A. S. & Lee, K. K. Efficient integration of short interspersed element-flanked foreign DNA via homologous recombination. *J. Biol. Chem* **274**, 36585–36591 (1999).
1029. Piedrahita, J. A. Gene targeting in domestic species: a new beginning. *Transgenic Res.* **9**, 261–262 (2000).
1030. Wang, B. & Zhou, J. Specific genetic modifications of domestic animals by gene targeting and animal cloning. *Reprod. Biol. Endocrinol.* **1**, 103 (2003).
1031. Flisikowska, T., Thorey, I. S., Offner, S., Ros, F., Lifke, V., Zeitler, B., Rottmann, O., Vincent, A., Zhang, L., Jenkins, S., Niersbach, H., Kind, A. J., Gregory, P. D., Schnieke, A. E. & Platzer, J. Efficient immunoglobulin gene disruption and targeted replacement in rabbit using zinc finger nucleases. *PLoS ONE* **6**, e21045 (2011).
1032. Vanamee, E. S., Santagata, S. & Aggarwal, A. K. FokI requires two specific DNA sites for cleavage. *J. Mol. Biol* **309**, 69–78 (2001).

1033. Kim, Y. G., Shi, Y., Berg, J. M. & Chandrasegaran, S. Site-specific cleavage of DNA-RNA hybrids by zinc finger/FokI cleavage domain fusions. *Gene* **203**, 43–49 (1997).
1034. Bibikova, M., Beumer, K., Trautman, J. K. & Carroll, D. Enhancing gene targeting with designed zinc finger nucleases. *Science* **300**, 764 (2003).
1035. Durai, S., Mani, M., Kandavelou, K., Wu, J., Porteus, M. H. & Chandrasegaran, S. Zinc finger nucleases: custom-designed molecular scissors for genome engineering of plant and mammalian cells. *Nucleic Acids Res* **33**, 5978–5990 (2005).
1036. Urnov, F. D., Miller, J. C., Lee, Y.-L., Beausejour, C. M., Rock, J. M., Augustus, S., Jamieson, A. C., Porteus, M. H., Gregory, P. D. & Holmes, M. C. Highly efficient endogenous human gene correction using designed zinc-finger nucleases. *Nature* **435**, 646–651 (2005).
1037. Porteus, M. H. Mammalian gene targeting with designed zinc finger nucleases. *Mol. Ther* **13**, 438–446 (2006).
1038. Moehle, E. A., Moehle, E. A., Rock, J. M., Rock, J. M., Lee, Y.-L., Lee, Y. L., Jouvenot, Y., Jouvenot, Y., DeKelver, R. C., Dekelver, R. C., Gregory, P. D., Gregory, P. D., Urnov, F. D., Urnov, F. D., Holmes, M. C. & Holmes, M. C. Targeted gene addition into a specified location in the human genome using designed zinc finger nucleases. *Proc. Natl. Acad. Sci. U.S.A* **104**, 3055–3060 (2007).
1039. Arnould, S., Perez, C., Cabaniols, J.-P., Smith, J., Gouble, A., Grizot, S., Epinat, J.-C., Duclert, A., Duchateau, P. & Pâques, F. Engineered I-CreI derivatives cleaving sequences from the human XPC gene can induce highly efficient gene correction in mammalian cells. *J. Mol. Biol* **371**, 49–65 (2007).
1040. Pruett-Miller, S. M., Connelly, J. P., Maeder, M. L., Joung, J. K. & Porteus, M. H. Comparison of zinc finger nucleases for use in gene targeting in mammalian cells. *Mol. Ther* **16**, 707–717 (2008).
1041. Maeder, M. L., Thibodeau-Beganny, S., Osiak, A., Wright, D. A., Anthony, R. M., Eichtinger, M., Jiang, T., Foley, J. E., Winfrey, R. J., Townsend, J. A., Unger-Wallace, E., Sander, J. D., Müller-Lerch, F., Fu, F., Pearlberg, J., Göbel, C., Dassie, J. P., Pruett-Miller, S. M., Porteus, M. H., Sgroi, D. C., Iafrate, A. J., Dobbs, D., McCray, P. B., Cathomen, T., Voytas, D. F. & Joung, J. K. Rapid "open-source" engineering of customized zinc-finger nucleases for highly efficient gene modification. *Mol. Cell* **31**, 294–301 (2008).
1042. Cathomen, T. & Joung, J. K. Zinc-finger nucleases: the next generation emerges. *Mol. Ther* **16**, 1200–1207 (2008).
1043. Whyte, J. J., Zhao, J., Wells, K. D., Samuel, M. S., Whitworth, K. M., Walters, E. M., Laughlin, M. H. & Prather, R. S. Gene targeting with zinc finger nucleases to produce cloned eGFP knockout pigs. *Mol. Reprod. Dev* **78**, 2 (2011).
1044. Whyte, J. J. & Prather, R. S. Zinc finger nucleases to create custom-designed modifications in the swine (Sus scrofa) genome. *Journal of animal science* (2011).
1045. Ramirez, C. L., Foley, J. E., Wright, D. A., Müller-Lerch, F., Rahman, S. H., Cornu, T. I., Winfrey, R. J., Sander, J. D., Fu, F., Townsend, J. A., Cathomen, T., Voytas, D. F. & Joung, J. K. Unexpected failure rates for modular assembly of engineered zinc fingers. *Nat. Methods* **5**, 374–375 (2008).
1046. Gabriel, R., Lombardo, A., Arens, A., Miller, J. C., Genovese, P., Kaeppel, C., Nowrouzi, A., Bartholomae, C. C., Wang, J., Friedman, G., Holmes, M. C., Gregory, P. D., Glimm, H., Schmidt, M., Naldini, L. & Kalle, C. von. An unbiased genome-wide analysis of zinc-finger nuclease specificity. *Nat. Biotechnol* **29**, 816–823 (2011).
1047. Gupta, A., Meng, X., Zhu, L. J., Lawson, N. D. & Wolfe, S. A. Zinc finger protein-dependent and -independent contributions to the in vivo off-target activity of zinc finger nucleases. *Nucleic Acids Res* **39**, 381–392 (2011).
1048. Pattanayak, V., Ramirez, C. L., Joung, J. K. & Liu, D. R. Revealing off-target cleavage specificities of zinc-finger nucleases by in vitro selection. *Nat. Methods* **8**, 765–770 (2011).
1049. Doyon, Y., Vo, T. D., Mendel, M. C., Greenberg, S. G., Wang, J., Xia, D. F., Miller, J. C., Urnov, F. D., Gregory, P. D. & Holmes, M. C. Enhancing zinc-finger-nuclease activity with improved obligate heterodimeric architectures. *Nat. Methods* **8**, 74–79 (2011).
1050. Christian, M., Cermak, T., Doyle, E. L., Schmidt, C., Zhang, F., Hummel, A., Bogdanove, A. J. & Voytas, D. F. Targeting DNA double-strand breaks with TAL effector nucleases. *Genetics* **186**, 757–761 (2010).
1051. Li, T., Huang, S., Jiang, W. Z., Wright, D., Spalding, M. H., Weeks, D. P. & Yang, B. TAL nucleases (TALNs): hybrid proteins composed of TAL effectors and FokI DNA-cleavage domain. *Nucleic Acids Res* **39**, 359–372 (2011).
1052. Li, T., Huang, S., Zhao, X., Wright, D. A., Carpenter, S., Spalding, M. H., Weeks, D. P. & Yang, B. Modularly assembled designer TAL effector nucleases for targeted gene knockout and gene replacement in eukaryotes. *Nucleic Acids Res* **39**, 6315–6325 (2011).
1053. Mahfouz, M. M., Li, L., Shamimuzzaman, M., Wibowo, A., Fang, X. & Zhu, J.-K. De novo-engineered transcription activator-like effector (TALE) hybrid nuclease with novel DNA binding specificity creates double-strand breaks. *Proc. Natl. Acad. Sci. U.S.A* **108**, 2623–2628 (2011).
1054. Sander, J. D., Cade, L., Khayter, C., Reyon, D., Peterson, R. T., Joung, J. K. & Yeh, J.-R. J. Targeted gene disruption in somatic zebrafish cells using engineered TALENs. *Nat. Biotechnol* **29**, 697–698 (2011).

1055. Huang, P., an Xiao, Zhou, M., Zhu, Z., Lin, S. & Zhang, B. Heritable gene targeting in zebrafish using customized TALENs. *Nat. Biotechnol* **29**, 699–700 (2011).
1056. Boch, J., Scholze, H., Schornack, S., Landgraf, A., Hahn, S., Kay, S., Lahaye, T., Nickstadt, A. & Bonas, U. Breaking the code of DNA binding specificity of TAL-type III effectors. *Science* **326**, 1509–1512 (2009).
1057. Moscou, M. J. & Bogdanove, A. J. A simple cipher governs DNA recognition by TAL effectors. *Science* **326**, 1501 (2009).
1058. Morbitzer, R., Römer, P., Boch, J. & Lahaye, T. Regulation of selected genome loci using de novo-engineered transcription activator-like effector (TALE)-type transcription factors. *Proc. Natl. Acad. Sci. U.S.A* **107**, 21617–21622 (2010).
1059. Cermak, T., Doyle, E. L., Christian, M., Wang, L., Zhang, Y., Schmidt, C., Baller, J. A., Somia, N. V., Bogdanove, A. J. & Voytas, D. F. Efficient design and assembly of custom TALEN and other TAL effector-based constructs for DNA targeting. *Nucleic Acids Res* **39**, e82 (2011).
1060. Zhang, F., Le Cong, Lodato, S., Kosuri, S., Church, G. M. & Arlotta, P. Efficient construction of sequence-specific TAL effectors for modulating mammalian transcription. *Nat. Biotechnol* **29**, 149–153 (2011).
1061. Morbitzer, R., Elsaesser, J., Hausner, J. & Lahaye, T. Assembly of custom TALE-type DNA binding domains by modular cloning. *Nucleic Acids Res* **39**, 5790–5799 (2011).
1062. Mussolino, C., Morbitzer, R., Lütge, F., Dannemann, N., Lahaye, T. & Cathomen, T. A novel TALE nuclease scaffold enables high genome editing activity in combination with low toxicity. *Nucleic Acids Res* **39**, 9283–9293 (2011).
1063. Hockemeyer, D., Wang, H., Kiani, S., Lai, C. S., Gao, Q., Cassady, J. P., Cost, G. J., Zhang, L., Santiago, Y., Miller, J. C., Zeitler, B., Cherone, J. M., Meng, X., Hinkley, S. J., Rebar, E. J., Gregory, P. D., Urnov, F. D. & Jaenisch, R. Genetic engineering of human pluripotent cells using TALE nucleases. *Nat Biotechnol* **29**, 731–734 (2011).
1064. Porteus, M. H. & Carroll, D. Gene targeting using zinc finger nucleases. *Nat. Biotechnol* **23**, 967–973 (2005).
1065. Carroll, D. Progress and prospects: zinc-finger nucleases as gene therapy agents. *Gene Ther* **15**, 1463–1468 (2008).
1066. Urnov, F. D., Rebar, E. J., Holmes, M. C., Zhang, H. S. & Gregory, P. D. Genome editing with engineered zinc finger nucleases. *Nat. Rev. Genet* **11**, 636–646 (2010).
1067. Boch, J. & Bonas, U. Xanthomonas AvrBs3 family-type III effectors: discovery and function. *Annu Rev Phytopathol* **48**, 419–436 (2010).
1068. Clark, K. J., Voytas, D. F. & Ekker, S. C. A TALE of two nucleases: gene targeting for the masses? *Zebrafish* **8**, 147–149 (2011).
1069. Hockemeyer, D., Soldner, F., Beard, C., Gao, Q., Mitalipova, M., DeKelver, R. C., Katibah, G. E., Amora, R., Boydston, E. A., Zeitler, B., Meng, X., Miller, J. C., Zhang, L., Rebar, E. J., Gregory, P. D., Urnov, F. D. & Jaenisch, R. Efficient targeting of expressed and silent genes in human ESCs and iPSCs using zinc-finger nucleases. *Nat. Biotechnol* **27**, 851–857 (2009).
1070. Jasin, M. & Berg, P. Homologous integration in mammalian cells without target gene selection. *Genes Dev.* **2**, 1353–1363 (1988).
1071. Sedivy, J. M. & Sharp, P. A. Positive genetic selection for gene disruption in mammalian cells by homologous recombination. *Proc. Natl. Acad. Sci. U.S.A.* **86**, 227–231 (1989).
1072. Kragl, M., Knapp, D., Nacu, E., Khattak, S., Maden, M., Epperlein, H. H. & Tanaka, E. M. Cells keep a memory of their tissue origin during axolotl limb regeneration. *Nature* **460**, 60–65 (2009).
1073. Khattak, S., Richter, T. & Tanaka, E. M. Generation of transgenic axolotls (Ambystoma mexicanum). *Cold Spring Harb Protoc* **2009**, pdb.prot5264 (2009).
1074. Wober, J., Möller, F., Richter, T., Unger, C., Weigt, C., Jandausch, A., Zierau, O., Rettenberger, R., Kaszkin-Bettag, M. & Vollmer, G. Activation of estrogen receptor-beta by a special extract of Rheum rhaponticum (ERr 731), its aglycones and structurally related compounds. *J. Steroid Biochem. Mol. Biol.* **107**, 191–201 (2007).
1075. Wanda, G. J. M. K., Starcke, S., Zierau, O., Njamen, D., Richter, T. & Vollmer, G. Estrogenic activity of griffonianone C, an isoflavone from the root bark of Millettia griffoniana: regulation of the expression of estrogen responsive genes in uterus and liver of ovariectomized rats. *Planta Med.* **73**, 512–518 (2007).
1076. Rando, T. A. Stem cells, ageing and the quest for immortality. *Nature* **441,** 1080-1086 (2006)
1077. Stenderup, K., Justesen, J., Clausen, C. & Kassem, M. Aging is associated with decreased maximal life span and accelerated senescence of bone marrow stromal cells. *Bone* **33**, 919-926 (2003)
1078. Dunwoodie, S. L. The role of hypoxia in development of the Mammalian embryo. *Dev. Cell* **17**, 755-7730 (2009)
1079. Ma, T., Grayson, W. L., Frohlich, M. & Vunjak-Novakovic, G. Hypoxia and stem cell-based engineering of mesenchymal tissues. *Biotechnol. Prog*. **25**, 32-42 (2009)

1080. Kim, J. H., Park, S. H., Park, S. G., Choi, J. S., Xia, Y. & Sung, J. H. The pivotal role of reactive oxygen species generation in the hypoxia-induced stimulation of adipose-derived stem cells. *Stem Cells Dev*. **20**, 1753-1761 (2011)
1081. Mazumdar, J., O'Brien, W. T., Johnson, R. S., LaManna, J. C., Chavez, J. C., Klein, P. S. & Simon, M. C. O2 regulates stem cells through Wnt/beta-catenin signalling. *Nat. Cell Biol*. **12**, 1007-1013 (2010)
1082. Mohyeldin, A., Garzon-Muvdi, T. & Quinones-Hinojosa, A. Oxygen in stem cell biology: a critical component of the stem cell niche. *Cell Stem Cell* **7**, 150-161 (2010)
1083. Dos Santos, F., Andrade, P. Z., Boura, J. S., Abecasis, M. M., da Silva, C. L. & Cabral, J. M. Ex vivo expansion of human mesenchymal stem cells: a more effective cell proliferation kinetics and metabolism under hypoxia. *J. Cell. Physiol*. **223**, 27-35 (2010)
1084. Grayson, W. L., Zhao, F., Bunnell, B. & Ma, T. Hypoxia enhances proliferation and tissue formation of human mesenchymal stem cells. *Biochem. Biophys. Res. Commun*. **358**, 948-953 (2007)
1085. Hung, S. P., Ho, J. H., Shih, Y. R., Lo, T. & Lee, O. K. Hypoxia promotes proliferation and osteogenic differentiation potentials of human mesenchymal stem cells. *J. Orthop. Res*. **30**, 260-266 (2012)
1086. Jin, Y., Kato, T., Furu, M., Nasu, A., Kajita, Y., Mitsui, H., Ueda, M., Aoyama, T., Nakayama, T., Nakamura, T. & Toguchida, J. Mesenchymal stem cells cultured under hypoxia escape from senescence via down-regulation of p16 and extracellular signal regulated kinase. *Biochem. Biophys. Res. Commun*. **391**, 1471-1476 (2010)
1087. Tsai, C. C., Chen, Y. J., Yew, T. L., Chen, L. L., Wang, J. Y., Chiu, C. H. & Hung, S. C. Hypoxia inhibits senescence and maintains mesenchymal stem cell properties through down-regulation of E2A-p21 by HIF-TWIST. *Blood* **117**, 459-469 (2011)
1088. Niebruegge, S., Bauwens, C. L., Peerani, R., Thavandiran, N., Masse, S., Sevaptisidis, E., Nanthakumar, K., Woodhouse, K., Husain, M., Kumacheva, E. & Zandstra, P. W. Generation of human embryonic stem cell-derived mesoderm and cardiac cells using size-specified aggregates in an oxygen-controlled bioreactor. *Biotechnol. Bioeng*. **102**, 493-507 (2009)
1089. Prado-Lopez, S., Conesa, A., Arminan, A., Martinez-Losa, M., Escobedo-Lucea, C., Gandia, C., Tarazona, S., Melguizo, D., Blesa, D., Montaner, D., Sanz-Gonzalez, S., Sepulveda, P., Gotz, S., O'Connor, J. E., Moreno, R., Dopazo, J., Burks, D. J. & Stojkovic, M. Hypoxia promotes efficient differentiation of human embryonic stem cells to functional endothelium. *Stem Cells* **28**, 407-418 (2010)
1090. Abaci, H. E., Truitt, R., Luong, E., Drazer, G. & Gerecht, S. Adaptation to oxygen deprivation in cultures of human pluripotent stem cells, endothelial progenitor cells, and umbilical vein endothelial cells. *Am. J. Physiol. Cell Physiol*. **298**, 1527-1537 (2010)
1091. Teramura T., Onodera Y., Takehara T., Frampton J., Matsuoka T., Ito S., Nakagawa K., Miki Y., Hosoi Y., Hamanishi C. & Fukuda K. Induction of Functional Mesenchymal Stem Cells from Rabbit Embryonic Stem Cells by Exposure to Severe Hypoxic Conditions. *Cell Transplant*. (2012) Aug 27. [Epub ahead of print]
1092. Takehara, T., Teramura, T., Onodera, Y., Kakegawa, R., Fukunaga, N., Takenoshita, M., Sagawa, N., Fukuda, K. & Hosoi, Y. Rho-associated kinase inhibitor Y-27632 promotes survival of cynomolgus monkey embryonic stem cells. *Mol. Hum. Reprod*. **14**, 627-634 (2008)
1093. Rostovskaya M., Fu J., Obst M., Baer I., Weidlich S., Wang H., Smith A. J., Anastassiadis K. & Stewart A. F. Transposon-mediated BAC transgenesis in human ES cells. *Nucleic Acids Res*. (2012) Jun 30. [Epub ahead of print]
1094. Muenthaisong S., Ujhelly O., Polgar Z., Varga E., Ivics Z., Pirity M. K. & Dinnyes A. Generation of mouse induced pluripotent stem cells from different genetic backgrounds using Sleeping beauty transposon mediated gene transfer. *Exp Cell Res*. **15**, 2482-2489 (2012)
1095. Kues W. A., Herrmann D., Barg-Kues B., Meena Haridoss S., Nowak-Imialek M., Buchholz T., Streeck M., Grebe A., Grabundzija I., Merkert S., Martin U., Hall V. J., Rasmussen M. A., Ivics Z., Maddox-Hyttel P. & Niemann H. Derivation and characterization of Sleeping Beauty transposon-mediated porcine induced pluripotent stem cells. *Stem Cells Dev*. (2012) Sep 18. [Epub ahead of print]
1096. Mostoslavsky G. Concise review: The magic act of generating induced pluripotent stem cells: many rabbits in the hat. *Stem Cells*. **30**, 28-32 (2012)
1097. Lin T. A., Chen C. H., Sung L. Y., Carter M. G., Chen Y. E., Du F., Ju J. C. & Xu J. Open-pulled straw vitrification differentiates cryotolerance of in vitro cultured rabbit embryos at the eight-cell stage. *Theriogenology*. **75**, 760-768 (2011)
1098. Xue F., Ma Y., Chen Y. E., Zhang J., Lin T. A., Chen C. H., Lin W. W., Roach M., Ju J. C., Yang L., Du F. & Xu J. Recombinant rabbit leukemia inhibitory factor and rabbit embryonic fibroblasts support the derivation and maintenance of rabbit embryonic stem cells. *Cell Reprogram*. **14**, 364-376 (2012)
1099. Tancos Z., Nemes C., Polgar Z., Gocza E., Daniel N., Stout T. A., Maraghechi P., Pirity M. K., Osteil P., Tapponnier Y., Markossian S., Godet M., Afanassieff M., Bosze Z., Duranthon V., Savatier P. & Dinnyes A. Generation of rabbit pluripotent stem cell lines. *Theriogenology*. (2012) Aug 24. [Epub ahead of print]

1100. Anokye-Danso F., Trivedi C. M., Juhr D., Gupta M., Cui Z., Tian Y., Zhang Y., Yang W., Gruber P. J., Epstein J. A. & Morrisey E. E. Highly efficient miRNA-mediated reprogramming of mouse and human somatic cells to pluripotency. *Cell Stem Cell*. **8**, 376-388 (2011)
1101. Luo J., Suhr S. T., Chang E. A., Wang K., Ross P. J., Nelson L. L., Venta P. J., Knott J. G. & Cibelli J. B. Generation of leukemia inhibitory factor and basic fibroblast growth factor-dependent induced pluripotent stem cells from canine adult somatic cells. *Stem Cells Dev*. **20**, 1669-1678 (2011)
1102. Nagy K., Sung H. K., Zhang P., Laflamme S., Vincent P., Agha-Mohammadi S., Woltjen K., Monetti C., Michael I. P., Smith L. C. & Nagy A. Induced pluripotent stem cell lines derived from equine fibroblasts. *Stem Cell Rev*. **7**, 693-702 (2011)
1103. Zhou L., Wang W., Liu Y., Fernandez de Castro J., Ezashi T., Telugu B. P., Roberts R. M., Kaplan H. J. & Dean D. C. Differentiation of induced pluripotent stem cells of swine into rod photoreceptors and their integration into the retina. *Stem Cells*. **29**, 972-980 (2011)
1104. Gardner R. L. & Munro A. J. Successful construction of chimaeric rabbit. *Nature*. **250**, 146-147 (1974)
1105. Kunisada Y., Tsubooka-Yamazoe N., Shoji M. & Hosoya M. Small molecules induce efficient differentiation into insulin-producing cells from human induced pluripotent stem cells. *Stem Cell Res*. **8**, 274-284 (2012)
1106. Shi Y. Mammalian RNAi for the masses. *Trends Genet*. **19**, 9-12 (2003)
1107. Chitwood D. H. & Timmermans M. C. Small RNAs are on the move. *Nature*. **467**, 415-419 (2010)
1108. Sliva K. & Schnierle B. S. Selective gene silencing by viral delivery of short hairpin RNA. *Virol J*. **7**, 248 (2010)
1109. Jinek M. & Doudna J. A. A three-dimensional view of the molecular machinery of RNA interference. *Nature*. **457**, 405-412 (2009)
1110. Kawasaki H., Taira K. & Morris K. V. siRNA induced transcriptional gene silencing in mammalian cells. *Cell Cycle*. **4**, 442-448 (2005)
1111. Schütze N. siRNA technology. *Mol Cell Endocrinol*. **213**, 115-119 (2004)
1112. Nacu E., Glausch M., Le H. Q., Damanik F. R., Schuez M., Knapp D., Khattak S., Richter T. & Tanaka E. M. Connective tissue cells, but not muscle cells, are involved in establishing the proximo-distal outcome of limb regeneration in the axolotl. *Development*. Submitted

10 ACKNOWLEDGMENT

I thank my supervisor Prof. Angelika Schnieke for giving the opportunity to perform this thesis at her research group, for discussions, suggestions and support. In particular I would like to thank her to give me the possibilities to attend conferences, to present posters and in addition to give me the possibility to present parts of my work in a talk in Slovenia.

Further, I thank the 2nd referee, PD Dr. Susanne Ulbrich, for evaluating this thesis and for friendly discussions.

Great thanks go to Prof. Dr. Oswald Rottmann who did all the microinjections and for his always friendly discussions.

A lot of help and advices I received from Dr. Tatiana Flisikowska. Further, she was always there for discussions and questions. In addition, there were a lot of nice moments full of fun. Thank you for the great time!

Further, I thank Dr. Alex Kind for helpful comments, discussions and advice.

I am very grateful to Prof. Elly Tanaka for providing vectors containing the CAGGs promoter and *mCherry*. I am also thankful to Dr. Martin Kragl for his efforts regarding the INS1-E cells.

A huge "Thank you" goes to Toronto, Canada, to Dr. Shahryar Khattak, who answered me a lot of questions and serving as a mentor.

I have to write the thanks to Xinxin in English. After more than three years, I would be happy to write them in German. ☺ Anyway, thank you for the great time!

Special thanks to my students Ala El Din Samara, Manuel Glaser, Lara Riehl, Miha Modic for their work and the nice time. With some I had a lot of fun. In particular, I am grateful to Miha Modic for the organisation of the trip through Slovenia.

Ein Riesendank geht an Peggy Müller, Anja Saalfrank und Marlene Edlinger für die vielen vielen schönen Momente auch und besonders abseits der Arbeit! Inbegriffen ist natürlich auch Benedikt Baumer, bei dem ich mich hoffentlich noch in vielen Jahren später bedanken kann. Denn auf jeden Fall: Der K2 ruft! ☺

Bei Dr. Claudia Merkl möchte ich mich für ihre vielen Diskussionen und praktischen Hinweise bedanken, und auch für viele schöne und lustige Momente. Simon Leuchs danke ich zusätzlich für die Einführung in die Welt der Münchner Weinmessen.

Ich möchte mich auch bei Magret Bahnweg, Sulith Christan, Barbara Bauer, Dr. Simone Kraner, Steffen und Viola Löbnitz, Angela Zaruba, Kristina Mosandl und Konrad Fischer

bedanken. Es waren schöne Jahre mit euch. Viele gute Erinnerungen bleiben und beim Schreiben dieser Zeilen habe ich ein Lächeln auf den Lippen.

Für die unheimliche und unendliche Unterstützung meiner Eltern über all die Jahre hinweg möchte ich mich von Herzen bedanken. Danke, dass ihr mir dies alles ermöglicht habt!

Ein besonderes Dankeschön geht an meine Frau, Anne. Es gibt keinen Menschen auf der Welt, der mich so gut versteht und mir so ähnlich ist. Mit dir kann ich so schön Lachen und Rumblödeln und einfach unbeschwert sein. In deiner Nähe bin ich einfach ich. Du bist immer bei mir, in meinem Herzen. Ich liebe dich!

11 CURRICULUM VITAE

Persönliche Daten

Name:	Tobias Roland Richter
Geburtsdatum:	09.05.1981
Geburtsort:	Bautzen, ehemalige Deutsche Demokratische Republik

Ausbildung

Seit 09/2012	Post-Doktorandenstelle University of Iceland, Reykjavik, Island Spatiotemporal role of fibronectin in branching morphogenesis of human mammary gland and lung
06/2008 – 08/2012	Promotion Technische Universität München, Deutschland New methods for transgenesis in rabbits: Cell-mediated transgenesis and transposons
10/2006 – 04/2008	Master of Science Molekulare Biotechnologie Technische Universität München, Deutschland Abschlussnote: 1,1 Master´s Thesis: Isolation and characterisation of a putative rabbit embryonic stem cell line
10/2001 – 09/2004	Bachelor of Science Molekulare Biotechnologie Technische Universität Dresden, Deutschland Abschlussnote: 1,7 Bachelor´s Thesis: Analysis of the expression of selected genes of the uteri of rats after treatment with griffonianone C extracted from *Millettia griffoniana*
09/1997 – 07/2000	Abitur Berufliches Gymnasium für Ernährungswissenschaft, Dresden, Deutschland Abschlussnote: 1,3

Veröffentlichungen

Nacu E *et al*. (2012) Connective tissue cells, but not muscle cells, are involved in establishing the proximo-distal outcome of limb regeneration in the axolotl. *Development*. Submitted [1112]

Zakhartchenko V *et al.* (2011) Cell-Mediated Transgenesis in Rabbits: Chimeric and Nuclear Transfer Animals. *Biology of Reproduction* 84:229–237. [516]

Kragl M *et al*. (2009) Cells keep a memory of their tissue origin during axolotl limb regeneration. *Nature* 460:60–65. (Acknowledgment) [1072]

Khattak S, Richter T, Tanaka EM (2009) Generation of transgenic axolotls (*Ambystoma mexicanum*). *Cold Spring Harb Protoc* 2009:pdb.prot5264. [1073]

Wober J *et al*. (2007) Activation of estrogen receptor-beta by a special extract of Rheum rhaponticum (ERr 731), its aglycones and structurally related compounds. *J. Steroid Biochem. Mol. Biol.* 107:191–201. [1074]

Wanda GJMK *et al*. (2007) Estrogenic activity of griffonianone C, an isoflavone from the root bark of Millettia griffoniana: regulation of the expression of estrogen responsive genes in uterus and liver of ovariectomized rats. *Planta Med.* 73:512–518. [1075]